CHLOROPHYLL DIAGENESIS IN THE WATER COLUMN AND SEDIMENTS OF THE BLACK SEA

by

Linda L. King

B.S., Chemistry
Mary Washington College
(1987)

SUBMITTED IN PARTIAL FULFILLMENT
OF THE REQUIREMENTS FOR THE DEGREE OF
DOCTOR OF PHILOSOPHY

at the

MASSACHUSETTS INSTITUTE OF TECHNOLOGY
and the
WOODS HOLE OCEANOGRAPHIC INSTITUTION

November 1992

ABSTRACT

This thesis examines the degradation pathways of chlorophyll in the Black Sea water column and sediments. Measurements are made of total chlorophyll in sediment traps from two locations and depths in the water column, and at two locations in surface sediments. Individual chlorophyll degradation products are also identified. This data is used to construct a mass balance of chlorophyll production and sedimentation showing the major pathways for chlorophyll loss and the ultimate sedimentary sinks. The distribution of chlorophyll degradation products is also analyzed down core and related to environmental changes in the Black Sea.

Several new sinks for chlorophyll degradation products are identified. Steryl esters of pyropheophorbide-*a* are identified in sediment trap and sediment samples. It is thought that these compounds are formed during grazing. In sediment traps it is found that the distribution of the sterols esterified to pyropheophorbide-*a* change with season and that the sterols esterified are related to the distribution of sterols synthesized by the phytoplankton living in the photic zone at the time of production. Analysis of pyropheophorbide-*a* steryl esters in sediments shows the distribution of sterols to be quantitatively and qualitatively more similar to the distribution of free sterols in sediment traps than in sediments. The esterification of the sterols to pyropheophorbide-*a* apparently prevents the preferential removal of 4-desmethylsterols relative to 4-methylsterols during degradation of the sterol esters.

Chlorophyll degradation products which are incorporated into high molecular weight material and material which is only accessible with strong acid are also identified. The chlorophyll degradation products incorporated into these structures represent only a few percent of the total structure. In the high molecular weight material, only phorbins derived from chlorophyll-a are identifies, where as in the acid extractable material, porphyrins are also identified. In surface sediments, the acid extractable chlorophyll degradations products and the solvent extractable macromolecular chlorophyll degradation products each comprise approximately 30% of total sedimentary chlorophyll degradation products. The acid extractable chlorophyll degradation products are identified in sediment trap samples, and evidence is presented for the occurrence of the solvent extractable macromolecular chlorophyll degradation products in sediment trap samples.

Using data from sediment traps, sediments, and the literature, a mass balance of chlorophyll flux, degradation, and accumulation in the Black Sea is presented. In the photic zone, chlorophyll degradation products are either destroyed by photo-oxidation and grazing, or they are transported into the anoxic water column in large, rapidly sinking particles. Once the chlorophyll degradation products have reached the anoxic water column, they survive to be deposited in the underlying sediments. As a comparison, 25 times more total organic carbon reaches the anoxic water column than does total phorbin, but 75% of total organic carbon which reaches the anoxic water column is degraded, either in the anoxic water column or in the very surface sediments. Though a larger percentage of total organic carbon passes out of the photic zone, the phorbin macrocycle appears to be more stable under anoxic conditions than is total organic carbon. The chlorophyll which can be detected below the chemocline of the Black Sea in the form of chlorophyll degradation products will survive to be deposited in surface sediments. Once in sediments, chlorophyll degradation products are found in four different reservoirs: phorbin steryl esters, free phorbins, solvent extractable macromolecular chlorophyll degradation products, and acid extractable chlorophyll degradation products. Evidence for the occurrence of porphyrins in surface Black Sea sediments is also presented.

The distribution of chlorophyll degradation products in Unit I Black Sea sediments varies greatly with sediment depth. The concentration of total phorbin generally increases with increasing burial depth, but the concentrations of the individual chlorophyll degradation products vary in a manner which is both dissimilar to total phorbin and to each

other. No parent/daughter relationships for the chlorophyll degradation products are indicated by the data. The distribution of sterols esterified to pyropheophorbide-a changes with sediment depth with the largest qualitative changes occuring in strata where the total phorbin concentration shows the largest quantitative changes. It is suggested that the variations seen in the esterified sterols are related to changes in the phytoplankton community over time. From the presented data, it is also suggested that total phorbin concentration, normalized to total organic carbon, in Black Sea Unit I sediments is related to paleoprimary production.

Several conclusions are drawn from the work presented in this thesis. There is approximately 3 times more chlorophyll-derived phorbin in Black Sea sediments than can be accounted for when considering only individual pheopigments, and therefore the sedimentary degradation of chlorophyll is much more complex than previously thought. In the anoxic sediments of the Black Sea, the total phorbin distribution can be accounted for with organically extractable high molecular weight degradation products, pyropheophorbide steryl esters, pheopigments, and acid extractable chlorophyll degradation products. The sterol distribution in the pyropheophorbide steryl esters may preserve the sterol distribution in surface waters as synthesized by the phytoplankton, and pyropheophorbide steryl esters are preserved in sediments over the long term.

ACKNOWLEDGEMENTS

Many people were instrumental in the successful completion of this thesis. My thesis supervisor, Dan Repeta discussed many ideas with me and after we settled on a research topic, he got me started in the right directions. Throughout my years of study, he provided direction, discussion, and insight not only on chlorophyll degradation but organic geochemistry and oceanography in general. For all his help, I owe him my sincerest thanks. My thesis committee consisted of Dr. Phil Gschwend from M.I.T., Dr. Mark Altabet from W.H.O.I., and Dr. Geoff Eglinton from the University of Bristol. Each member provided lively discussion, both in committee meetings and out, and asked questions which made me consider aspects of my research which I had not previously though of. The impact of their help is reflected greatly in this thesis.

I also owe many thanks to all those who provided assistance with the actual lab work, either through the giving of advice, teaching me new methods, or performing analysis. Carl Johnson collected all the mass spectral data in this thesis and taught me to use the nuclear magnetic resonance spectrometer. He also helped fix our visible spectrophotometer that seemed to always be on the fritz. Thanks also go to Niel Blough for letting me use his spectrophotometer when ours was down. Bob Johnson provided many suggestions about how to obtain chromatographic separations for many of my samples. He also let us beg and barrow his printer from which all the chromatograms in this thesis obtained from the diode array detector were printed. Many people helped with the CHN analysis including Bob Nelson, Mark Dennet, Alan Fleer, and Brit. The analysis were performed on instruments in the labs of Phil Gschwend and Joel Goldman. I could not have performed the gas chromatographic analysis with out the help of Sussie McGroddy and Loraine Eglinton. I also thank John Farrington for allowing me to use his GCs. I also would like to thank Dr. Niel Blough, Dr. Kathleen Ruttenberg, Dr. Tim Eglinton, Dr. Jean Whelan, Dr. John Volkman, Dr. Stuart Wakeham, Dr. Joanne Muramoto, Dr. Dan Simpson, Steve Manganini, and Carl Johnson for many useful discussions (and not always about organic geochemistry and oceanography).

Much of this research could not have been carried out without the samples provided by Susumu Honjo. He and Steve Manganini provided the sediment trap samples and the gravity core which are discussed in Chs. 5, 6, and 7. The box core samples discussed throughout the thesis were collected and provided by Dan Repeta. I would also like to thank Geoff Eglinton and James Maxwell for the invitation to come to Bristol to analyze samples by liquid chromatography/mass spectrometry. I also owe a very sincere thank you to John Farrington, Karen Rauss, Susan Merrifield, Dan Repeta, Jean Whelan, and Ellen

Druffel. Without their help and support this thesis may never have been written. The work in this thesis was funded by grants from the Woods Hole Oceanographic Insitution's Ocean Ventures Fund and the National Science Foundation contract numbers OCE88-14398, OCE90-17626, and OCE92-01178. This support is greatfully acknowledged.

I also would like to thank Mom, Dad, and Steve. Steve not only provided moral support, but helped get me through organic chemistry class and to figure out some of the chemical reactions in this thesis. Barb and Kathy have been wonderful friends; Barb for many years now, and Kathy, a new friend, for the past few years. May we always be friends. To all these people, my friends in Fye, and Gene Roddenberry: I couldn't have done it without you. Thanks!!

TABLE OF CONTENTS

LIST OF FIGURES

LIST OF TABLES

Chapter 7

LIST OF ABBREVIATIONS

Abbreviations found in text, tables, and figures

chl-*a*	chlorophyll-*a*
chl-*b*	chlorophyll-*b*
ptn-*a*	pheophytin-*a*
ptn-*b*	pheophytin-*b*
pptn-*a*	pyropheophytin-*a*
pptn-*b*	pyropheophytin-*b*
pbd-*a*	pheophorbide-*a*
pbd-*b*	pheophorbide-*b*
ppbd-*a*	pyropheophorbide-*a*
ppbd-*b*	pyropheophorbide-*b*
Znppbtn-*a*	Zn-pyropheobutin-*a*
AEX	acid extractable chlorophyll degradation products
HMW	high molecular weight solvent extractable chlorophyll degradation products
PSE	pyropheophorbide-a steryl esters
MeOH	methanol
n-PrOH	*n*-propanol
gdw	gram dry weight
S/R	ratio of absorbances at Soret maximum and red band
C:chl	ratio of g organic carbon to g total phorbin

Abbreviations found in figures

B	blank impurity
I	impurity
IS	internal standard
S	solvent
W	water

CHAPTER 1

THE DEGRADATION OF CHLOROPHYLL-*A* IN THE MARINE ENVIRONMENT and A DESCRIPTION OF THE BLACK SEA

CHAPTER 1

THE DEGRADATION OF CHLOROPHYLL-*A* IN THE MARINE ENVIRONMENT AND A DESCRIPTION OF THE BLACK SEA

I. INTRODUCTION

Since the initial work on the fate of chlorophyll in sediments done in the 1930's (Treibs, 1936), the study of chlorophyll degradation has proceeded in several different directions in response to different research questions. These questions are concerned with tracing photic zone biological activity, linking the sedimentary record of chlorophyll degradation products to past phytoplankton production, tracing the diagenetic pathways of organic compounds, and understanding the carbon cycle. As a result of the diversity of problems under study, research on chlorophyll degradation has proceeded in a manner which has led to a large body of literature on as yet unlinked aspects of chlorophyll degradation.

The existence of a link between the concentration of chlorophyll degradation products in sediments and the magnitude of paleoprimary production was first suggested by Fogg and Belcher (1961) and Gorham (1961). Since these early studies, work has been done in various sedimentary environments to establish this link (Czeczuga, 1964; Wetzel, 1970; Brown *et al.*, 1977; Daley *et al.*, 1977; Guilizzoni *et al.*, 1983; Swain, 1985). More recently, this line of research has been expanded to examine the link between paleoprimary production and the C/chl (g carbon/g chlorophyll) ratio in sediments (Lorenzen, 1968; Clayton and Michael, 1990). Investigations have also been undertaken to examine the factors which affect the ratio of C/chl produced by phytoplankton (Owens *et al.*, 1980; Hunter and Laws, 1981; Welschmeyer and Lorenzen, 1984; Laws *et al.*, 1984; Laws *et al.*, 1987; Sakshaug *et al.*, 1991) and the preservation of this ratio in sediment traps and sediments (Welschmeyer and Lorenzen, 1984; Cole *et al.*, 1985; Downs and Lorenzen, 1985). The major problem with using total phorbin or C/chl as an indicator of paleoprimary production, is loss of chlorophyll through unknown degradation pathways in the water column and sediment.

The biologically mediated degradation of chlorophyll in the water column is studied as a means of monitoring zooplankton grazing and phytoplankton senescence (Schoch *et al.*, 1981; Carpenter and Berquist, 1985; Burkill *et al.*, 1987; Ziegler *et al.*, 1988; Downs, 1989; Roy *et al.*, 1990; Bianchi *et al.*, 1991). The goal of this research is to establish a link between specific chlorophyll degradation products and grazing or senescence. Such a link could be used to quantify the relative contribution of both senescence and grazing to the

removal of phytoplankton from the photic zone and deposition of chlorophyll degradation products in sediments.

Chlorophyll degradation products in sediments have been analyzed by organic geochemists in order to advance their understanding of transformation pathways for organic compounds. These studies have taken two different paths. The first involves looking for specific compounds believed to be necessary intermediates in the degradation of chlorophyll to porphyrins as postulated by Treibs (1936) (Gillan and Johns, 1980; Keely and Brereton, 1986; Furlong, 1986; Furlong and Carpenter, 1988; Keely *et al.*, 1988; Keely *et al.*, 1990), or by looking for any compound which may have been produced in the transformation of chlorophyll to porphyrins (Smith and Baker, 1974; Baker et al., 1976; Baker et al., 1977, 1978a, 1978b; Baker and Palmer, 1979; Louda and Palmer, 1980; Louda and Baker, 1981, 1986; Baker and Louda, 1980, 1982, 1983, 1986). The second approach is to look for any sedimentary phorbin, chlorin, or porphyrin, determine its structure, and to postulate a transformation mechanism from a specific chlorophyll or heme type starting material (Fookes, 1983; Chicarelli *et al.*, 1984; Chicarelli and Maxwell, 1984; Ocampo *et al.*, 1984, 1985; Kauer *et al.*, 1986; Verne-Mismer *et al.* 1988,1990; Bauder *et al.*, 1990; Callot *et al.*, 1990).

Chlorophyll degradation products are also used in the study of carbon cycling since chlorophyll is one of a few compounds unique to photoautotrophic activity. Tracing chlorophyll degradation products in the water column and sediments is simplified due to its characteristic visible spectrum. The use of chlorophyll degradation products in the study of carbon cycling has evolved to using the stable carbon isotope ratios of chlorophyll and its degradation products to look for changes in carbon dioxide partial pressure and tropodynamics (Hayes *et al.*, 1987; Popp *et al.*, 1989; Hayes *et al.*, 1989; Hayes *et al.*, 1990).

For the most part, each of the above investigations have been carried out independently of each other. Few attempts have been made to link the formation and distribution of specific chlorophyll degradation products in the water column with those found in sediments. There is also evidence that chlorophyll degradation products analyzed in sediments by high pressure liquid chromatography represent only a fraction of the chlorophyll degradation products actually in sediments (Furlong and Carpenter, 1988; Repeta, unpublished). The research in this thesis was undertaken with three objectives in mind: (1) to develop methods for identifying and quantifying chlorophyll degradation products in samples from sediments and sediment traps, (2) to identify major sedimentary sinks for chlorophyll in sediments and assess the relative contribution of each to the pathway of chlorophyll degradation, and (3) to construct a quantitative model of

chlorophyll degradation in the Black Sea water column and sediments. The following provides an introduction to the state of knowledge of the different aspects of chlorophyll degradation which are involved in this research project. This paper also describes the Black Sea which is the chosen oceanographic setting for the work presented in this thesis.

II. CHLOROPHYLL DIAGENESIS IN THE WATER COLUMN

Chlorophyll is synthesized in the euphotic zone by algae during the process of primary production. The distribution of algae, and therefore chlorophyll, in the photic zone depends on the light regime and nutrient distribution. The particular phytoplankton in the producer community will also affect the photic zone chlorophyll distribution, as different plankton groups produce varying amounts of diverse chlorophylls (Lorenzen, 1968; Laws and Bannister, 1980; Sharp et al., 1980), though all phytoplankton, with the exception of pyrochlorophytes, produce chlorophyll-a_1. Once formed, chlorophyll may be degraded in the photic zone through the processes of zooplankton grazing, photo-oxidation, and senescence. The chlorophyll degradation products formed through grazing and senescence are pheophorbides and pheophytins, with the pheopigment (pheophytin, pyropheophytin, pheophorbide, pyropheophorbide as a group) formed being dependent on the organisms involved (Schoch *et al.*, 1981; Carpenter and Berquist, 1985; Burkill *et al.*, 1987; Ziegler *et al.*, 1988; Downs, 1989; Roy *et al.*, 1990; Bianchi *et al*, 1991). The products of photo-oxidation are as yet unidentified in the marine environment, but are believed to be either linear tetrapyrroles or colorless products (Matile et al., 1987). Chlorophylls of many different structures undergo degradative processes in the surface water column.

Phytoplankton produce the chlorophylls (Fig. 1-1) chlorophyll-a_1, chlorophyll-a_2, chlorophyll-b_1, chlorophyll-b_2, chlorophyll-c_1, chlorophyll-c_2, chlorophyll-c_3, phytol substituted chlorophyll-*c*, and Mg 2,4-divinylpheoporphyrin-a_5 monomethyl ester (Ricketts, 1966; Fawley , 1989; Nelson and Wakeham, 1989; Bidigare *et al.*, 1990; Goericke and Repeta, 1992), with the major photosynthetic pigments found in the marine environment being chlorophylls-*a* and -*c*. Chlorophyll-*a* occurs in all green photosynthetic organisms (except prochlorophytes) with chlorophylls-*b*,-c_1,-c_2, and -c_3 occuring as accessory pigments. After the death of the algae, the pigments may be transfered out of the photic zone on sinking particles. Chlorophylls are usually found only in the surface waters but may occur in low concentrations on particles in the deeper ocean. Very rarely are chlorophylls found in marine sediments. Pheophytins and pheophorbides, which are produced in the water column, are commonly found in surface sediments.

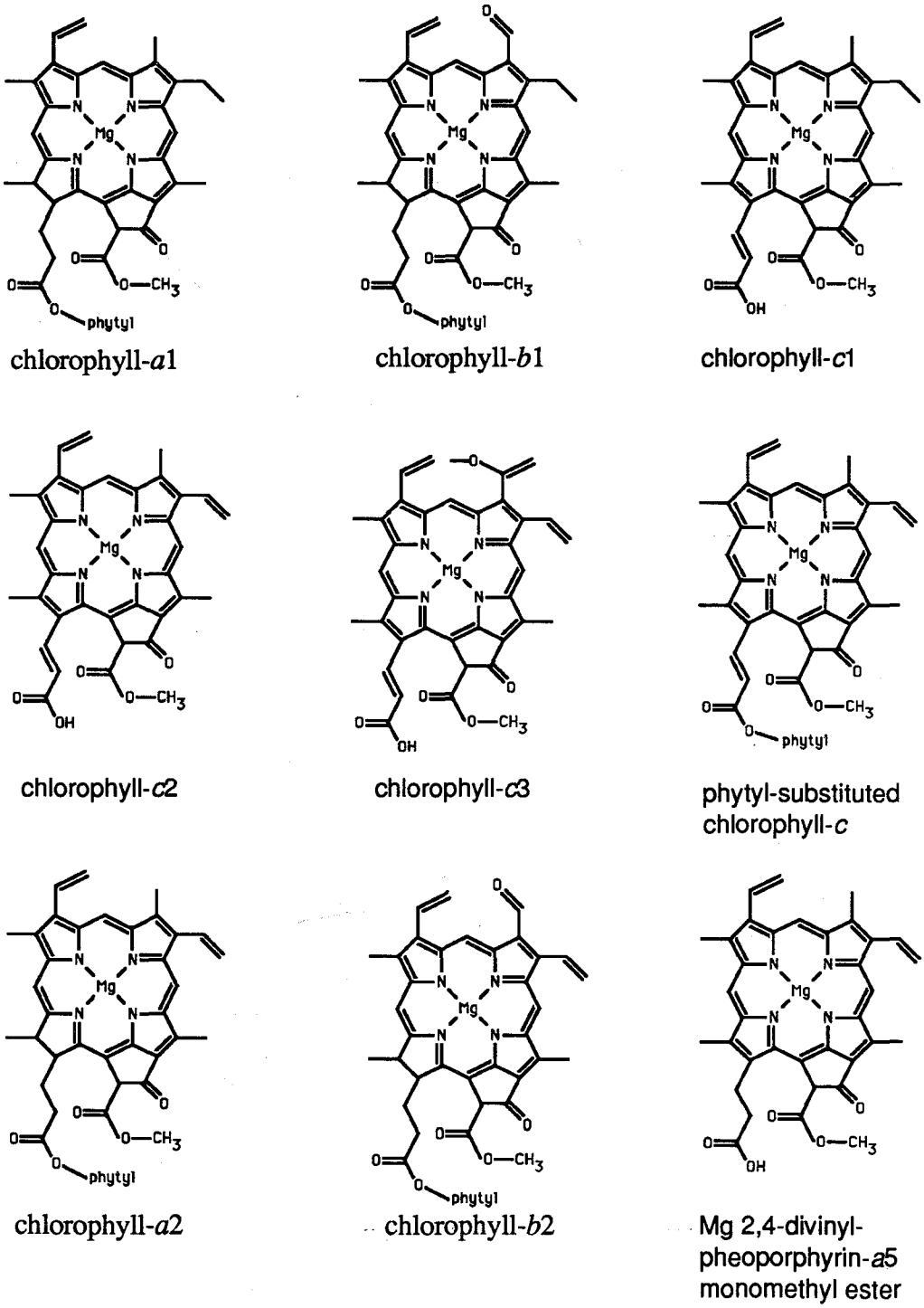

Fig. 1-1 Structures of the different chlorophylls identified in marine phytoplankton.

In the water column, chlorophyll may be lost through grazing. In grazing, zooplankton eat phytoplankton and assimilate part of the organic material and pass the remaining material, in altered form, packaged in fecal pellets. Grazed chlorophyll will either be converted to pheopigments or lost through conversion to colorless material or through assimilation (Conover *et al.*, 1986; Kiorboe and Tisselius, 1987; Lopez *et al.*, 1988; Roy *et al.*, 1989; Penry and Frost, 1991; Mayzaud and Razouls, 1992). The pheopigments formed during grazing are pheophytin (**1**, Fig. 1-2), pyropheophytin **2**, pheophorbide **3**, pyropheophorbide **4**, and unidentified phorbins (Burkill *et al.*, 1987; Downs, 1989; Bianchi *et al.*, 1991). The efficiency of the chlorophyll to pheopigment conversion during grazing is dependent on the grazing organism, food concentration, food quality, and feeding history of the grazing organism (Kiorboe and Tisselius, 1987; Lopez *et al.*, 1988; Roy *et al.*, 1989; Penry and Frost, 1991; Mayzaud and Razouls, 1992). The chlorophyll degradation product produced during grazing may be specific for the grazing organism (Carpenter and Berquist, 1985; Klein *et al.*, 1986; Burkhill et al., 1987), and the pheopigment flux resulting from grazing is related to the size of the grazing organism (Welschmeyer and Lorenzen, 1985; Carpenter *et al.*, 1986; Carpenter *et al.*, 1988). The products of zooplankton grazing are packaged into fecal pellets which will either remain suspended in the surface water column or sink out of the photic zone (Welschmeyer and Lorenzen, 1985; Bathmann and Liebezeit, 1986).

In the photic zone, chlorophyll may be removed by photo-oxidation as well as by grazing (Daley and Brown, 1973; SooHoo and Kiefer, 1982a, 1982b). Chlorophyll contained in living or dead phytoplankton (Daley and Brown, 1973) or in fecal pellets small enough to remain suspended (SooHoo and Kiefer, 1982a, 1982b) is subject to photo-oxidation. Rate constants for photo-oxidation are higher for chlorophyll-*a* than for pheopigments (Carpenter *et al.*, 1986) and, for chlorophyll, range from 0.04 to 0.09 m^2/Einst (SooHoo and Kiefer, 1982b; Welschmeyer and Lorenzen, 1985;.Carpenter *et al.*, 1986). Photo-oxidation of chlorophyll and its degradation products in surface waters may account for 75 to 90% of chlorophyll loss and 40% of pheopigment loss (Welschmeyer and Lorenzen, 1984; Carpenter *et al.*, 1986), and photo-oxidation may be a major mechanism for removal of chlorophyll and its degradation products from the surface ocean.

Removal of chlorophyll from the photic zone also occurs during algal senescence. Degradation of chlorophyll in senescing cells may occur through photo-oxidation or enzymatically during cellular lysis. In cultures of nutrient starved algae and cyanobacteria , Daley and Brown (1973) found the concentration of chlorophyll-*a* to decrease during algal senescence with no increase in pheopigments, suggesting degradation of chlorophyll-*a* to colorless products is occuring, but in light starved cultures of cyanobacteria, they found

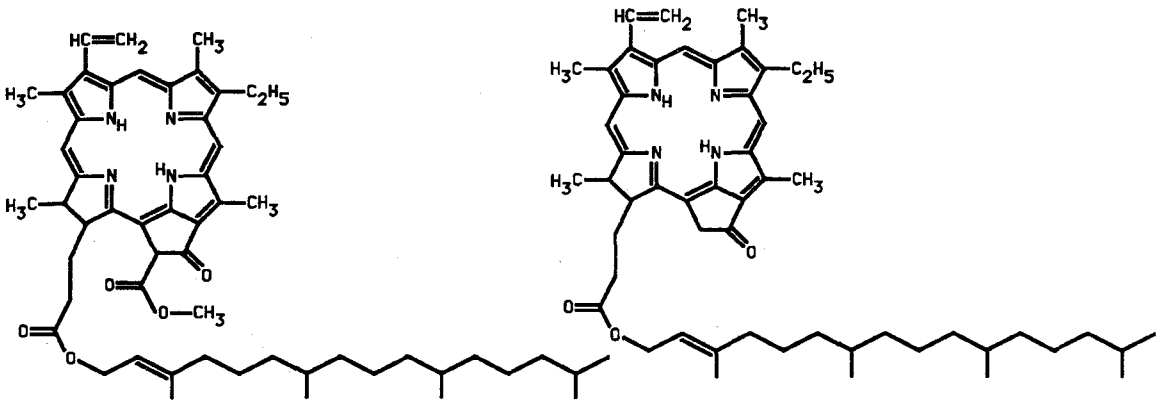

1 pheophytin-*a*

2 pyropheophytin-*a*

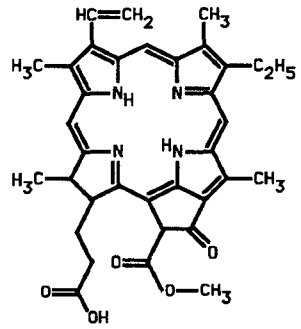

3 pheophorbide-*a*

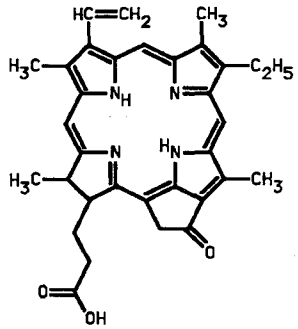

4 pyropheophorbide-*a*

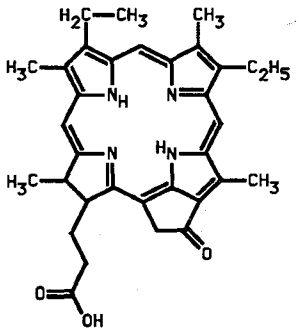

5 mesopyropheophorbide-*a*

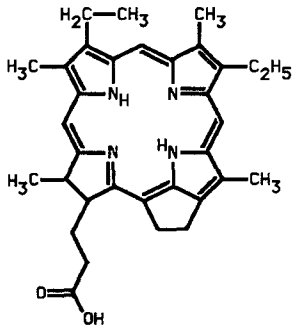

6 deoxomesopyropheophorbide-*a*

Fig. 1-2 Structures of degradation products of chlorophyll-*a* discussed in the text. Numbers are keyed to the discussion.

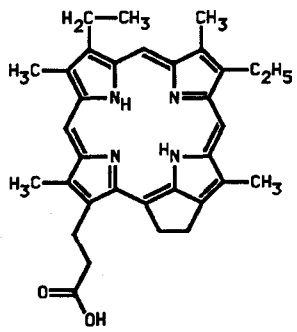

7 acid of deoxophylloerythroetioporphyrin

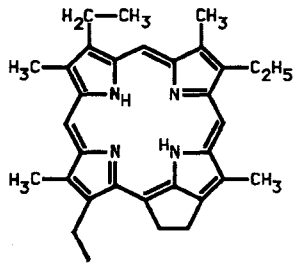

8 deoxophylloerythroetioporphyrin

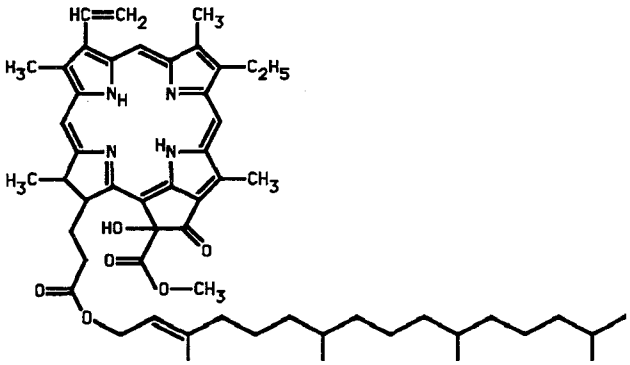

9 10-oxypheophytin

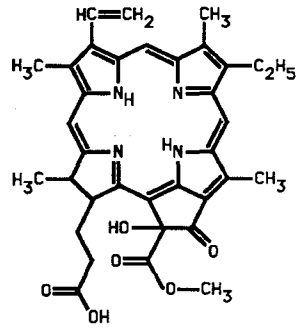

10 10-oxypheophorbide

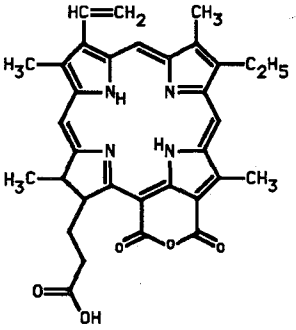

11 purpurin 18

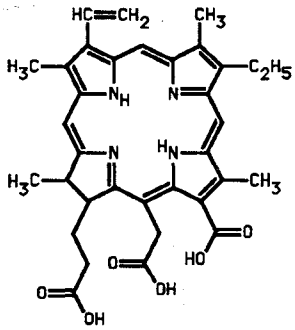

12 chlorin-e6

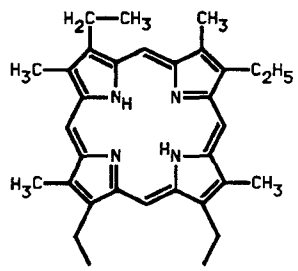

13 etioporphyrin

Fig. 1-2 continued.

concentrations of pheophytin-*a* and pheophorbide-*a* to increase as chlorophyll-*a* decreased, suggesting that conversion of chlorophyll-*a* to pheopigments is occuring during senescence. In light-starved cultures of *Euglena*, both pheophytin and pyropheophytin were found to form through enzymatic reactions (Schoch *et al.*, 1981), and in cultures of *Clorella fusca*, pheophorbide-*a* and pyropheophorbide-*a* were formed (Ziegeler *et al.*, 1988). The result of these studies suggests that during senescence, the many different pheopigment are formed and the pigments produced may be species specific.

The primary controls on the amount and form of chlorophyll degradation products that leave the photic zone are photo-oxidation (SooHoo and Kiefer, 1982b; Welschmeyer and Lorenzen, 1984; Leavitt and Carpenter, 1990) and grazing (Owen and Falkowski, 1982; Klein *et al*, 1986; Conover *et al.*, 1986; Downs, 1989). Once degradation products of chlorophyll are formed in the photic zone, whether through grazing or senescence, they will be transported to the underlying sediments in large particles, but during sedimentation, further loss of chlorophyll and its degradation products will occur through enzymatic reactions in intact algal cell and during grazing of sinking particles (Bathmann and Liebezeit, 1986). Phorbins found in the water column below the photic zone are chlorophyll-*a*, pheophytin-*a*, and pheophorbide-*a*. The total concentration of these compounds decreases with water depth (Vernet and Lorenzen, 1987; Furlong and Carpenter, 1988; Downs, 1989). Concentrations of chlorophyll-*a* rapidly decrease below the chlorophyll maximum with pheophytin and pheophorbide reaching a concentration maximum slightly below the depth of the maximum in chlorophyll concentration (Vernet and Lorenzen, 1987; Downs, 1989). The concentration of all chlorophyll-derived compounds then rapidly decreases. Once the phorbins arrive at the sediment surface, they may be further degraded.

III. CHLOROPHYLL DIAGENESIS IN SEDIMENTS

Once chlorophyll degradation products are deposited in sediments, they may degrade by several different pathways, some of which are known, but many of which are still unclear (Fig. 1-3). These pathways include complete remineralization of chlorophyll to CO_2, and transformation of the deposited pheopigments through a series of phorbins and chlorins with porphyrins. Studies also suggest that chlorophyll degradation products may be incorporated into macromolecular compounds. The way in which chlorophyll and its degradation products degrade in sediments may be controlled by the redox conditions under which the phorbins are deposited (Orr *et al.*, 1958; Baker and Louda, 1982).

Once chlorophyll, or degradation products of chlorophyll, are deposited in sediments they continue to degrade, ultimately through catagenesis where the chlorophyll skeleton is lost through thermal cracking of C-C bonds (Baker and Louda, 1983). Before the onset of catagenesis, during diagenesis, the phorbin macrocycle may be lost through remineralization with the ultimate end product being CO_2. The mechanism through which remineralization occurs is unknown, but is presumed to occur through cleavage of the macrocycle, and has been compared to the process in which other compounds containing macrocycles, such as heme, are removed from living organisms. Heme, a biologically produced porphyrin, is cleaved to biliverdin, a linear tetrapyrrole, as part of the process which removes heme from living tissue (Brown and King, 1978). With chlorophyll, the rate and extent to which macrocycle cleavage occurs may be influenced by bacteria and light (Jen and Mackinney, 1970; Brown, *et al.*, 1980; Matile *et al.*, 1987). The occurrence of a pigment in *euphausiids* with a linear tetrapyrrole type absorption spectrum and with a structure that suggests this compound is formed from chlorophyll-*a* (Shimomura, 1980) supports the occurrence of macrocycle cleavage in the marine environment. The *euphausiid* study does not deal with sedimentary phorbin degradation, but does suggest that macrocycle cleavage may occur under marine conditions without the necessity of light.

The most commonly studied sedimentary chlorophyll degradation pathway is the formation of porphyrins from chlorophyll as first proposed by Treibs in 1936. Treibs (1936) proposed a series of transformations necessary to convert chlorophyll to the porphyrins he isolated from oils (Treibs, 1936). These steps are: (1) demetallation; (2) ester hydrolysis, loss of phytol to form pheophorbide and loss of methanol from the carbomethoxy group; (3) hydrogenation of the vinyl group; (4) dehydrogenation, aromatization of the ring to form a porphyrin; (5) reduction of the carboxyl group; (6) decarboxylation, loss of the acids formed in ester hydrolysis as CO_2; and (7) complex formation, insertion of a metal in the macrocycle. Intermediates formed by each transformation have been isolated except the diacid formed in step 2. It is believed that instead of hydrolysis of the carbomethoxy ester, as suggested in step 2, the entire carbomethoxy group is removed (as in the formation of pyropheophorbide). With this one difference, all the intermediates in this reaction scheme, commonly referred to as the Treibs scheme, have now been identified (Keely, 1989; Keely *et al.*, 1990).

The first intermediates in the Treibs scheme are found in the water column and in surface sediments. These are pheophytin, pyropheophytin, pheophorbide, and pyropheophorbide (Brown *et al.*, 1977; Daley *et al.*, 1977; Gillan and Johns, 1980; Keely and Brereton, 1986; Keely *et al.*, 1988). In sediments, the decrease in concentration of these compounds occurs rapidly with sediment depth (Gillan and Johns, 1980; Keely and

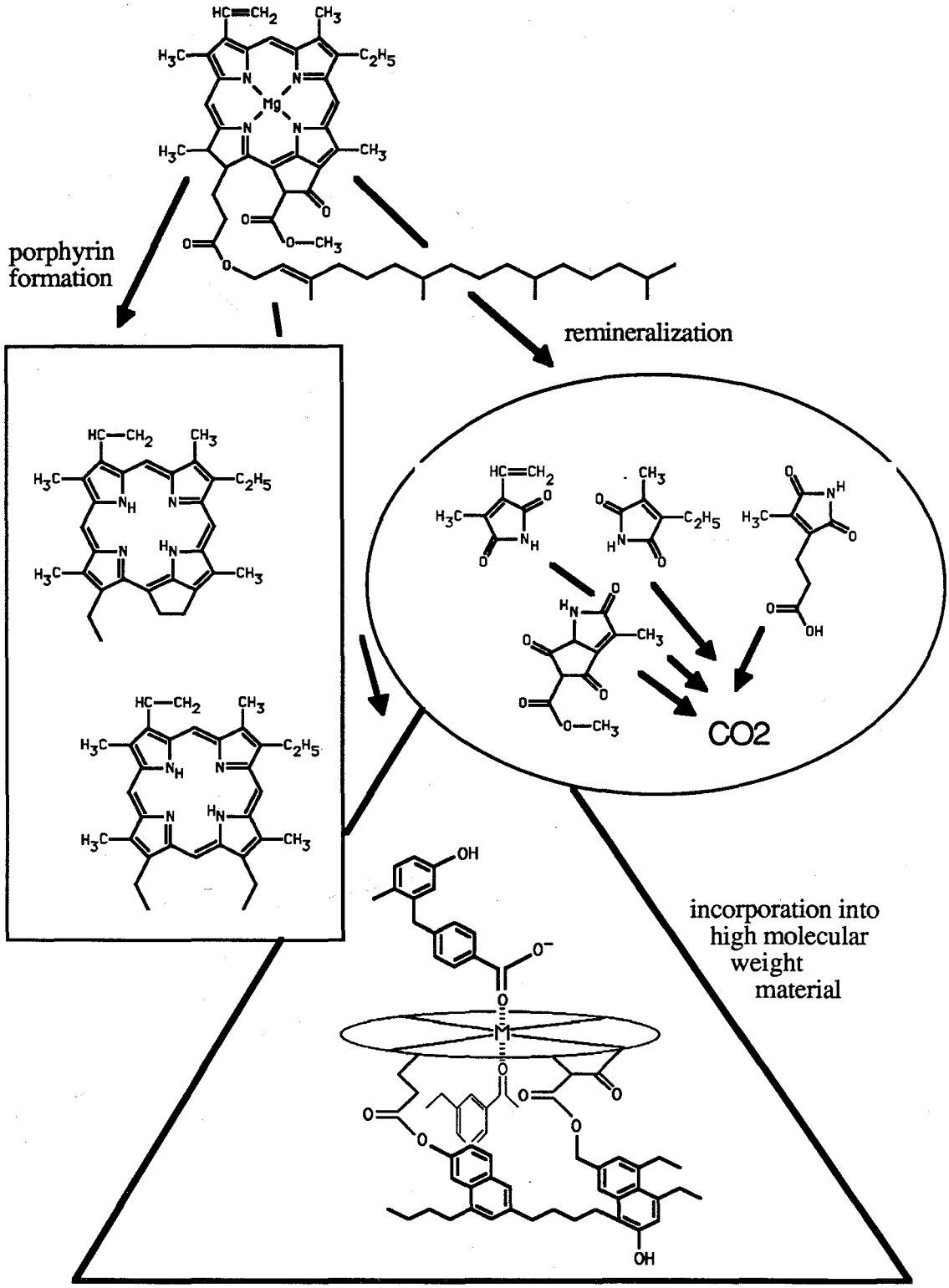

Fig. 1-3 Conceptual degradation pathway for chlorophyll-*a* in sediments.

Brereton, 1986; Keely *et al.*, 1988), with the concentration of chlorophyll decreasing much more rapidly than pheophytin, due to the faster rate of demetallation of chlorophyll relative to competing reactions (Keely and Brereton, 1986). An intensive investigation of the Treibs scheme degradation intermediates was undertaken by Keely *et al.* (1990). In the Marau shale, they identified mesopyropheophorbide-*a* **5** and deoxomesopyropheophorbide-*a* **6** (Keely *et al.*, 1990). The last intermediates in the Treibs scheme, the carboxylic acids of deoxophylloerythroetioporphyrin (DPEP) **7** and DPEP **8** were found in the Willershausen shale (Keely *et al.*, 1990). The transformations suggested by Keely's work generally fit the Treibs scheme, though the order in which the reactions occur is not the same. Degradation of chlorophyll to porphyrins, along the lines suggested by Treibs (1936), appears to be one degradation pathway of chlorophyll but it is not the only one (Baker and Louda, 1982; Habermehl *et al.*, 1984; Ocampo *et al.*, 1985a)

Intermediates of chlorophyll degradation other than those suggested by Treibs (1936) and Keely *et al.*, (1990) have been isolated. The rapid decrease in pheopigment concentration which is seen in oxic sediments is not apparent in anoxic sediments (Orr *et al.*, 1958; Swain, 1985; Furlong, 1986; Furlong and Carpenter, 1988; Hurley and Armstrong, 1991; Yacobi *et al.*, 1991) suggesting that variations exist in the degradation pathway of chlorophyll in oxic and anoxic environments. In oxic sediments, pheophytin, pyropheophytin, pheophorbide, and pyropheophorbide occur as in anoxic sediment, but 10-oxypheophytin **9** and 10-oxypheophorbide **10** (allomerized pheophytin and pheophorbide) also occur (Baker and Louda, 1982, 1983). Due to the rapid conversion of these allomerized compounds to purpurins **11** and chlorins **12** (Baker and Louda, 1982, 1983), the decrease in concentration of phorbins in oxic recent sediments occurs rapidly (Baker and Louda, 1983). On the basis of their visible spectra, approximately eight chlorins have been identified in Deep Sea Drilling Project (DSDP) samples from the Gulf of California (Louda and Baker, 1981; Baker and Louda, 1982). These compounds increase in concentration in sediment strata below those strata which contain pheophytins and pheophorbides, suggesting that chlorins and purpurins are formed diagenetically from pheopigments (Baker and Louda, 1980, 1982; Louda and Baker, 1981). With increase in sediment age, the chlorins found become increasingly defunctionalized (Baker and Louda, 1980).

The last steps in the diagenesis of chlorophyll, whether in oxic or anoxic environments, are metallation and aromatization to form metallated porphyrins from pheophorbides and chlorins. Both metallated and free base porphyrins have been found in sediments, as well as metallated and free base phorbins (Prowse *et al.*, 1990). This suggests that metallation and aromatization are competing reactions. The order in which

these reactions occur may depend on sediment Eh (Lipiner *et al.*, 1988) and the distribution of metals present in the sediment (Lipiner *et al.*, 1988). The formation of porphyrins represents the end-product of diagenesis along the route first suggested by Treibs (1936) and later augmented by Baker and Louda (1982) (Fig. 1-4).

A third possible sink of chlorophyll degradation products in sediments is the incorporation of the phorbin macrocycle into macromolecular structures. In sediments, porphyrins are believed to be incorporated into kerogen since the concentration of porphyrins has been shown to increase in oil shales in the region of thermal cracking (Quirke et al., 1980; Mackenzie et al., 1980; Barwise and Roberts, 1984); and alkyl pyrroles, believed to be formed from porphyrins, are produced during pyrolysis of kerogens (Sinninghe Damste *et al.*, 1992). The incorporation of the phorbin macrocycle into macromolecular material may also occur before kerogen formation begins. In size exclusion chromatography of total extracts of recent sediments, a fraction with a molecular weight greater than 1000 daltons which possesses a phorbin-type visible spectrum can be isolated (Repeta and Simpson, unpublished), and porphyrins with molecular weights up to 20,000 daltons have been identified in extracts of oil shales (Blumer and Snyder, 1967; Blumer and Rudrum, 1970). Phorbins are also believed to occur in humic material. Visible spectra of humic material isolated from marine sediments are phorbin-like (Sato, 1980; Cronin and Morris, 1982; Poutanen and Morris, 1983; Ertel and Hedges, 1983) and oxidation of humic acids produces maleimides; oxidation products of phorbins and porphyrins (Furlong and Carpenter, 1988). The results of these studies provide evidence for the incorporation of chlorophyll-*a* into a non-organic solvent extractable form early in the degradation of chlorophyll, and the phorbins incorporated in these macromolecular fractions could represent an unquantified reservoir of chlorophyll degradation products in high pressure liquid chromatography (HPLC) studies. Studies which quantify total sedimentary phorbins by visible spectrophotometry would include only those high molecular weight phorbins which are solvent extractable.

In sediments, chlorophyll degradation products degrade through numerous pathways including remineralization to CO_2, porphyrin formation, and incorporation into macromolecular material. The relative importance of each path may depend on diagenetic conditions. In order to account for the total quantity of chlorophyll degradation products in sediments, the phorbins in macromolecular material, as well as free phorbin, must be quanitified.

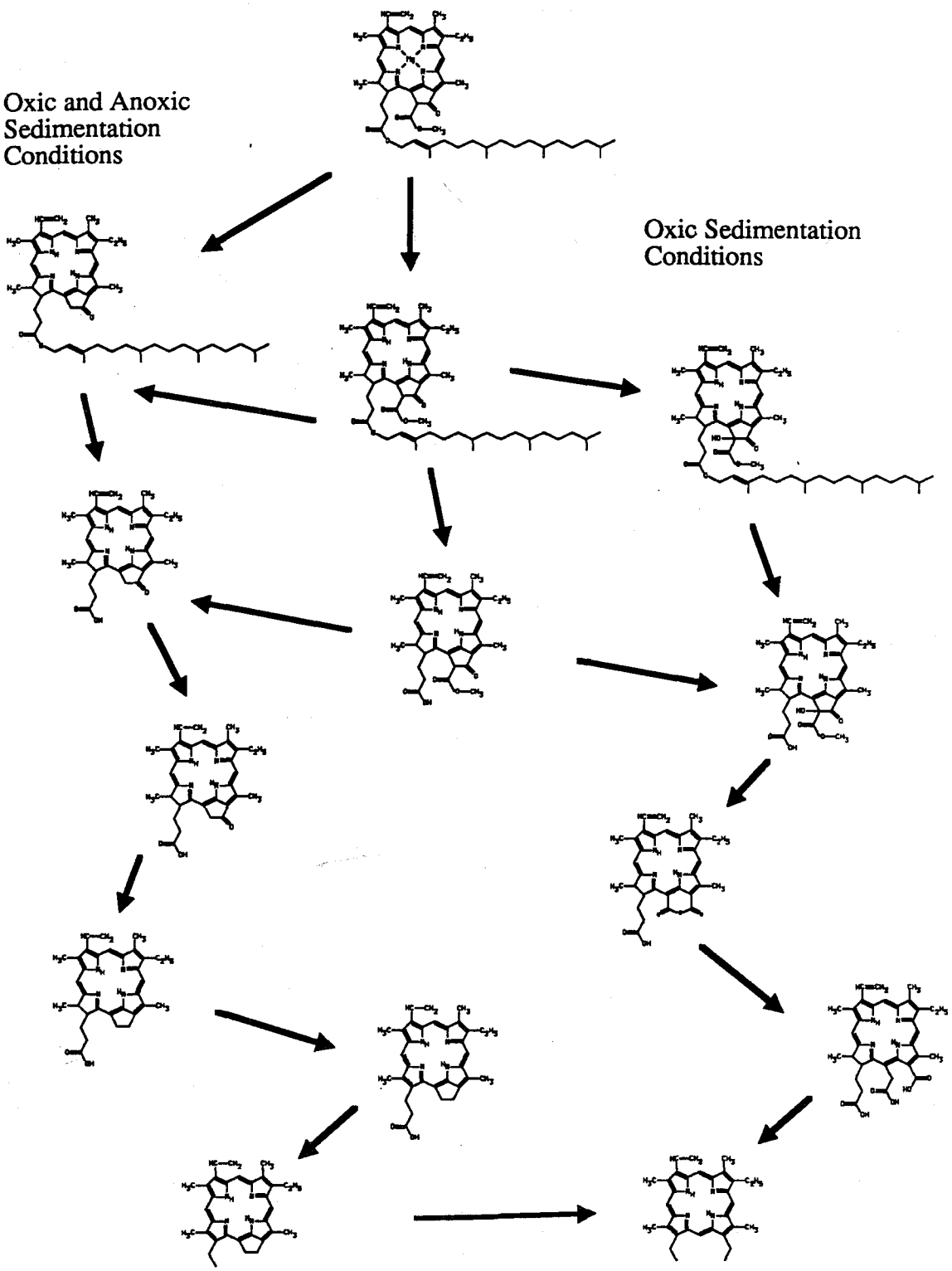

Fig. 1-4 Degradation pathway for chlorophyll-*a* proposed by Treibs (1936) and augmented by Baker and Louda (1982).

IV. OTHER STUDIES OF SEDIMENTARY COMPOUNDS POSSIBLY DERIVED FROM CHLOROPHYLL

The sedimentary degradation of chlorophyll has also been studied from two additional points of view not considered by traditional studies of the diagenesis of organic compounds: by looking for any organic structure in sediments with a phorbin or porphyrin-type chromophore as indicated by visible spectroscopy and by relating the ratio of $^{13}C/^{12}C$ in the phorbin or porphyrin to the environment of formation for the diagenetic precursor of the phorbin or porphyrin. In looking for compounds in sediments that might be related to chlorophyll, many unusual structures have been identified which are believed to originate from precursors other than chlorophyll-*a* (Fookes, 1983; Chicarelli *et al*, 1984; Chicarelli

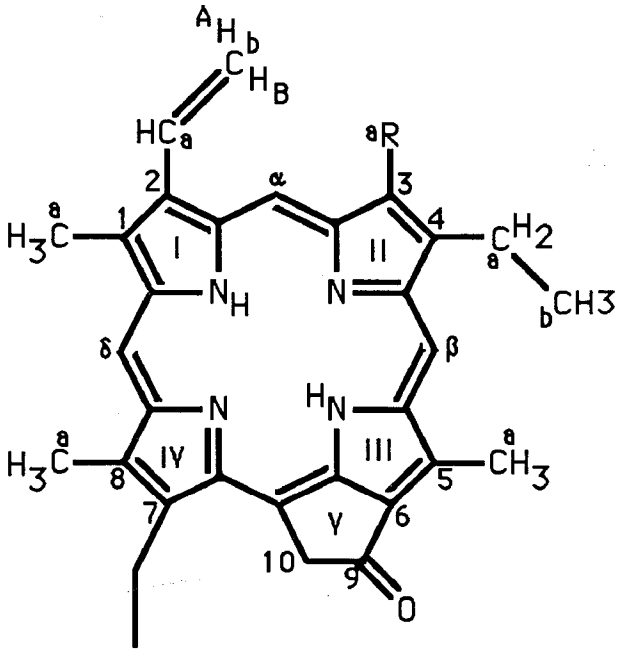

and Maxwell, 1984, 1986; Ocampo *et al.*, 1984, 1985b; Kauer *et al.*, 1986; Verne-Mismer *et al.*, 1988,1990; Bauder *et al.*, 1990). Several porphyrins have been isolated with a five-membered isocyclic ring on the side of the structure opposite to that of chlorophyll-*a* and are believed to be derived from one or more of the chlorophylls-*c* (Ocampo *et al*, 1984, Verne-Mismer *et al.*, 1988, 1990; Callot *et al.*, 1990). Porphyrins with seven-membered isocyclic rings have been isolated from oil shales and are thought to derive from rearrangement of the propionic acid group of chlorophyll-*a* derivatives (Fookes, 1983; Chicarelli and Maxwell, 1986), but there is as yet no assigned precursor for porphyrins with six-membered isocyclic rings (Chicarelli *et al.*, 1984). Monobenzoporphyrins (rhodoporphyrins) with the benzene ring on ring II of the porphyrin and porphyrins with extended alkyl chains at C-4 are thought to derive from input of bacteriochlorophylls

(Ocampo *et al.*, 1985b; Kaur *et al.*, 1986; Callot *et al.*, 1990; Quirke *et al.*, 1990) or chlorophylls-*b* or -*d* (Quirke *et al.*, 1990).

By combining structural analysis with isotopic analysis, degradation products of cytochrome or heme have been tentatively identified in sediments. Etioporphyrins **13** which possess propionic acids at both C-6 and C-7 can not be derived from any known chlorophylls but are structurally similar to heme. The appearance of these diacids along with the two possible mono acid homologues in sediments suggests that at least a portion of sedimentary etioporphyrins are derived from heme (Bauder *et al.*, 1990; Callot *et al.*, 1990). Stable carbon isotope ratios of C_{32} etioporphyrins in the Julia Creek formation are 2-3 ‰ lower (depleted in ^{13}C) than the remaining etio and DPEP porphyrins, indicating a source other than chlorophyll for the C_{32} etioporphyrins in this sample (Boreham *et al.*, 1989; Ocampo *et al.*, 1989; Hayes *et al.*, 1990). Inferences as to the source of porphyrins have been made based on their ^{13}C depletion relative to other lipids in the same sample. Stable carbon isotopes of porphyrins have also been used to infer sources of given porphyrins from specific chlorophyll precursors. Precursor information is used in combination with the stable carbon isotope ratios of other lipids to reconstruct the flow of carbon through ancient ecosystem (Hayes et al., 1987; Boreham et al., 1990).

V. THE BLACK SEA

All the research described in this thesis was conducted on sediment and sediment trap samples from the Black Sea. In choosing this site, we hoped that the anoxic conditions which exist in the Black Sea water column below approximately 100 m and which exist in the sediments would simplify the degradative route of chlorophyll by removing the oxic degradation pathway. Due to the largely anoxic and enclosed conditions, the Black Sea has environmental conditions which are not typical of the world's oceans.

The Black Sea is an inland sea situated in eastern Europe, bordered by Rumania, Bulgaria, Turkey, Moldova, Ukraine, Russia, and Georgia (Fig. 1-5), and is the world's largest anoxic water body. The only connection between the Black Sea and Atlantic Ocean is through the 300 km long Turkish Straits (Gunnerson and Ozturgut, 1974) which connects the Black Sea with the Mediterranean Sea. Mediterranean Deep Water entering the Black Sea must pass from the Aegean Sea, and through the Turkish Straits which consist of the Dardanelles, the Sea of Marmara, and the Straits of Bosphorus. Three kilometers from the exit of the Straits of Bosphorus into the Black Sea is a sill with a maximum depth

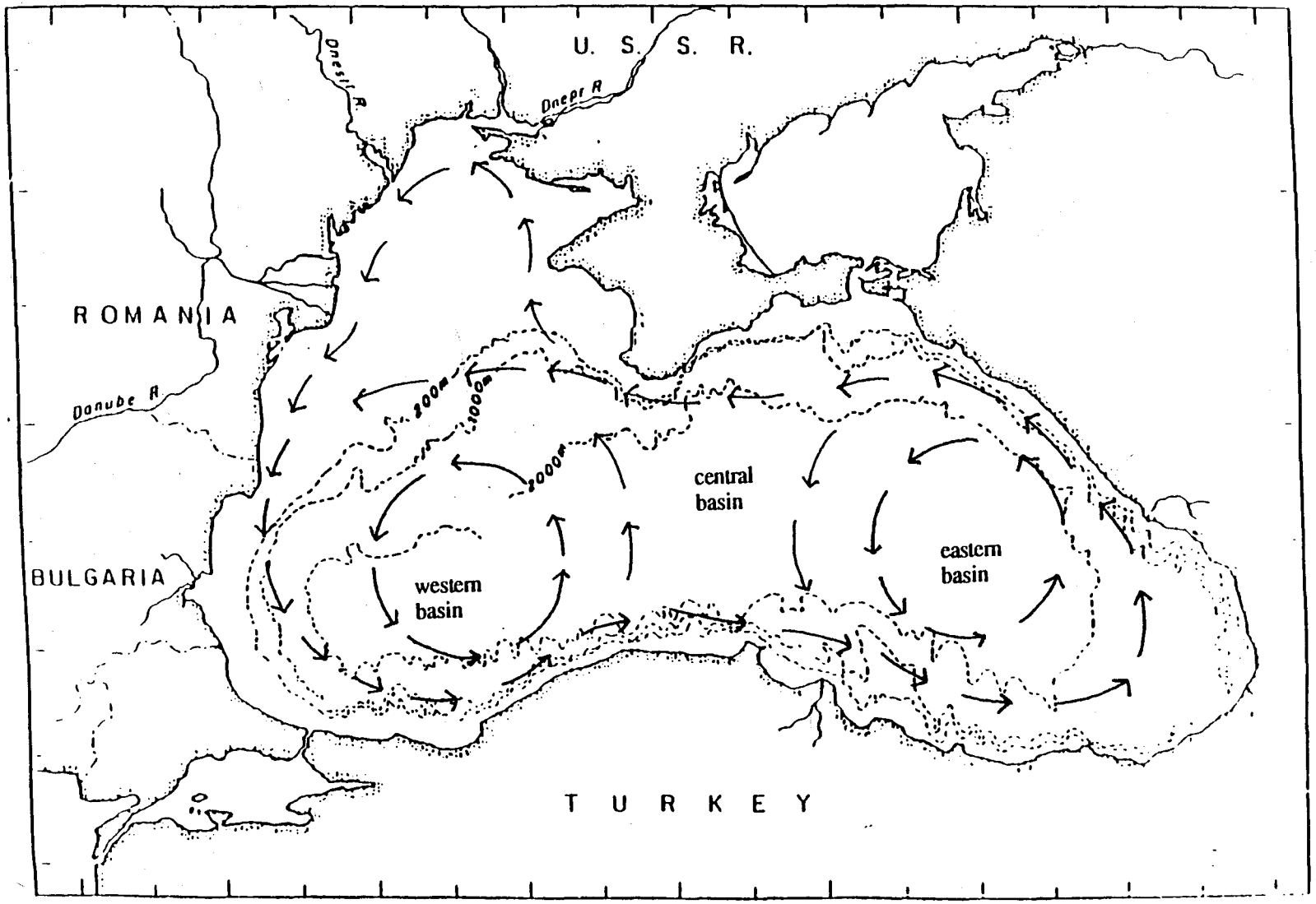

Fig. 1-5 Map showing the location of the Black Sea and the surface currents.
(Ross et al., 1974)

of between 32 and 34 m (Gunnerson and Ozturgut, 1974). This sill restricts the flow of water into and out of the Black Sea basin.

The Black Sea basin consists of a narrow shelf averaging only 20 km wide and 100 m deep (Ross *et al.*, 1974). Only west of the Crimea, where the Danube, Dnestr, Bug, and Dnepr Rivers enter the Black Sea, does the shelf become 190 km wide. The basin slope is steep down to depths of 2000 m, and then levels out into the Abyssal Plain with a maximum depth of 2206 m (Ross *et al.*, 1974). The basin is generally divided into two regions, the eastern and western basins, with the Danube Fan occupying much of the western basin. The eastern basin is connected to the Sea of Azov, which lies to the north, via the 5 m deep Kerch' Strait.

Of the water entering the Black Sea, 75% is fresh, entering from rivers and precipitation (Shimkus and Trimonis, 1974). The only inflow of saline water is from the Mediterranean Sea, flowing over the sill at the Straits of Bosphorus (Scholten, 1974; Sorokin, 1983). Water exits the Black Sea through evaporation and through surface outflow also at the Straits of Bosphorus. Due to the salinity differences between the surface Black Sea water and Mediterranean Sea Deep Water, Mediterranean Deep Water flows into the Black Sea beneath the outflow of Black Sea surface water (Fig. 1-6). At the interface between these two opposite flowing water bodies, mixing and entrainment occurs so that the salinity of the Mediterranean Deep Water which arrives in the Black Sea is greatly reduced, but is still much higher than Black Sea surface waters. The saline water entering the Black Sea flows down into the basin and mixes with Black Sea bottom waters (Stanev, 1990).

The surface layer of the Black Sea water column can be divided into four layers: mixed layer, seasonal thermocline, cold intermediate layer, and permanent halocline (Stanev, 1989, 1990). The upper three layers are oxic and the permanent halocline marks the beginning of the permanently anoxic basin. The cold intermediate layer persists throughout the year from 50 - 70 m (Stanev, 1989), and deep Black Sea water exists below 300 m (Stanev, 1990). Surface water circulation of the Black Sea can be divided into two gyres surrounded by the main gyre which follows the continental slope (Stanev, 1990). Cyclonic currents are driven by wind stress. Density in the Black Sea is determined predominantly by salinity and not temperature, and in the western gyre which has more intense circulation than the eastern gyre, the halocline shoals to a shallower depth than in the eastern gyre (Stanev, 1990). Increased wind forcing in winter causes increased shoaling of the halocline in the gyre centers and corresponding sinking along the basin edges. The cold intermediate layer forms through winter cooling in the northwestern Black

Sea and sinks until it reaches water of the same density. It then spreads out across the basin (Stanev, 1990), helping to maintain the stratification of the Black Sea water column.

The water column of the Black Sea is stratified due to the large salinity and temperature differences between surface and deep waters (Fig. 1-6). The surface water is oxygenated and of low salinity: 18.33‰ increasing to 21.09‰ at 100 m (Murray *et al.*, 1989). The salinity then slowly increases to 22.22‰ at 2050 m (Murray *et al.*, 1989). The combination of a strong thermocline with a strong halocline creates a pycnocline which prevents, or greatly reduces mixing of oxygenated surface waters with anoxic water below the pycnocline. The inflow of Mediterranean Deep Water into the Black Sea does not supply enough oxygen to maintain oxygenated conditions in the deep basin, and therefore the pycnocline of the Black Sea also causes there to be an H_2S chemocline in which the water above is oxygen rich and the water below is oxygen depleted.

The surface of the chemocline is dome-shaped, being shallower in the center of the basin and deeper along the shelves. Of the Black Sea's 523,000 km^3 of water, 80-90% are anoxic (Deuser, 1974; Sorokin, 1983). In June, 1988, oxygen decreased from approximately 300 μM in at the surface to less than 5 μM by 55 m in the central part of the western basin, and a suboxic zone existed between 55 and 95 m with sulfide appearing at 95 m (Murray *et al.*, 1989). This represent a shallowing of the chemocline from April, 1969 conditions, but this may not represent a continuous upward movement in the depth of the chemocline since there is evidence that the surface of the chemocline shifts up and down over time (Bryantsev et al., 1988; Kempe *et al.*, 1990). When the concentration of H_2S is plotted against density, the isopycnal surface where H_2S goes to zero is the same in 1969, 1988, and in 1991 (Tugrul *et al.*, 1992). Comparisons of nutrient data for 1969, 1988, and 1992, suggests that the net upward movement of the depth at which oxygen conditions become suboxic may be due to eutrophication and changes in the Black Sea ecosystem since 1975 (Tugrul *et al.*, 1992).

The entire aerobic ecosystem of the Black Sea must exist in the surface waters. The photic zone supports a rich community of phytoplankton. At times and locations where the chemocline intersects the photic zone, brown sulfur bacteria grow (Simpson and Repeta, 1988; Repeta *et al.*, 1989) and contribute to primary production (Karl and Knauer, 1991). Primary production is highest along the coasts and in the central basin, and lowest in the centers of the eastern and western basins (Shimkus and Trimonis, 1974; Sorokin, 1983; Izdar *et al.*, 1987). The cycle of phytoplankton species succession is well characterized. This cycle follows the cycle of primary production. There are two major phytoplankton blooms, the first, and largest bloom occurs in February to April and the second, smaller bloom, in August to September (Sorokin, 1983; Benli, 1987). Production may reach 1-3

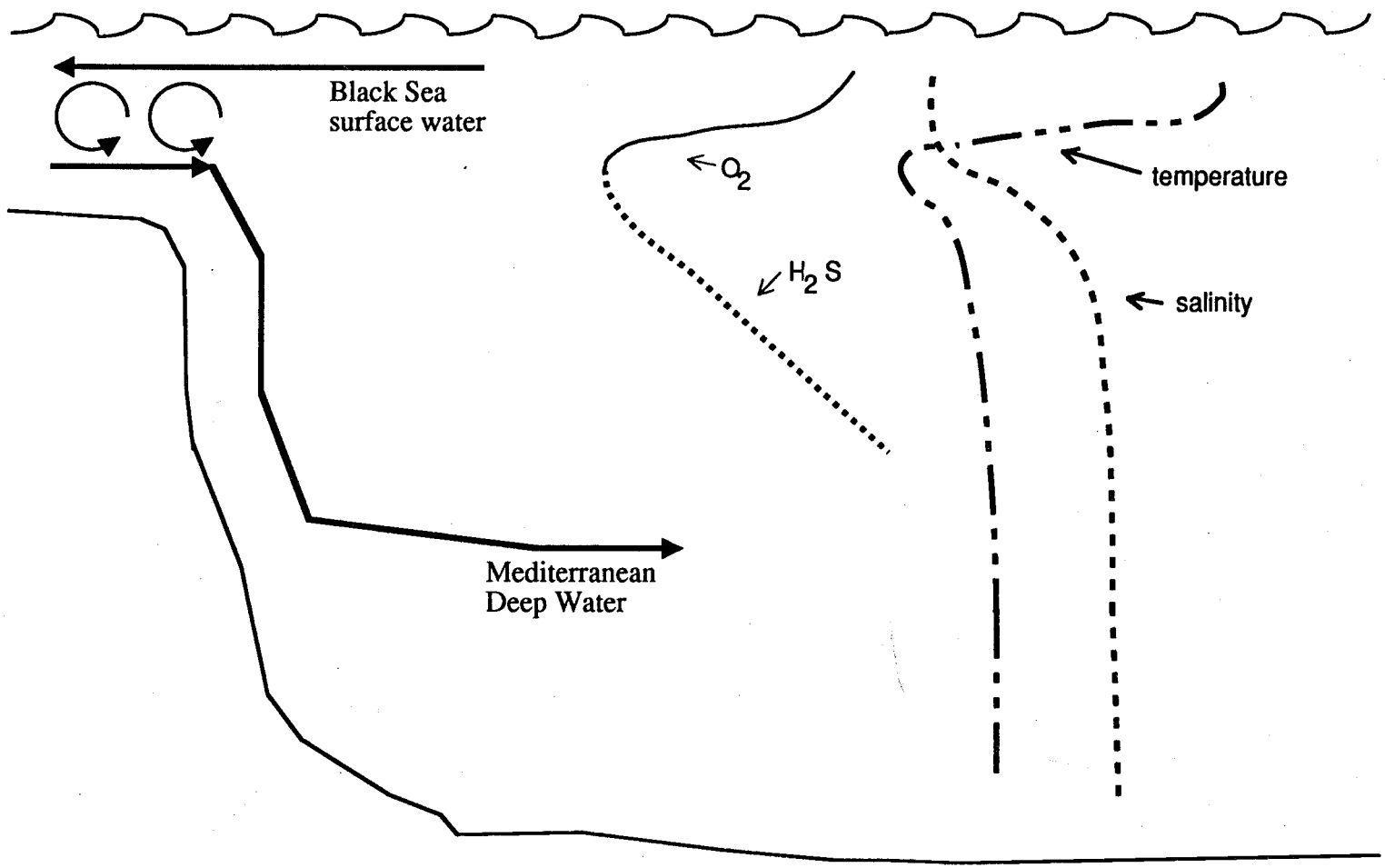

Fig. 1-6 Schematic representation of the water flow into the Black Sea and some of the properties of the water column.

$gC/m^2/d$ in the late winter/early spring and 1 $gC/m^2/d$ in the fall (Sorokin, 1983). The most abundant phytoplankton species in the Black Sea are diatoms and dinoflagellates (Benli, 1987). These are also the most abundant species in the spring bloom. In the fall bloom, coccolithophorids are the dominant species (Honjo *et al.*, 1987; Benli, 1987).

The cycle of primary production drives the flux of components through the water column, but total flux is also influenced by turbidity currents and lateral mixing. A five-year biweekly sediment trap study at two depths at a station near the Turkish coast in the western basin found the flux at 1200 m to be greater than at 250 m due to input of resuspended material (Hay et al., 1990). Whether this increase in flux with depth is common throughout the Black Sea or is caused by the location of the sediment traps near the coast is unclear. The flux of biogenic components is driven by the phytoplankton species inhabiting the photic zone, with the biogenic silica flux increasing in spring when diatoms are in bloom, and the carbonate flux increasing in the fall when coccolithophorids are in bloom (Honjo *et al.*, 1987; Hay, 1987; Hay *et al.*, 1990). The flux of lithogenic components reaches a maximum in early winter (Honjo *et al.*, 1987). In winter, approximately 50% of sediment trap material is estimated to be lithogenic. Winter storms also resuspend material deposited on the shelves and transport it off shore where it is redeposited (Honjo *et al.*, 1987). Resuspended material may be composed of biogenic silica and carbonate as well as terrigenous material introduced by rivers.

The components of the total flux falling through the water column are deposited in sediments. Since the bottom water and sediments are anoxic, the sediments are not bioturbated (Fig. 1-7). The surface sediment is made up of two layers of unconsolidated material, the fluff and floc layers. The floc layer resides above the fluff layer and contains organic compounds chemically distinct from the fluff layer (Beier *et al.*, 1991). To account for the higher concentrations of reduced compounds in the fluff compared to the floc, Beier *et al.* (1991) suggested that a bacterial community resides between the two layers. Microbial mats on the surface of the fluff layer were observed during box core collection on the 1988 Black Sea expedition (Honjo and Broda, 1988).

The sediments below the fluff layer consist of distinct lithologic units which can be correlated throughout the Black Sea. Only the upper two units were deposited in the Holocene. Unit I, the uppermost unit, is made of laminated dark and light bands, and Unit II is a sapropel (Ross *et al.*, 1970; Ross and Degens, 1974; Degens and Stoffers, 1980). Unit III is a calcareous clay deposited during the last glacial maximum (Ross *et al.*, 1970; Ross and Degens, 1974; Degens and Stoffers, 1980). The source of the laminations in Unit I is uncertain but the light bands consist almost exclusively of tests of the coccolithophore *Emiliania huxleyi* (Bukry *et al.*, 1970), and it is currently felt that $CaCO_3$

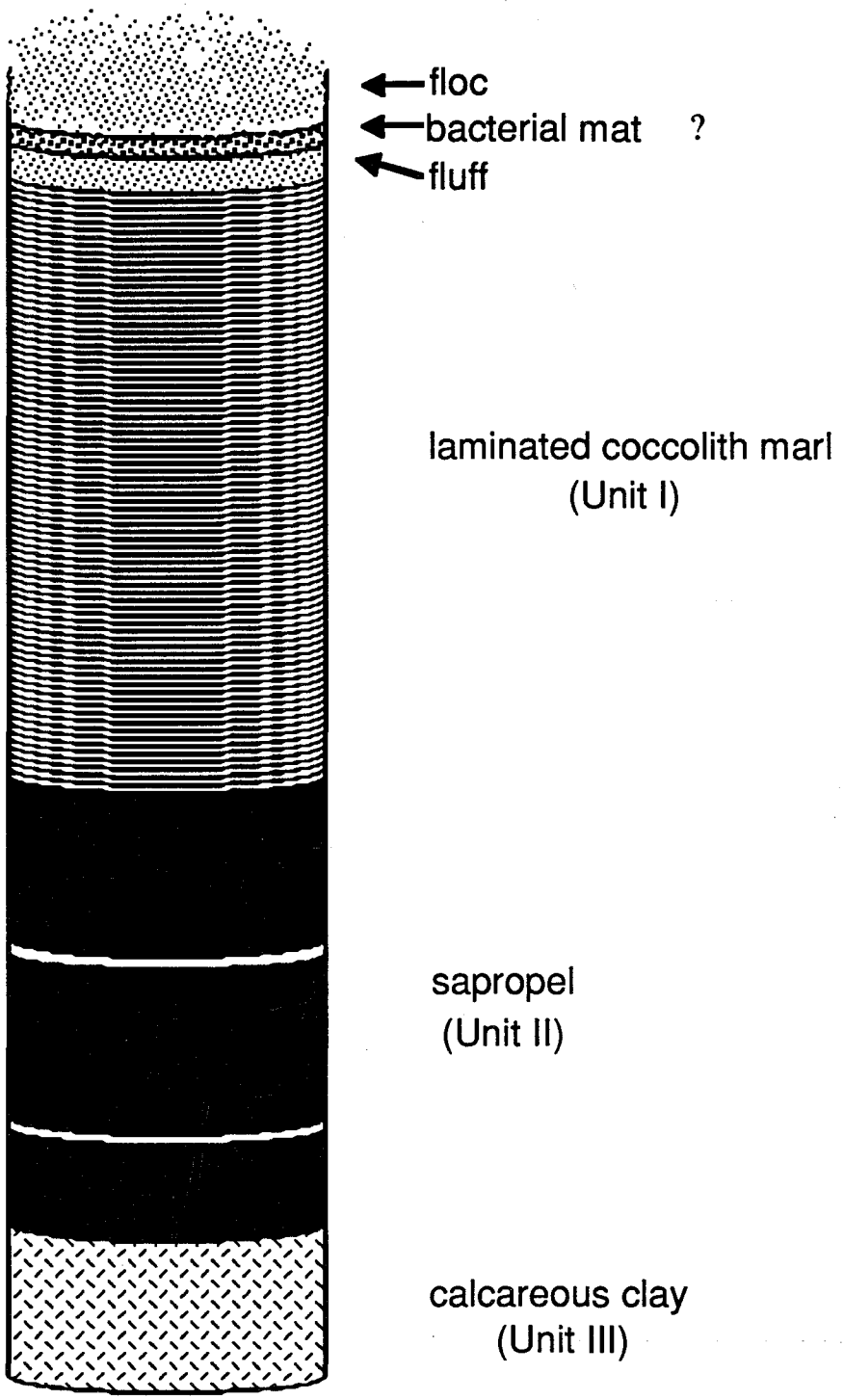

Fig. 1-7 Schematic representation of Black Sea sediments.

is deposited in pulses against a constant background of material, mostly clays, making up the dark bands (Hay, 1988). Total organic carbon (TOC) in Unit I averages 4% and is fairly constant over the length of the sedimentary sequence (Calvert and Fontugne, 1987; Hay, 1988; Calvert *et al.*, 1991). Detailed measurements of the concentration of sedimentary organic carbon in the very surface sediments reveals that there is a surface maximum in TOC (Honjo and Broda, 1988; Calvert *et al.*, 1991; Lyons, 1991). Surface TOC is approximately twice the average Unit I value suggesting that rapid remineralization of total organic carbon is occuring in Black Sea surface sediments. Calcium carbonate in Unit I varies between 15 and 30% (Calvert and Fontugne, 1987). In Unit II, total organic carbon varies between 10 and 15% and calcium carbonate is fairly constant at about 10% (Calvert and Fontugne, 1987). There is much dispute about the age of the interface between Unit I and Unit II, but radioisotope measurements place the age of the boundary at between 1600-3000 yrs (Jones, 1990; Calvert *et al.*, 1991; Crusius and Anderson, 1992; Jones and Gagnon, 1992). In Unit III, TOC is approximately 1% with $CaCO_3$ reaching 50% (Ross and Degens, 1974). The age of the Unit II/Unit III boundary is between 6600 and 8200 years (Calvert *et al.*, 1991; Jones and Gagnon, 1992).

VI. DISTRIBUTION OF CHLOROPHYLL DEGRADATION PRODUCTS IN THE WATER COLUMN AND SEDIMENTS OF THE BLACK SEA

Very few studies have been made of the distribution of chlorophyll degradation products in Black Sea sediments, and even fewer of chlorophyll degradation products in the Black Sea water column. During the 1988 R/V *Knorr* Black Sea expedition, Repeta and Simpson (1991) analyzed chlorophyll degradation products in suspended and sinking particulate matter in the surface 300 m of the water column. Only chlorophylls were identified in the water column; no pheopigments were found. In examining the distribution of chlorophyll degradation products on suspended particulate matter in the chemocline, Repeta *et al* (1989) isolated a suite of bacteriochlorophylls-*e*, providing the first evidence of bacterial photosynthesis in the Black Sea.

Chlorophyll degradation products in Black Sea sediments were analyzed in cores collected during the 1969 R/V *Atlantis II* expedition, and the 1971 R/V *Chain* cruise to the Black Sea. The concentration of chlorophyll degradation products as determined spectrometrically was found to increase with sediment depth through Units I and II. Below Unit II, the concentration decreased by an order of magnitude (Lorenzen, 1974). In surface sediments, concentrations of total phorbin varied between 400 and 1000 μg/gdw

and increased to over 2000 μg/gdw in Unit II (Lorenzen, 1974). Mass spectrometric and visible spectrometric analysis of total organic extract, fractionated by partitioning into solvents of varying polarity, provided evidence for homologous series of chlorins (Peake *et al.*, 1974) and porphyrins (Peake *et al.*, 1974; Cassagrande and Hodgson, 1976).

Chlorophyll degradation products were also analyzed in samples obtained from Deep Sea Drilling Project Leg 42. All these samples were taken from below Unit II and contained only low levels of tetrapyrrole pigments with concentrations that decreased with depth (Baker *et al.*, 1978). The distribution of porphyrins found in these samples, as determined by mass spectrometry, was different from that of open ocean samples. As well as finding the nickel porphyrins found in marine sediments, copper containing porphyrins were also found in the Black Sea samples (Palmer and Baker, 1978). It was suggested that these copper containing compounds are remnants of terrigenous inputs (Palmer and Baker, 1978).

VII. ORGANIZATION OF THIS THESIS

The objectives of my thesis work are explored in five chapters which each examine a different aspect of chlorophyll degradation and one methods chapter which describes techniques for synthesizing and purifying authentic compounds. Much of the work described required the use of standard compounds for spectroscopic and chromatographic comparisons and for methods development. The methods used to synthesize the authentic standards and to gather spectrographic data, along with the spectroscopic and chromatographic properties of these standards are described in Chapter 2. Each of chapters 3-7 describe chlorophyll degradation from different points of reference and required the development of new techniques relevant to the individual chapters. Chapter 3, "Novel Pyropheophorbide-a Steryl Esters in Black Sea Sediments," describes a series of esters in which pyropheophorbide-*a* is esterified to a variety of sterols. Chapter 4, "High Molecular Weight and Acid Extractable Chlorophyll Degradation Products in Black Sea Sediments," describes chlorophyll degradation products which are incorporated into a macromolecular structure and a structure which can only be extracted from the sediment matrix with strong acid. The research in chapters 3 and 4 was conducted on two samples each consisting of over 200 g of sediment. Sediment trap samples are also analyzed to explore water column degradation of chlorophyll. A detailed study of the sterol distribution in the pyropheophorbide-*a* steryl esters in the sediment trap material is presented in Chapter 5, "Pyropheophorbide-*a* Steryl Esters in Sediment Traps Samples from the Black Sea". The

distribution of all phorbins in sediment trap samples is described in Chapter 6, "A Mass Balance of Chlorophyll Degradation Products in the Black Sea". Also presented in Chapter 6 is a mass balance of chlorophyll degradation in the water column and sediments using the the detailed inventory of sedimentary chlorophyll degradation products carried out in Chapters 3 and 4, in conjunction with the sediment trap data described in Chapter 6. Chapter 7 describes a detailed down-core analysis of chlorophyll degradation products in Unit I and Unit II sediments from the Black Sea and uses the data obtained to build describing ecological changes in the Black Sea over the past 1000 years in the Black Sea. Finally, chapter 8 presents my overall conclusions formed from my four years of work on this project and important areas of future research.

VII. REFERENCES

Baker E. W. and Louda J. W. (1980), Products of chlorophyll diagenesis in Japan Trench sediments, DSDP sites 438, 439, and 440, In: *Initial Reports of the Deep Sea Drilling Project,* **57**: Washington (U.S. Govt. Printing Office), 1397-1408.

Baker E. W. and Louda J. W. (1982), Geochemistry of tetrapyrrole, tetraterpenoid and perylene pigments in sediments from the Gulf of CA: DSDP Leg 64, Sites 474, 477, 479, and 481, and the SIO Guaymas Basin Survey Cruise Leg 3, Sites 10 and 18G, In: *Initial Reports of the Deep Sea Drilling Project,* **64**: Washington (U.S. Govt. Printing Office), 789-814.

Baker E. W. and Louda J. W. (1983), Thermal aspects in chlorophyll geochemistry, In: *Advances in Organic Geochemistry 1981*, 401-421.

Baker E.W. and Louda J.W. (1986) Porphyrins in the geological record. In: Biological Markers in the Sedimentary Record. (R. B. Johns, ed.) , 125-225.

Baker E. W. and Palmer S. E. (1979) Chlorophyll diagenesis in IPOD Leg 47A, Site 397 core samples, In: *Initial Reports of the Deep Sea Drilling Project,* **47A**: Washington (U.S. Govt. Printing Office), 547-551.

Baker E. W., Palmer S. E., and Huang W. Y. (1977) Intermediates and late diagenetic tetrapyrrole pigments, Let 41: Cape Lerde Rise and Basin, In: *Initial Reports of the Deep Sea Drilling Project,* **41**: Washington (U.S. Govt. Printing Office), 825-837.

Baker, E. W., Palmer S. E., and Huang W. Y. (1978) Chlorin and porphyrin geochemistry of DSDP Leg 40 sediments, In: *Initial Reports of the Deep Sea Drilling Project,* **40**: Washington (U.S. Govt. Printing Office), 639-647.

Baker E. W., Palmer S. E., and Parrish K. L. (1976) Tetrapyrole pigments in DSDP Leg 38 sediments, In: *Initial Reports of the Deep Sea Drilling Project,* **38**: Washington (U.S. Govt. Printing Office), 785-789.

Barwise A. J. G. and Roberts I. (1984) Diagenetic and catagenetic pathways for porphyrins in sediments. *Org. Geochem.* **6**, 167-176.

Bathmann U. and Liebezeit G. (1986) Chlorophyll in copepod faecal pellets: Changes in pellet numbers and pigment content during a declining Baltic spring bloom. *Mar. Ecol.* **7**, 59-73.

Bauder C., Ocampo R., Callot H. J., and Albrecht P. (1990) Structural evidence for heme fossils in Messel oil shale (FRG). *Naturwissenschaften* **77**, 378-379.

Beier J. A., Wakeham S. G., Pilskaln C. H., and Honjo S. (1991) Enrichment in saturated compounds of Black Sea interfacial sediment. *Nature* **351**, 642-644.

Benli H. A. (1987) Investigation of plankton distribution in the southern Black Sea and its affect on particle flux. SCOPE/UNEP Sonderband Heft 62, Mitt. Geol.-Palaeont. Inst. Univ. Hamburg, 77-87.

Bianchi T. S., Findlay S., and Fontvieille D. (1991) Experimental degradation of plant materials in Hudson river sediments. I. Heterotrophic transformations of plant pigments. *Biogeochem.* **12**, 171-187.

Bidigare R. R., Kennicutt M. C., and Ondrusek M. E. (1990) Novel chlorophyll-related compounds in marine phytoplankton: distributions and geochemical implications. *Energy and Fuels* **4**, 653-657.

Blumer M., and Rudrum, M. (1970), High molecular weight fossil porphyrins: Evidence for monomeric and dimeric tetrapyrroles of about 1100 molecular weight, *J. Inst. Petr.* **56**, 99-106.

Blumer M. and Snyder W. D. (1967) Porphyrins of high molecular weight in a Triassic oil shale: Evidence by gel permeation chromatography. *Chem. Geo.* **2**, 35-45.

Boreham C. J., Fookes C.J. R., Popp B. N., and Hayes J. M. (1989) Origins of etioporphyrins in sediments: Evidence from stable carbon isotopes. *Geochim Cosmochim Acta* **53**, 2451-2455.

Boreham C J., Fookes C. J. R., Popp B. N., and Hayes J. M. (1990) Origins of etioporphyrins in sediments: 2. Evidence from stable carbon isotopes. *Energy and Fuels* **4**, 658-661.

Brown S. R., Daley R. J., and McNeely R. N. (1977) Composition and stratigraphy of the fossil phorbin derivatives of Little Round Lake, Ontario. *Limnol. Oceanogr.* **22**, 336-348.

Brown S. B. and King R. F. G. J. (1978) The mechanism of haem catabolism. *Biochem J.* **170**, 297-311.

Brown S. B., Smith K. M, Bisset G. M. F., and Troxler R. F. (1980) Mechanism of photooxidation of bacteriochlorophyll *c* derivatives. *J. Bio. Chem.* **255**, 8063-8068.

Bryantsev V. A., Fashchuk D. Y., Ayzatullin T. A., Bagotskiy S. V., and Leonov A. V. (1988) Variation in the upper boundary of the hydrogen sulfide zone in the Black Sea: Analysis of field observations and modeling results. *Oceanology* **28**, 180-185.

Bukry, D., King, S. A., and Horn, M. K. (1970), Geological significance of coccoliths in fine-grained carbonate bands of past glacial Black Sea sediments, *Nature* **226**, 156-158.

Burkhill P. H., Mantoura R. R. C., Llewellyn C. A., and Owens N. J. P. (1987) Microzooplankton grazing and selectivity of phytoplankton in coastal waters. *Mar. Bio.* **93**, 581-590.

Callot H. J., Ocampo R., and Albrecht P. (1990) Sedimentary porphyrins: Correlations with biological precursors. *Energy and Fuels* **4**, 635-639.

Calvert S. E. and Fontugne M. R. (1987) Stable carbon isotopic evidence for the marine origin of the organic matter in the Holocene Black Sea Sapropel. *Chem. Geo.* **66**, 315-322.

Calvert S. E., Karlin R. E., Toolin L. J., Donahue D. J., Southon J R., and Vogel J. S. (1991) Low organic carbon accumulation rates in Black Sea Sediments. *Nature* **350**, 692-695.

Carpenter S. R., and Berquist A. M. (1985) Experimental tests of grazing indicators based on chlorophyll-a degradation products. *Arch. Hydrobiol.* **102**, 303-317.

Carpenter, S. R., Elser M. M., and Elser J. J. (1986), Chlorophyll production, degradation, and sedimentation: Implications for paleolimnology, *Limnol. Oceanogr.* **31**,112-124.

Carpenter S. R., Leavitt P. R., Elser J. J., and Elser M. M. (1988) Chlorophyll budgets: response to food web manipulation. *Biogeochem.* **6**, 79-90.

Casagrande D.J. and Hodgson G. W. (1976) Geochemistry of porphyrins: The observation of homologous tetrapyrroles in a sediment sample from the Black Sea. *Geochim. Cosmochim. Acta* **40**, 479-482.

Chicarelli M. I. and Maxwell J. R. (1984) A naturally occurring, chlorophyll *b* related porphyrin. *Tetrahedron Lett* **25**, 4701-4704.

Chicarelli M.I and Maxwell J.R. (1986) A novel fossil porphyrin with a fused ring system: Evidence for water column transformation of chlorophyll: *Tetrahedron Lett.* **27**, 4653-4654.

Chicarelli M. I., Wolff G. A., Murray M., and Maxwell J. R. (1984) porphyrins with a novel exocyclic ring system in an oil shale. *Tetrahedron* **40**, 4033-4039.

Clayton J. L., and Michael G. E. (1990) Controls on porphyrin concentrations of Pennsylvanian organic-rich shales, Western U.S.A. *Energy and Fuels* **4**, 644-646.

Cole J. J., Honjo S., and Caraco N. (1985) Seasonal variation in the flux of algal pigments to a deep-water site in the Panama Basin. *Hydrobiologia* **122**, 193-197.

Conover R. J., Durvasula R., Roy S., and Wang R. (1986), Probable loss of chlorophyll-derived pigments during passage through the gut of zooplankton, and some of the consequences, *Limnol. Oceanogr.* **31**, 878-887.

Cronin J. R. and Morris R. J. (1982) The occurrence of high molecular weight humic material in recent organic-rich sediment from the Nambian Shelf. *Esturine, Coastal and Shelf Sciences* **15**, 17-27.

Crusius J., and Anderson R. F. (1992) Inconsistencies in accumulation rates of Black Sea sediments inferred from Records of Laminae and ^{210}Pb. *Paleoceanography* **7**, 215-227.

Czeczuga B. (1964) Quantitative changes in sedimentary chlorophyll in the bed sediment of the Mikolajki Lake during the post-glacial period. *Hydrologie* **27**, 88-98.

Daley, R. J., and Brown S. R. (1973), Experimental characterization of lacustrine chlorophyll diagenesis.Physiological and Environmental Affects, *Arch. Hydrobiol*, **72,** 277-304.

Daley R. J., Brown S. R., and McNeely R. N. (1977) Chromatographic and SCDP measurements of fossil phorbins and the postglacial history of Little Round Lake, Ontario. *Limnol. Oceanogr.* **22**, 349-360.

Degens, E. T., and Stoffers, P. (1980), Environmental events recorded in Quaternary sediments of the Black Sea, *J. Geol. Soc. London* **137**, 131-138.

Deuser W. G. (1974) Evolution of anoxic conditions in Black Sea during Holocene, In: The Black Sea--Geology, Chemistry, and Biology, E.T. Degen and D.A. Ross, Eds. Am. Assoc. Petrol. Geol.

Downs, J. N. (1989), Implications of the phaeopigment, carbon and nitrogen content of sinking particles for the origin of export production, Phd thesis, University of Washington.

Downs J. N., and Lorenzen C. J. (1985) Carbon:pheopigment ratios of zooplankton fecal pellets as an index of herbivorous feeding. *Limnol. Oceanogr.* **30**, 1024-1036.

Ertel J. R. and Hedges J. I. (1983) Bulk chemical and spectroscopic properties of marine and terrestrial humic acids, melanoidins and catechol-based synthetic polymers. In *Aquatic and Terrestrial Humic Materials* (Ed. R. F. Christman and E. T. Gjessing). pp 143-163, Ann Arbor Science.

Fawley M. W. (1989) A new form of chlorophyll *c* involved in light-harvesting. *Plant Physiol.* **91**, 727-732.

Fogg G. E. and Belcher J. H. (1961) Pigments from the bottom deposits of an English lake. *New Phycol.* **23**, 129-142.

Fookes C. J. R. (1983) Structure determination of nickel(II) deoxophylloerythroetioporphyrin and a C_{30} homologue from an oil shale: Evidence that petroporphyrins are derived from chlorophyll. *J. Chem. Soc., Chem. Commun.* **1983**, 1472-1473.

Furlong E.(1986), Sediment geochemistry of photosynthetic pigments in oxic and anoxic marine and lacustrine sediments: Dabob Bay, Saanich Inlet, and Lake Washington, Ph.d. thesis, University of. Washington.

Furlong E., and Carpenter S. R. (1988), Pigment preservation and remineralization in oxic coastal marine sediments, *Geochim. Cosmochim. Acta* **52**, 87-100.

Gillan F. T. and Johns R. B. (1980) Input and early diagenesis of chlorophyll in a temperate intertidal sediment. *Mar. Chem.* **9**, 243-253.

Goericke R., and Repeta D. J. (1992) The pigments of *Procloracoccus marinus*: The presence of divinyl chlorophyll *a* and *b* in a marine procaryote. *Limnol. Oceanogr.* **37**, 425-433.

Gorham E. (1961) Chlorophyll derivatives, sulphur, and carbon in sediment cores from two English lakes. *Can. J. Botany* **39**, 333-338.

Guilizzoni F., Bonomi G., Balanit G., and Ruggiu D. (1983) Relationship between sedimentary pigments and primary production: evidence from core analyses of twelve Italian lakes. *Hydorbiologia* **103**, 103-106.

Gunnerson C. G. and Ozturgut E. (1974) The Bosphorus, In: The Black Sea--Geology, Chemistry, and Biology, E.T. Degen and D.A. Ross, Eds. Am. Assoc. Petrol. Geol.

Habermehl G., Springer G., and Frank M. H. (1984) X-ray structure analysis of a nickle petroporphyrin confirms hypothesis of Treibs. *Naturwissenschaften* **71**, 261-263.

Hay, B. J. (1987), Particle Flux in the Western Black Sea in the Present and Over the Last 5,000 years: Temporal Variability, Sources, Transport Mechanisms, Ph.d. Thesis, Massachusetts Institute of Technology and the Woods Hole Oceanographic Institution Joint Program in Oceanography, 201p.

Hay B. J. (1988) Sediment accumulation in the central western Black Sea over the past 5100 years. *Paleoceanogr.* **3**, 491-508.

Hay B. J., Honjo S., Kempe S., Ittekkot V. A., Degens E. T., Konuk T., and Izdar E. (1990) Iterannual variability in particle flux in the southwestern Black Sea. *Deep-Sea Research* **37**, 911-928.

Hayes J. M., Freeman K. H., Popp B. N., and Hoham C. H. (1990) Compound-specific isotopic analyses: A novel tool for reconstruction of ancient biogeochemical processes. *Org. Geochem.* **16**, 1115-1128.

Hayes J. M., Popp B. N., Takigiku R., and Johnson M. W. (1989), An isotopic study of biogeochemical relationships between carbonates and organic carbon in the Greenhorn Formation, *Geochim. Cosmochim.Acta.***53**, 2961-2972.

Hayes J.M., Takigiku R., Ocampo R., Callot H.J., and Albrecht P. (1987), Isotopic compositions and probable origins of organic molecules in the Eocene Messel shale, *Nature* **329**, 48-51.

Honjo S. and Broda J. E. (1988) The first recovery of fluff layer from the Black Sea bottom; onboard observation. In: Temporal and Spatial Variability in Sedimentation in the Black Sea: Cruise Report R/V Knorr 134-8, Black Sea Leg 1. WHOI-88-35. 135-140.

Honjo S., Hay B. J., Manganini S. J., Asper V. L., Degens E. T., Kempe S., Ittekkot V., Izdar E., Konuk Y. T., and Benli H. A. (1987) Seasonal cyclicity of lithogenic particle fluxes at a southern Black Sea sediment trap station. SCOPE/UNEP Sonderband Heft 62, Mitt. Geol.-Palaeont. Inst. Univ. Hamburg, 19-39.

Hunter B. L. and Laws E. A. (1981) ATP and chlorophyll a as estimators of phytoplankton carbon biomass. *Limnol. Oceanogr.* **26**, 944-956.

Hurley J. P. and Armstrong D. E. (1991) Pigment preservation in lake sediments: A comparison of sedimentary environments in Trout Lake, Wisconsin. *Can. J. Fish. Aquat. Sci.* **48**, 472-486.

Izdar, E., Konuk, T., Ittekkot, V., Kempe, S., and Degens, E. T. (1987), Particle flux in the Black Sea: Nature of the Organic Matter, SCOPE/UNEP Sonderband Heft 62, Mitt. Geol.-Palaeont. Inst. Univ. Hamburg, 1-18.

Jen J. J. and Mackinney G. (1970) On the photodecomposition of chlorophyll in vitro -- II. Intermediates and breakdown products. *Photochem. Photobiol.* **11**, 303-308.

Jones G. A. (1990) AMS radiocarbon dating of sediments and waters from the Black Sea: An integrated approach. *EOS* **71**, 152.

Karl D. M. and Knauer G. A. (1991) Microbial production and particle flux in the upper 350 m of the Black Sea. *Deep-Sea Research* **38 suppl. 2**, S921-S942.

Kaur S., Chicarelli, M. I., and Maxwell J. R. (1986) Naturally occurring benzoporphyrins: Bacterial marker pigments? *J. Am. Chem. Soc.* **108**, 1347-1348.

Keely, B. J. (1989), Early diagenesis of chlorophyll and chlorin pigments, Phd thesis, University of Bristol.

Keely, B. J., and Brereton R. G. (1986), Early chlorin diagenesis in a recent aquatic sediment, *Adv. Org. Geo. 1985*, 975-980.

Keely, B. J., Brereton, R. G., and Maxwell, J. R. (1988), Occurrence and significance of pyrochlorins in lake sediment, Advances in Organic Geochemistry 1987, *Org. Geo.*, **13**, 801-805.

Keely, B.J., Prowse, W.G., and Maxwell, J.R. (1990), The Treibs Hypothesis: An evaluation based on structural studies, *Energy Fuels*, **4**, 628-634.

Kempe S., Liebezett S., and Diericks A.-R. (1990) Water balance in the Black Sea. *Nature* **346**, 419.

Kiorboe T., and Tiselius P. T. (1987) Gut clearance and pigment destruction in a herbivorous copepod, *Acartia tonsa*, and the determination of *in situ* grazing rates. *J. Plankton Res.* **9**, 525-534.

Klein B., Gieskes W. C. C., and Kraay G. G. (1986) Digestion of chlorophylls and carotenoids by the marine protozoan Oxyrrhis marina studied by HPLC analysis of algal pigments, *J Plankton Res*, **8**, 827-836.

Laws E. A. and Bannister T. T. (1980) Nutrient- and light-limited growth of *Thalassiosira fluviatilis* in continuous culture, with implications for phytoplankton growth in the ocean. *Limnol. Oceanogr.* **25**, 457-473.

Laws E. A., DiTullio G. R., and Redalje D. G. (1987) High phytoplankton growth and production rates in the North Pacific subtropical gyre. *Limnol. Oceanogr.* **32**, 905-918.

Laws E. A., Redalje D. G., Haas L. W., Bienfang P. K., Eppley R. W., Harrison W. G., Karl D. M., and Marra J. (1984) High phytoplankton growth and production rates in oligotrophic Hawaiian coastal waters. *Limnol. Oceanogr.* **29**, 1161-1169.

Leavitt P. R., and Carpenter S. R. (1990) Regulation of pigment sedimentation by photo-oxidation and herbivore grazing. *Can. J. Fish. Aquat. Sci.* **47**,1166-1176.

Leavitt P. R., and Carpenter S. R. (1990) Aphotic pigment degradation in the hypolimnion: Implications for sedimentation studies and paleolimnology. *Limnol. Oceanogr.* **35**, 520-534.

Lipiner G., Willner I., Aizenshtat Z. (1988) Correlation between geochemical environments and controlling factors in the metallation of porphyrins. *Org. Geochem.* **13**, 747-756.

Lopez M. D. G., Huntley M. E., and Sykes P. F. (1988) Pigment destruction by *Calanus pacificus*: impact on the estimation of water column fluxes. *J. Plank. Res.* **10**, 715-734.

Lorenzen C.J . (1968) Carbon/chlorophyll relationships in an upwelling area. *Limnol. Oceanogr.* **13**, 202-204.

Lorenzen C. J. (1974) Chlorophyll-degradation products in sediments of Black Sea. In: The Black Sea -- Geology, Chemistry, and Biology (E. Degens and D. A. Ross, eds.). *Mem. Am. Assoc. Pet. Geol.* **20**, 426-428.

Louda J. W. and Baker E. W. (1981) Geochemistry of the tetrapyrrole, carotenoid, and perylene pigments in sediments from the San Miguel Gap (Site 467) and Baja California borderland (Site 471), Deep Sea Drilling Project Leg 63. In *Initial Reports of the Deep Sea Drilling Project* (Ed. B. Haq, and R. S. Yeats). Vol. 63, pp. 785-818. U. S. Government Printing Office.

Louda, J. W, and E. W. Baker (1986), The Biogeochemistry of chlorophyll, In: Organic Marine Geochemistry (ed. M. Sohn), ACS Symposium series 305, Chap. 7, p. 107-126. American Chemical Society.

Louda J. W., Palmer S. E., and Baker E. W. (1980) Early products of chlorophyll diagenesis in Janpan Trench sediments of Deep Sea Drilling Project sites 434, 435, and 436, In: *Initial Reports of the Deep Sea Drilling Project*, **56**: Washington (U.S. Govt. Printing Office), 1391-1396.

Lyons T. W. (1991) Upper Holocene sediments of the Black Sea: Summary of leg 4 box cores (1988 Black Sea Oceanographic Expedition). In: Black Sea Oceanography (E. Izdar and J. W. Murray, ed.) NATO ASI Series, Kluwer Academic Publishers, 401-441.

Mackenzie A. S., Quirke J. M. E., and Maxwell J. R. (1980) Molecular parameters of maturation in the Toarcian shales, Paris Basin, France -- II. Evolution of metalloporphyrins. *Adv. Org. Geochem. 1979*, 239-248.

Matile P., Ginsburg S., Schellenberg M., and Thomas H. (1987) Catabolites of chlorophyll in senescent leaves. *J. Plant. Physiol.* **129**, 219-228.

Mayzaud P. and Razouls S. (1992) Degradation of gut pigment during feeding by a subantarctic copepod: Importance of feeding history and digestive acclimation. *Limnol. Oceanogr.* **37**, 393-404.

Murray J. W., Jannasch H. W., Honjo S., Anderson R. R., Reeburgh W. S., Top Z., Friederich G. E., Codispoti L. A., and Izdar E. (1989) Unexpected changes in the oxic/anoxic interface in the Black Sea, *Nature* **338**, 411-413.

Nelson J. R., and Wakeham S. G. (1989) A phytol-substituted chlorophyll *c* from Emiliania huxleyi (Prymnesiophyceae). *J. Phycol.* **25**, 761-766.

Ocampo R., Callot H. J., and Albrecht P. (1985a) Identification of polar porphyrins in oil shale. *J. Chem. Soc., Chem. Commun.* **1985**, 198-200.

Ocampo R., Callot H. J., and Albrecht P. (1985b) Occurrence of bacteriopetroporphyrins in oil shale. *J. Chem. Soc., Chem. Commun.* **1985**, 200-201.

Ocampo R., Callot H. J., and Albrecht P. (1989) Different isotope compositions of C-DPEP and C_{32} Etioporphyrin III in oil shale. *Naturwissenschaften* **76**, 419-421.

Ocampo. R., Callot H. J., Albrecht P., and Kintzinger J. P. (1984) A novel chlorophyll c related petroporphyrin in oil shale. *Tetrahedron Lett.* **25**, 2589-2592.

Orr W. L., Emery K. O., and Grady J. R. (1958), Preservation of chlorophyll derivatives in sediments off Southern California, *Bull. Amer. Assoc. Petrol. Geo.* **42**, 925-958.

Owens T.G., and Falkowski P.G. (1982), Enzymatic degradation of chlorophyll *a* by marine phytoplankton *in vitro*, *Phytochem.* **21**, 979-984.

Owens T.G., Falkowski P.G., and Whitledge T.E. (1980) Diel periodicity in cellular chlorophyll content in marine diatoms. *Mar. Biol.* **59**, 71-77.

Palmer S.E. and Baker E. W. (1978), Copper porphyrins in deep-sea sediments: A possible indicator of oxidized terrestrial organic matter, *Science* **201**, 49-51.

Peake E., Casagrande J., and Hodgson G. W. (1974) Fatty acids, chlorins, hydrocarbons, sterols, and carotenoids from a Black Sea core. In: The Black Sea -- Geology, Chemistry, and Biology (E. Degens and D. A. Ross, eds.). *Mem. Am. Assoc. Pet. Geol.* **20**, 505-523.

Penry D. L., and Frost B. W. (1991) Chlorophyll *a* degradation by *Calanus pacificus*: Dependence on ingestion rate and digestive acclimation to food resources. *Limnol. Oceanogr.* **36**, 147-159.

Popp B. N., Takigiku R., Hayes J. M., Louda J. W., and Baker E. W. (1989) The post-paleozoic chronology and mechanism of 13C depletion in primary marine organic matter. *Am. J. Science* **289**, 436-454.

Poutanen E.-L. and Morris R. J. (1983) The occurrence of high molecular weight humic compounds in the organic-rich sediments of the Peru continental shelf. *Oceanogogica Acta* **6**, 21-28.

Prowse W. G., Keely B. J., and Maxwell J. R. (1990) A novel sedimentary metallochlorin. *Org. Geochem.* **16**, 1059-1065.

Quirke J. M. E., Dale T., Britton E. D., Yost R. A., Trichet J., and Belayouni H. (1990) Preliminary characterization of porphyrins from the Gafsa Basin, Tunisia: Evidence for metal-free benzo porphyrins from an immature sediments. *Org. Geochem.* **15**, 169-177.

Quirke J. J. E., Shaw G. J., Soper P. D., and Maxwell J. R. (1980) The presence of porphyrins with extended alkyl substituents. *Tetrahedron* **36**, 3261-3267.

Repeta D. J. and Simpson D. J. (1991) The distribution and recycling of chlorophyll, bacteriochlorophyll and carotenoids in the Black Sea. *Deep-Sea Research* **38 suppl. 2**, S969-S984.

Repeta D. J., Simpson D. J., Jorgensen B. B., and Jannasch H. W. (1989) Evidence from anoxygenic photosynthesis form the distribution of bacteriochlorophylls in the Black Sea. *Nature* **342**, 69-72.

Ricketts T. R. (1966) Magnesium 2,4-divinylphaeoporphyrin a_5 monomehyl ester, a protochlorophyll-like pigment in some unicellular flagellates. *Phytochem.* **5**, 223-229.

Ross D. A., and Degens E. T. (1974) Recent sediments of the Black Sea, In: The Black Sea--Geology, Chemistry, and Biology, E.T. Degen and D.A. Ross, Eds. Am. Assoc. Petrol. Geol. pp 183-199.

Ross D. A., Degens E. T., and MacIlvaine J. (1970) Black Sea: Recent sedimentary history. *Science* **170**, 163-165.

Ross D. A., Uchupe E., and Bowin C. O. (1974) Shallow structure of the Black Sea, In: The Black Sea--Geology, Chemistry, and Biology, E. T. Degen and D. A. Ross, Eds. Am. Assoc. Petrol. Geol. pp 1-10.

Roy S., Harris R. P., and Poulet S. A. (1989) Inefficient feeding by *Calanus Helgolandicus* and *Temora longicornis* on *Coscinodiscus wailesii*: quantitative estimation using chlorophyll-type pigments and affects on dissolved free amino acids. *Mar. Ecol. Prog. Ser.* **52**, 145-153.

Sakshaug E., Johnson G., Andresen K., and Vernet M. (1991) Modeling of light-dependent algal photosynthesis and growth: experiments with the Barents Sea diatoms *Thalassiosira norkenshioeldii* and *Chaetoceros furcellatus*. *Deep-Sea Res.* **38**, 415-430.

Sato S. (1980) Diagenetic alteration of organic matter in leg 57 sediments, deep sea drilling project. In *Initial Reports of the Deep Sea Drilling Project* (Ed. Scientific Party), Vol. 61-62, pp 1305-1312. U.S. Government Printing Office.

Schoch S., Scheer H., Schiff J.A., Rudiger W., and Siegelman H. W. (1981) Pyropheophytin a accompanies pheophytin a in darkened light grown cells of *Euglena*. *Z. Naturforsch* **36**, 827-833.

Scholten R. (1974) Role of the Bosphorus in Black Sea chemistry and sedimentation. n: The Black Sea--Geology, Chemistry, and Biology, E.T. Degen and D.A. Ross, Eds. Am. Assoc. Petrol. Geol. pp 115-126.

Sharp J. H., Perry M. J., Renger E.H., and Eppley R. W. (1980) Phytoplankton rate processes in the oligotrophic waters of the central North Pacific Ocean. *J. Plank. Res.* **2**, 335-353.

Shimkus L. M. and Trimonis E. S. (1974) Modern sedimentation in Black Sea, In: The Black Sea--Geology, Chemistry, and Biology, E.T. Degen and D.A. Ross, Eds. Am. Assoc. Petrol. Geol. pp 249-278.

Shimomura O (1980) Chlorophyll-derived bile pigments in bioluminescent Euphausids, *FEBS Letters*, **116**, 203-206.

Simpson D. J., and Repeta D. J. (1988) Aneorobic primary production in the Black Sea: The distribution of photosynthetic pigments, *EOS*, **69**, 1241.

Sinninghe Damste J. S., Eglinton T. I., and De Leeuw J. W. (1992) Alkylpyrroles in a kerogen pyrolysiate: Evidence for abundant tetrapyrrole pigments. *Geochim. Cosmochim. Acta* **56**, 1743-1751.

Smith G. D. and Baker E. W. (1974) Chlorophyll derivatives in DSDP leg 22 sediments, *In: Initial Reports of the Deep Sea Drilling Project*, **22**: Washington (U.S. Govt. Printing Office), 677-679.

SooHoo J. B. and Kiefer D. A. (1982a) Vertical distribution of phaeopigments--I. A simple grazing and photooxidative scheme for small particles, *Deep-Sea Res.* **29**, 1539-1551.

SooHoo J. B. and Kiefer D. A. (1982b) Vertical distribution of phaeopigments--II. Rates of production and kinetics of photooxidation. *Deep-Sea Res.* **29**, 1553-1563.

Sorokin Y. I. (1983) The Black Sea. In: Ecosystems of the world 26 -- Estuaries and Enclosed Seas (B. H. Ketchum, ed.). Elsevier, 253-307.

Stanev E. V. (1989) Numerical modelling of the circulation and the hydrogen sulphide and oxygen distribution in the Black Sea. *Deep-Sea Res.* **36**, 1053-1065.

Stanev E. V. (1990) On the mechanisms of the Black Sea circulation. *Earth-Science Reviews* **28**, 185-319.

Swain E. B. (1985) Measurement and interpretation of sedimentary pigments. *Freshwater Biol.* **15**, 53-75.

Treibs A. (1936), Chlorophyll- und Haeminderivate in organischen mineralstoffen, *Angewandte Chemie*, **49**, 682-686.

Tugrul S., Basturk O., Saydam C., and Yilmaz A. (1992) Changes in the hydrochemistry of the Black Sea inferred from water density profiles. *Nature* **359**, 137-139.

Verne-Mismer J., Ocampo R., Callot H. J., and Albrecht P. (1988) Molecular fossils of chlorophyll-*c* of the 17-nor0DPEP series. Structure determination, synthesis, and geochemical significance. *Tetrahedron Lett.* **29**, 371-374.

Verne-Mismer J., Ocampo R., Callot H. J., and Albrecht P. (1990) New chlorophyll fossils from moroccan oil shales. Porphyrins derived from chlorophyll c_3 or a related pigment? *Tetrahedron Lett.* **31**, 1751-1754.

Vernet M. and Lorenzen C. J. (1987), The relative abundance of pheophorbide-a and pheophytin-a in temperate marine waters, *Limnol. Oceanogr*, **32**, 352-358.

Welschmeyer N. A., and Lorenzen C.J . (1984) Carbon-14 labeling of phytoplankton carbon and chlorophyll a carbon: Determination of specific growth rates. *Limnol. Oceanogr.* **29**, 135-145.

Welschmeyer N. A. and Lorenzen C. J. (1985), Chlorophyll budgets: Zooplankton grazing and phytoplankton growth in a temperate fjord and the Central Pacific Gyres, *Limnol. Oceanogr.* **30**, 1-21.

Wetzel R. G. (1970) Recent and postglacial production rates of a marl lake. *Limnol. Oceanogr.* **15**, 491-503.

Yacobi Y. Z., Mantoura R. F. C, and Llewellyn C. A. (1991) The distribution of chlorophylls, carotenoids and their breakdown products in Lake Kinneret (Israel) sediments. *Freshwater Biol.* **26**, 1-10.

Ziegler R., Blaheta A., Guha N., and Schonegge B. (1988) Enzymatic formation of pheophorbide and pyropheophorbide during chlorophyll degradation in a mutant of *Chlorella fusca* SHIHIRA et KRAUS. *J. Plant. Physiol.* **132**, 327-332.

CHAPTER 2

SYNTHESIS OF AUTHENTIC COMPOUNDS and SPECTRAL METHODS

CHAPTER 2

SYNTHESIS OF AUTHENTIC COMPOUNDS AND SPECTRAL METHODS

I. INTRODUCTION

As part of this research project, a variety of analytical methods were developed to isolate, purify, and identify sedimentary chlorophyll degradation products. Authentic chlorophyll degradation products of known structure were synthesized to test and calibrate separation methods. These standards were also used to learn how structural changes affect spectral properties of chlorophyll degradation products, information which was necessary for the identification of unknown compounds. In this chapter, the partial synthesis of authentic chlorophyll degradation products is described, as well as the spectral methods used to analyze and characterize these authentic compounds.

II. METHODS

A. ISOLATION AND SYNTHESIS OF STANDARD COMPOUNDS

The procedures for synthesis of the authentic chlorophyll degradation products used in this research have many aspects in common. All the standards were synthesized from chlorophylls-*a* and -*b* isolated from fresh spinach. The solvents used were Burdrick and Jackson HPLC grade, and immediately prior to use, CH_2Cl_2 and benzene were redistilled under nitrogen over $CaCl_2$ to remove acid, water, and non-volatile contaminants. Distilled water was redistilled from $KMnO_4$. Several types of thin layer chromatography (TLC) plates were used: Whatman PLKC18F (reversed phase, C_{18}) 1000 μm (preparative) and 200 μm (analytical), Merck silica gel 60 250 μm, and Whatman microcrystalline cellulose 250 μm. Prior to their use, all TLC plates were washed in 100% acetone, and the silica gel plates were activated at 250°C for 2 hours. Unless otherwise specified, reversed-phase plates were developed with MeOH, silica gel plates with 30% acetone/hexane, and cellulose plates with 20% acetone/hexane. Once the TLC plates were developed and scraped, the pigment was recovered from the gel by washing with 100% acetone.

Transfer and filtering pipets, chromatographic grade sand, and $NaSO_4$ were each Soxhlet extracted for 24 hours with toluene/MeOH (25/75, v/v), and allowed to air dry. The $NaSO_4$ was further dried for 24 hours at 250°C. The sand and $NaSO_4$ were stored in

a desiccator. As a first step in purifying the authentic compounds, peaks containing the desired compound were isolated by reversed-phase high pressure liquid chromatography (HPLC). The HPLC was performed at a flow rate of 1.5 ml/minute on a 30 x 0.5 cm column packed with 5μ Alltech Absorbosphere C_{18} gel. Sample tubes for nuclear magnetic resonance spectrometry (NMR) were cleaned with HCl/HNO_3 (2/1), rinsed with $KMnO_4$ distilled water, dried at 250°C, and stored in a desiccator. The purity of the standards was checked by NMR (Katz *et al.*, 1966) and comparison of extinction coefficients with literature values (Vernon, 1960; Pennington *et al.*, 1964; Hoffman and Werner, 1966; Jeffrey and Humphrey, 1975; Fuhrhop and Smith, 1975; Watanabe *et al.*, 1985; Keely, 1989). Once purified, the authentic compounds were dissolved in benzene, purged with He, sealed in ampules under He, and stored in the dark at -30°C.

Isolation of chlorophylls-*a* and -*b*

Chlorophylls-*a* and -*b* were isolated from spinach that was obtained fresh, then frozen overnight at -30°C to facilitate cell rupture, and finally crushed to a powder. The pigments were sonic extracted in acetone, and the solvent (water and acetone) decanted and filtered. This procedure was repeated until the extraction solvent was colorless. The extract was concentrated by rotary evaporation, and the residual solution was extracted (3x) with an equal volume of diethyl ether. The ether extracts were combined, washed with distilled water, dried over Na_2SO_4 (anhyd), and evaporated to dryness. Chlorophylls-*a* and -*b* ware isolated from the spinach extract by column chromatography using silica gel (320-345 mesh) eluted with 30% acetone/hexane. The crude chlorophylls were subsequently purified by analytical reversed-phase TLC, followed by HPLC. Using a solvent mixture of 95% $MeOH/H_2O$, chl-*a* eluted in 27 minute, and chl-*b* in 15 minute.

Preparation of pheophytins-*a* and -*b*

Pheophytins-*a* and -*b* were prepared from crude chls-*a* and -*b* by shaking an ether solution of the appropriate chlorophyll with an equal volume of 1N HCl for 15 minutes (Hynninen, 1973). A noticeable color change, from green to brown, signified that demetallation had occurred. The ether was allowed to separate from the aqueous acid which was extracted twice more with ether. The combined ether extracts were washed with $KMnO_4$ distilled water and dried over Na_2SO_4 (anhyd). The crude pheophytins were purified by analytical TLC on silica followed by HPLC. On HPLC, ptn-*a* eluted in 18 minute using a solvent mixture of 20% acetone/MeOH, and ptn-*b* in 15 minute using 10% acetone/MeOH.

Preparation of pheophorbides-*a* and -*b*

Pheophorbides-*a* and -*b* were prepared from purified ptns-*a* and -*b* by shaking an acetone solution of the appropriate pheophytin with an equal volume of concentrated HCl for 15 minute (Hynninen, 1973). The mixture was then allowed to stand 15 minute Distilled water and CH_2Cl_2 were added to the acid solution. Dilution of the acid with water facilitated transfer of the pigment into CH_2Cl_2. The acid solution was extracted twice more with CH_2Cl_2 and the three extracts combined, washed with $KMnO_4$ distilled water, and dried over Na_2SO_4 (anhyd). The individual crude pheophorbides were purified by analytical reversed-phase TLC to remove any unhydrolyzed pheophytin, followed by cellulose TLC to remove contamination introduced by the reversed-phase TLC plates.

Preparation of pyropheophytins-*a* and -*b* and pyropheophorbides-*a* and -*b*

Pyropheophytins-*a* and -*b*, and pyropheophorbides-*a* and -*b* were prepared by dissolving the appropriate pheophytin or pheophorbide in collidine and refluxing under nitrogen for 90 minute (Fuhrhop and Smith, 1975). After allowing the mixture to cool under nitrogen, the collidine was removed by vacuum distillation. The crude pyropheophytins were purified by silica TLC, followed by HPLC (HPLC conditions same as for pheophytins). The crude pyropheophorbides were purified by reversed-phase TLC, followed by cellulose TLC (as for pheophorbides).

Synthesis of Zn pyropheobutin-*a*

Zinc pyropheobutin-*a* (Znppbn-*a*) was synthesized from ppbd-*a* in two steps. First, ppbd-*a* butyl ester was prepared from ppbd-*a* by dissolving the ppbd-*a* in a minimum amount of CH_2Cl_2. To this was added 1.1 equivalents of N,N-dicyclohexylcarbodiimide (DCC), 1.1 equivalents of *n*-butanol, and 0.1 equivalents of dimethylaminopyridine. The reaction mixture was stirred at room temperature overnight under N_2 (Hassner and Alexanian, 1978). The next day, the reaction mixture was diluted with CH_2Cl_2, extracted three times with 0.01N HCl, and then washed with $KMnO_4$ distilled water. Pyropheophorbide-*a* butyl ester was isolated from any unreacted pyropheophorbide by reversed-phase TLC (spectroscopic yield: 51%).

Pyropheophorbide-*a* butyl ester was dissolved in CH_2Cl_2, and saturated zinc acetate in MeOH added. The solution was refluxed under N_2 for 20 minutes (Fuhrhop and Smith, 1975), cooled to room temperature, washed with distilled water, dried, and then purified by silica TLC (30% acetone/hexane), and HPLC (10% water/MeOH) to give pure Zn pyropheobutin-*a*. After TLC, 72% (spectroscopic yield) of the butyl ester was

recovered as Zn(II) pyropheobutin-*a*. The pure Znppbn-*a* was stored dissolved in benzene and sealed under He in ampules frozen at -30°C.

B. SPECTRAL METHODS

All the authentic standards were characterized by visible, nuclear magnetic resonance (NMR), infrared (IR), and mass (MS) spectrometry. By comparing these spectra of the authentic compounds which have known structures, it was possible to learn how changes in molecular structure affect the appearance of the spectra. Comparison of spectra of authentic compounds with those of unknown compounds from samples helped provide details of the molecular structure of the unknown compounds.

In the following section, the methods used for taking visible, NMR, IR, and MS are described. These methods were applied to both the known authentic standards and unknown chlorophyll degradation products uncovered during the course of this research project. By using a consistent set of methods for gathering spectral data, the data was standardized and spectra of unknown compounds were readily comparable.

Visible spectrophotometry

The visible spectrum of each standard in 100% acetone was measured from 350-750 nm using a Varian DMS-200 dual-beam scanning spectrophotometer referenced to 100% acetone. Extinction coefficients were determined by preparing a 10^{-4} M acetone solution of each pigment and measuring its absorption spectrum. The extinction coefficient of each pigment was then calculated for the Soret maximum using the Lambert-Beer Law:

$$A = \varepsilon bc \text{ or } A = \alpha bc$$

where A is the absorbance (AU); ε, the extinction coefficient (L·cm/mole); α, the absorptivity (L·cm/g); b, the pathlength (cm); and c, the concentration (molarity for ε and g/L for α).

Mass Spectrometry

Mass spectral data for the demetallated chlorophyll derivatives were collected on a Finnigan 4500 mass spectrometer. The methane chemical ionization mass spectrum was collected for each non-metallated pigment by applying the pigment dissolved in CH_2Cl_2 to a gold-tipped direct insertion probe. The mass spectrometer source temperature was 100°C, and the probe temperature was heated from ambient to 350°C in one minute. The

ionization potential used was 130eV with the methane pressure set at 0.5 torr. The hydrogen chemical ionization mass spectrum was also collected for each non-metallated pigment. The pigment, dissolved in CH_2Cl_2, was applied to a copper-tipped direct insertion probe. The source temperature was 100±10°C, hydrogen pressure was 0.5 torr, and the filament was at 40 eV. As soon at the probe was inserted, the source was heated at the maximum rate to 350°C.

Liquid secondary ion mass spectra were collected for chlorophyll-*a* and chlorophyll-*b* on a VG AutoSpec Q mass spectrometer in the magnetic scan mode. The sample was dissolved in acetone with 0.5% *m*-nitrobenzyl alcohol added as matrix and introduced into the mass spectrometer using a VG dynamic FAB probe and ionized using a cesium ion gun.

Infrared spectrometry

Infrared data for each pigment were collected on a Mattson Sirius 100 FTIR. Data were collected from neat samples prepared by evaporating a concentrated CH_2Cl_2 solution of the pigment on a NaCl plate. The NaCl plate was then placed in the IR beam, and the optics bench was sealed and purged with dry air to remove interfering H_2O and CO_2 from the optics. Two hundred fifty six scans of each sample were gathered from 4000 to 500 cm^{-1} at 2 nm resolution using a MCT detector. The spectra were referenced to a clean NaCl plate.

Nuclear Magnetic Resonance spectrometry

The proton nuclear magnetic resonance (NMR) spectrum of each pigment was collected on a Bruker AC300 300 MHz NMR either in deuterated acetone (C_3D_6O, 100 atom % D), or deuterated benzene (C_6D_6, 100 atom % D). All chemical shifts for the spectra were reported using the δ convention referenced to the solvent absorption signal. Benzene and acetone were assigned chemical shifts of 7.4 ppm and 2.2 ppm, respectively. It was sometimes necessary to perform a background subtraction to remove impurities introduced by the deuterated solvent. The presence of the impurities in the solvent was confirmed by the supplier (Aldrich).

III. RESULTS AND DISCUSSION

In the infrared, nuclear magnetic resonance, and mass spectra of the ten authentic compounds analyzed, clear differences exist between the chl-*a* and chl-*b* series phorbins, as well as subtle differences between each of the compounds in a given series. The tabulated data (Tables 2-1 to 2-5) from the spectral analyses are presented in the following discussions along with representative spectra. The complete NMR, IR, MS, and visible spectra of the individual compounds appear in Appendix I.

A. VISIBLE SPECTROPHOTOMETRY

The visible spectra of phorbins all exhibit similar features. Each spectrum has two main bands in the visible region. The shortest wavelength band, known as the Soret band, has the largest absorption intensity and occurs in the region of 350 - 450 nm. The specific wavelength of the Soret band is compound specific. The second main band occurs in the region of 650 nm and is known as the "red band". This band has a much lower absorption intensity than the Soret band. The ratio of absorbance intensities for the Soret/red band is between 1-2 for metallated phorbins, 2-5 for chlorins and phorbins, and 5 - 10 for porphyrins (Baker and Louda, 1986). Three weaker bands occur between the Soret and red bands. The position and intensity of these bands depend on the specific structure of the compound. For the compounds discussed in this study, the arrangement of these minor bands are similar.

The visible spectra from 350-750 nm, in acetone, of each of the authentic compounds display features which are easily comparable (Table 2-1, Fig. 2-1, and Appendix I). The main differences between the visible spectra of the chlorophylls and pheopigments under study occur between the spectra of metallated and non-metallated compounds, and between the spectra of the *a* and *b* series pigments. These differences are in the wavelength of maximum absorbance and in the intensity ratios of the Soret and red bands. A theoretical description of the origin of the absorptions in the visible region of chlorophyll degradation products will not be presented here, but rather an explanation of the variations in the absorption wavelengths and intensities. The differences between each member of the chlorophyll-*a* and its corresponding chlorophyll-*b* series pigment are the same. Structural changes which affect the conjugation of the macrocycle or which affect a functionality conjugated to the macrocycle give rise to changes in the visible spectra of

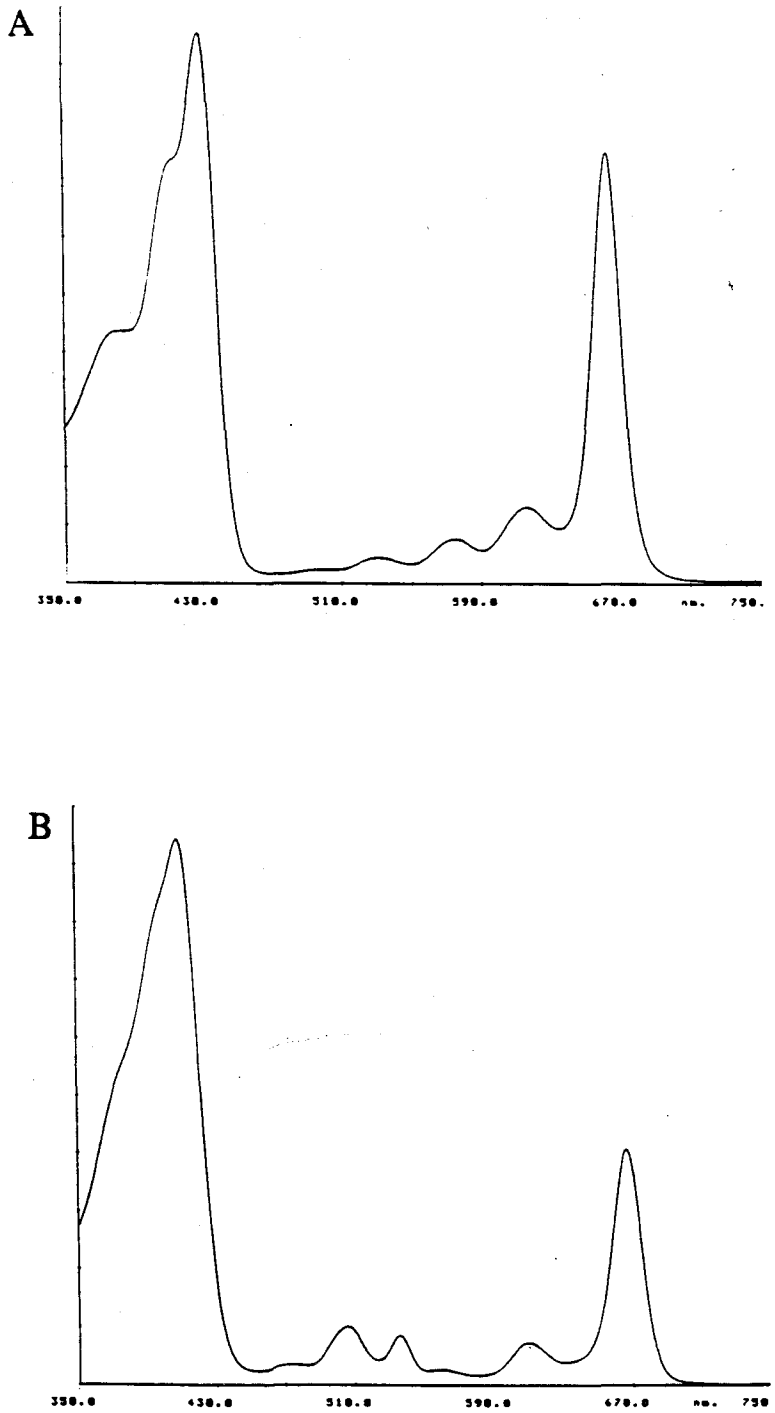

Fig. 2-1 The visible spectra of (a) chlorophyll-*a* and (b) pheophytin-*a* in 100% acetone.

Table 2-1

VISIBLE ABSORBANCE DATA FOR THE CHLOROPHYLLS AND THEIR DERIVATIVES

	MW(g)	α(l/g·cm)* this work	α(l/g·cm)* Keely,1989	ε(l/mole·cm)*	S/R**	λmax	major bands in spectra, nm (α, l/g·cm)
chl-*a*	893.50	112	101	1.00×10^5	1.26	429.1	429.1 (112), 529.8 (4.9), 574.3 (8.5), 614.8 (15.3), 661.8 (89.0)
ptn-*a*	871.21	116	120	1.01×10^5	2.22	409.3	409.3 (111), 505.0 (11.6), 534.7 (9.7), 609.0 (8.2), 665.9 (50.0)
pptn-*a*	813.18	128	121	1.04×10^5	2.27	410.2	410.2 (128), 506.7 (12.7), 535.6 (10.1), 609.0 (8.7), 666.7 (56.3)
pbd-*a*	592.69	128	162	7.55×10^4	2.39	410.2	410.2 (128), 505.0 (14.7), 534.7 (12.5), 609.8 (10.3), 665.9 (53.6)
ppbd-*a*	534.66	211	195	1.13×10^5	2.26	410.2	410.2 (211), 506.7 (22.2), 535.6 (17.7), 609.0 (15.3), 666.7 (93.5)
chl-*b*	907.49	145	109	1.32×10^5	2.94	455.5	455.5 (145), 550.4, 595.8(10.8), 645.3 (49.3)
ptn-*b*	885.20	176	129	1.55×10^5	5.04	434.9	434.9 (176), 526.5 (13.6), 599.1 (9.2), 653.5 (34.9)
pptn-*b*	827.16	140	28	1.16×10^5	4.24	435.7	435.7 (140), 527.3 (12.1), 599.9, 654.4 (26.7)
pbd-*b*	606.68	212	127	1.29×10^5	4.92	434.9	434.9 (212), 525.7 (19.9), 598.3 (14.2), 653.5 (43.1)
ppbd-*b*	580.64	210		1.22×10^5	5.18	435.7	435.7 (210), 538.1 (22.5), 599.9, 654.4 (40.5)

*α and ε are for the Soret band

**the ratio of absorbances of the Soret and red bands

chlorophyll degradation products. Structural changes which cause changes in the three dimensional structure of the phorbin macrocycle also cause variations in the visible spectra.

The wavelengths of maximum absorbance for the Soret and red bands are different for the visible spectra of chl-*a* and chl-*b* , and the ratios of the absorbance intensity of the Soret to red band (S/R ratio) also vary. In chl-*b*, the aldehyde group on C-3 acts to lengthen the conjugated system as compared to that of chl-*a*, which has a methyl group on C-3. The visible spectra of phorbins and porphyrins are explained through a HOMO-LUMO molecular orbital theory (Gouterman, 1961; Hoff and Amesz, 1991), in which the highest occupied molecular orbitals (HOMO) and the lowest unoccupied molecular orbitals (LUMO) of porphyrins are degenerate. Therefore, the transitions which account for the visible bands in the spectrum are forbidden and their absorption is of low intensity (The Soret band is considered in most discussions to occur in the UV). Any change in the π system of the macrocycle which places the two HOMO at different energy levels, makes the red band transition allowed and thus increases the intensity of this band. The greater the energy difference between the two HOMO, the greater the intensity of the red band (Gouterman, 1961). In phorbins, in which ring IV is reduced, the energy of one HOMO and one LUMO in increased, relative to the situation in porphyrins, through reduced electron density, and the red band absorbance becomes allowed (Gouterman, 1961). The aldehyde group at C-3 in chl-*b*, brings the two HOMO closer in energy relative to chl-*a*, and therefore reduces the intensity of red band absorption (Hoff and Amesz, 1991). Insertion of a metal into the ring also splits the energy levels of the HOMO (Gouterman, 1961), and explains the difference in intensity of red band absorption between the chlorophylls and their associated pheopigments. Any change in the energy levels of one HOMO and one LUMO, will change the energy gap between the HOMO and LUMO and produce the observed changes in the absorbance wavelength of both the Soret and red bands (Gouterman, 1961; Hoff and Amesz, 1991).

The differences between the spectra of the pheopigments and their parent chlorophylls follow the same trends for the *a* and *b* series pigments. The most pronounced effect upon demetallation is the shift in the Soret band to shorter wavelengths and the red band to longer wavelengths. The π electrons of the Mg atom found in the center of the chlorophylls are conjugated with the π electrons of the macrocycle, reducing the energy of the a_{2u} HOMO. The increase in the length of the conjugated system shifts the absorption wavelength of the Soret band to lower energies, and reduces the degeneracy of the two HOMO, which increases the intensity of absorbance of the red band (Gouterman, 1961). The change in the fine structure of the spectra seen between the chlorophylls and

pheopigments results from the ability of the macrocycle to flex in the pheopigments (Gouterman, 1961).

B. MASS SPECTROMETRY

In methane chemical ionization mass spectrometry, demetallated derivatives of chlorophyll-*a* and -*b* fragment in a specific manner which makes it possible to determine if a compound has a phytyl group esterified to the C-7 propionic acid, and if it has a carbomethoxy group at C-10. This information is conveyed by the appearance or absence of an ion. The pseudo-molecular ion occurs in methane CI-MS at one a.m.u. above the nominal molecular weight, and a second ion occurs at 29 a.m.u. above the nominal molecular weight of the molecule analyzed. Fragments of the parent molecule may also possess ions at M+29 a.m.u. Chlorophylls are not stable on the direct insertion probe under the conditions used in this study, and chemical ionization mass spectra could therefore not be collected (the chl-*a* and chl-*b* spectra in Appendix I are FAB spectra). Chlorophyll-*b* derivatives tend to be less stable on the probe than chl-*a* derivatives, and do not give clean mass spectra, therefore the mass spectrum of the chl-*b* derivatives presented in Appendix I are of low quality.

The mass spectra of the eight demetallated authentic compounds studied contain ions which form through similar fragmentation pathways. Each contains a pseudo-molecular ion at 1 a.m.u. (M+1) above the nominal molecular weight of the compound and an ion at 29 a.m.u. (M+29) above the molecular weight (Table 2-2; Fig. 2-2a; Appendix I). The pseudo-molecular ion (M+1) forms when the charged reagent gas (CH_5^+) protonates the sample molecule, and the M+29 ion, characteristic of methane chemical ionization, forms when the sample molecule abstracts $C_2H_5^+$ from the reagent gas. The molecular ion then looses neutral fragments. It is the ions formed from the loss of these fragments which comprise the mass spectrum.

After formation of the molecular ion, the pheophytins and pyropheophytins of both chl-*a* and chl-*b* fragment through loss of the phytyl chain esterified at C-7. The major fragment ion seen in both the pheophytins and pyropheophytins corresponds to the molecular ions of the appropriate pheophorbide and pyropheophorbide. The mass spectra of chlorophyll derivatives also exhibit the loss of 58 a.m.u. This fragmentation represents the loss of the C-10 carbomethoxy group and is known as pyrolysis. The loss of this functional group is shown by the presence of an ion at 813 a.m.u. in the mass spectrum of ptn-*a*. This ion is not seen in the mass spectrum of ptn-*b*, but the lack of the ion may be due to poor spectral quality. The formation of this ion on the direct insertion probe, and not in the gas phase, can be seen in the total ion chromatogram (RIC) of the evolution of

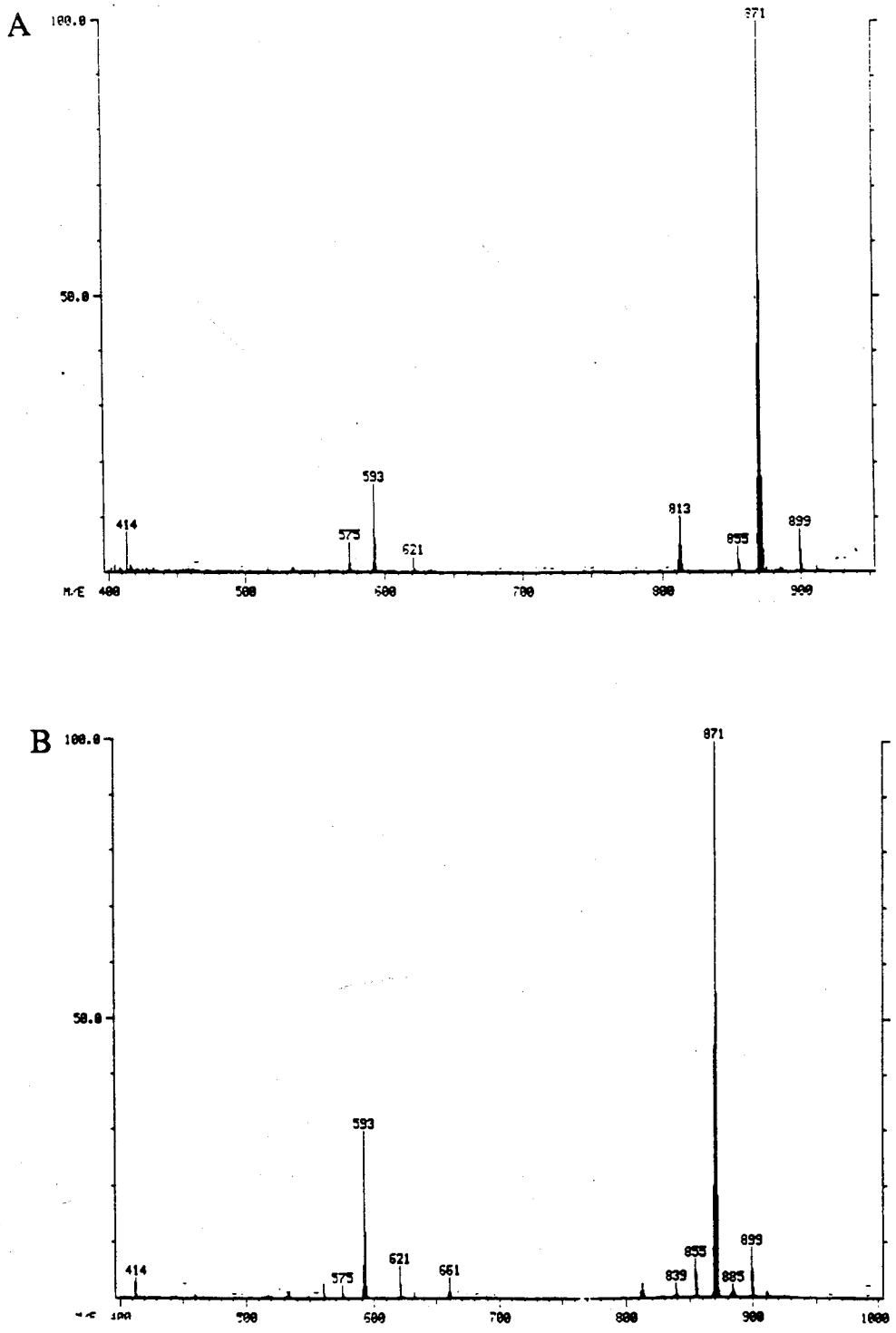

Fig. 2-2 Methane chemical ionization mass spectra of pheophytin-*a* evolved from the (a) gold direct insertion probe, and (b) platinum wire direct insertion probe. Note the different mass range for the two spectra.

Table 2-2

METHANE CHEMICAL IONIZATION MASS SPECTROMETRIC DATA FOR DERIVATIVES OF CHLOROPHYLL-*A* AND CHLOROPHYLL-*B*

CHLOROPHYLL-*A* DERIVATIVES

	ptn-*a*	pptn-*a*	pbd-*a*	ppbd-*a*
Nom. mol. wt.	870	812	592	534
M+1	871	813	593	535
M+29	899	841	621	563
M+1-16	855	797		
M+1-H_2O			575	517
M+1-$COOCH_2$	813			
M+1-phytol	593	535		
M+29-phytol	621	563		
M+1-phytol-H_2O	575	517		

CHLOROPHYLL-*B* DERIVATIVES

	ptn-*b*	pptn-*b*	pbd-*b*	ppbd-*b*
Nom. mol. wt.	884	826	606	548
M+1	885	827		549
M+29	901	855		577
M+1-16		811		
M+1-$COOCH_2$				
M+1-phytol	607	549		
M+29-phytol		577		

the MS of ptn-*a* on the gold tipped probe. In the RIC of ptn-*a* on the gold-tipped probe, the peaks for masses 813 and 871 do not co-occur, indicating that the ions with mass 871 and 813 are not formed at the same time. Additional evidence for this reaction occuring on the gold-tipped probe in the mass spectrum of ptn-*a* comes from comparing the mass spectrum of ptn-*a* on the gold probe to that on the platinum wire probe (DCI probe) (Fig. 2-2). The

lower 813/871 ratio seen in the mass spectra of ptn-*a* from the platinum wire versus that of the gold probe may be due to the much faster heating rate of the platinum wire versus the solid gold probe (Frew *et al.*, 1988). The study by Baker (1970) suggests that chlorophyll derivatives pyrolyze upon prolonged exposure to source temperatures of 300°C.

C. INFRARED SPECTROMETRY

The IR spectra of the chlorophylls and their derivatives exhibit many differences and similarities. The spectra all exhibit the same basic pattern of peaks with variations caused by changes in the side chain substituents. Each spectrum has absorbances for the vinylic C-H stretch between 3000 and 3080 cm^{-1}, for aliphatic C-H stretching between 2950 and 2850 cm^{-1}, for C=O stretching between 1730 and 1670 cm^{-1}, and for C=C stretching between 1600 and 1620 cm^{-1}. The chl-*b* series pigments, which have an aldehyde group at C-3, also exhibit bands for an aldehyde C-H stretch at 2730 cm^{-1}. Within each pigment series, a reduction in the absorbance in the C-H stretching region is seen when comparing the phytyllated with the dephytyllated species (Table 2-3, Fig. 2-3, and appendix I). In the following paragraphs, only absorptions arising from general functionalities are described; the fingerprint region of the spectra is not discussed.

The major absorbances in the infrared spectra of the synthetic chlorophyll degradation products occur in the region 2750 - 3080 cm^{-1}. The main band, from 2850 - 2950 cm^{-1}, is caused by the aliphatic C-H stretching absorption of the methyl and methylene groups of the side chains. The four acidic compounds, pbd-*a*, ppbd-*a*, pbd-*b*, and ppbd-*b* show reduced intensity of this band, as compared with the chlorophylls and pheophytins, due to the loss of the C-H stretching absorbances in the phytyl ester. The absorbances in the aliphatic region of the infrared spectrum appear as 3 bands. Of these, the highest frequency band, appearing in the region of 2950 cm^{-1} is due to the asymmetric C-H stretching vibration of the methyl groups (Houssier and Sauer, 1969). The most intense of the aliphatic bands (2923 - 2925 cm^{-1}) is due to the asymmetric C-H stretching mode of the methylene groups (Houssier and Sauer, 1969). The lowest frequency aliphatic band which appears in each of the compounds studied occurs from 2850 - 2860 cm^{-1} and is caused by the overlap of the symmetric stretching of the methyl and methylene groups (Houssier and Sauer, 1969). The IR spectrum of each of the ten pigments studied also contains one absorption between 3010 - 3080 cm^{-1} due to vinyl C-H stretching.

Of the ten chlorophyll derived compounds studied, four are acidic. In the C-H stretching region of the IR spectra, these four compounds differ from those of the non-acids due to the lack of the C-H stretching absorbances contributed by the phytyl chain in the structure of the phytyllated compounds. The acidic compounds studied have a greatly

Table 2-3

INFRARED ABSORBANCE MAXIMA FOR CHLOROPHYLL DERIVATIVES

CHLOROPHYLL-*A*

	chl-*a*	ptn-*a*	pptn-*a*	pbd-*a*	ppbd-*a*
N-H		3400[1]	3400	3400	3400
vinyl C-H	3080	3096	3017	3011	3053
aliphatic C-H	2950	2950	2950	2957	2960
	2923	2925	2924	2923	2924
	2851	2856	2850	2853	2858
C=O	1733	1739	1731	1737	1725
	1717	1717	1694	1693	1691
	1698	1693		1668	
C=C (chlorin band)	1604	1617	1618	1618	1618

CHLOROPHYLL-*B*

	chl-*b*	ptn-*b*	pptn-*b*	pbd-*b*	ppbd-*b*
N-H		3400	3400	3400	3400
vinyl C-H	3004	3044	3014	3008	n.d.[2]
aliphatic C-H	2951	2953	2953	2921	2954
	2924	2925	2925	2862	2922
	2852	2853	2854	n.d.	2851
aldehyde C-H	2750	2726	2725	2732	2726
C=O	1733	1734	1733	1733	1733
	1717	1706	1699	1700	1699
	1699	1662	1662	1684	1654
	1664	n.d.		1675	
C=C (chlorin band)	1604	1619	1621	1621	1618

[1]all values are in wavenumbers (cm^{-1})
[2]not determined

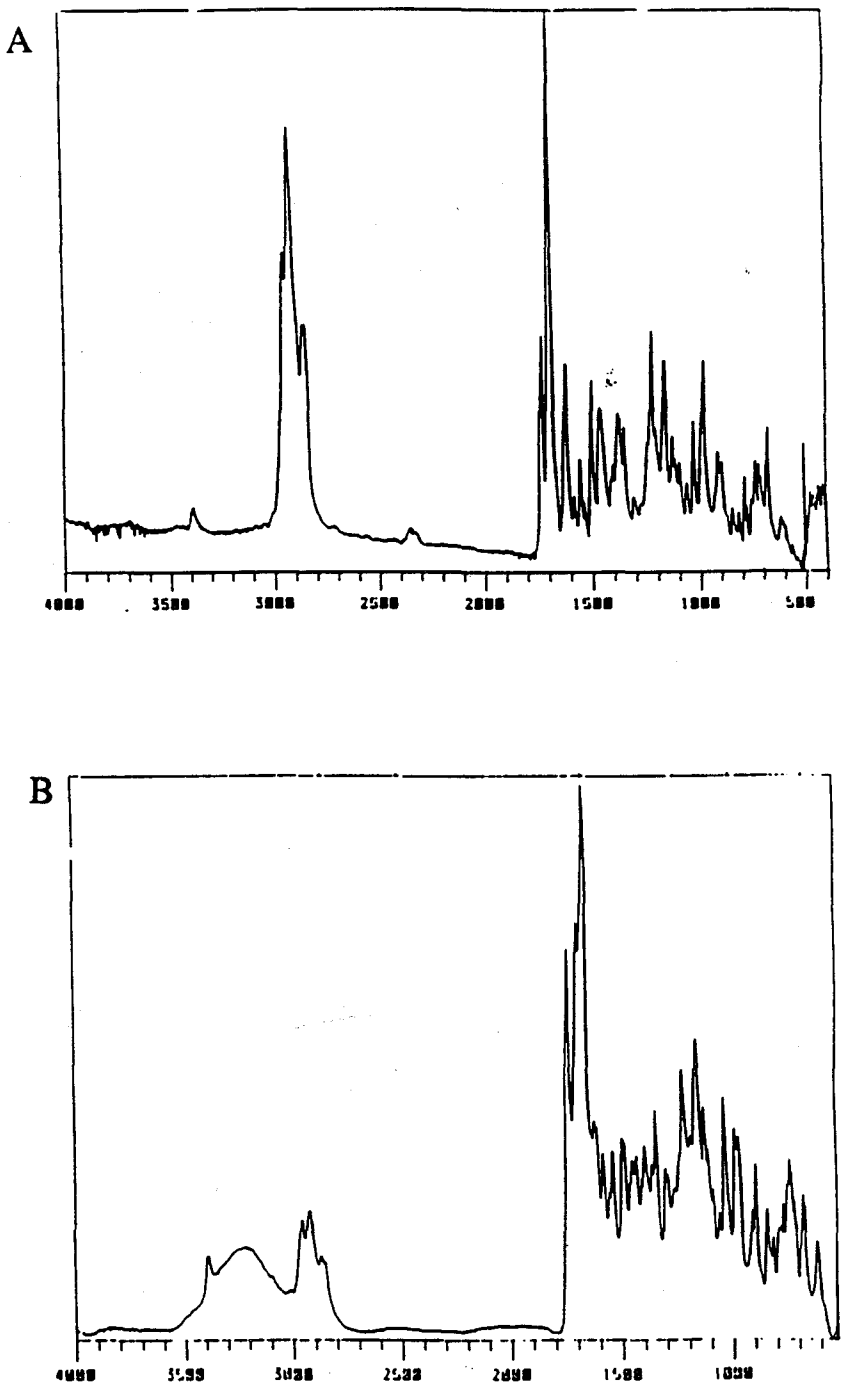

Fig. 2-3 Infrared spectra collected from neat samples of (a) pheophytin-*a*, and (b) pyropheophorbide-*a*.

reduced number of methyl groups which reduces the intensity of the C-H stretching absorbance in the region of 2950 cm^{-1} as compared with the phytyllated compounds. The lack of the phytyl chain in the structure of pbd-*a*, pbd-*b*, ppbd-*a*, and ppbd-*b* also reduces the intensity of the methylene stretching absorbance between 2923 - 2925 cm^{-1} as compared with the phytyllated compounds.

One additional C-H stretching absorption occurs in the IR spectra of the chlorophyll-*b* series pigments which does not occur in the IR spectra of the chl-*a* pigments. Each of the five chlorophyll-*b* derived compounds has an aldehyde group at C-3 whereas the chlorophyll-*a* pigments have a methyl group at this position. The aldehyde group in the chlorophyll-*b* pigments produces an additional C-H stretch between 2725 - 2750 cm^{-1}. The IR spectra of chlorophyll-*b* and its degradation products also contain one additional absorption in the carbonyl region.

The IR spectra of the pheopigments of chlorophyll-*a* and -*b*, contain an additional stretch at 3400 cm^{-1} due to N-H stretching (Katz, 1966). This band is partially hidden by the O-H stretching of the water absorbance in each spectrum. Since chlorophyll-*a* and -*b* have Mg in the center of the macrocycle and do not have pyrrolic hydrogens, the N-H stretching band is not present in these compounds.

The carbonyl region of the infrared spectrum occurs from 1650 - 1850 cm^{-1}. The spectra in this region are complicated by the possible formation of chlorophyll oligomers through the coordination of the keto carbonyl with Mg. The formation of aggregates through coordination of the ketone with the Mg of chlorophyll causes a substantial reduction in the intensity of the free keto carbonyl stretch at approximately 1695 cm^{-1} and the appearance of the coordinated keto (C=O---Mg) stretch at 1652 cm^{-1}. The aggregates can be broken into monomers by the addition of a nucleophile (Ballschmitter and Katz, 1969), and the presence of water, a nucleophile, in the spectra collected neat during this study can be seen by the large O-H stretch. In this study, chlorophyll-*a* and its pheopigments appear as monomers as evidenced by the presence of the free keto carbonyl band at 1691 - 1698 cm^{-1} and the lack of the coordinated keto band at 1652 cm^{-1}.

Dimers of chlorophyll degradation products can also form through hydrogen bonding. The carbonyl region of monomeric chlorophyll and its pheopigments has two IR absorbances. The first, at approximately 1735 cm^{-1} arises from stretching of the C-7 and C-10 esters and the band at 1695 cm^{-1} arises from ketone stretching. The formation of dimers through hydrogen bonding results in the splitting of the ester carbonyl band into two peaks with subsequent reduction in the intensity of the band at 1735 cm^{-1} and the appearance of a band at approximately 1715 cm^{-1} (Ballschmitter and Katz, 1969). The appearance of the band at 1717 cm^{-1} in the pheopigments lacking the carbomethoxy group,

indicates that the chlorophylls and pheopigments in this study are dimers formed through hydrogen bonding.

In the carbonyl region of the IR spectrum, one stretching band occurs for each carbonyl group in the structure of the compound analyzed. The maximum number of C=O stretches seen in the IR spectra of the chlorophyll-*a* pigments is 3 with only 2 occurring in the IR spectra of the two decarbomethoxylated compounds, pptn-*a* and ppbd-*a*. An additional C=O stretch occurs in the IR spectrum of each chlorophyll-*b* pigment, as compared with that of each chlorophyll-*a* pigment, due to the aldehyde group at C-3 in the structure of the chlorophyll-*b* pigments. Four C=O stretches occur in the spectrum of chl-*b*, ptn-*b*, and pbd-*b*, and three in pptn-*b*, and ppbd-*b*. The assignments in the carbonyl region of the IR spectra are based on the explanation of Katz *et al.* (1966), and Ballschmitter and Katz (1969).

Each absorption in the carbonyl region of the IR spectra of the chlorophyll degradation products can be assigned as resulting from a specific C=O in their structure. The stretching vibration of the C-7 proprionic ester C=O occurs near 1733 cm^{-1} in the IR spectrum of each compound studied, and the C-10 methyl ester C=O stretch, near 1717 cm^{-1} in the IR spectra of the *a* series and 1700 cm^{-1} in the *b* series compounds. The C=O stretch from the C-10 methyl ester is absent in pptn-*a*, ppbd-*a*, pptn-*b*, and ppbd-*b* since these compounds lack the C-10 carbomethoxy group. The C-9 ketone C=O stretch occurs between 1690 and 1700 cm^{-1} in the IR spectrum of all ten pigments studied. The lower frequency of the C=O ketone band is due to conjugation with the aromatic macrocycle in the chlorophyll pigment structure. In the IR spectrum of the *b* series compounds, a fourth band is found near 1660 cm^{-1}. This band arises from the C=O stretch of the C-3 aldehyde. The unusually low frequency of this absorption is due to the extended conjugated system of the macrocycle in which the aldehyde is also a part.

The absorptions in the carbonyl region of the IR spectrum of each of the four acidic chlorophyll degradation products studies, pbd-*a* and -*b*, and ppbd-*a* and -*b*, are shifted compared to that of the non-acidic compounds studied. The acid carbonyl stretch occurs near 1730 cm^{-1}, and the C-10 ester, found only in IR spectra of pbd-*a* and pbd-*b*, occurs between 1684 and 1668 cm^{-1}. The C-10 ester carbonyl occurs at 1680 cm^{-1} in the spectra of the acidic chlorophyll degradation products. This frequency is lower than normal and this assignment is made based on the lack of the 1680 cm^{-1} absorption in the decarbomethoxylated compounds, as compared with the compounds containing a carbomethoxy group. The unusually low frequency of this stretch may be due to intramolecular hydrogen bonding between the acidic hydrogen and the methyl ester carbonyl in the structure of the chlorophyll degradation products studied. Hydrogen

bonding has an electron withdrawing effect which acts to lower the absorption frequency. The band at 1733 cm^{-1} must, by default, be due to the acid carbonyl stretch. This unusually high frequency for an acid stretch could indicate a lack of hydrogen-bonding between the acid groups of adjacent molecules caused by the methods used to obtain these spectra.

The final absorption studied in the IR spectra of the authentic chlorophyll compounds is the chlorin band. This band occurs at 1604 cm^{-1} in the IR spectra of the two metallated compounds and at 1617 - 1621 cm^{-1} in the IR spectra of the other eight compounds studied. The source of this band is the C=C stretch of the extended conjugated system of the phorbin macrocycle (Andersson *et al.*, 1989). The lowering of the frequency of this band in the metallated compounds is caused by the extension of the conjugated system through the central magnesium atom.

D. NUCLEAR MAGNETIC RESONANCE SPECTROMETRY

The proton nuclear magnetic resonance spectra of chl-*a* and its derivatives, and chl-*b* and its derivatives are similar (Table 2-4 and 2-5; Fig. 2-4). Each of the chlorophyll derivatives studied has a H/C ratio of 1.3 for the phytyllated compounds and 1 for the acids. Because of these low H/C ratios, the NMR spectra have relatively few absorbances. Each spectrum has three absorbances between 9 - 11 ppm due to the three meso protons. Each also displays a doublet of doublets between 8 - 8.3 ppm and two doublet of doublets between 6.1 - 6.6 ppm due to the absorbance of the vinyl protons at C-2. The protons on the methyl substituents on rings I, II, and III, and on the carbomethoxy group resonate between 3.2 and 3.8 ppm. The absorbances between 1 - 3 ppm result from the protons on the propyl and phytyl groups. The most downfield absorbances, at 1 ppm and -1.2 ppm result from the absorbances of the pyrrole protons (N-H) in the center of the macrocycle in the demetallated compounds. Variations in these absorbances result from loss of phytol, from decarbomethoxylation, and from the replacement of the C-3 methyl group of chl-*a* and its derivatives with an aldehyde group on chl-*b* and its derivatives.

The dominant aspect of the chlorophyll structure effecting the NMR spectra is the paramagnetic and diamagnetic anisotropy of the phorbin macrocycle (Abraham *et al.*, 1982, 1987). All the protons attached to carbons which are part of the macrocycle, and protons on carbons which are attached to the macrocycle, are deshielded (shifted downfield 3.6 - 6.5 ppm and 3.5 - 4.0 ppm, respectively) by the magnetic field of the ring current, and the two protons inside the ring in the structures of the eight metal-free derivatives are shielded (shifted upfield 8 ppm). Differences in the NMR spectra of the chl-*b* and chl-*a* series pigments arise due to the aldehyde group at C-3 in chl-*b* and its derivatives. The

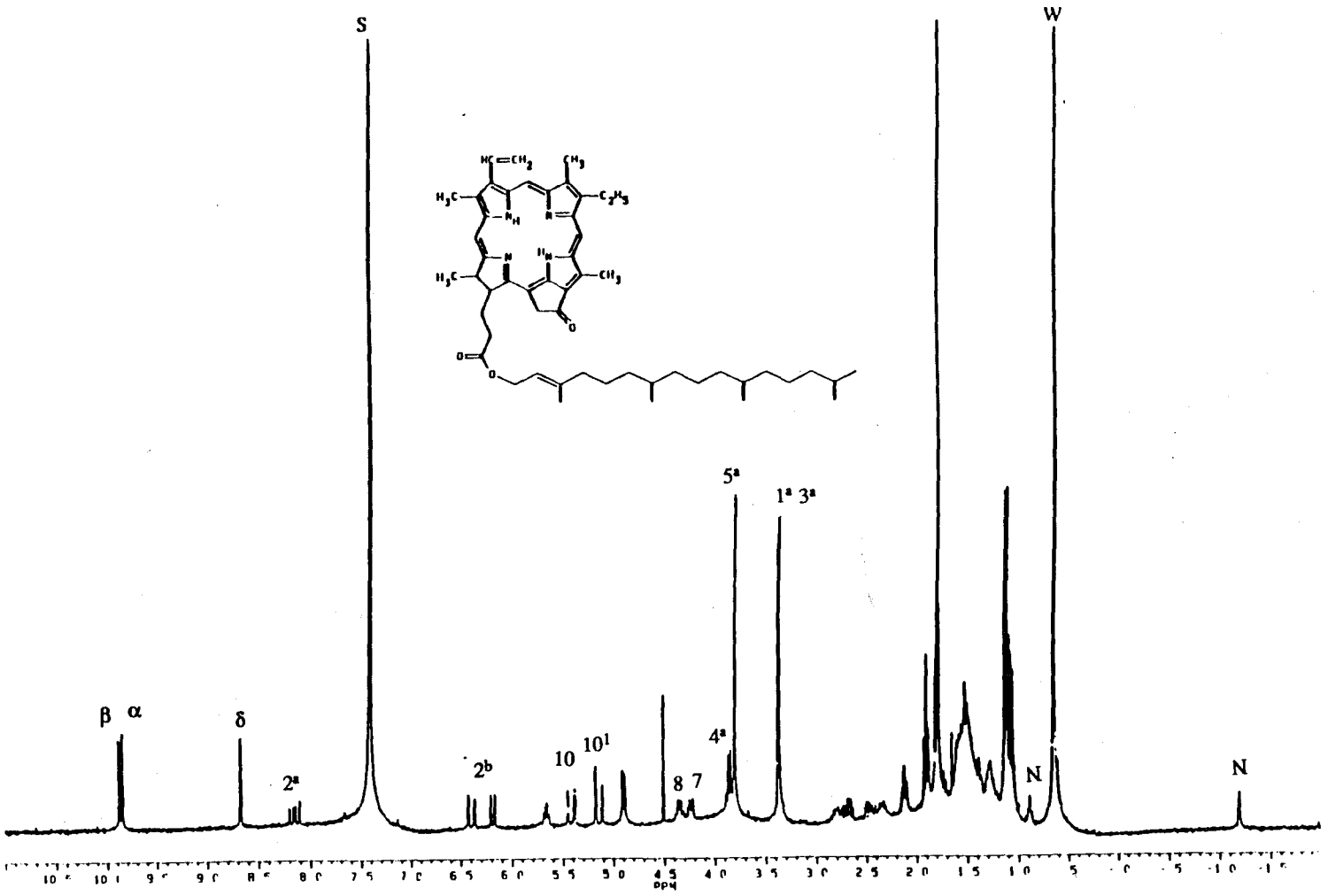

Fig. 2-4 300 MHz proton NMR spectrum of pyropheophytin-*a* in d6-benzene.

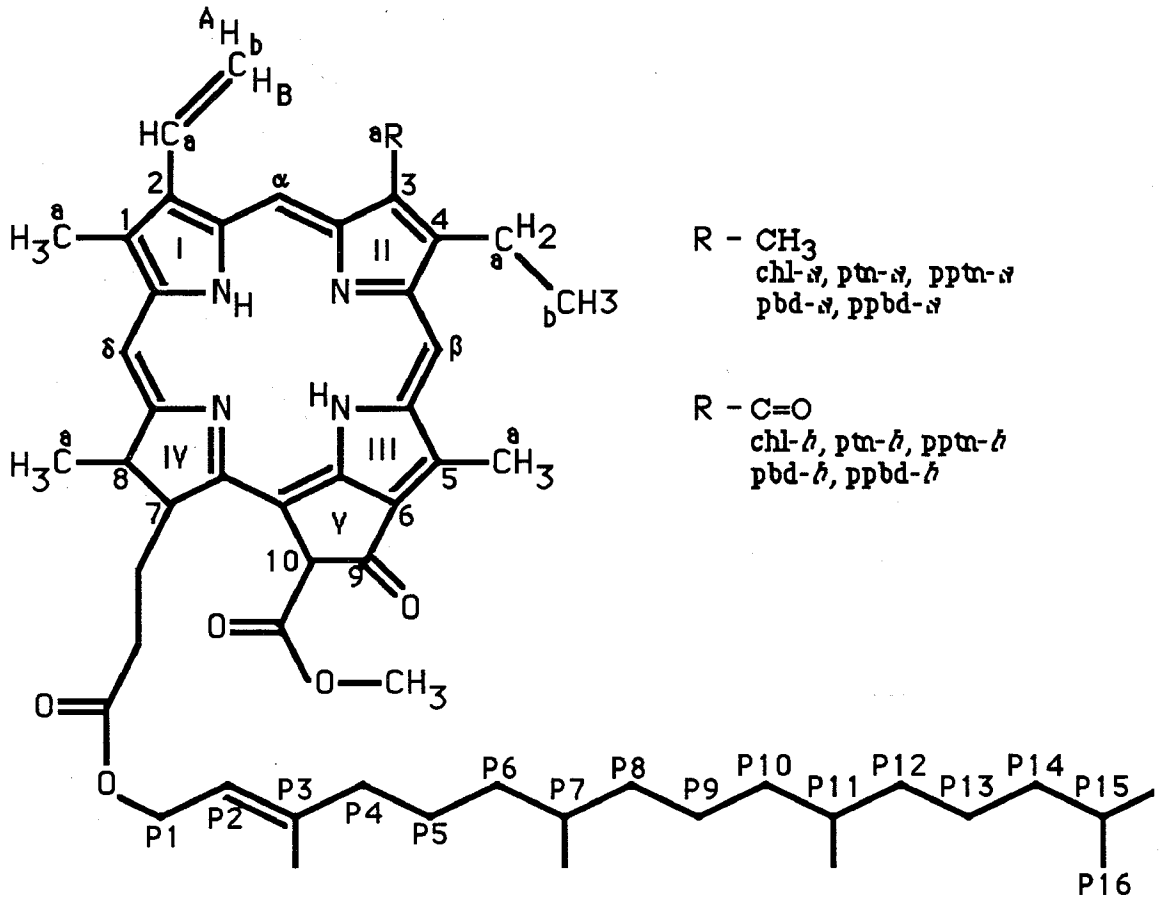

paramagnetic anisotropy of the C-3 aldehyde group in chl-*b* further deshields the α meso proton, shifting its absorbance downfield of its position in chl-*a* pigments (from 9.7 to 11), so that the aldehyde proton appears in the NMR spectra of chl-*b* series pigments as the most deshielded absorbance (10.9 - 11.3 ppm). The NMR spectra of the chl-*b* pigments also lack the absorbance due to the C-3 methyl protons seen in the spectra of the chl-*a* pigments. The chemical shifts of the protons in the ten authentic compounds analyzed are tabulated in Tables 2-2 and 2-3, and the complete spectra appear in Appendix I.

The paramagnetic anisotropy of the phorbin macrocycle of the ten compounds studied produces the large downfield chemical shifts seen in the NMR absorbances of the meso protons and the protons on the side chains. The meso protons of chl-*a* and its derivatives resonate between 8.6 ppm and 10 ppm. The δ proton is the most shielded of the three meso protons, due to its position adjacent to the the partially saturated pyrrole ring, ring IV (Closs *et al.*, 1963). In the chl-*a* pigments, the β proton is slightly further downfield than the α proton due to additional deshielding by the anisotropy of the C-9 ketone (Closs *et al.*, 1963).

In the NMR spectra of the chl-*b* derived pigments, the three meso protons resonate between 8.3 ppm and 11.4 ppm. As compared with NMR spectra of the chl-*a* pigments,

the order of the chemical shifts of the α and β meso protons is reversed in the NMR spectra of the chl-*b* pigments. The β meso proton in the chl-*b* pigments resonates at the same frequency as in the chl-*a* pigments, but the α proton appears further downfield in the chl-*b* pigments due to the added deshielding of the C-3 aldehyde carbonyl. Another example of the effect of the macrocycle ring current is the diamagnetic anisotropy experienced by the two N-H protons inside the macrocycle. The shielding produced by the ring current inside the macrocycle causes upfield shifts in the resonance of the pyrrolic protons to between 1 ppm and -2 ppm. As a comparison, the chemical shift of the proton on the N in pyrrole is 7.0 ppm (Pavia *et al.*, 1979).

The deshielding caused by the macrocycle ring current also produces the downfield shifts in the absorbances of the methyl groups adjacent to the ring. The structures of the five chl-*a* derived pigments studied each have methyl groups at C-1, C-3, C-5, and C-8 . The 1a and 3a methyl protons of the chl-*a* pigments are nearly equivalent, absorbing as singlets between 3.3 and 3.5 ppm. The very slight downfield shift in the 1a protons relative to the 3a protons may be due to the additional deshielding of the vinyl group on C-2. The 5a methyl protons are 0.3 ppm further downfield in the NMR spectra than the 1a and 3a methyl protons due to the presence of the C-9 ketone. The 8a methyl protons,which absorb between 1.68 - 1.85 ppm, are removed from the anisotropic effect of the ring current and absorb in the region expected for methyl protons. These protons' resonance signal appears as a doublet due to coupling with the C-8 proton. The structures of the five chl-*b* derived pigments which were studied each have methyl groups at C-1, C-5, and C-8. The resonances for these methyl protons appear in the same positions at they do in their corresponding chl-*a* derived structures. In the chl-*b* pigments, an aldehyde group replaces the methyl group which appears at C-3 in the chl-*a* pigments. The ring current contributes to the deshielding of the chl-*b* C-3 aldehyde proton which absorbs at 11.4 ppm. Aldehyde protons uneffected by anisotropy absorb between 9 - 10 ppm (Pavia, *et al.*, 1979).

The macrocycle of each of the ten authentic chlorophyll compounds also has two side chains which are only partially influenced by the macrocycle ring current. Both the chl-*a* and chl-*b* pigments have a vinyl group at C-2. Due to the lack of free rotation around the double bond, each of the three protons on this moiety experience different electronic environments. The 2a proton appears as a doublet of doublets at approximately 8.1 ppm (8.3 in the metallated compounds) with coupling constants of 11.5 Hz and 17.9 Hz. The absorbance of 2a is split to two peaks, with a *J* value of 11.5 Hz, by the cis proton, 2b-H_B. Each of these two peaks is further split to doublets, with a *J* value of 17.9 Hz, by the *trans* proton, 2b-H_A. The 2b-H_A proton also (trans to 2a) appears as a doublet of doublets.

Table 2-4

CHEMICAL SHIFTS OF CHLOROPHYLL-*A* DERIVATIVES IN d_6-BENZENE

	chl-*a**	ptn-*a*	pptn-*a*	pbd-*a*	ppbd-*a*
N-H		-1.16(s)	-1.20(s)	-1.17(s)	-1.17(s)
N-H		.90(s)	.90(s)	1.17(s)	1.15(s)
α-H	9.65(s)	9.74(s)	9.87(s)	9.73(s)	9.80(s)
β-H	9.96(s)	9.83(s)	9.84(s)	9.82(s)	9.82(s)
δ-H	8.81(s)	8.62(s)	8.67(s)	8.60(s)	8.63(s)
1a-CH_3	3.51	3.32(s)	3.37(s)	3.31(s)	3.36(s)
2a-H	8.30(dd)	8.13(dd)	8.15(dd)	8.10(dd)	8.12(dd)
2b-H_A	6.39(dd)	6.38(dd)	6.40(dd)	6.37(dd)	6.37(dd)
2b-H_B	6.17(dd)	6.22(dd)	6.19(dd)	6.17(dd)	6.18(dd)
3a-CH_3	3.47(s)	3.30(s)	3.36(s)	3.30(s)	3.34(s)
4a-CH_2	3.99(q)	3.80(q)	3.86(q)	3.81(q)	3.82(q)
4b-CH_3	1.86(t)	1.87(t)	1.90(t)	1.85(t)	1.89(t)
5a-CH_3	3.74(s)	3.66(s)	3.79(s)	3.66(s)	3.77(s)
7-H	4.31(d)	4.34(d)	4.23(d)	4.26(d)	4.17(d)
7a,7b-CH_2	2.68(m)	2.5-3.0	2.2-2.8	2.2-2.8	2.1-2.8
8-H	4.70	4.60(d)	4.34(d)	4.51(d)	4.27(d)
8a-CH_3	1.72(d)	1.78(d)	1.85(d)	1.74(d)	1.76(d)
10^1-H	6.23(s)	6.65(s)	5.42(d)	6.61(s)	5.41(d)
10-$COOCH_3$	3.80(s)	3.78(s)		3.77(s)	
10^2-H			5.14(d)		5.15(d)
P1-CH_2	4.64(m)	4.88(m)	4.89(d)		
P2-H	5.34(t)	5.60(t)	5.66(t)		
P3-CH_3	1.76(s)	1.72(s)	1.80(s)		
P7,P11-CH_3	.96(t)	1.07(t)	1.06(t)		
P15,P16-CH_3	1.00(d)	1.12(d)	1.11(d)		

*Spectrum taken in d_6-acetone

Table 2-5

CHEMICAL SHIFTS OF CHLOROPHYLL-*B* DERIVATIVES IN d_6-BENZENE

	chl-*b*	ptn-*b*	pptn-*b*	pbd-*b*	ppbd-*b*
N-H		-1.09(s)	-1.06(s)	-1.08(s)	-1.05(s)
N-H		.87(s)	.95(s)	1.12(s)	1.00(s)
α-H	10.93(s)	11.26(s)	11.31(s)	11.30(s)	11.33(s)
β-H	9.80(s)	9.61(s)	9.74(s)	9.66(s)	9.75(s)
δ-H	8.35(s)	8.48(s)	8.51(s)	8.46(s)	8.48(s)
1a-CH_3	3.36(s)	3.20(s)	3.26(s)	3.18(s)	3.21(s)
2a-H	8.31(dd)	8.17(dd)	8.20(dd)	8.14(dd)	8.18(dd)
2b-H_A	6.59(dd)	6.53(dd)	6.54(dd)	6.54(dd)	6.54(dd)
2b-H_B	6.19(dd)	6.19(dd)	6.20(dd)	6.19(dd)	6.19(dd)
3a-CHO	11.39(s)	11.39(s)	11.46(s)	11.41(s)	11.46(s)
4a-CH_2	4.08(m)	3.86(m)	3.94(m)	3.89(m)	3.95(m)
4b-CH_3	1.85(t)	1.72(t)	1.77(t)	1.75(t)	1.78(t)
5a-CH_3	3.64(s)	3.54(s)	3.67(s)	3.55(s)	3.67(s)
7-H	4.20(d)	4.26(m)	4.15(d)	4.16(m)	4.06(d)
7a,7b-CH_2	2.2-2.9	2.4-3.0	2.2-2.9	2.15-2.9	2.0-2.8
8-H	4.34(m)	4.55(d)	4.25(d)	4.44(d)	4.13(d)
8a-CH_3	1.72(d)	1.78(d)	2.11(t)	1.70(d)	1.68(d)
10^1-H	6.62(s)	6.58(s)	5.30(d)	6.52(s)	5.27(d)
10-$COOCH_3$	3.73(s)	3.80(s)		3.78(s)	
10^2-H			5.05(d)		5.01(d)
P2-H	5.47(t)	5.60(t)	5.68(t)		
P1-CH_2		4.88(m)	4.89(m)		
P3-CH3					
P7,P11-CH_3	1.16(t)	1.08(t)	1.07(t)		
P15,P16-CH_3	1.18(d)	1.13(d)	1.12(d)		

This resonance is split to two peaks with a *J* value of 1.8 Hz by the geminal proton 2b-H_B, and each of these peaks is further split into two peaks with a *J* value of 17.9 Hz by the trans proton 2a. Proton 2b-H_B (*cis* to 2a) is also split into two with a *J* value of 1.8 by the geminal proton, 2b-H_A, and again into two by the cis proton, 2a, with a coupling constant of 11.5 Hz. The chemical shifts of the two 2b protons are in the region expected for vinyl protons but the 2a protons are shifted further downfield, to 8.1 ppm, by the deshielding effect of the ring current.

The ethyl group of C-4 also shows NMR absorbances shifted by the ring current as well as absorbances uneffected by the ring anisotropy. The 4b protons occur as a triplet, split by the two 4a protons, with a chemical shift at 1.9 ppm as expected for methylene protons uneffected by shielding or deshielding. The 4a protons, shifted downfield by the deshielding effect of the ring current, occur as a quadruplet at 4.0 ppm. The resonance of these two protons is split by the three protons at 4b.

The partially saturated pyrrole ring (ring IV) of both the chl-*a* and chl-*b* pigments has two protons attached directly to the ring, one at C-7 and one at C-8. Though ring IV is not part of the conjugated system, these protons are still effected by the paramagnetic anisotropy of the conjugated ring, since they are only one carbon removed from the conjugated system. Being one carbon removed from the ring, the deshielding effect is not as large as that acting on the meso protons, and the C-7 and C-8 protons occur at resonances of 4.2 ppm and 4.5 ppm respectively. Proton C-8 occurs in the NMR spectra of the ten authentic compounds studied as a doublet split to a quadruplet, though in trying to determine the coupling constants, higher order splitting was also observed. The absorbance of the C-8 proton is split to a doublet by the proton at C-7, and further to a quadruplet by the three 8a methyl protons. The resonance signal for proton C-7 is split to a doublet by the proton on C-8, and further split by the methylene protons 7a and 7b.

The arrangement of functional groups at C-10 varies among the compounds studied. Six of the compounds, chl-*a*, ptn-*a*, pbd-*a*, chl-*b*, ptn-*b*, and pbd-*b* each have one proton and one carbomethoxy group at the C-10 position, while the four decarbomethoxylated compounds, pptn-*a*, ppbd-*a*, pptn-*b*, and ppbd-*b*, each have two protons at C-10. The chemical shift of the single C-10 proton on the six compounds containing the carbomethoxy group, which resonates as a singlet, is concentration dependent in d_6-benzene, the solvent used in these NMR experiments. As concentration increases, the C-10 proton shifts further downfield, absorbing between 5.5 and 7 ppm. The three methyl protons on the C-10 carbomethoxy group occur as a singlet at 3.8 ppm. The shift of these protons away from the 0 - 2 ppm region usually expected for methyl protons is due to the electron withdrawal of the adjacent oxygen atom. In these

compounds, the two protons at C-10 occur as a pair of doublets between 5 and 5.5 ppm. Since these protons can not freely rotate, they experience different electronic environments, produce individual nuclear magnetic resonance signals, and couple with each other. The electronic environments of these two protons, though different, are nearly equivalent and second order splitting is therefore observed. The two peaks in each doublet are uneven and the chemical shifts of C-10^1 and C-10^2 are displaced slightly from the center of the doublet towards the larger of the two peaks. Protons C-10^1 and C-10^2 strongly couple, with a J value of 20 Hz. The behavior of these proton resonances in the NMR spectra of both the chl-*a* and chl-*b* derived compounds is similar.

The protons of the propionic ester and phytyl chain are not discussed in detail here. The protons of the C-7a, C-7b, and P-1 methylene groups are slightly deshielded by the C-7 propionic ester group, and are therefore shifted slightly downfield of the other phytyl protons, and have complex NMR splitting patterns. The remaining protons of the phytyl chain do not feel the deshielding effect of the C-7 ester, and therefore these protons resonate in the region expected for protons on aliphatic carbons. The chemical shifts for the propionic ester and phytyl protons in the chl-*b* pigments is similar to that of the chl-*a* pigments.

IV. CONCLUSIONS

In this chapter, I describe the methods used to synthesize authentic compounds used throughout this thesis to standardize procedures. I also describe the spectral methods used to structurally identify the chlorophyll degradation products. Spectral analysis of authentic compounds provides a means to determine how structural modifications of chlorophylls and their derivatives effect the IR, MS, NMR, and visible spectra. Further purification of the isolated degradation products in a manner similar to those used for the standards has shown that the spectral methods described are useful in elucidating the structure of unknown sedimentary chlorophyll degradation products.

V. REFERENCES

Abraham R. J., Medforth C. J., Smith K. S., Goff D. A., and Simpson D. J. (1987) NMR spectra of porphyrins. 31. Ring Currents in hydroporphyrins. *J. Am. Chem. Soc.* **85**, 4789-4791.

Abraham R. J., Smith K. M., Goff D. A., and Lai J.-J. (1982) NMR Spectra of porphyrins. 18. A ring-current model for chlorophyll derivatives. *J. Am. Chem. Soc.* **104**, 4332-4337.

Anderson L. A., Loehr T. M., Cotton T. M., Simpson D. J., and Smith K. M. (1989) Spectroscopic analysis of chlorophyll model complexes: methyl ester ClFe(III)pheophorbides. *Biochem. Biophys Acta* **974**, 163-179.

Baker E. W. (1970) tetrapyrole pigments. In *Initial Reports of the Deep Sea Drilling Project* (eds. R. G. Bader, *et al.*), 4, pp 431-438. U. S. Government Printing Office.

Baker E. W. and Louda J. W. (1986) Porphyrins in the geological record. In: Biological Markers in the Sedimentary Record (R. B. Johns, Ed.) Elsevier. p 125-225.

Baker E. W. and Smith G. D. (1974) Pleistocene changes in chlorophyll pigments. In: Advances in Organic Geochemistry, 1973. p. 649-660.

Ballschmitter K. and Katz J. J. (1969) An infrared study of chlorophyll-chlorophyll and chlorophyll-water interactions. *J. Am. Chem. Soc.* **91**, 2661-2677.

Closs G. L., Katz J. J., Pennington F. C., Thomas M. R., and Strain H. H. (1963) Nuclear magnetic resonance spectra and molecular association of chlorophylls *a* and *b*, methyl chlorophyllides, pheophytins, and methyl pheophorbides. *J. Am. Chem. Soc.* **304**, 3809-3821.

Frew N. M., Johnson C. G., Bromund R. H. (1988) Supercritical fluid chromatography -- Mass spectrometry of carotenoid pigments. In *Supercritical Fluid Extraction and Chromatography: Techniques and Applications* (eds. B. A. Charpentier and M. R. Sevenants), Ch. 12, pp. 208-228, American Chemical Society.

Fuhrhop J.-H. and Smith K. M. (1975) *Laboratory Methods in Porphyrin and Metalloporphyrin Research.* Elsevier Scientific Publishing Company.

Furlong E. T. and Carpenter R. (1989) Pigment preservation and remineralizaiton in oxic coastal marine sediments. *Geochim. Cosmochim. Acta* **52**, 87-99.

Gouterman M. (1961) Spectra of porphyrins. *J. Mol. Spectrosc.* **6**, 138-163.

Hassner A. and Alexanian V. (1978) Direct room temperature esterification of carboxylic acids. *Tetrahedron. Lett.* **46**, 4475-4478.

Hoff A. J. and Amesz J. (1991) Visible absorption spectroscopy of chlorophylls. In *Chlorophylls* (ed. H. Scheer), Ch. 4.1, pp. 723-735.

Hoffman P. and Werner D. (1966) Spectrometric chlorophyll determination having special regard to various types of equipment. *Jena Rev.* **11**, 300-303.

Houssier C., and Sauer K. (1969) Optical properties of the protochlorophyll pigments. I. Isolation, characterization, and infrared spectra. *Biochem. Biophys. Acta* **172**, 476-491.

Hynninen P. H. (1973) Chlorophylls. IV. Preparation and purification of some derivatives of chlorophylls *a* and *b*. *Acta Chemica Scandinavica* **27**, 1771-1780.

Jeffrey S. W. and Humphrey, G. F. (1975) New spectrophotometric equations for determining chlorophylls a, b, c1, and c2 in higher plants, algae and natural phytoplankton. *Biochem. Physiol. Pflanzen* **167**, 191-194.

Katz J. J., Dougherty R. C., and Boucher L. J. (1966) Infrared and nuclear magnetic resonance spectroscopy of chlorophyll. In *The Chlorophylls* (eds. L. P. Vernon and G. R. Seely), Chap. 7, pp. 186-252. Academic Press

Keely B. J. (1989) Early diagenesis of chlorophyll and chlorin pigments. Ph.D. dissertation, Univ. of Bristol.

Keely B. J. and Maxwell J. R. (1990) Fast atom bombardment mass spectrometric and tandem mass spectrometric studies of some functionalized tetrapyrroles derived from chlorophylls *a* and *b*. *Energy Fuels* **4**, 737-741.

Ourisson G. (1974) response to Baker and Smith, 1974. In: Advances in Organic Geochemistry, 1973. p. 660.

Pavia D. L., Lampman G. M., and Kriz G. S. (1979) *Introduction to Spectroscopy*. Saunders College.

Pennington F. C., Strain H. H., Svec W. A., and Katz J. J. (1964) Preparation and properties of pyrochlorophyll-a, methyl pyrochlorophyllide-a, pyrophaeophytin-a, and methyl pyropheophorbide-a derived from chlorophyll by decarbomethoxylation. *J. Am. Chem. Soc.* **86**, 1418-1426.

Fuhrop J.-H. and Smith K. M. (1975) In: Laboratory methods in porphyrin and metalloporphyrin research. Elsevier, Amsterdam. 132-135.

Vernon L. P. (1960) Spectrophotometric determination of chlorophylls and phaeophytins in plants. *Anal. Chem.* **32**, 1144-1150.

Watanabe T., Hangu A., Honda K., Nakazato M., Konno M., and Saitoh S. (1984) Preparation of chlorophylls and pheophytins by isocratic liquid chromatography. *Anal. Chem.* **56**, 251-256.

CHAPTER 3

NOVEL PYROPHEOPHORBIDE STERYL ESTERS IN BLACK SEA SEDIMENTS

The work presented in this chapter is an expansion of the work which appeared as:

Pyropheophorbide-*a* Steryl Esters in Black Sea Sediments

in

Geochimica et Cosmochimica Acta
Vol 55, pp. 2067-2074, 1991

CHAPTER 3

NOVEL PYROPHEOPHORBIDE STERYL ESTERS IN BLACK SEA SEDIMENTS

I. INTRODUCTION

Studies suggest that ptn-*a*, pptn-*a*, pbd-*a*, and ppbd-*a* are the most abundant pheopigments in the water column and recent sediments (Brown *et al.*, 1977; Gillan and Johns, 1980; Keely and Brereton, 1986; Furlong and Carpenter, 1988; Hurley and Armstrong, 1990), but these four compounds, along with undegraded chl-*a* , account for only 10-20% of the total phorbins in organic solvent extracts of sediment as measured by visible spectroscopy (665 nm; Furlong and Carpenter, 1988). In Black Sea surface sediments, 0.12 μmol/g dry weight (gdw) of phorbin is needed to account for the absorption at 665 nm in the solvent extract, yet only 0.03 μmol/gdw of chl-*a* and pheopigments is measured by HPLC. The contributions of chl-*b*, chl-*c*, and bacteriochlorophyll degradation products as measured by HPLC are minor. Additional sinks for chlorophyll degradation products in surface sediments are needed to account for the absorption of the total sediment extract as measured at 665 nm.

During the course of our study of chlorophyll degradation in recent sediments from the Black Sea, we observed a series of very nonpolar chlorophyll degradation products with chromatographic properties similar to the post-depositional degradation products (PDDs) described by Furlong and Carpenter (1988) in extracts of Dabob Bay sediment. On reverse-phase HPLC, PDD elute after pptn-*a*, the least polar chlorophyll degradation product reported to date. The PDD were quantitatitively minor in Dabob Bay, but in Black Sea sediment these nonpolar chlorophyll degradation products are nearly equal in abundance to the sum of all other HPLC characterizable chl-*a* degradation products, and therefore represent a major preservational sink for chlorophyll in Black Sea sediments. In the following, we describe the structure and synthesis of pyropheophorbide-*a* steryl esters and discuss their geochemical significance.

II. METHODS

Surface sediment was collected by box core from a water depth of 2129 m in the Euxine Abyssal Plain (Fig. 3-1) during the 1988 Black Sea Expedition (R/V Knorr, 134-9,

May 14-28, 1988). Once on deck, the core was immediately sectioned and frozen. A composite sediment sample (899 g wet wt) encompassing a depth of 0-10 cm was extracted with acetone (9x, sediment was completely covered by acetone), followed by CH_2Cl_2 (3x) by vigorous stirring for at least 2 hours. The combined extracts were concentrated by rotary evaporation, an equal volume of 30/70 (v/v) hexane/diethyl ether was added, and the pigments were partitioned into the organic phase. The organic extract was washed, dried over $NaSO_4$, and evaporated to dryness. Pigments were redissolved in acetone and split 78:2:20, with 78% of the sample being set aside for later study. All procedures were performed at room temperature with minimum exposure to light, and all samples were stored in the dark at -30°C.

Phorbin steryl esters (PSEs) were separated from 20% of the total extract by reverse-phase column chromatography (RPLC). The sample was dissolved in MeOH and one-sixth was applied to a 10 mm i.d. column, dry-packed with 7 g of octadecylsilyl bonded silica (ODS) (Waters Assoc. C18 Sep-Pak). Pigments were eluted in two fractions with *n*-propanol/MeOH and acetone. The first fraction, containing carotenoids, chlorophylls, and pheopigments, was eluted with 50 mL of MeOH followed by 130 mL of 20/80 (v/v) *n*-propanol/MeOH. The second fraction, containing the PSEs, was eluted with 100 mL of acetone. With each solvent change, the sample vial was rinsed with fresh solvent and the rinse applied to the column. The column was reused 4-5 times, by removing all solvent and reequilibrating with MeOH, to isolate PSEs from the remaining sample. Preparatory HPLC using 20% *n*-propanol/MeOH was used to isolate eight PSE containing peaks (PSE 1 to 8, Fig. 3-2). Immediately prior to mass spectral analysis, individual PSE fractions were further purified by thin layer chromatography (Merck Kieselgel 60, plate washed with acetone and activated 2 hr at 250°C), developed with 25/75 (v/v) acetone/hexane. Total phorbin steryl esters (not individual PSE containing peaks) were isolated from the RPLC phorbin steryl ester isolate using HPLC with 40% *n*-propanol/MeOH.

Non-esterified solvent-extractable sterols were isolated from 2% of the remaining extract according to the procedure of Farrington *et al.* (1988). Briefly, the extract was fractionated by liquid chromatography on 5% deactivated silica gel. Lipids were eluted with hexane, toluene/hexane, and ethyl acetate/hexane. The 4-methyl- (F_6; Farrington *et al.*, 1988) and 4-desmethylsterols (F_7) were eluted with 15/85 (v/v) ethyl acetate/hexane and 20/80 (v/v) ethyl acetate/hexane, respectively. Non-esterified solvent-extractable sterols and sterols derived from the hydrolysis of total phorbin steryl esters (acetone/12 N HCl, 1/1, 20 min. (In Chl. 5 a better method is introduced using 5% H_2SO_4/MeOH)) were acetylated (acetic anhydride/pyridine (1/1) overnight at room temperature; Volkman *et al.*,

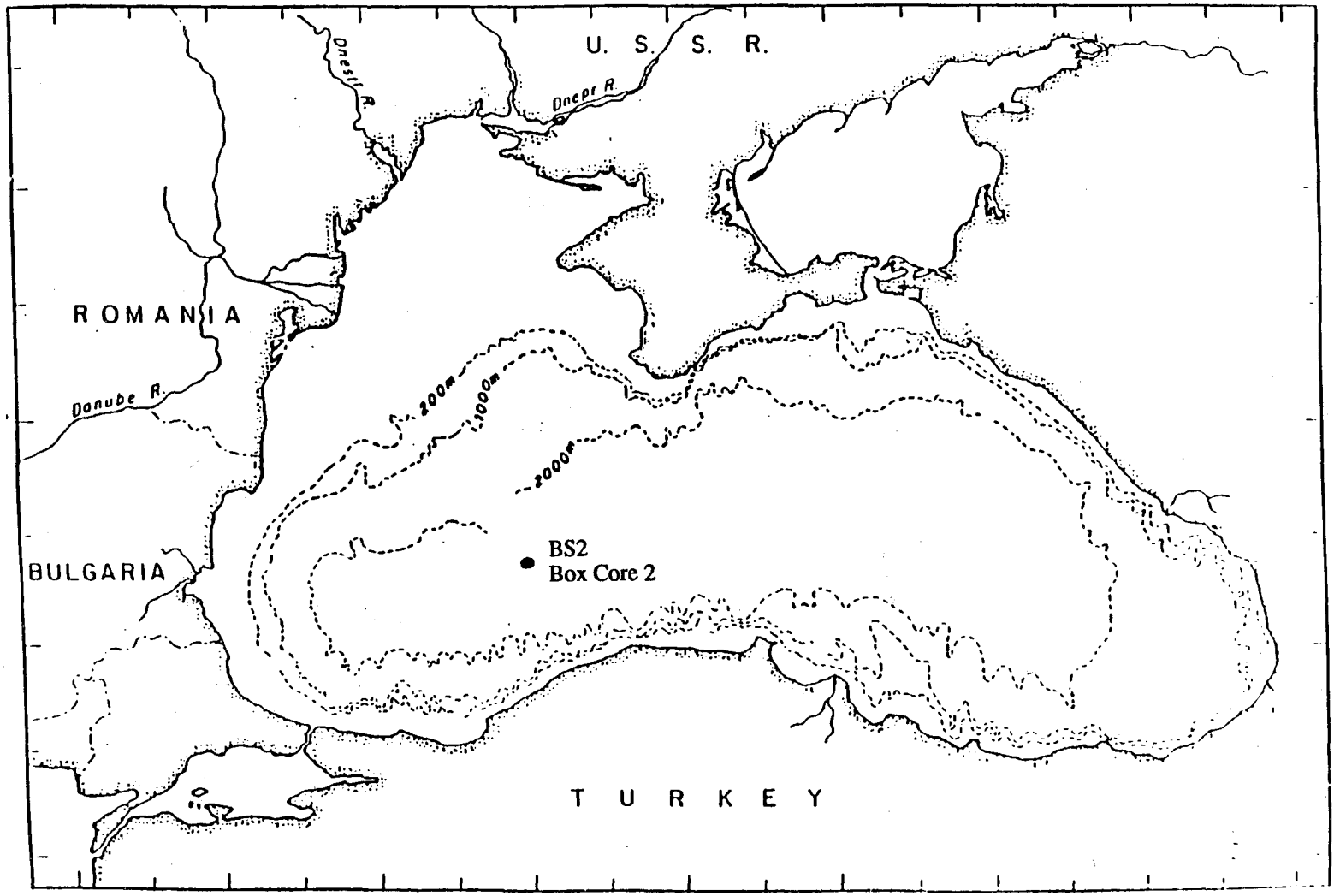

Fig. 3-1 Map of the Black Sea. Sampling locations are indicated.
(Ross *et al.*, 1974)

1984; McCaffrey, 1990), and analyzed by gas chromatography (GC) and gas chromatography/mass spectrometry (GC/MS).

Desorption chemical ionization mass spectra (CI-MS; methane reagent gas) and visible spectra were collected of each PSE fraction using the procedures described in Ch. 2. The hydrolysis products of PSE fraction 4 and acetylation products of the non-esterified solvent-extractable sterols and total PSE-derived sterols were analyzed by GC and GC/MS. Gas chromatographic analyses were performed on a Carlo Erba 4160 gas chromatograph equipped with a 30 m, 0.25 mm i.d. fused silica capillary column coated with phenylmethylsilicone (DB-5; J & W Scientific), using H_2 as carrier gas and temperature programmed from 80 - 260°C at 3.5°/min then 4°/min to a final temperature of 310°C. A Finnigan 4510 quadropole mass spectrometer was used for all CI-MS and GC/MS work. Identification of sterols was made by comparison of mass spectra and GC retention times with published data.

Authentic pyropheophorbide-*a* steryl esters were synthesized in yields of 50 - 60% from pyropheophorbide-*a* and four sterols found in high concentrations in our total PSE isolate: cholesterol, stigmasterol (24-ethylcholesta-5,22-dien-3β-ol), brassicasterol (24β-methylcholesta-5,22-dien-3β-ol), and β-sitosterol (24-ethylcholest-5-en-3β-ol). Esterification was performed by dissolving 1 mg of pyropheophorbide-*a* in 1 mL of CH_2Cl_2. To this was added 1.1 equivalents of N,N-dicyclohexylcarbodiimide, 1.1 equivalents of sterol , and 0.1 equivalents of 4-pyrrolidinopyridine. The reaction mixture was stirred at room temperature under N_2 overnight (Hassner and Alexanian, 1978). The reaction mixture was diluted with CH_2Cl_2, and washed with 3 x 15 mL permanganate distilled water, 3 x 15 mL 5% acetic acid, again with 3 x 15 mL distilled water, and then allowed to dry over Na_2SO_4. The pyropheophorbide-*a* sterol ester was then separated from any unreacted pyropheophorbide-*a* by thin layer chromatography on SiO_2 using 25% (v/v) acetone/hexane, and further purified by prep-scale HPLC using 20% (v/v) *n*-PrOH/MeOH. Each authentic pyropheophorbide-*a* steryl ester was characterized by visible spectrophotometry, CI-MS, and NMR according to the methods in Ch. 2. The extinction coefficient of pyropheophorbide-*a* cholesteryl ester was determined by preparing three 10^{-4} M acetone solutions of the pigment and determining the average extinction coefficient at the Soret maximum (410 nm).

III. RESULTS AND DISCUSSION

A. STRUCTURAL IDENTIFICATION

Chromatographic (HPLC) analysis of the total sediment extract for the surface 10 cm of sediment in the Black Sea (Fig. 3-2) shows a series of compounds with visible spectra similar to that of ptn-*a*, but eluting 15 - 25 minutes after pptn-*a* . These compounds constitute ~17% of the total solvent extractable chlorophyll degradation products (determined by absorbance of total solvent extract at 665 nm). Each fraction isolated by HPLC was analyzed by visible spectrophotometry and CI-MS. The visible spectrum of each fraction is identical (Fig. 3-3), with $\lambda_{max\ (acetone)}$ at 410, 507, 536, 609, and 667 nm and S/R ratio an 2.31. This compares well to pptn-*a* with $\lambda_{max\ (acetone)}$ at 410, 505, 535, 609, and 667 nm and S/R ratio of 2.27. The close similarities in these spectra suggest structural similarities between these compounds. Chemical ionization MS shows each of the isolated PSE fraction to contain a mixture of compounds (Fig. 3-4a), all with a common fragment ion of m/e 535.

The CI-MS pseudo-molecular ions (M+1) for this complex mixture range from m/e 887 - 945 (Table 3-1). Loss of the alcohol esterified to the propionic acid group through ester cleavage followed by hydrogen transfer has been shown to occur in chlorophyll degradation products (Baker, 1970; Keely and Maxwell, 1990). The absence of an ion at m/e 593 indicates that the macrocycle is not pbd-*a*, and the occurrence of the single major ion at m/e 535 as the common fragment indicates that this series of compounds has a single common macrocycle, ppbd-*a*. The individual components of the complex mixture must therefore differ only in the esterifying alcohols. The identity of the macrocycle as ppbd-*a* is further substantiated by comparison of MS with that of authentic PSEs, and by co-elution of the hydrolysis product of the total PSEs with authentic ppbd-*a*.

To account for the range in molecular weights suggested by the CI-MS data, the molecular weights of the esterified alcohols must range from 370 to 428 a.m.u. In order to determine the identity of the esterified alcohols, PSE fraction 4 was hydrolyzed and the hydrolysis products analyzed by GC and GC/MS. Analysis by GC/MS shows that only sterols are produced upon hydrolysis of PSE fraction 4, and the major sterol in PSE fraction 4 is 24-methylcholesta-5,22-dien-3β-ol (Fig. 3-4b). To determine the identities of the remaining alcohols esterified to total PSEs, a fraction of total PSEs was hydrolyzed, acetylated, and analyzed by GC and GC/MS (Fig. 3-5). Pyropheophorbide steryl esters were also isolated from a second sediment sample and hydrolyzed. Qantitative analysis of the PSE hydrolysis products indicates a 90% recovery of the expected yield of sterols. No alcohols, other than sterols are present in the hydrolysis products of total PSEs (Ch. 5).

Table 3-1

MOLECULAR WEIGHTS AND ABUNDANCES AS DETERMINED BY CI-MS AND HPLC OF PSEs ISOLATED FROM BLACK SEA SEDIMENT

PSE Fraction	M+1	Intensity	Esterified Sterol	nmol/g dry wt
1	887[1]	95	24-norcholesta-5,22-dien-3β-ol	2.0
	901[2]	5	cholesta-5,22-dien-3β-ol	0.10
2	889	5	unknown	0.17
	901	82	cholesta-5,22-dien-3β-ol	2.8
	915	13	24-methylcholesta-5,24(28)-dien-3β-ol	0.45
3	901	16	cholesta-5,22-dien-3β-ol	0.18
	915	76	24-methylcholesta-5,24(28)-dien-3β-ol	0.87
	931	8	unknown	0.092
4	903	15	cholest-5-en-3β-ol	0.63
	915	81	24-methylcholesta-5,22-dien-3β-ol	3.4
	931	4	unknown	0.17
5	903	58	cholest-5-en-3β-ol	1.8
	917	16	unknown	0.48
	929	22	24-ethylcholesta-5,22-dien-3β-ol	0.70
	945	4	4α,23,24-trimethyl-5α-cholest-22-en-3β-ol	0.13
6	901	4	unknown	0.061
	903	8	cholest-5-en-3β-ol	0.12
	917	24	24-methylcholest-5-en-3β-ol	0.37
	929	41	24-ethylcholesta-5,22-dien-3β-ol	0.62
	943	9	unknown	0.14
	945	14	4α,23,24-trimethyl-5α-cholest-22-en-3β-ol	0.21
7	905	20	5α-cholestanol	0.27
	917	40	24-methylcholest-5-en-3β-ol	0.54
	929	9	24-ethylcholesta-5,22-dien-3β-ol	0.12
	931	20	24-ethylcholest-5-en-3β-ol	0.27
	943	4	unknown	0.054
	945	7	4α,23,24-trimethyl-5α-cholest-22-en-3β-ol	0.095
8	905	4	5α-cholestanol	0.087
	917	7	24-methylcholest-5-en-3β-ol	0.15
	919	6	unknown	0.13
	931	76	24-ethylcholest-5-en-3β-ol	1.7
	945	7	unknown	0.15

[1]Underlined M+1 values signify the major pseudo-molecular ion in CI-MS of each HPLC peak collected.
[2]Our HPLC separation does not completely resolve the mixture of pyropheophorbide steryl esters in our sample. Co-eluting sterols therefore appear in more than one PSE fraction.

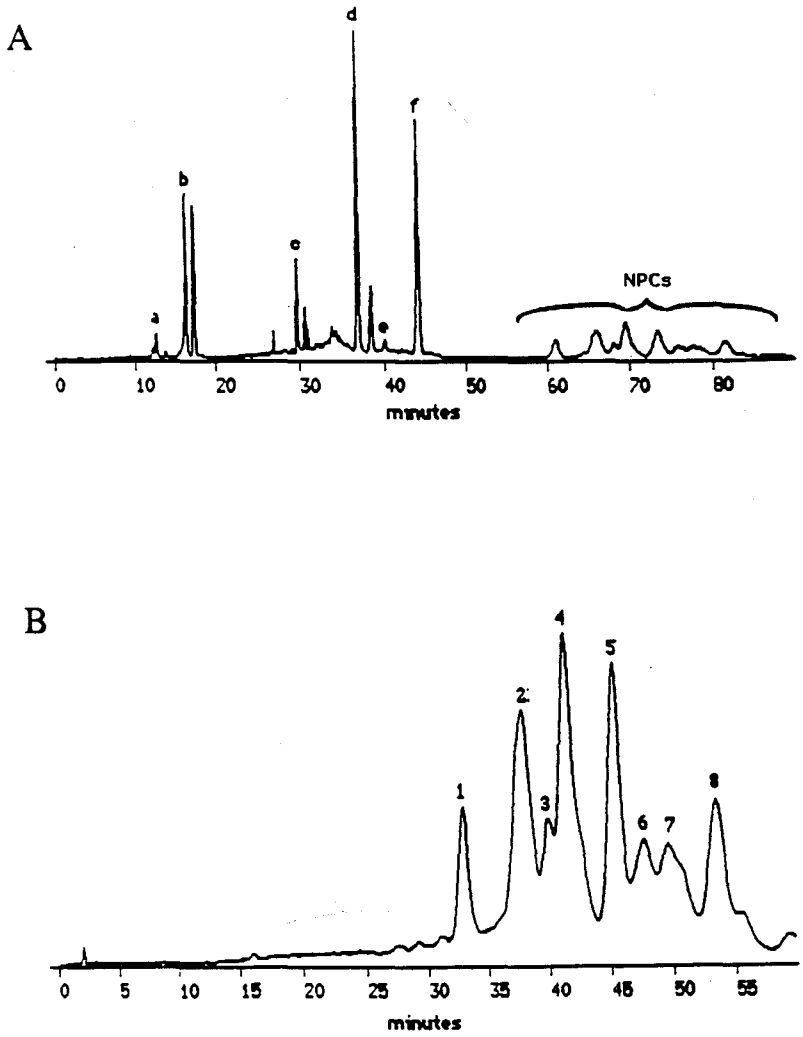

Fig. 3-2 (a) Fluorescence HPLC trace of the total solvent extract of sample BS2-0-10. Peak identifications are as follows: **a**) pheophorbide-*a*; **b**) pyropheophorbide-*a*, **c**) chlorophyll-*a*, **d**) pheophytin-*a*, **e**) pheophytin-*b*, **f**) pyropheophytin-*a*. (b) Fluorescence HPLC trace of the PSE isolate. Numbered peaks refer to the isolated PSE fractions.

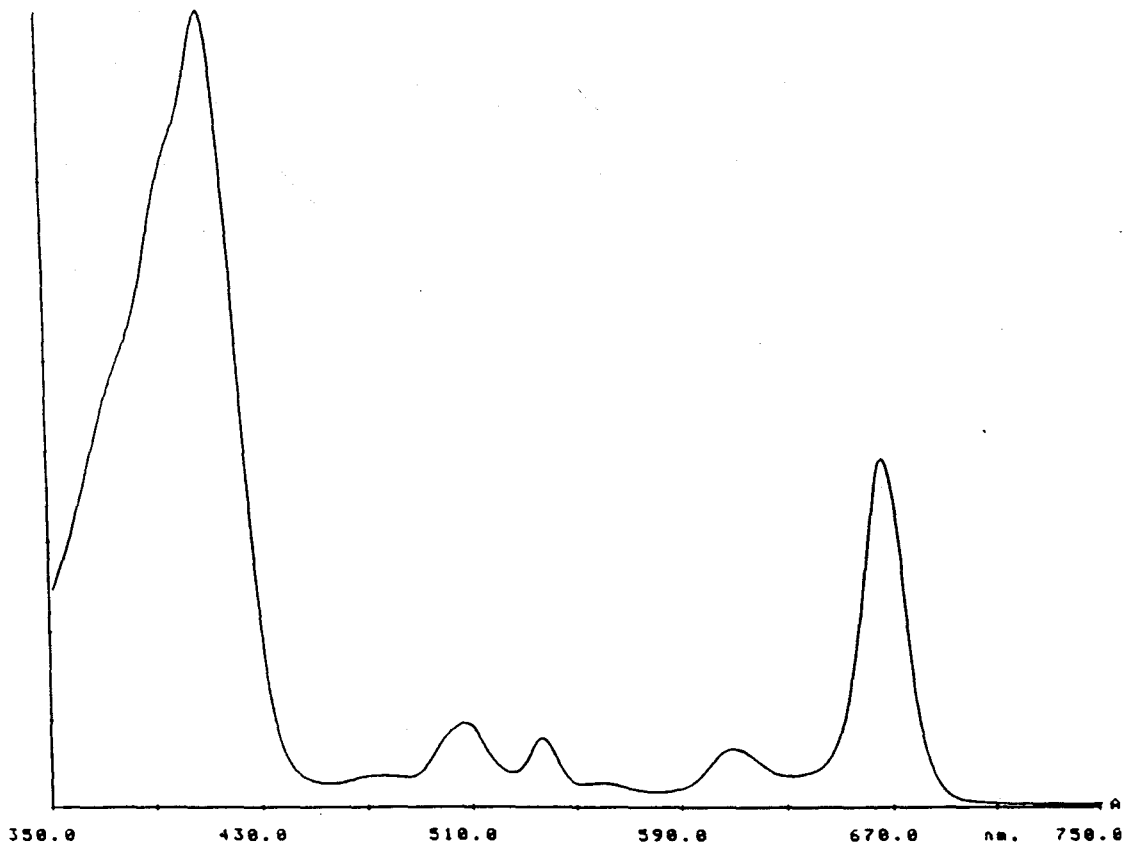

Fig. 3-3 Visible spectrum in 100% acetone of purified PSE fraction 4 from Black Sea sediment.

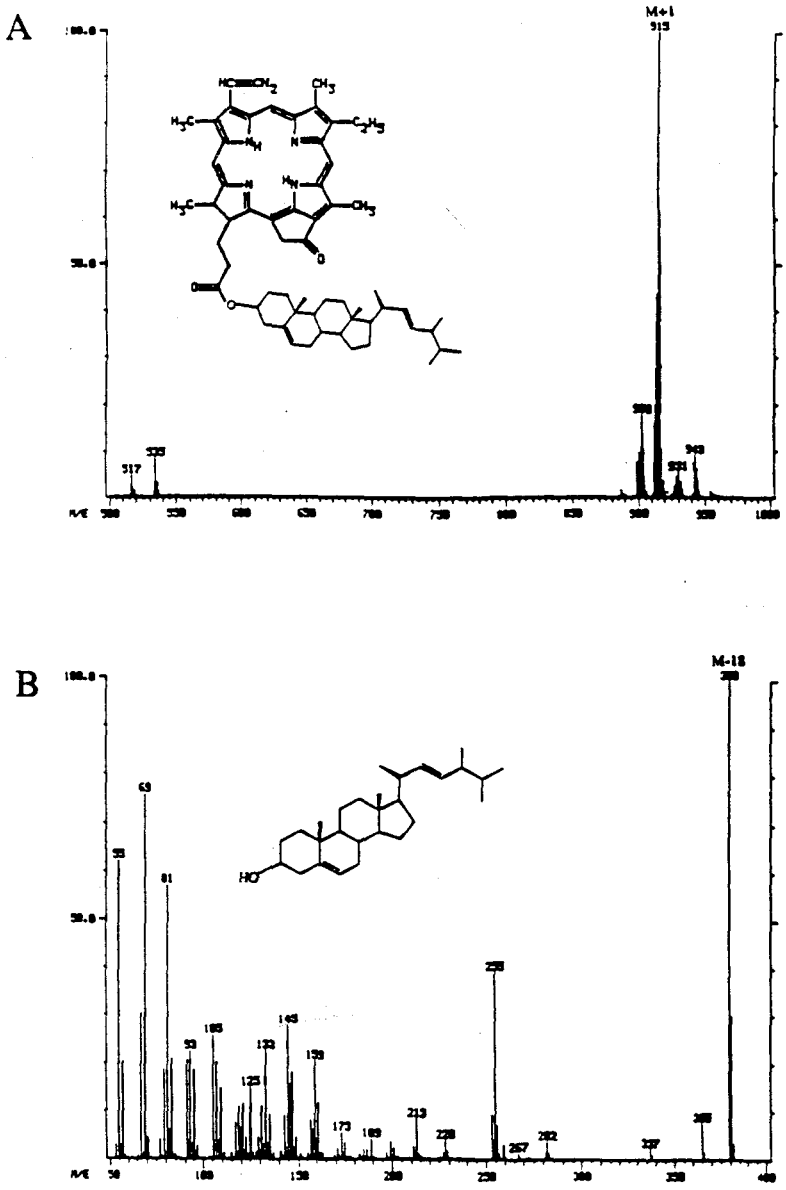

Fig. 3-4 (a) CI-MS of PSE4. (b) Mass spectrum from GC/MS of hydrolyzed PSE4.

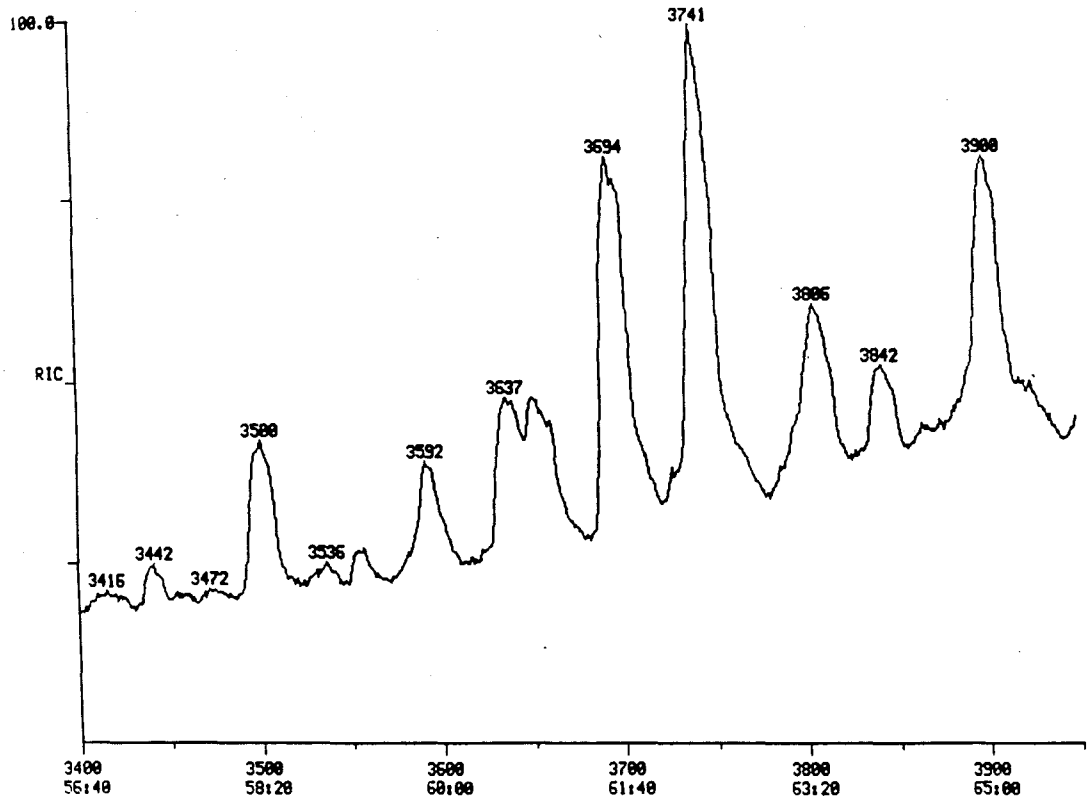

Fig. 3-5 GC/MS total ion chromatogram of sterols as acetates, hydrolyzed from total PSEs.

By comparing mass spectra with published data, the series of sterols was found to be (in order of decreasing abundance): 24-methylcholesta-5,22-dien-3β-ol, cholest-5-en-3β-ol (cholesterol), 24-ethylcholest-5-en-3β-ol, cholesta-5,22(Z)-dien-3β-ol, cholesta-5,22(E)-dien-3β-ol, 24-norcholesta-5,22-dien-3β-ol, 24-methylcholest-5-en-3β-ol, and 24-ethylcholesta-5,22-dien-3β-ol. Minor amounts of 24-methylcholesta-5,24(28)-dien-3β-ol, 5α(H)-cholestan-3β-ol (cholestanol), 24-ethyl-5α(H)-cholestan-3β-ol, 4α,23,24-trimethyl-5α(H)-cholest-22-en-3β-ol (dinosterol), and 4α,24-dimethyl-5α(H)-cholestan-3β-ol were also detected. The identity of pyropheophorbide-*a* cholesterol ester is further supported by co-elution of this compound with authentic pyropheophorbide-*a* cholesterol ester.

The only other reported occurrence of steryl esters of chlorophyll degradation products is by Prowse and Maxwell (1991) and Eckardt *et al.* (1991). In a Miocene oil shale, Prowse and Maxwell (1991) isolated pyropheophorbide-*a* and mesopyropheophorbide-*a* esterified to 24-ethyl-4α-methylcholestan-3β-ol, and from a eutrophic lake sediment, Eckardt *et al.* (1991) isolated pyropheophorbide-*a* esterified to 16 different sterols.

B. SPECTROSCOPIC CHARACTERIZATION OF AUTHENTIC COMPOUNDS

We synthesized four authentic pyropheophorbide-*a* steryl esters from pyropheophorbide-*a* and the sterols brassicasterol, β-sitosterol, cholesterol, and stigmasterol. These four sterols were chosen since they occur in high concentrations in both non-esterified solvent-extractable sedimentary sterols and PSE sterols. The authentic compounds were characterized by visible spectrophotometry, NMR, and CI-MS. Their HPLC behavior was also investigated. The visible spectrum of each pyropheophorbide-*a* steryl ester was identical with λ_{max} at 410 and 666 nm and S/R of 2.23. Using pyropheophorbide-*a* cholesteryl ester, the extinction coefficient at the Soret maximum (410 nm) was determined to be 9.5×10^4 L/molxcm. This value is only 91% of that for pyropheophytin-*a*, though the NMR and MS data suggests that the synthetic pyropheophorbide-*a* cholesterol ester is pure.

The methane CI-MS of each authentic pyropheophorbide-*a* steryl ester was taken for comparison with PSEs isolated from sediments, and to compare the fragmentation pathway of the PSEs with other chlorophyll-*a* degradation products. Each PSE produced a pseudo-molecular ion at 1 a.m.u. above the nominal mass of the compound and a single major fragment at 535 a.m.u. (Fig. 3-6 and Appendix II). The pseudo-molecular ions for pyropheophorbide-*a* brassicasteryl ester, β-sitosteryl ester, cholesteryl ester, and stigmasteryl ester occur at m/z 915, 931, 903, and 929 respectively. The fragment at m/z

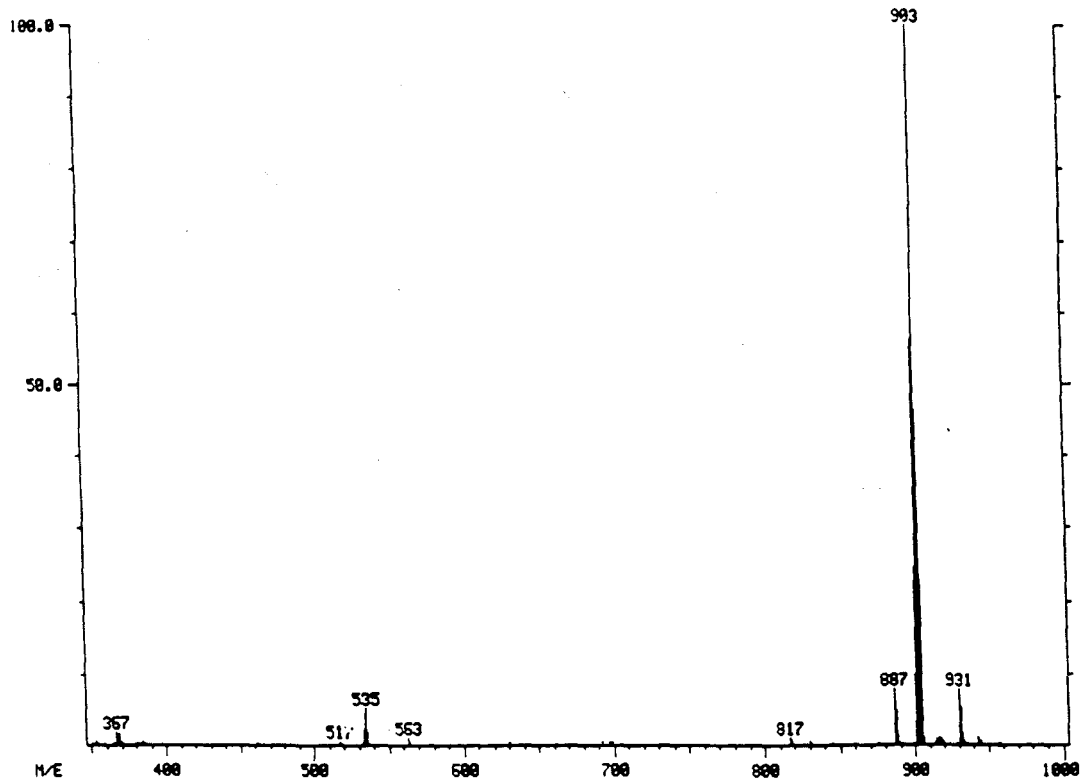

Fig. 3-6 CI-MS of authentic pyropheophorbide-*a* cholesteryl ester.

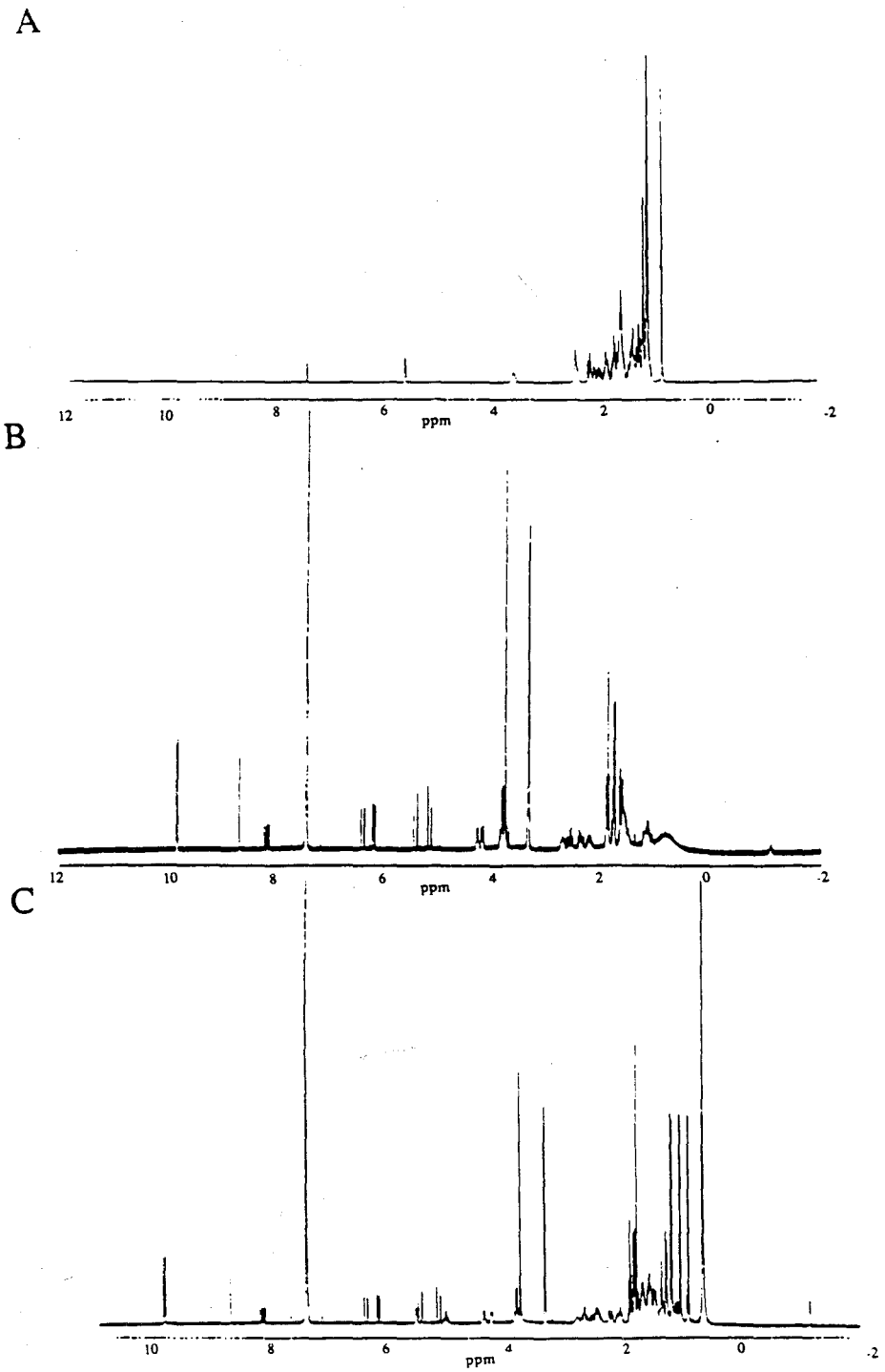

Fig. 3-7 300 MHz NMR spectra in d_6-benzene. a) authentic cholesterol. b) authentic pyropheophorbide-*a*. c) authentic pyropheophorbide-*a* cholesteryl ester.

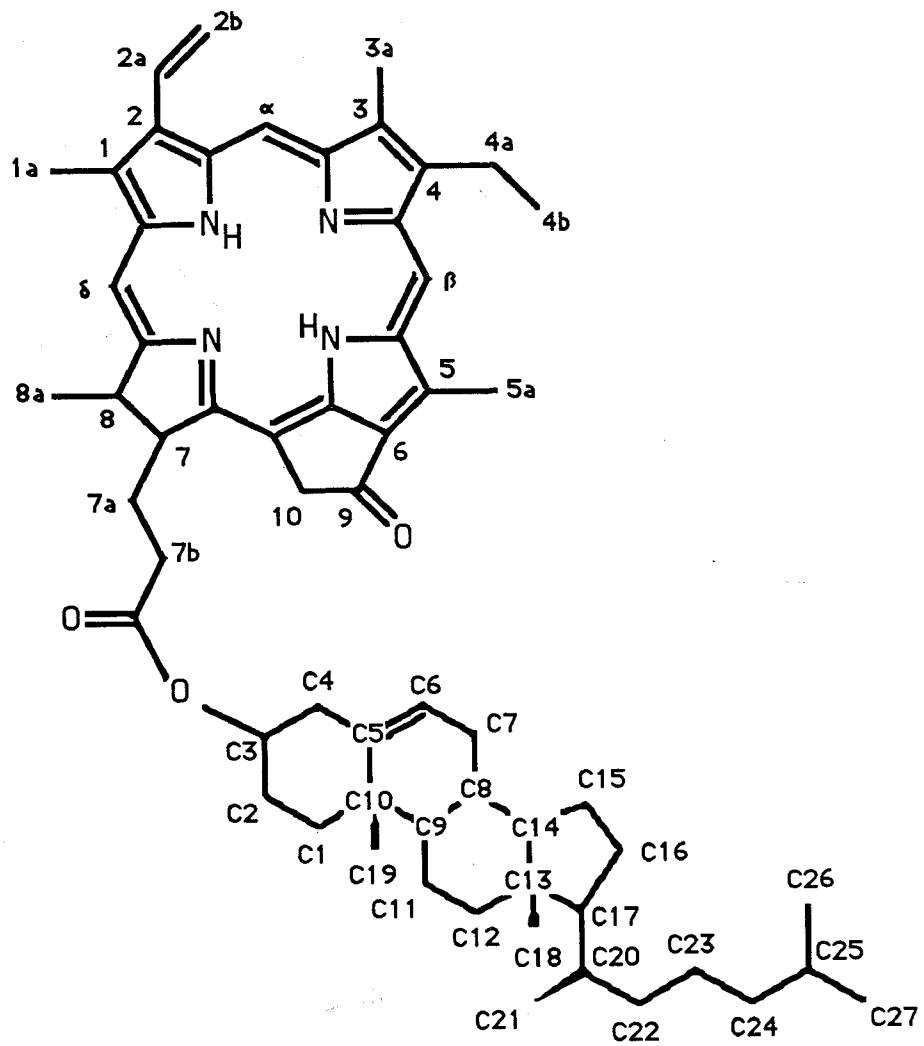

Fig. 3-8 Structure of pyropheophorbide-*a* cholesteryl ester showing the numbering system used in the spectroscopic studies.

535, common to each MS, represents the loss of the sterol and formation of pyropheophorbide-*a*.

The NMR spectra of the authentic PSEs are similar to each other and to pyropheophorbide-*a*. The NMR spectra of pyropheophorbide-*a* cholesteryl ester, pyropheophorbide-*a* and cholesterol are shown in Fig. 3-7. Due to the strong paramagnetic anisotropy of the phorbin macrocycle ring current, the majority of the resonance attributable to the phorbin portion of pyropheophorbide-*a* cholesteryl ester are shifted downfield of the resonances of cholesterol. The resonances caused by protons on the parent pyropheophorbide-*a* compound are (numbering shown in Fig. 3-8): N-H, -1.17(s); N-H, 0.92(s); α-H, 9.85(s); β-H, 9.88(s); δ-H, 8.71(s); 1a-CH_3, 3.37(s); 2a-H, 8.15(dd); 2b-H_A, 6.39(dd); 2b-H_B, 6.18(dd); 3a-CH_3, 3.36(s); 4a-CH_2, 3.85(q); 4b-CH_3, 1.19(t); 5a-CH_3, 3.79(s);7-H, 4.28(m); 7a,7b-CH_2, 2.05-2.90; 8-H, 4.41(q); 8a-CH_3, 1.83(d); 10^1-H, 5.41(d); and 10^2-H, 5.17(d). The protons on the methyl groups of the cholesterol esterified to the C7 propionic acid group on pyropheophorbide-*a* can also be identified: C-18, 0.88(s); C-19, 1.03(s); C-26 and C-27, 1.18(dd); and C-21, 1.27(d). The protons at C-3 and C-6 resonate at 5.05(m) and 5.55(d) respectively. With the exception of the resonances for the protons on the C-3, C-6, and C-19 carbons of the esterified cholesterol, the chemical shifts for the protons of pyropheophorbide-*a* cholesteryl ester are nearly identical to those of pyropheophorbide-*a* and cholesterol.

C. ORIGIN OF PYROPHEOPHORBIDE-*A* STERYL ESTERS

The possible sources of pyropheophorbide-*a* steryl esters (PSEs) are direct biosynthesis by phytoplankton, production in sediments through bacterial activity, or production in the water column through heterotrophic activity. The direct biosynthesis of these compounds is unlikely since extensive surveys of phytoplankton pigments have never revealed the existence of these compounds.

In order to differentiate between a water column and sedimentary source, the solvent-extractable sedimentary sterols were analyzed by GC and GC/MS (Fig. 3-9) and their distributions compared to that of the PSE sterols. Analysis of solvent-extractable sedimentary sterols shows the distribution of these compounds to differ from those in the PSEs (Fig. 3-10). In order of decreasing concentration, the non-esterified solvent-extractable sedimentary sterols are: 4α,23,24-trimethylcholest-22-en-3β-ol (dinosterol), 4α,24-dimethyl-5α-cholestan-3β-ol, 24-ethylcholest-5-en-3β-ol, 4α,23,24-trimethyl-5α-cholestan-3β-ol, 24-methylcholesta-5,22-dien-3β-ol, 23,24-methylcholest-22-en-3β-ol, 4α,24-dimethyl-5α-cholest-22-en-3β-ol, 24-methyl-5α-cholestan-3β-ol, 4α,22,23-trimethyl-5α-cholestan-3β-ol, 24-ethylcholesta-5,22-dien-3β-ol, 24-methylcholest-22-en-

3β-ol, cholest-5-en-3β-ol, cholesta-5,22Z-dien-3β-ol, 24-ethyl-5α-cholestan-3β-ol, 24-methylcholest-5-en-3β-ol, 24-methylcholesta-5,24(28)-dien-3β-ol, 23,24-dimethylcholesta-5,22-dien-3β-ol, 24-ethylcholest-22-en-3β-ol, cholesta-5,22E-dien-3β-ol, 5α-cholestan-3β-ol, 22,23-methylene-4α,24-dimethyl-5α-cholestan-3β-ol, 27-nor-24-methyl-5α-cholestan-3β-ol, and 24-norcholesta-5,22-dien-3β-ol. This sterol distribution agrees both quantitatively and qualitatively with earlier studies of sedimentary sterols by Lee *et al.* (1980) de Leeuw *et al.* (1983) and Wakeham and Beier (1991).

The large differences in the distribution of non-esterified solvent-extractable sterols and PSE-derived sterols are apparent from Fig. 3-10; the most notable difference being the low levels of 4-methyl sterols in the PSE sterol distribution, compared to the solvent-extractable sterol distribution. A comparison of the PSE sterol distribution with the solvent extractable esterified sedimentary sterols and the base-extractable sterols can be made using literature data. Using the data of de Leeuw *et al.* (1983), the PSE sterol distribution is most similar to that of the base-extractable sterol distribution. In the base-extractable sterols, 4-desmethyl sterols are the major sterols with 24-methylcholesta-5,22-dien-3β-ol being the major sterol. This sterol is also the major sterol in the PSE sterols and in the 4-desmethyl non-esterified solvent-extractable sterols, but in the non-esterified solvent-extractable sterols, the 4-methyl sterols are the most important sterols quantitatively. For the distribution of sterols to be different in the PSE and non-esterified solvent-extractable sterol fractions, the esterification of sterols with pyropheophorbide-*a* must be selective or formation of PSEs must occur in the water column or at the sediment water-interface. It is therefore necessary to examine the likelihood of a water column source for PSEs.

To examine the possibility of a water column source for the PSEs, PSE sterol data was compared with Black Sea water column sterol data from the literature (Fig. 3-11). The analysis of water column sterols provides a means of examining the sterol distribution in the water column at a single point in time, whereas the analysis of the PSE sterols in sediments from 0-10 cm represents an integration over 500 years. Comparison of the PSE sterols with the suspended particulate matter (oxic zone) data of Gagosian and Heinzer (1979), and sediment trap data of Wakeham and Beier (1991) shows the PSE sterols to be more similar quantitatively to water column sterol distributions than sediment sterol distributions, although not all the sterols analyzed in the sediments and PSEs were reported for the water column samples. In their water column suspended particulate matter sterols, Gagosian and Heinzer (1979) do not report the distribution of 4-methyl sterols, but these sterols are reported by Wakeham and Beier (1991). The major difference between sedimentary and water column sterol distributions is the presence of considerably less dinosterol and other 4-methyl sterols in sediment trap samples (Wakeham and Beier, 1991)

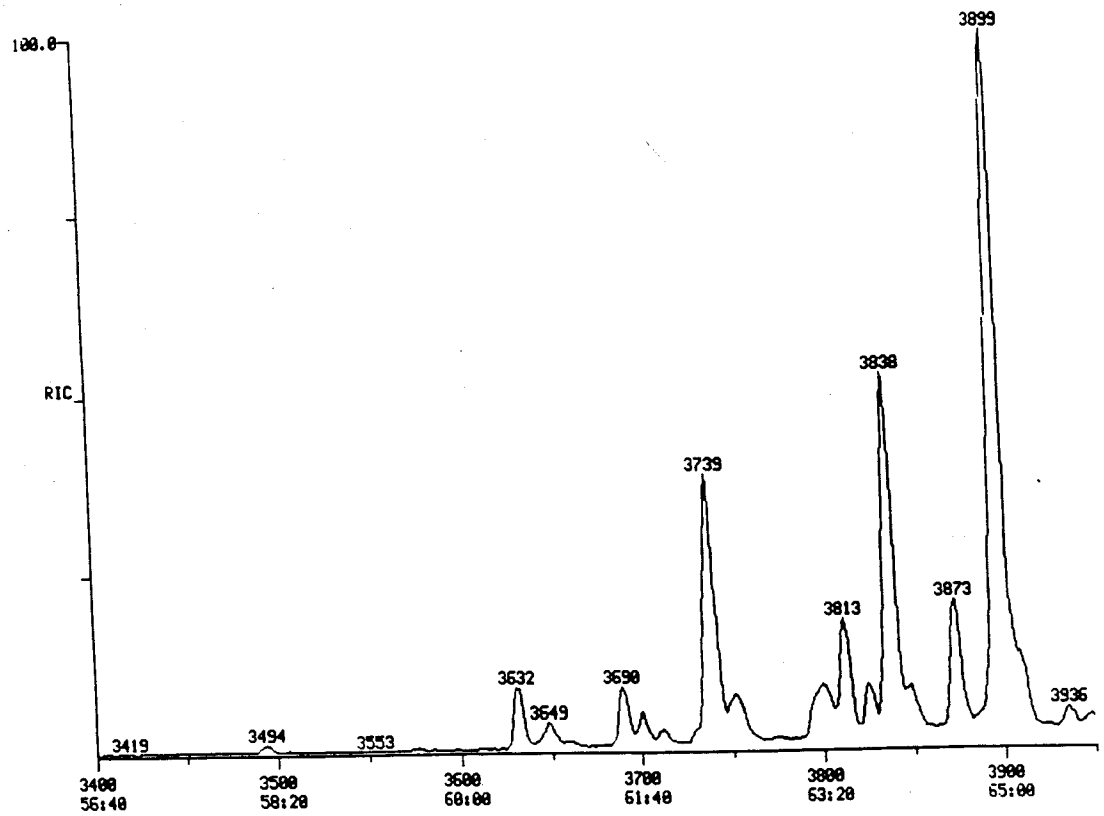

Fig. 3-9 GC/MS total ion chromatogram of solvent-extractable sedimentary sterols.

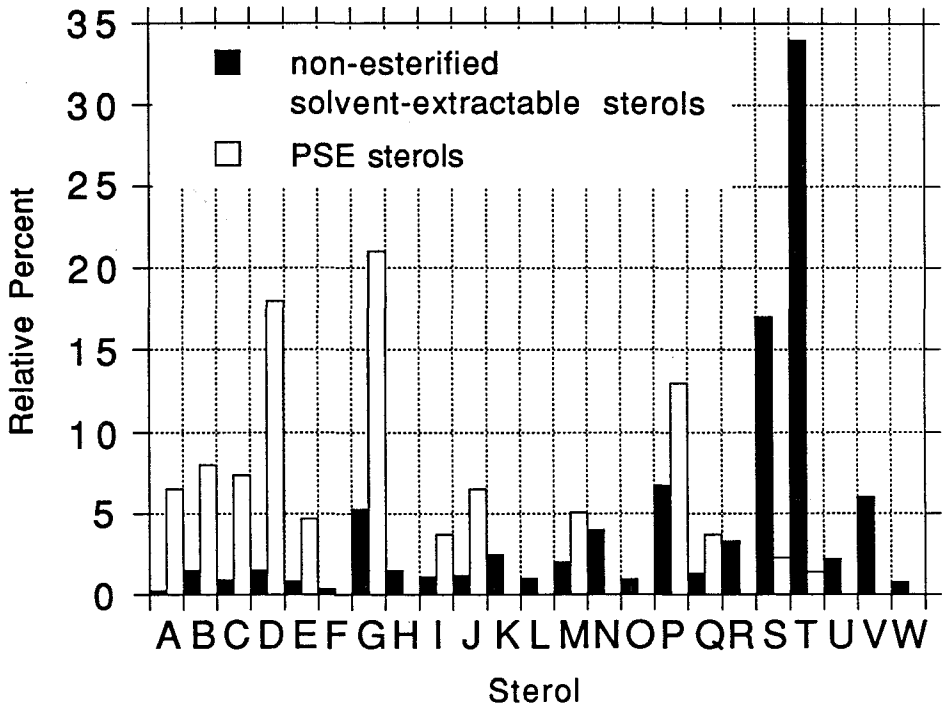

Fig. 3-10 A comparison of the relative contribution of individual sterols to the PSE sterols and solvent extractable sedimentary sterols. Sterol identifications: **A**) 24-norcholesta-5,22-dien-3β-ol, **B**) cholesta-5,22Z-dien-3β-ol, **C**) cholesta-5,22E-dien-3β-ol, **D**) 5α-cholesten-3β-ol, **E**) 5α-cholestan-3β-ol, **F**) 27-nor-24-methyl-5a-cholestan-3β-ol (tentative identification based on molecular weight and retention time only), **G**) 24-methylcholesta-5,22-dien-3β-ol, **H**) 24-methyl-5α-cholest-22-en-3β-ol, **I**) 24-methylcholesta-5,24(28)-dien-3β-ol, **J**) 24-methylcholest-5-en-3β-ol, **K**) 24-methyl-5α-cholestan-3β-ol, **L**) 23,24-dimethylcholesta-5,22-dien-3β-ol, **M**) 24-ethyl-5,22-dien-3β-ol, **N**) 23,24-dimethylcholest-22-en-3β-ol, **O**) 24-ethylcholest-22-en-3β-ol, **P**) 24-ethylcholest-5-en-3β-ol, **Q**) 24-ethyl-5α-cholestan-3β-ol, **R**) 4α,24-dimethyl-5α-cholest-22-en-3β-ol, **S**) 4α,24-dimethyl-5α-cholestan-3β-ol, **T**) 4α,23,24-trimethylcholest-22-en-3β-ol, **U**) 4α,22,23-(or 4α,22,24-)trimethyl-5α-cholestan-3β-ol **V**) 4α,23,24-trimethyl-5α-cholestan-3β-ol, and **W**) 22,23-methylene-4α,24-dimethyl-5α-cholestan-3β-ol.

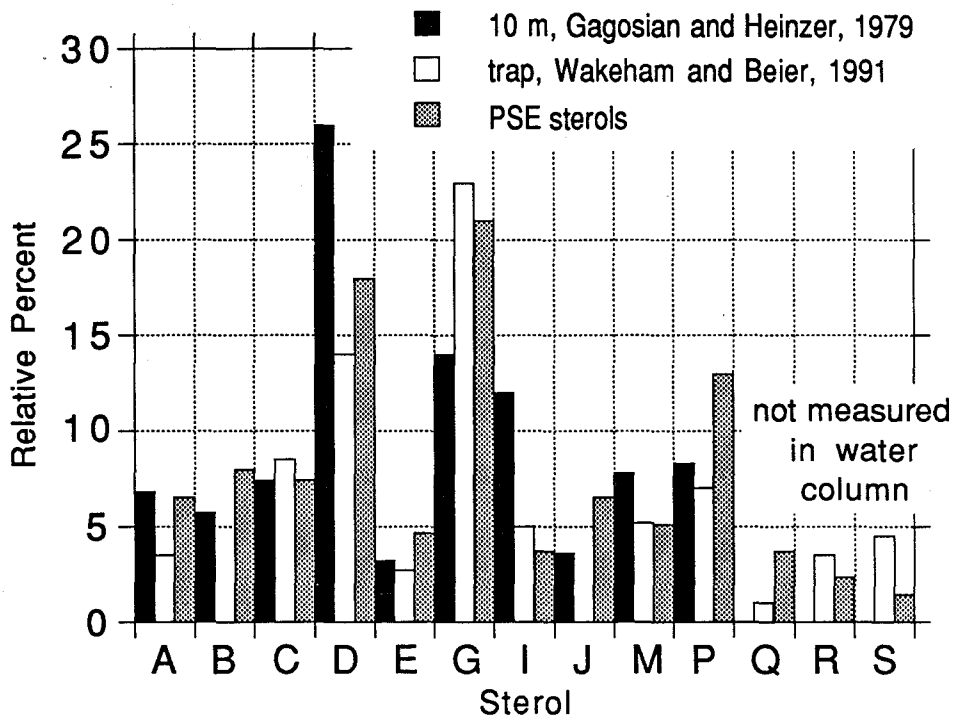

Fig. 3-11 A comparison of the relative contribution of individual sterols to water column samples, sediment trap samples, and sedimentary PSE sterols. Data from water column sterols collected at 10 m, Gagosian and Heinzer, 1979; solvent-extractable sterols from a sediment trap sample, Wakeham and Beier, 1991; hydrolyzed PSE sterols, this study. Sterols are identified as they are in Fig. 3-10.

than in sediments. The low abundance of 4-methyl sterols in sediment trap samples relative to sedimentary sterols agrees favorably with the PSE sterol distribution. This conclusion is supported by studies of sterols and PSEs in sediment and sediment trap samples from the Black Sea central basin (Ch. 5). Differences between the distribution of solvent-extractable sterols in sediment traps and sediments can be explained by differences between the degradation rates of 4-methyl and 4-desmethyl sterols in sediments. In sediments, sterols are dehydrated to sterenes. The 4-desmethyl sterols are dehydrated more readily than 4-methyl sterols possibly due to hinderence by the 4-methyl group on 4-methyl sterols (Gagosian *et al.*, 1980; Wolf *et al.*, 1986). It is this latter process, which may be microbially mediated (Gagosian *et al.*, 1980), which most likely accounts for the observed rapid decrease in 4-desmethyl sterols between sediment traps placed in the anoxic water column and underlying sediments. As a comparison, the contribution of 4-desmethylsterols to total base-hydrolyzable solvent-extractable and total base-hydrolyzable residual sterols is 2 - 4 times greater than in total non-esterified solvent-extractable sterol (de Leeuw *et al.*, 1983).

Rapidly sinking fecal pellets egested by zooplanktonic herbivores transport sterols from suspended particulate matter in the euphotic zone to surface sediments. Michaelis *et al.* (1987) measured the seasonal flux of sterols to sediments using a sediment trap deployed at 1200 m. Two distinct flux maxima, one during June - July and one during August - September, contributed greater than 98% of the total sterols to sediments, with nearly 50% of the total flux occurring in two 10 day periods between July 2 - 13 and August 28 - September 8. During these high flux periods, the distribution of sterols in the sediment trap samples was qualitatively similar to the distribution of sterols in our PSE sample, with cholesterol, 24 methyl- and 24-ethylcholesta-5,22-dien-3β-ol, and 24-ethylcholest-5-en-3β-ol being relatively abundant.

Further evidence for a water column source for the PSEs is found in the stanol/stenol ratios. Conversion of stenols to stanols can occur through microbially mediated hydrogenation (Eyssen *et al.*, 1973), and an increase in the stanol/stenol ratio with depth has been shown to occur in anoxic sediments (Gaskel and Eglinton, 1975, 1976; Nishimura and Koyama, 1977; Nishimura, 1978). Non-esterified solvent-extractable sterols in Black Sea sediments have stanol/stenol ratios of 0.5 - 3.9. The stanol/stenol ratios of both the base-hydrolyzable solvent-extractable and the base-hydrolyzable residue sterols are greater than 1 (de Leeuw *et al.*, 1983). Sterols in Black Sea suspended particulate matter from the oxic water column (Gagosian *et al.*, 1979; Wakeham and Beier, 1991) and in sediment traps (Wakeham and Beier, 1991) have stanol/stenol ratios of 0.1 - 0.3. Stanol/stenol ratios in PSE sterols were difficult to

determine due to contaminant hydrocarbons introduced from the RPLC column which coeluted with the sterols during GC and GC/MS. From molecular ion intensity in probe MS analysis and from GC analysis, estimates of cholestanol/cholesterol are ≤ 0.1. This ratio is much closer to water column stanol/stenol ratio values and suggests that some process has protected the PSE stenols from reduction to stanols.

The stanol/stenol ratios of PSE sterols suggests an upper water column source for the PSEs with rapid removal of the PSEs from the water column to the sediments. Wakeham (1989) compared stanol/stenol ratios of sterols in sediment, suspended particulate matter, and sediment trap samples from environments with anoxic water columns: Black Sea, Carioco Trench, and the oxygen minimum zone of the Eastern Sub-tropical Pacific. Wakeham's (1989) data shows suspended particulate matter to have low stanol/stenol ratios in oxic surface waters. Below the oxic/anoxic interface in the Black Sea and Cariaco Trench and below the onset of suboxic conditions in the Pacific, the stanol/stenol ratio in suspended particulate matter increases to that of the sediment sterols. Sediment trap samples from the anoxic portion of the water column have low stanol/stenol ratios, similar to those of samples from the upper oxic water column. The difference in the stanol/stenol ratios in the two types of samples arises from the very rapid sinking rate of large particles collected in sediment traps and the negligible to low sinking rate of suspended particulate matter. The oxic/anoxic interface of the Black Sea is a strong redox boundary and is inhabited by a community of sulfate reducing bacteria (Jannasch *et al.*, 1974). The suspended particulate matter sinks slowly through the chemocline, giving the microbial community inhabiting the redox interface time to reduce stenols to stanols (Wakeham, 1989). The faster sinking particles caught in sediment traps pass through the oxic/anoxic interface with little stenol to stanol conversion. The incorporation of PSEs into large sinking particles suggests a means by which the PSE sterols can be protected from stenol to stanol conversion during passage through the chemocline.

There are two ways in which the PSEs could be introduced as part of large particles in the upper water column: through sediment resuspension or through grazing. Georicke (unpublished data) found a complex mixture of PSEs in suspended particulate matter from the Sargasso Sea. In the euphotic zone, the potential for very rapid photooxidation places an upper limit on the lifetime of pheopigments at approximately 10 days (SooHoo and Kiefer, 1982; Welschmeyer and Lorenzen, 1985), and grazing reduces the lifetime to less than 2.5 days (Burkill *et al.*, 1987). Rapid rates of photooxidation and grazing make it unlikely that pheopigments in the Sargasso Sea, such as the PSEs, have an origin from a detrital component advected into the open ocean from the adjacent continental margin. Photo-oxidation and grazing of pigments in the surface ocean would remove the pigments

before significant lateral transport could occur. The studies of Downs (1989) suggests a source for these compounds from zooplankton grazing on phytoplankton. Reversed-phase HPLC analysis of the total organic extract of fecal pellet material from feeding studies using cultured *Euphausiid pacifica*, *Pleuroncodes planipes* (crabs), *Phialidium* (medusae), *Pleurobrachia* (ctenophore) and *Calanus pacifica* (copepods) fed phytoplankton show pigments at the retention time appropriate for PSEs. From the data provided by Downs (1989) we could not unambiguously identify these compounds as PSEs, but the data does provide supporting evidence for a grazing origin for PSEs. Prowse and Maxwell (1991) also concluded that the formation of pyropheophorbide-*a* steryl esters was biologically mediated, and not the result of the degradation of a directly biosynthesized unidentified chlorophyll steryl ester.

IV. CONCLUSIONS

Structural analysis of a series of compounds eluting well after pptn-*a* has shown this complex mixture of compounds to be a series of ppbd-*a* steryl esters. The sterol distribution, stanol/stenol ratio, and Down's (1989) grazing data suggest ppbd-*a* steryl esters are formed during grazing. The formation of a series of products, each with the same macrocycle, ppbd-*a*, suggests a specific mechanism of formation. The sterol distribution and stanol/stenol ratios are consistent with an upper water column source with rapid removal to sediments, such as would occur during grazing. If grazing is the mode of formation of PSEs, then the differences in PSE sterol distributions and non-esterified solvent-extractable sterol distributions suggests that non-esterified solvent-extractable sterols are not a good indicator of the distribution of organism living in the surface ocean, but PSE sterols may provide a means of determining the distribution of sterols as found in sediment trap samples.

V. REFERENCES

Downs J. N. (1989) Implications of the phaeopigments, carbon and nitrogen content of sinking particles for the origin of export production. Ph.D. dissertation, Univ. of Washington.

Eyssen H. J., Parmentier G. G., Compernolle G. C., De Pauw G., and Piessens-Denef M. (1973) Biohydrogenation of sterols by *Eubacterium* ATCC 21,408 -- *Nova* Species. *Eur. J. Biochem.* **36**, 411-421.

Farrington J. W., Davis A. C., Sulanowski J., McCaffrey M. S., McCarthy M. A., Clifford C. H., Dickinson P., and Volkman J. K. (1988) Biogeochemistry of lipids in surface sediments of the Peru upwelling area - 15°S. In: *Advances in Organic Geochemistry 1987* (eds. L. Mattavelli and L. Novelli). *Org Geochem.* **13**, 607-617.

Furlong E. T. and Carpenter R. (1988) Pigment preservation and remineralization in oxic coastal marine sediments. *Geochim. Cosmochim. Acta* **52**, 87-99.

Gagosian R. B. and Heinzer R. (1979) Stenols and stanols in the oxic and anoxic waters of the Black Sea. *Geochim. Cosmochim. Acta* **43**, 471-486.

Gagosian R. B., Lee C., and Heinzer F. (1979) Processes controlling the stanol/stenol ratio in Black Sea seawater and sediments. *Nature* **280**, 575-576.

Gagosian R. B., Smith S. O., Lee C. L., Farrington J. W., and Frew N. E. (1980) Steroid transformations in recent marine sediments. In: Advances in Organic Geochemistry 1979 (Ed. A.G. Douglas and J.R. Maxwell) pp. 407-419.

Gaskel S. J. and Eglinton G. (1975) Rapid hydrogenation of sterols in a contemporary lacustrine sediment. *Nature* **254**, 209-211.

Gaskel S. J. and Eglinton G. (1976) Sterols of a contemporary lacustrine sediment. *Geochim. Cosmochim. Acta***40**, 1221-1228.

Gillan F. T. and Johns R. B. (1980) Input and early diagenesis of chlorophyll in a temperate intertidal sediment. *Mar. Chem.* **9**, 243-253.

Harvey H. R., O'Hara S. C. M., Eglinton G., and Corner D. S. (1989) The comparative fate of dinosterol and cholesterol in copepod feeding: Implications for a conservative molecular biomarker in the marine water column. *Org. Geochem.* **14**, 635-641.

Hurley J. P., and Armstrong D. E. (1990) Fluxes and transformations of aquatic pigments in Lake Mendota, Wisconsin. *Limnol. Oceanogr.* **35**, 384-398.

Jannasch H. W., Truper H. G., and Tuttle J. H. (1974) Microbial sulfur cycle in Black Sea. In *The Black Sea -- Geology, Chemistry, and Biology* (eds. E. T. Degens and D. A. Ross) pp. 419-425. American Association f Petroleum Geologists.

Keely B. J. (1989) Early diagenesis of chlorophyll and chlorin pigments. Ph.D. dissertation, Univ. of Bristol.

Keely B. J., and Brereton R. G. (1986) Early chlorin diagenesis in a recent aquatic sediment. In *Advances in Organic Geochemistry 1985*, *Org. Geochem.* **10**, 975-980.

Keely, B. J., Prowse, W. G., and Maxwell, J. R. (1990) The Treibs hypothesis: An evaluation based on structural studies, *Energy Fuels* **4**, 628-634.

Keely B. J. and Maxwell J. R. (1990) Fast atom bombardment mass spectrometric and tandem mass spectrometric studies of some functionalized tetrapyrroles derived from chlorophylls *a* and *b*. *Energy Fuels* **4**, 737-741.

de Leeuw J. W., Rijpstra W. I. C., Schenck P. A., and Volkman J. K. (1983) Free, esterified and residual bound sterols in Black Sea Unit I sediments. *Geochim. Cosmochim. Acta* **47**, 455-465.

Lee C., Gagosian R. B., and Farrington J. W. (1980) Geochemistry of sterols in sediments from Black Sea and the southwest African shelf and slope. *Org. Geochem.* **2**, 103-113.

McCaffrey M. A. (1990) Sedimentary lipids as indicators of depositional conditions in the coastal Peruvian upwelling regime. Ph.D. dissertation, MIT/WHOI, WHOI-90-29.

Michaelis W., Schumann P., Ittekkot V., and Konuk T. (1987) Sterol markers for organic matter fluxes in the Black Sea. *SCOPE/UNEP Sonderband Heft 62, Mitt. Geol.-Palaeont. Inst. Univ. Hamburg*, 89-98.

Nishimura M. (1978) Geochemical characteristics of the high reduction zone of stenols in Suwa sediments and the environmental factors controlling the conversion of stenols into stanols. *Geochim. Cosmochim. Acta* **42**, 349-357.

Nishimura M. and Koyama T. (1977) The occurrence of stanols in various living organisms and the behavior of sterols in contemporary sediments. *Geochim. Cosmochim. Acta* **41**, 379-385.

Ross D. A., Uchupe E., and Bowin C. O. (1974) Shallow structure of the Black Sea, In: The Black Sea--Geology, Chemistry, and Biology, E. T. Degen and D. A. Ross, Eds. Am. Assoc. Petrol. Geol. pp 1-10.

SooHoo J. B. and Kiefer D. A. (1982) Vertical distribution of phaeopigments: I. A simple grazing and photooxidative scheme for small particles. *Deep Sea Res.* **29**, 1982.

Treibs A. (1936) Chlorophyll- and Haminderivate in organischen Mineralstoffen. *Angew. Chem.* **49**, 682-686.

Verne-Mismer J., Ocampo R., Callot H. J., and Albrecht P. (1988) Molecular fossils of chlorophyll-*c* of the 17-nor0DPEP series. Structure determination, synthesis, and geochemical significance. *Tetrahedron. Lett.* **29**, 371-374.

Volkman J. K., Gagosian R. B., and Wakeham S. G. (1984) Free and esterified sterols of the marine dinoflagellates *Gonyaulax polygramma*. *Lipids* **19**, 457-465.

Wakeham S. G. (1989) Reduction of sterols to stanols in particulate matter at oxic-anoxic boundaries in seawater. *Nature* **342**, 787-790.

Wakeham S. G. and Beier J. A. (1991) Organic biomarkers as indicators of particulate matter source and alteration processes in the water column of the Black Sea. *NATO Advanced Research Workshop on Black Sea Oceanography.*

Welshmeyer N. A. and Lorenzen C. J. (1985) Chlorophyll Budgets: Zooplankton grazing and phytoplankton growth in a temperate fjord and the Central Pacific gyres. *Limnol. Oceanogr.* **30**, 1-21.

Wolff G. A., Lamb N. A., and Maxwell J. R. (1986) The origin and fate of 4-methyl steroids -- II. Dehydration of stanols and occurrence of C_{30} 4-methyl steranes. *Org. Geochem.* **10**, 965-974.

CHAPTER 4

HIGH MOLECULAR WEIGHT AND ACID EXTRACTABLE CHLOROPHYLL DEGRADATION PRODUCTS IN BLACK SEA SEDIMENTS

CHAPTER 4

HIGH MOLECULAR WEIGHT AND ACID EXTRACTABLE CHLOROPHYLL DEGRADATION PRODUCTS IN BLACK SEA SEDIMENTS

I. INTRODUCTION

Many naturally occurring organic compounds are known to be deposited in sediments either in a complex macromolecular form (biomacromolecules), or incorporated into a macromolecular structure during degradation (geomacromolecules). Biomacromolecules include algaenan, cutins, and lignins. Examples of geomacromolecules include fulvic and humic acids, bitumen, and kerogen. Incorporation of chlorophyll degradation products into macromolecular organic structures is one potential sink for chlorophyll degradation products which appear to be lost during early diagenesis. Evidence for the formation of high molecular weight chlorophyll degradation products was first proffered by Blumer (Blumer and Snyder, 1967; Blumer and Rudrum, 1970) who isolated compounds from shales with porphyrin-like visible spectra having molecular weights of up to 20,000 a.m.u.. Since this work, additional evidence for the inclusion of porphyrins into high molecular weight organic matter and kerogen has been obtained.

Using gel permeation chromatography (GPC) and thin layer chromatography, Blumer and Rudrum (1970) isolated vanadyl porphyrins from maltenes and asphaltenes extracted from Serpiano oil shale and Leo shale with molecular weights of greater than 1000 a.m.u.. From mass spectrometric and infrared spectroscopic evidence, Blumer and Rudrum (1970) suggested these high molecular weight structures were porphyrin dimers. Porphyrins are also believed to occur in kerogens. Studies of shales using reflectance spectroscopy show that porphyrins are incorporated in the kerogen (Holden and Gaffey, 1990; Holden *et al.*, 1991). These studies also indicate that after bitumen is removed from sediment, porphyrins, which may or may not be part of the kerogen, still remain bound in the mineral matrix (Holden *et al.*, 1991). The generation of porphyrins from kerogen through thermal cracking has been proposed to explain the presence of porphyrins with extended alkyl side chains in oils (Quirke *et al.*, 1980), to explain the occurrence of vanadyl porphyrins below strata containing only nickel porphyrins (Louda and Baker, 1981; Baker and Louda, 1983), and to explain the increase in abundance of C_{28} and C_{29} vanadyl etioporphyrins below the zone of hydrocarbon generation in the Toarcian shale (Mackenzie *et al.*, 1980). Similarly, etioporphyrin concentrations have been seen to increase to levels

above the initial DPEP concentration in the hydrocarbon generation zone in the El Lajjun oil shale suggesting etioporphyrins are being produced through thermal cracking of the kerogen (Barwise and Roberts, 1984). These data suggest that at some point during the degradation of chlorophyll, prior to the onset of thermal cracking, the phorbin macrocycle becomes incorporated into a macromolecular structure.

Additional studies suggest that chlorophyll degradation products are incorporated into high molecular weight material and material which is not readily extracted with organic solvents. Several lines of evidence indicate that incorporation of the macrocycle into non-solvent extractable and macromolecular material occurs during the very early stages of chlorophyll degradation. Visible spectra of marine humic substances show the presence of a Soret band reminiscent of a chlorophyll or phorbin-type absorption spectrum (Sato, 1980; Cronin and Morris, 1982; Poutanen and Morris, 1983; Ertel and Hedges, 1983) suggesting that phorbins are contained within humic substances. Furlong and Carpenter (1988) demonstrated the presence of phorbins in humic substances by chromic acid oxidation of Dabob Bay humic and fulvic acids. The maleimides released upon oxidation of the humics were inferred to originate from chlorophyll degradation products incorporated into the sedimentary humic material (Furlong and Carpenter, 1988).

Evidence also exists for the occurrence of a phorbin-containing, high molecular weight fraction in recent sediments which is organic solvent extractable. Separation of total organic extracts of recent sediments by GPC (Repeta, unpublished) produces a high molecular weight fraction with a phorbin-type visible spectrum suggesting this fraction contains incorporated chlorophyll degradation products. Many lines of evidence indicate that at some stage in chlorophyll diagenesis, the degradation products of chlorophyll may become bound into a macromolecular or not easily extractable structure.

The results of laboratory studies signify chlorophyll may become incorporated into high molecular weight material through the burial and diagenesis of whole algae. Upon heating of whole algae under anoxic conditions, chlorophyll becomes non-solvent extractable, yet visible spectroscopy shows the phorbin macrocycle is still present in the algae (Oehler *et al.*, 1974). Similar results have been found for sedimentary humic material. Ertel and Hedges (1983) found the phorbin-type absorption to be more intense in humic acids isolated from reducing sediments than in oxic sediments. The compounds contributing the phorbin-like absorption could not be solvent extracted from the humic acids in anoxic Saanich Inlet (Ertel and Hedges, 1983) nor from those in Nambian Shelf sediments (Cronin and Morris, 1982), whereas in material from the Peru Upwelling Zone, those compounds producing the phorbin-like absorption could be solvent extracted from the humic acids (Poutanen and Morris, 1983). Chlorophyll degradation products may

therefore be bound into macromolecular structures before they are deposited in sediments, or their ultimate fate in sediments may be determined by sedimentary conditions.

In studies of the degradation of chlorophyll in Black Sea sediments, we found that only 50% of the absorbance at 665 nm of the total sediment extract is due to chlorophyll-*a*, chlorophyll-*b*, the pheopigments of chlorophyll-*a* and -*b*, and pyropheophorbide-*a* steryl esters (King and Repeta, 1991). In an attempt to account for the remaining 50%, we degraded and analyzed the high molecular weight fraction isolated by gel permeation chromatography. This fraction accounts for another 30% of organically extracted sedimentary chlorophyll. In order to learn if more sedimentary chlorophyll exists than can be extracted using organic solvents, sediment was further extracted with base and acid. An additional 50% of the quantity of organic solvent extractable chlorophyll degradation products can be extracted using methanolic sulfuric acid. In this paper, we present evidence for the incorporation of chlorophyll degradation products into a non-solvent extractable form early in the chlorophyll diagenetic sequence. We also report the extraction, chemical degradation, separation, and partial structural analysis of the solvent extractable high molecular weight and acid extractable chlorophyll degradation products.

II. METHODS

A. ISOLATION OF SOLVENT EXTRACTABLE HIGH MOLECULAR WEIGHT MATERIAL

Surface sediment was collected by box core from a water depth of 2129 m in the Euxine Abyssal Plain (Fig. 4-1) during the 1988 Black Sea Expedition (*R/V Knorr*, 134-9, May 14-28, 1988), and immediately sectioned and frozen. A composite sediment sample (0-10 cm; 899 g wet wt.) was extracted by vigorous stirring for at least 2 hours with acetone (9x), and then CH_2Cl_2 (3x) (analysis scheme shown in Fig. 4-2). The combined extracts were concentrated by rotary evaporation, an equal volume of 30/70 (v/v) hexane/diethyl ether added, and the pigments partitioned into the organic phase. The organic extract was washed, dried, and evaporated to dryness. Solvent extractable high molecular weight chlorophyll (HMW) was isolated by gel permeation chromatography on a 1 m x 1.5 cm column packed with polystyrene gel (Ch 7) in CH_2Cl_2. The high molecular weight (HMW) fraction was the first fraction to elute off the column and eluted 60 to 98 mL after loading the sample.

Reversed-phase high pressure liquid chromatography (HPLC) was performed on the HMW fractions, using a 15 cm 3 μm absorbosphere column (Alltech) with a Waters

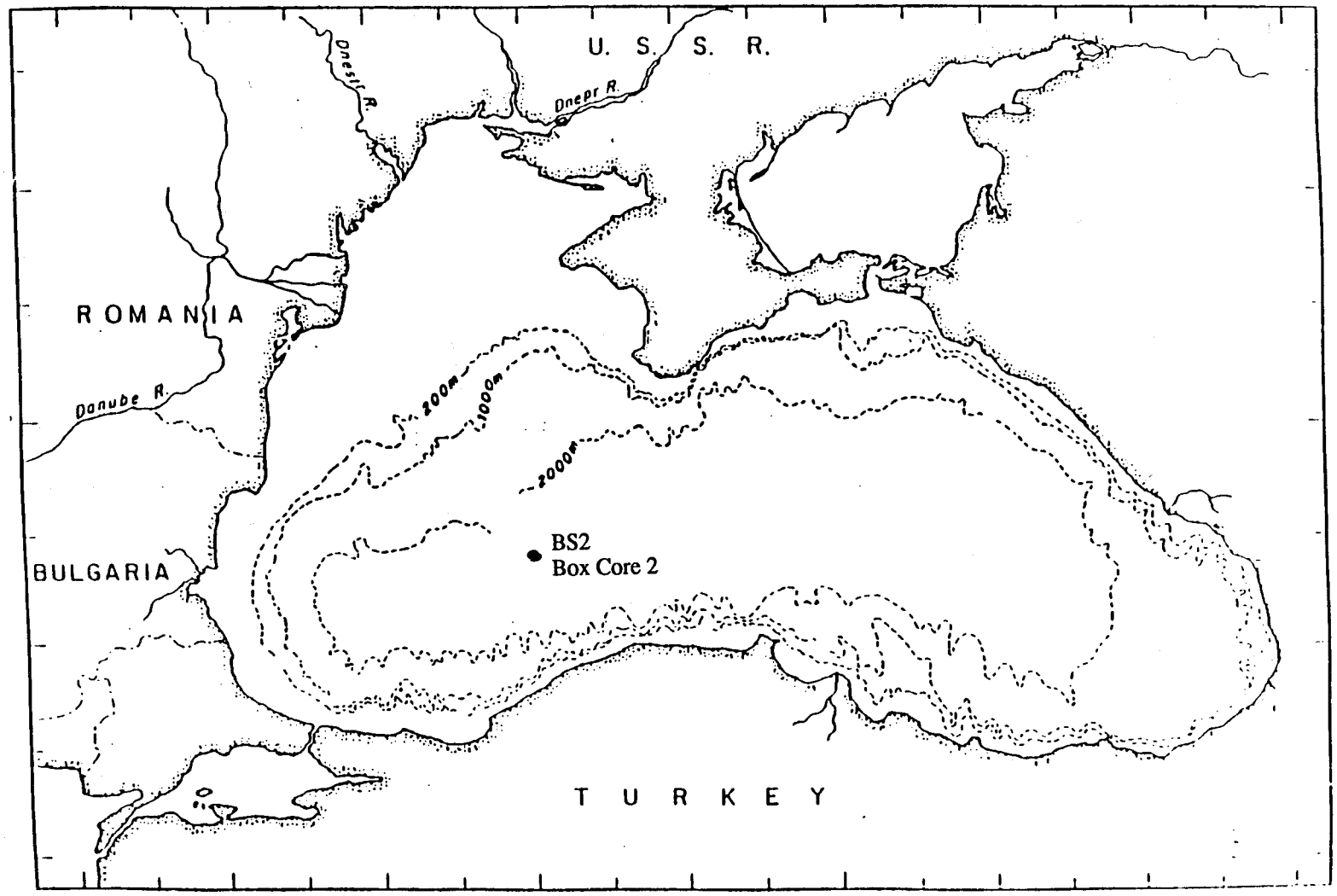

Fig. 4-1 Map of the Black Sea. Sampling locations are indicated.
(Ross *et al.*, 1974)

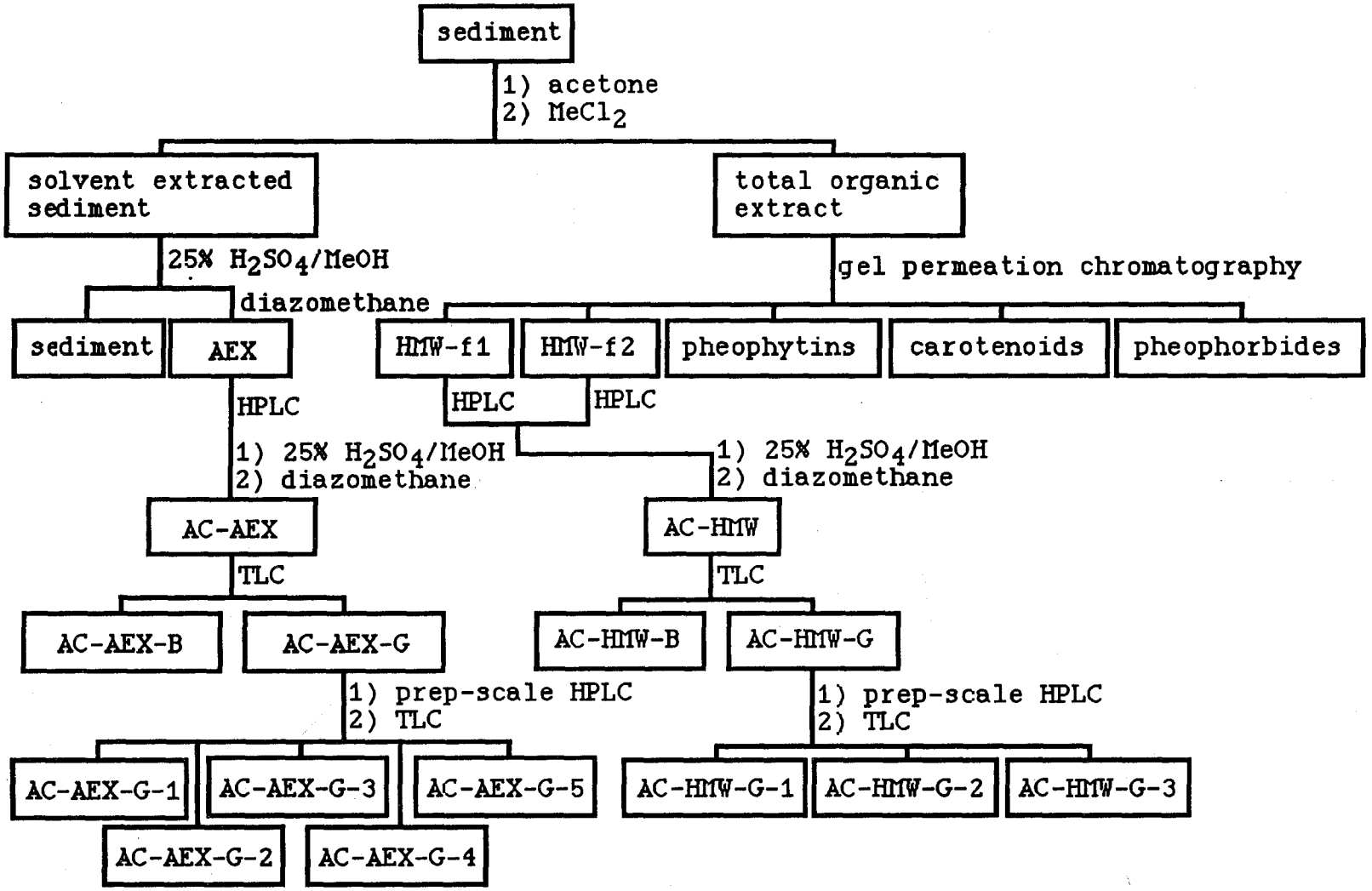

Fig. 4-2 Isolation scheme for high molecular weight and acid extractable chlorophyll degradation products.

600 low pressure mixing system and a Waters 990 photodiode array detector set to detect between 350 nm and 750 nm. The solvent program was a 30 minute linear gradient from 100% A to 100% B followed by 15 minutes of isocratic B at a flow rate of 1.5 mL/minutes Solvent A was 20/80 (v/v) 0.5N NH_4OAc(aq)/MeOH, and solvent B was 20/80 (v/v) *n*-PrOH/MeOH.

B. ISOLATION OF ACID EXTRACTABLE MATERIAL

Aliquots (2g) of sediment which had been previously extracted with organic solvents were treated with 15 mL of methanolic sulfuric acid (3, 6, 12, 25, and 50% (w/w)), HCl, or NaOH (3, 6, and 12% (w/w)) to release non-solvent-extractable chlorophyll degradation products. The HCl solution was prepared so that the sediment was exposed to the same number of acid equivalents as in the 50% H_2SO_4/MeOH extraction (19.5 mL conc HCl/15 mL MeOH/2 g sed. vs. 2 mL conc. H_2SO_4/15 mL MeOH/2 g sed.). All base extractions and initial acid extractions were performed by adding methanolic acid or base drop-wise to the sediment and stirring under a nitrogen atmosphere. After performing extractions with 25% and 50% H_2SO_4/MeOH, we found that the extracted chlorophyll degradation products were highly oxidized; the suite of pigments released contained large amounts of purpurins. Therefore, a closed sparged system was used to prevent formation of oxidation products. Extractions were performed in a three-necked flask fitted with a sparging tube, dropping funnel, and drying tube. The sediments were suspended in MeOH by stirring, and purged 30 min with nitrogen. The concentrated acid was then dripped into the reaction flask while continuing to stir and purge the solution.

To optimize extraction conditions, the effect of H_2SO_4 concentration was examined. A plot of H_2SO_4 concentration vs. chlorophyll degradation product recovery (Fig. 4-3) shows that recovery is linear over low acid concentrations, reaches a maximum at 25% H_2SO_4, then levels off or decreases at 50% H_2SO_4. From this data, 25% H_2SO_4/MeOH was chosen as the concentration to be used in the rest of the experiments. To determine the effect of reaction time, extractions were run for 1 hour, overnight, and 3 days using 25% H_2SO_4/MeOH. The results are plotted in Fig. 4-4. Reaction time has no effect on recovery, suggesting that extraction of the chlorophyll degradation products is relatively rapid under the conditions used in this experiment. All further acid extractions were performed for 1 hr using 25% H_2SO_4/MeOH. Extraction efficiency was tested by sequentially extracting a sample eight times with fresh aliquots of acid. The results are plotted in Fig. 4-5. After the fourth extraction, each additional extraction produces an average of 1.2 nmol/gdw. The recovery of low concentrations of acid extractable

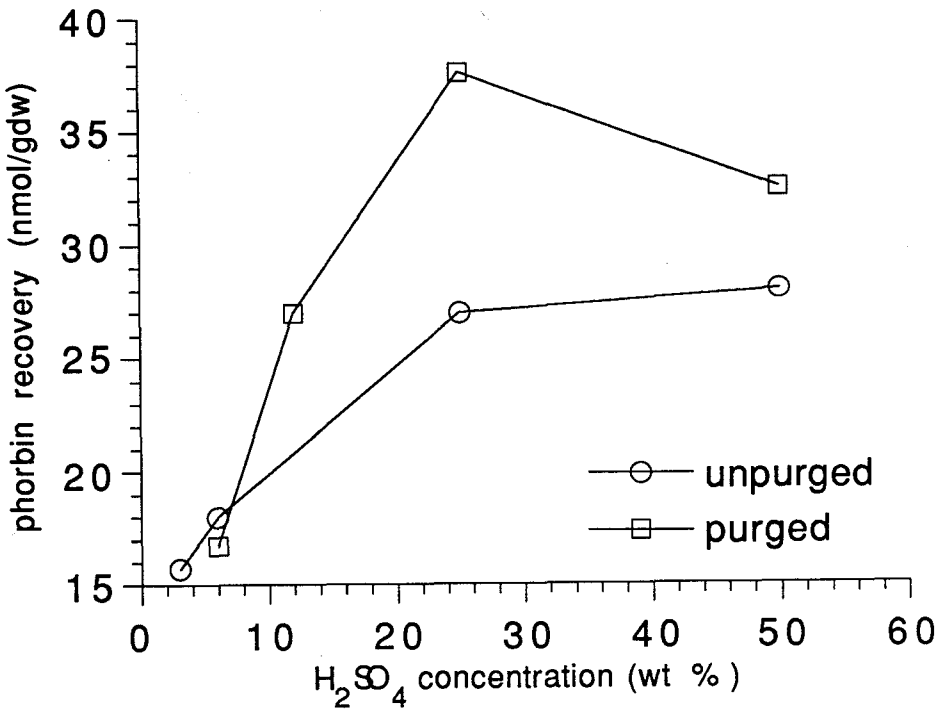

Fig. 4-3 Plot of acid concentration used to extract sediments versus pigment recovery.

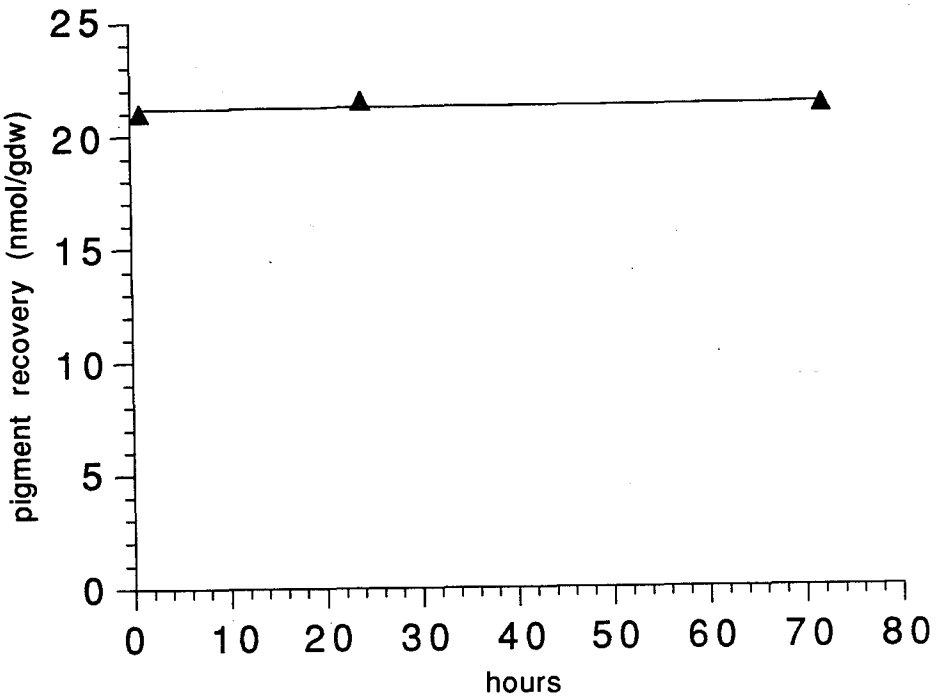

Fig. 4-4 Plot of pigment recovery from Black Sea sediments versus number of hours extracted with 25% H_2SO_4.

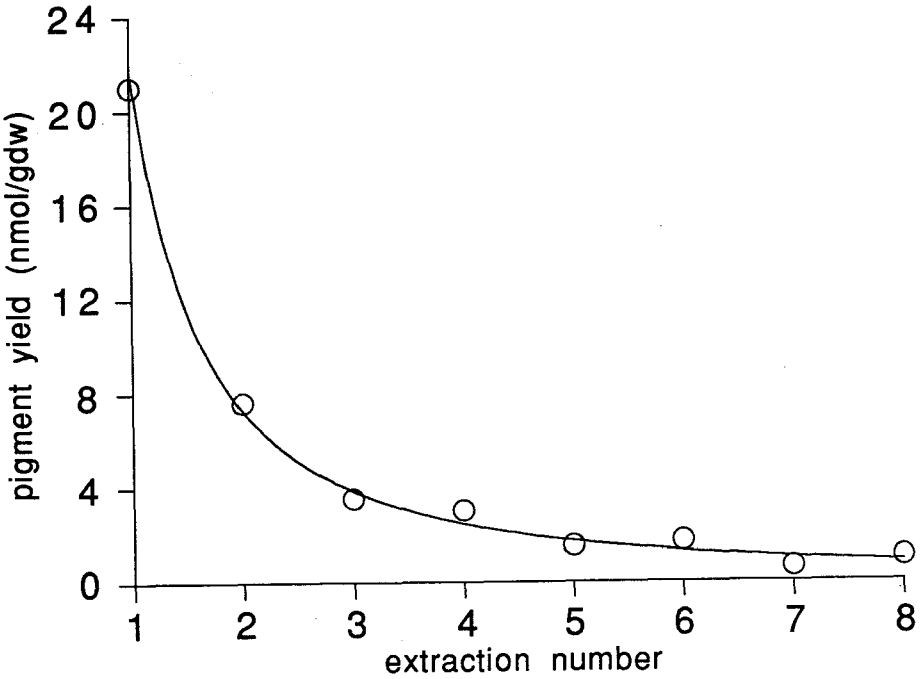

Fig. 4-5 The results of the sequential extraction experiment plotted as the concentration of additional pigment recovered with each extraction versus the number of times extracted.

chlorophyll degradation products (AEX) in extracts 5 - 8 suggests that the material recovered in extracts 5-8 is very tightly bound to the sediment matrix or is unaccessible to extraction and is therefore only slowly extracted using this method. These results further suggest that there may be additional chlorophyll degradation products in the sediments which have yet to be extracted and analyzed.

Once the sediment was extracted with acid, the acidic methanol solution was vacuum filtered through Whatman #1 paper and the sediment rinsed several times with methanol. The filtrate was diluted with 100 mL permanganate distilled water, and the solution extracted with three 20 mL volumes of CH_2Cl_2. The CH_2Cl_2 solution was dried over Na_2SO_4 and the CH_2Cl_2 removed by rotary evaporation. The sample was then redissolved in acetone and methylated with diazomethane using a modification of the method of Fales *et al.* (1973). The sample, dissolved in 2 mL of acetone, was placed in the diazomethane generator. Upon generation of the diazomethane, methylation occured concomitantly with the dissolution of the diazomethane in the acetone. High pressure liquid chromatography was performed on the AEX fraction in the manner described for the HMW fraction.

C. SEPARATION OF CHLOROPHYLL DEGRADATION PRODUCTS FROM THE HIGH MOLECULAR WEIGHT AND ACID EXTRACTABLE FRACTIONS

After HPLC analysis the HMW and AEX fractions were further treated with 3% (w/w) and 25% (w/w) H_2SO_4/MeOH (to produce the "acidified HMW" (AC-HMW) and "acidified AEX" (AC-AEX) fractions). A solution of the isolate in methanol, at a ratio of $2.2x10^{-9}$ moles phorbin/mL methanol, was purged with nitrogen and acid added in the same manner as in the acid extraction of sediments. After 1 hour, the acidic solution was diluted and extracted into CH_2Cl_2, dried, and methylated with diazomethane. The acidified HMW and AEX fractions were analyzed by HPLC in the same manner as described for the HMW and AEX fractions. The 3% acid solution had little effect on the HMW and AEX structures whereas the 25% acid solution cleaved phorbins from the remaining organic matrix in the HMW and AEX structures. All further degradations of the macromolecular structures were therefore carried out with 25% H_2SO_4/MeOH.

The methylated AC-HMW and methylated AC-AEX fractions were then separated into two sub-fractions by thin layer chromatography (Merk Kieselgel 60 plastic backed plates, washed in acetone and stored in desiccator prior to use) using 80/20 (v/v) CH_2Cl_2/*n*-propanol. Two closely eluting bands were separated (AC-HMW-G, AC-HMW-B and AC-AEX-G, AC-AEX-B (G = green, B = brown)). The bands were scraped and eluted from the silica with methanol, and each was analyzed by HPLC. The more rapidly

eluting band (AC-HMW-G and AC-AEX-G), was further analyzed by isocratic HPLC (10/10/80 (v/v/v) water/n-propanol/MeOH) using a Hitachi F1000 fluorescence detector with excitation at 410 nm and emission at 665 nm. Phorbins eluting as individual peaks using this isocratic HPLC system were collected for structural analysis.

D. CHARACTERIZATION OF CHLOROPHYLL DEGRADATION PRODUCTS

Visible, infrared, and nuclear magnetic resonance spectra were obtained of the HMW and AEX prior to separation by TLC. Visible spectra were obtained from 350-750 nm in acetone on a Varian DMS-200 dual beam scanning spectrophotometer. Concentrations were determined at the red band, assuming an extinction coefficient of 5 x 10^4 L/(mole x cm). The spectra were base-line corrected (by imposing a line connecting the minima on either side of the red band) to remove the influence of the absorbance of non-phorbin material upon which the phorbin-type spectrum is superimposed. Infrared spectra were obtained on a Mattson Sirius 100 FTIR at 2 cm^{-1} resolution, taking 256 scans. The samples were prepared neat on NaCl plates by evaporation from CH_2Cl_2 and the spectrophotometer mirrors were aligned in the microbeam configuration. Proton NMR spectra were obtained in d_6-acetone on a Bruker AC300 NMR using a dual $^1H/^{13}C$ probe. Individual compounds, isolated by prep-scale HPLC from AC-HMW-G and AC-AEX-G, were analyzed by visible spectrophotometry in acetone from 350-750 nm and by chemical ionization mass spectrometry. Individual compounds were further purified by SiO_2 TLC developed with 30% acetone/hexane prior to mass spectrometric analysis. The samples were introduced into a Finnigan 4500 mass spectrometer by applying the sample in CH_2Cl_2 to a gold-tipped direct insertion probe and heating from ambient temperature to 350°C in 1 minutes The mass spectrometer source temperature was 100°C; ionization potential, 130 eV; and the methane pressure, 0.5 torr.

E. SYNTHESIS AND ELUTION CHARACTERISTICS OF GEL PERMEATION CHROMATOGRAPHY COLUMN

The concentration of HMW chlorophyll degradation products was determined by column gel permeation chromatography (GPC) eluted with CH_2Cl_2. The polystyrene size exclusion gel was synthesized according to the method of Moore (1964). Briefly, 500 mL of distilled water and 11 g poly vinyl alcohol (PVA) was heated to 80°C while stirring with an EMI Incorporated Minarik model 5VB paddle stirrer at a setting of 45. To this solution was added 2 g of benzoyl peroxide. A mixture of 120 mL toluene, 20 mL divinyl benzene, and 60 mL styrene, was then added dropwise into the stirring PVA solution over a period of 30 min. The solution was allowed to mix while heating at 80°C for five hours, after

which the gel was filtered while still warm, and then washed with warm distilled water repeatedly until the rinse was clear. The gel was then rinsed with room temperature acetone. The gel was allowed to air dry overnight and then covered with excess CH_2Cl_2 (distilled from $CaCl_2$) and allowed to swell for 48 hours prior to packing in a 100 cm x 1.5 cm I.D. column fitted at the top and bottom with adjustable plungers. The molecular weight elution characteristics of the column were determined using polystyrene standards (Fig. 4-6). The molecular weight of the polystyrene standard which was only slightly retained was 7000 a.m.u..

The separation characteristics of the gel column were determined using the total sediment extract of sample BS2-0-10. In order to determine the elution volume of phorbin containing fractions in the sediment extract, 2 mL aliquots were collected throughout the analysis. The visible absorbance of each aliquot was measured at 410 nm, 450 nm, and 665 nm, and for each wavelength, the absorbances were plotted versus total elution volume (Fig. 4-7). The 2 mL aliquots were grouped into four fractions which were analyzed by HPLC to determine their pigment content (Fig. 4-8). The first fraction to elute, fraction **A**, contained the HMW chlorophyll degradation products; the second, fraction **B**, phorbin steryl esters and pheophytins; fraction **C** primarily carotenoids; and the last fraction, **D**, pheophorbides and chlorophylls. The recovery of pigment from the column was determined to be 96%.

III. RESULTS AND DISCUSSION

A. EXTRACTION

In studying the distribution of chlorophyll degradation products in Unit I Black Sea sediments, we identified a fraction of solvent extractable organic matter which elutes prior to any known chlorophyll degradation products by GPC and which possesses a phorbin-type visible spectrum. This fraction elutes between the solvent front and the pyropheophorbide-*a* steryl esters (PSEs) on our GPC column. The molecular weight of this fraction is therefore approximately greater than 1000 a.m.u. The size exclusion limit for our gel column is 7000 a.m.u. as determined by polystyrene standards (see Ch. 7). Based on visible spectrophotometric measurements, this high molecular weight (HMW) fraction contains approximately 25% of all solvent extractable chlorophyll degradation products in our sediment sample.

Earlier studies have shown that not all chlorophyll degradation products in sediments can be extracted with organic solvent (Cronin and Morris, 1982; Poutanen and

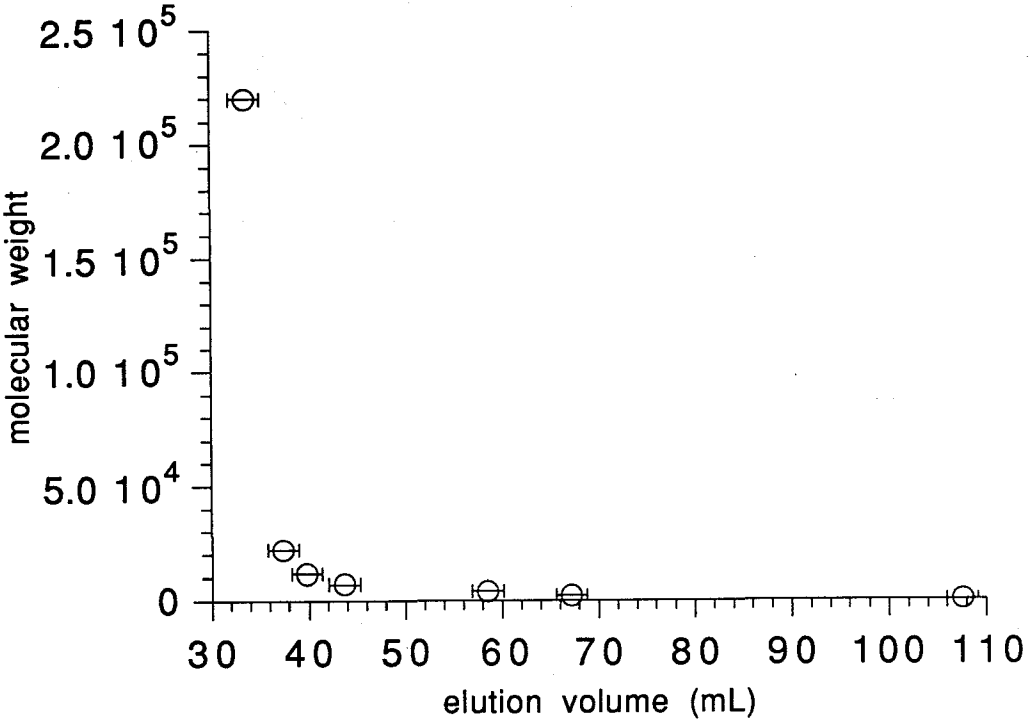

Fig. 4-6 Plot of the molecular weight of polystyrene standards versus their elution volume. This curve was used to determine the molecular weight cut off of the gel column used in this study.

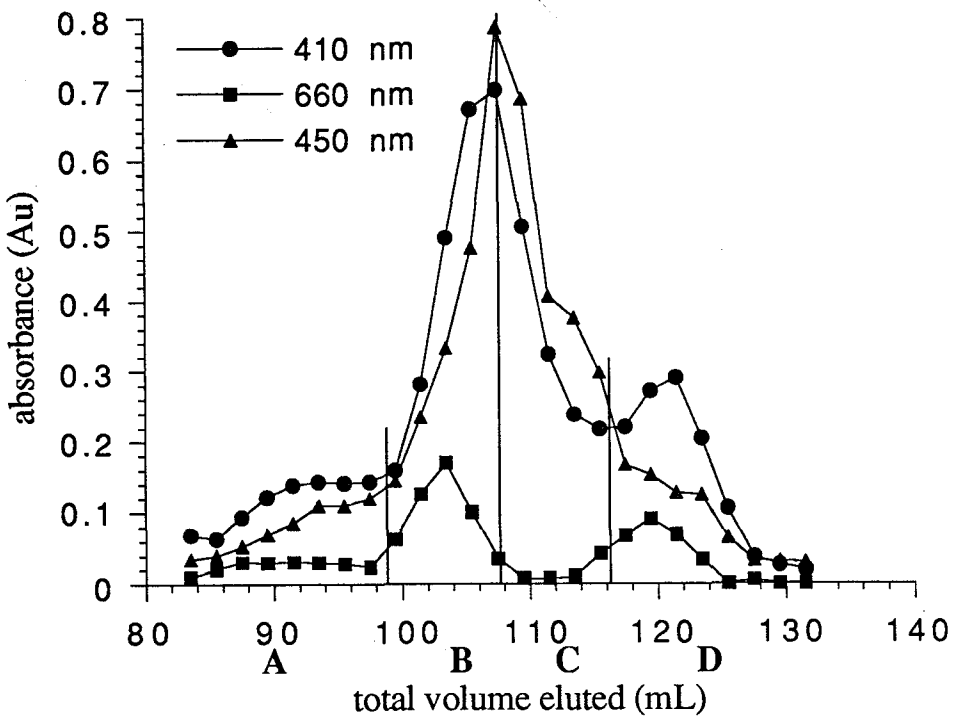

Fig. 4-7 Gel chromatogram of total sediment extract of sample BS2-0-10. Chromatogram was constructed from absorbance measurements on 2 mL fractions.

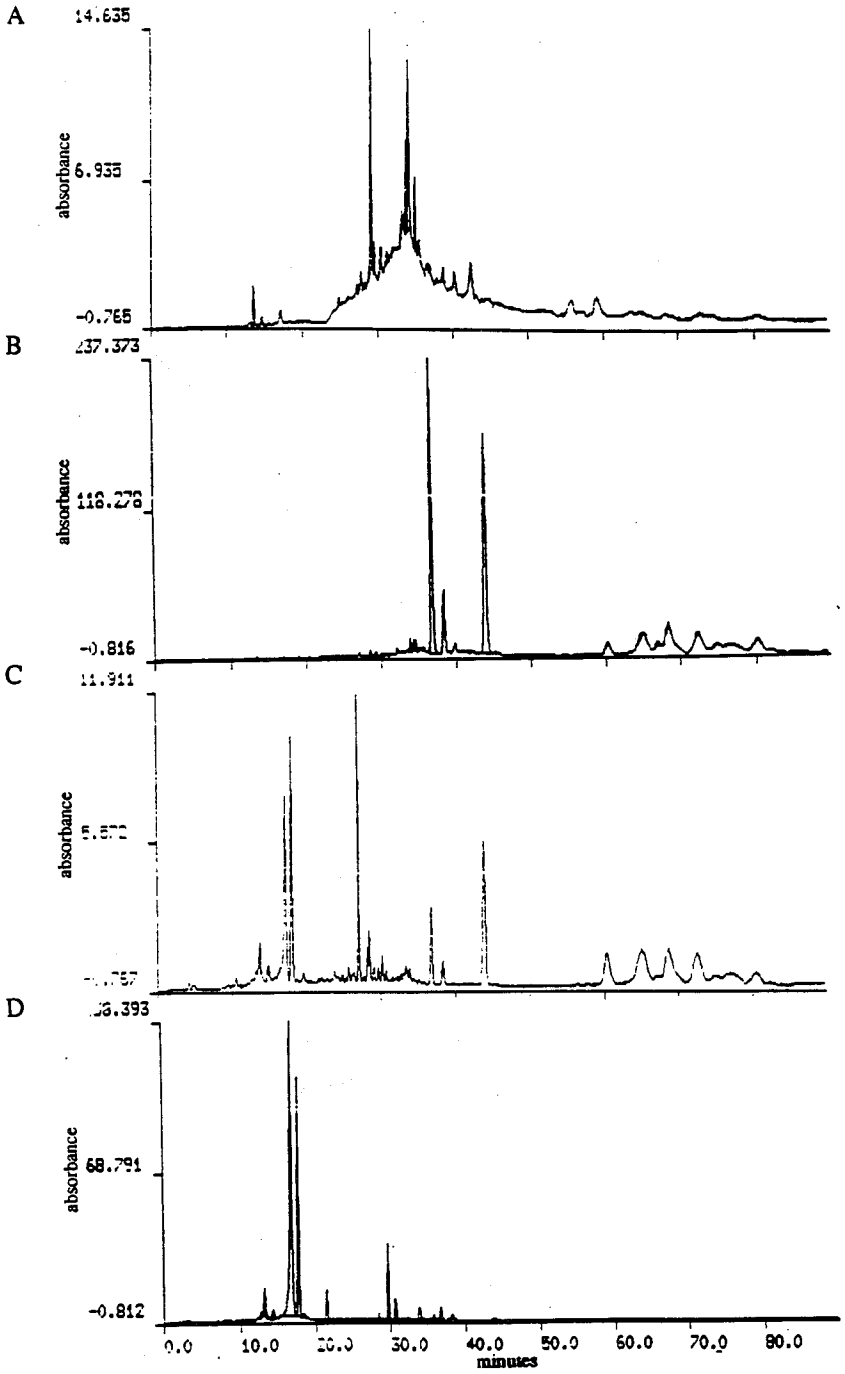

Fig. 4-8 HPLC chromatograms of the individual fractions isolated from the total sediment extract of sample BS2-0-10 by gel chromatography. Note the different absorbance scales in each chromatogram. The samples were analyzed at the same dilution.

Table 4-1

Concentration of Chlorophyll Degradation Products Extracted with Acid and Base

acid/base	concentration[1]	recovery (nmol/gdw) not purged	purged
KOH	15	7.5	
KOH	30	2.4	
H_2SO_4	3	15.7	
H_2SO_4	6	18.0	16.7
H_2SO_4	12		27.0
H_2SO_4	25	27.0	37.6
H_2SO_4	50	28.0	32.5
HCl	[2]62		18.8

[1]%w in MeOH

[2]acid equivalents equal to that in the 50% H_2SO_4/MeOH experiment

Morris, 1982; Ertel and Hedges, 1983; Furlong and Carpenter, 1987). Following solvent extraction, sediments were treated with acid and base (Table 4-1). Solutions of NaOH/MeOH were initially used since there are numerous reports of humic substances having phorbin-like visible spectra superimposed on the visible spectra of the humic substances (Cronin and Morris, 1982; Ertel and Hedges, 1983). Acid was then used to determine if chlorophyll degradation products existed in sediments in a form not accessible to solvent or base. After much experimentation, we found that a solution of 25% H_2SO_4/MeOH (w/w) extracted the greatest concentration of chlorophyll degradation products. In Black Sea Unit I sediments, which are approximately 20% $CaCO_3$, 2% H_2SO_4/MeOH used at a dilution of 7.5 mL MeOH/g of sediment is sufficient to cause total carbonate dissolution.

Visible spectra of both the acid and base extracts consist of a phorbin-type spectrum superimposed on a spectrum which decreases with increasing wavelength (Fig. 4-9). We quantified the amount of chlorophyll degradation products in our extract by correcting the red band absorbance for the background absorbance, and using an average extinction coefficient for chlorophyll and its degradation products (5×10^4 L/mol·cm). The results of the initial extractions are shown in Table 4-1. To determine if other acids worked as well

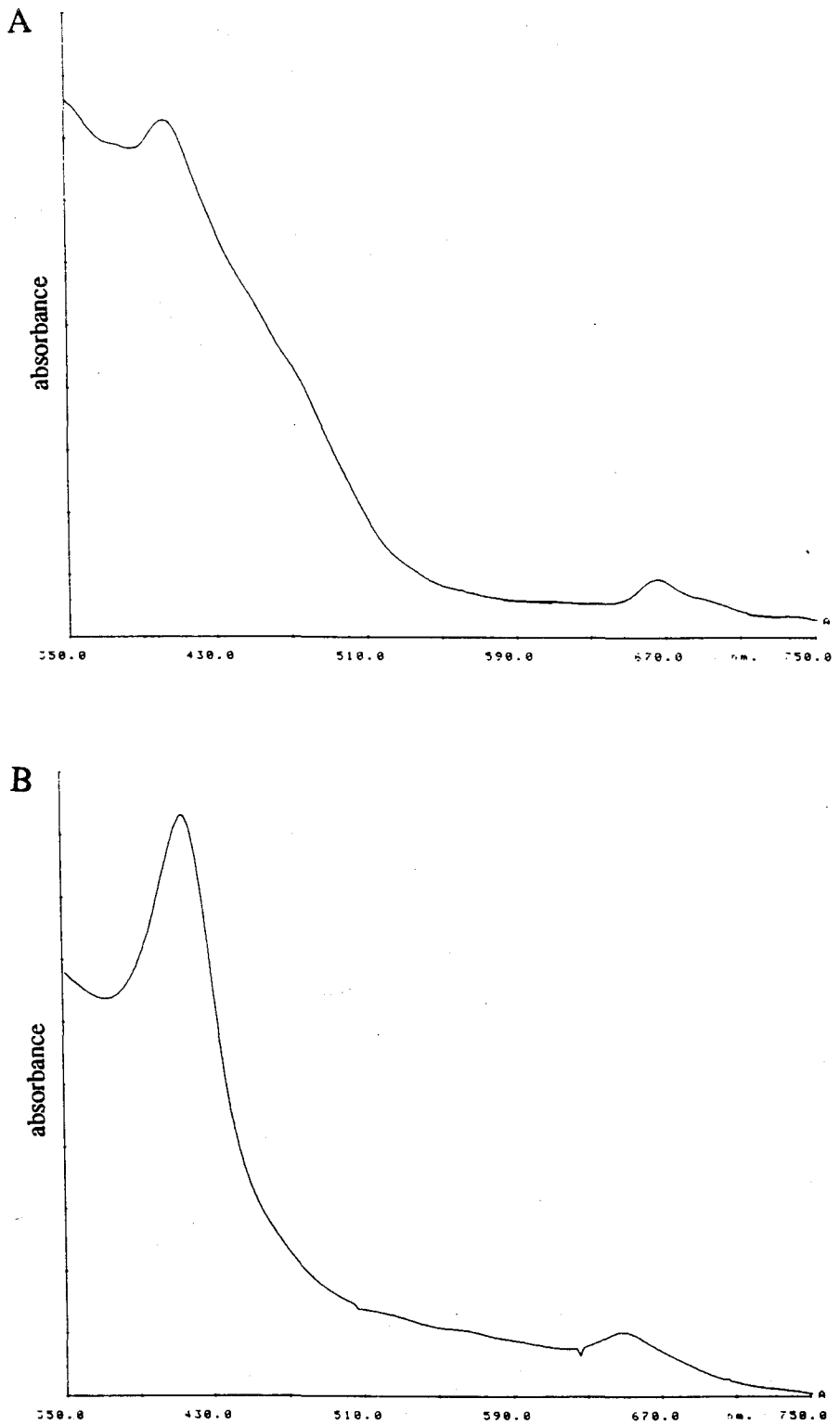

Fig. 4-9 Visible spectra of (a) base and (b) acid extracts of sediment in 100% acetone.

or better than H_2SO_4, solvent extracted sediment was extracted with HCl. Extraction with HCl recovered approximately one-half the concentration of pigment that the corresponding H_2SO_4/MeOH solution recovered (Table 4-1).

B. CHARACTERIZATION

Characterization of the high molecular weight and acid extractable material

The HMW and AEX fractions isolated from Unit I Black Sea sediments were characterized both spectrally and chromatographically. The chromatographic and spectral properties of these fractions and their subfractions are summarized in Table 4-2. The total HMW and AEX fractions were characterized by visible spectrophotometry, FTIR spectrometry, and FTNMR spectrometry. Visible spectrophotometry was used to quantify both the chlorophyll degradation products and the non-chlorophyll derived material in each isolate. As discussed previously, the visible spectra appear as a phorbin-type spectrum superimposed on a base-line whose absorption decreases with increasing wavelength. The shape of the visible spectra of the HMW and AEX fractions is distinctly different. The visible spectrum of the AEX decreases from the Soret maximum at 400 nm to an absorption minimum at 375 nm and then the absorption increases to 350 nm. This compares with the HMW where the absorption decreases from the Soret maximum at 404 nm to 350 nm. The base-line absorption acts to shift the frequencies of the Soret and red bands in the phorbin spectrum to shorter wavelengths. The red band in the visible spectrum of the AEX isolate shifts from 665 nm for a free pheopigment of chlorophyll-*a* to 648 nm, and in the HMW isolate, the red band is shifted from 665 nm to 663 nm. The greater wavelength shift of the red band in the phorbin absorption of the AEX as compared to the HMW suggests that there is a greater contribution of non-phorbin material to the AEX than the HMW.

The relative contribution of phorbin material to the visible spectrum of the HMW and AEX isolates can be measured by projecting a base-line from the intersection of the visible spectrum with 350 nm (the low wavelength cut-off of our measurements) to the absorption minimum to the high wavelength side of the Soret band, and ratioing the fraction of the absorbance occuring above the projected line (phorbin absorption) to the total absorption at the Soret maximum. The relative contribution of phorbins to the Soret band of the HMW fraction is 0.54 and to the AEX is 0.57. As a comparison, this ratio is 0.92 for chl-*a* and 0.87 for ptn-*a*. In pure chlorophyll-a and pheophytin-a, the absorbance of the Soret band is due only chlorophyll-*a* and pheophytin-*a*. The difference of this ratio from 1.0 suggests that the base-line correction method underpredicts the contribution of phorbin to the Soret band. In determining the quantity of phorbin in each fraction, a base-line is projected across the red band to correct for non-phorbin absorbance, and the

Table 4-2

PROPERTIES OF HIGH MOLECULAR WEIGHT AND ACID EXTRACTABLE ISLOLATES AND THEIR SUBFRACTIONS

	HPLC	visible spectroscopy	IR	NMR
AEX	continuously rising base-line with large hump at 35 minutes and then drops to zero absorbance	phorbin spectrum with red band absorbance at 648 nm superimposed upon a baseline which increases with decreasing wavelength	C-H stretching region similar to HMW no olefinic or aromatic C-H stretching absorances	little similariy to HMW no characteristic phorbin resonances broad doublet at 1 ppm, singlet at 1.5 ppm, absorbances between 7.5 and 8 ppm major absorbances all below 2.5 ppm
AC-AEX	rising base-line with five well defined peaks eluting bwteen 23 and 28 minutes - greatly reduced hump at 35 min.	S/R = 9.5 phorbin spectrum with red band absorbance at 648 nm superimposed upon a baseline which increases with decreasing wavelength		
AC-AEX-G	five well defined peaks eluting between 23 and 28 minutes with very little base-line rise	28% of bound phorbin-like with very little of the decaying baseline		
AC-AEX-B	continuously rising-baseline which returns to zero absorbance at approximately 35 minutes	72% of bound similar to AC-AEX but with greatly reduced phorbin character		

Table 4-2 continued

	HPLC	visible spectroscopy	IR	NMR
HMW	rising baseline with broad peak at 35 minutes		C-H stretching region similar to the AC-AEX and AEX noolefinic or aromatic C-H stretching absorances	little similariy to AEX no characteristic phorbin resonances broad doublet at 1 ppm, singlet at 1.5 ppm major absorbance is a doublet at 3.0 ppm
AC-HMW (combined HMW-f_1 and HMW f_2)	rising baseline with three peaks eluting between 22 and 28 minutes	S/R = 5.2 phorbin-like visible spectrum with red band absorption at 663 nm superimposed upon a baseline which decreases with increasing wavelength		
AC-HMW-G	three will defined peaks eluting between 22 and 28 minutes	36% of HMW phorbin-like visible spectrum with little or no baseline		
AC-HMW-B	rising baseline which returns to zero absorbance at 35 minutes	64% of HMW visible spectrum with very little phorbin-like character		

extinction coefficient for the red band is assumed to be the same for both AEX and HMW. In the HMW fraction the red band of the phorbin spectrum contributes 88% of the total absorption whereas in the AEX, the phorbin contribution is 59%. The differences between the relative contribution of non-phorbin absorption in the HMW and AEX isolates as determined at the Soret and red bands may be due either to the structures of the phorbins which may have different S/R ratios (the extinction coefficient of phorbins and porphyrins at the Soret band is similar whereas the extinction coefficient at the red band varies widely), or to differences in the non-phorbin material. The mass of phorbin in a known mass of both AEX and HMW was spectrophotometrically determined. The AEX contains approximately 9 mg phorbin /g AEX extract and the HMW contains 15 mg phorbin/g HMW extract. By mass, the HMW isolate contains approximately 1.7 times as much phorbin as does the AEX. As in the determinations of the contribution of the phorbin absorbance to the red band, the contributions of phorbin to the total isolate determined by mass may be biased if the red band extinction coefficient of the phorbins in the two samples is drastically different.

Similarities between the HMW and AEX fractions are seen in the IR spectra of these samples. The aliphatic C-H stretching region of the IR spectra of the two samples are identical. There is no absorbance in the C-H stretching region for olefinic or aromatic compounds which suggests that these fractions have a low degree of aromaticity. The IR spectra of these samples also indicate that the structures are dominated by the non-phorbin material and that the phorbins contribute very little to the overall spectroscopic properties of the sample.

Proton NMR spectra of the AEX and HMW material show little similarity (Fig. 4-10). The NMR spectra of the HMW and AEX fractions both lack the resonances characteristic of chlorophylls and their pheopigments. The NMR spectra of both the HMW and AEX material have broad doublets at approximately 1 ppm and broad singlets at approximately 1.5 ppm in d_6-acetone (Fig 4-7). The major absorbances in the NMR of the AEX material are all below 2.5 ppm (Fig. 4-10a) whereas in the NMR of the HMW material, the major absorbance is a doublet at 3.0 ppm (Fig. 4-10b). NMR resonances at these locations suggest a large contribution of lipid-like material to these structures. These two NMR spectra also differ in that the AEX sample has absorbances between 7.5 and 8 ppm suggesting that the AEX material may have a higher degree of aromaticity than the HMW material. The NMR data agree with the IR, visible spectroscopic, and mass data in that all four data sets suggest that the HMW and AEX structures consist mostly of non-phorbin material.

The HMW and AEX isolates were also characterized chromatographically. The HPLC chromatogram, with visible detection between 350 and 750 nm, of HMW displayed a rising base-line with a broad peak at 35 minutes (Fig. 4-11a). In the acid extraction experiments, the 6%, 12%, and 25% H_2SO_4 acid experiments produced HPLC chromatograms similar to each other and to HMW. The shape of the peak at 35 minutes was similar to that of HMW and the only difference between the chromatograms of the different acid extracts was the size of the broad peak eluting at 35 minutes (Fig. 4-11b). With increase in acid strength, the size of the broad peak increased until a concentration of 50% H_2SO_4/MeOH was reached. When 50% H_2SO_4/MeOH was used, the HPLC chromatogram did not possess a broad peak at 35 minutes, but instead had 5 well resolved peaks eluting between 23 and 28 minutes The visible spectrum from 350 - 750 nm across any point in the chromatogram of the HMW and AEX fractions was similar to that of the visible spectrum of the total isolate. This indicates that the phorbins in both isolates are bound into a structure which slowly elutes off the reversed-phase HPLC column.

Two possible explanations present themselves for the appearance of the broad peak eluting at 35 minutes in the HPLC chromatograms of the AEX and HMW isolates (Fig. 4-11). The broad peak in both fractions may be formed from a large quantity of similar but not equivalent molecules. The similarities in structures are such that the compounds elute very closely together, but not so similar that they coelute. An alternate explanation for the appearance of the broad peak which elutes at the end of the solvent gradient by HPLC is a possible large increase in solubility of the HMW and AEX in the mobile phase once water is removed from the mobile phase. The HPLC solvent gradient goes to 0% aqueous buffer at 30 minutes, just prior to the elution of the broad peak The HMW and AEX material which had been slowly eluting from the column when water was present in the mobile phase could then become solubilized and rapidly pass through the column to elute as an unresolved complex mixture.

The similar behavior of the HMW and AEX fractions by HPLC and similarities in the spectral data suggests that the HMW and AEX structurally resemble each other. Chromatographically, both fractions display a rising base-line which is more pronounced in the AEX fraction than in the HMW fraction, and a large broad peak at 35 minutes In both the HMW and AEX, a large percentage of the material is very non-polar, eluting at or near the end of the solvent gradient. This large peak contributes approximately 35% of the total integrated absorbance measured at 665 nm in the HPLC trace of the HMW fraction and approximately 50% of the total integrated absorbance in the AEX fraction.

Structural differences between the HMW and AEX fractions can be seen in the visible and NMR spectra of the total fractions. In the visible spectra of both the HMW and

A

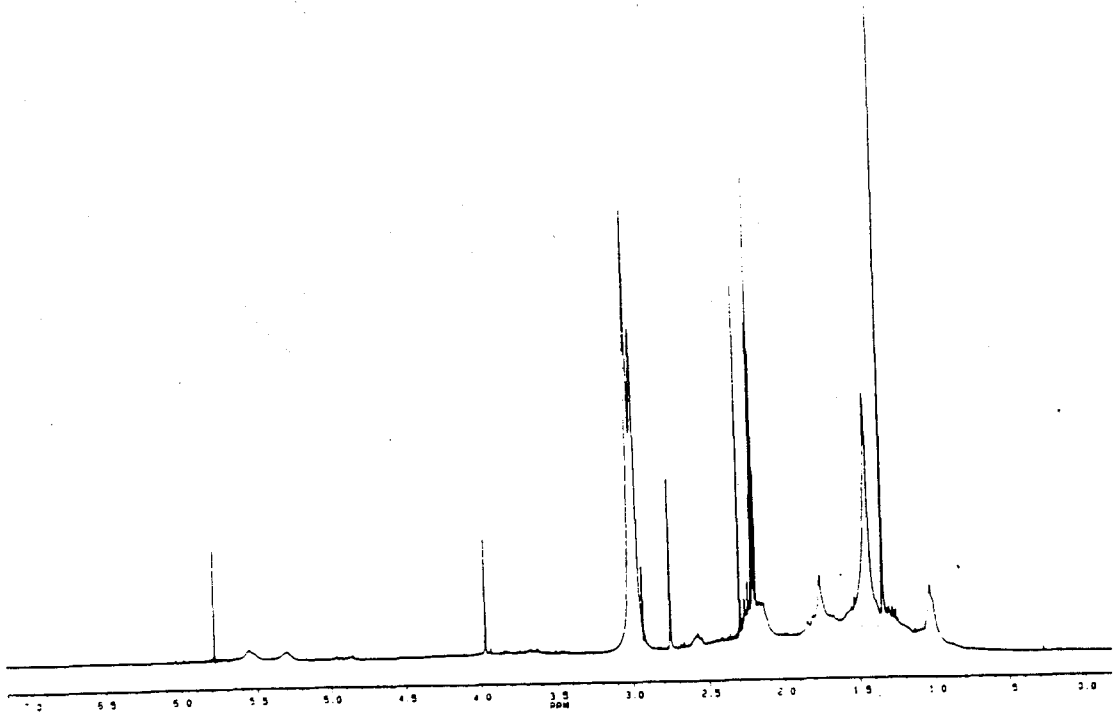

B

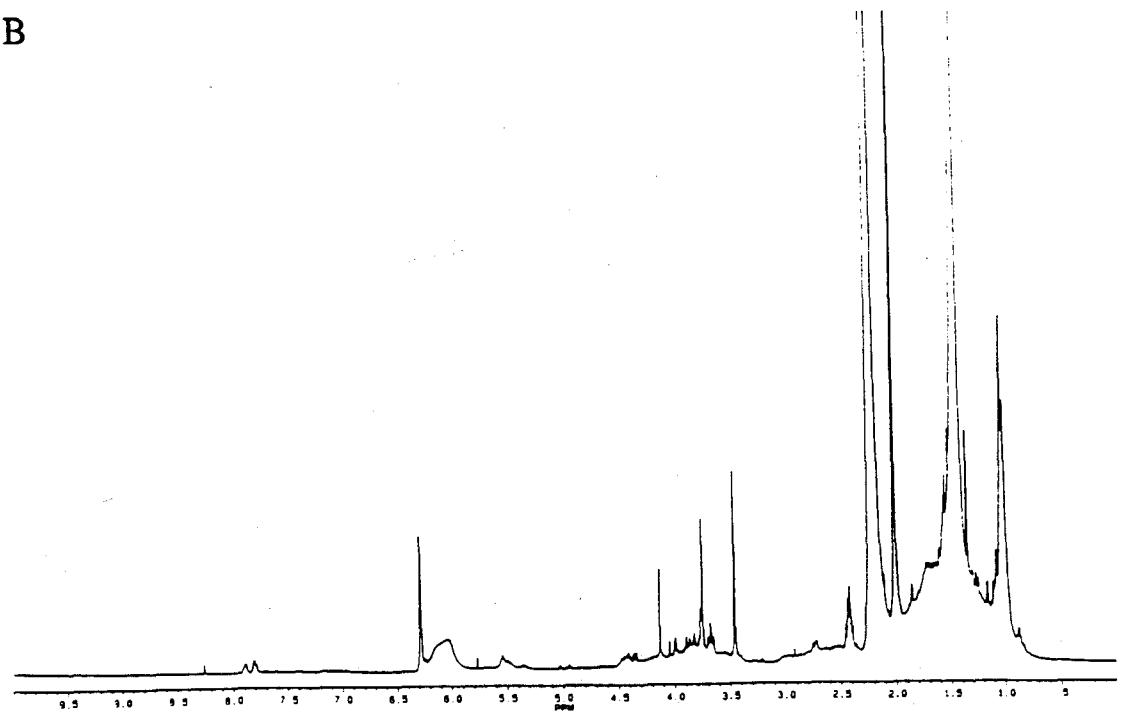

Fig. 4-10 300 MHz NMR in *d*6-acetone of the (A) HMW and (B) AEX isolates.

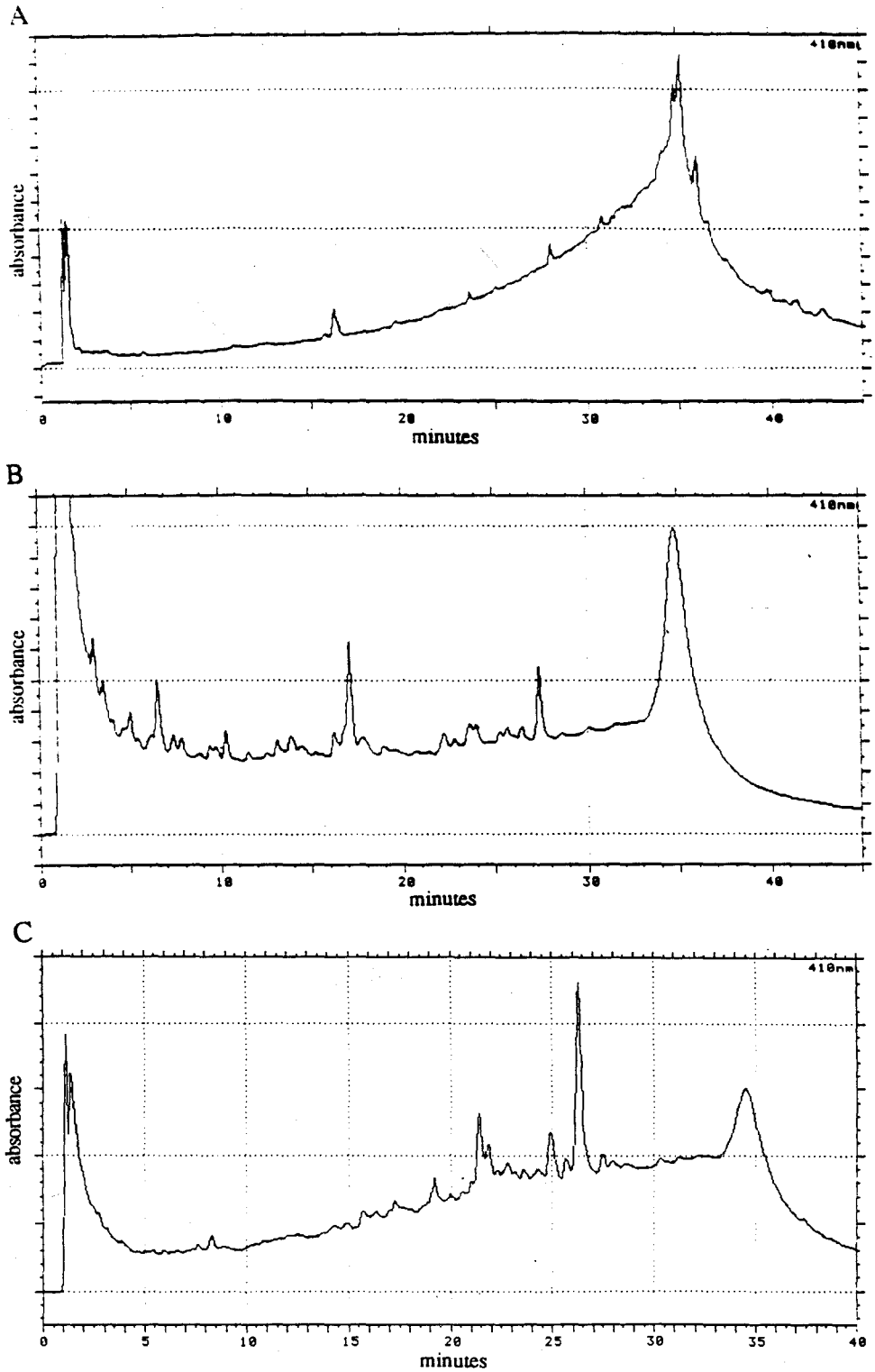

Fig. 4-11 Comparison of reversed-phase HPLC chromatograms with detection at 410 nm of (a) HMWand (b) AEX isolates, and (c) 50% H_2SO_4/MeOH extraction experiment. Note the smaller time scale for (c).

AEX fractions, it is necessary to correct the absorbance of the red band for absorbance of non-chlorophyll material. In the AEX fraction, the correction is larger than in the HMW fraction, and the absorbance at 350 nm in the AEX fraction is larger than in the HMW fraction. The NMR and IR spectra both suggest high degrees of aliphaticity for both the HMW and AEX fractions. The region from 2000 - 4000 cm^{-1} in the two IR spectra are identical, and the NMR spectra both have broad peaks of similar shape but different intensities between 0 and 2 ppm. A high degree of aliphatic character is further supported by preliminary pyrolysis GC-MS studies of the HMW and AEX isolates which show sterols to be present in the fractions. No evidence for pyrroles, which are formed upon pyrolysis of phorbins and porphyrins, was found in these studies. These studies suggest that phorbins contribute very little to the overall mass of the HMW and AEX structures and that both structures are highly aliphatic.

Additional differences in the structures of the HMW and AEX fractions are also apparent. The NMR spectrum of the AEX material possess absorbances between 7.5 and 8.0 ppm which are shifted downfield of the aliphatic region by an amount which is characteristic of the anisotropy of an aromatic system. No such peaks are present in the NMR of the HMW material. These data imply that the AEX has a higher degree of aromaticity than the HMW. The major difference between the two fractions is the need to use acid to extract the AEX fraction from the sediment while the HMW fraction can be extracted with organic solvent only. One explanation for the spectroscopic data is that the AEX and HMW fractions represent structures with incorporated phorbins as well as other lipids, but are formed through two totally different pathways. The need to use acid to extract the AEX indicates differences in the solubility properties of the two isolates.

Another explanation for the observed data is that the molecular weight of the AEX fraction may be such that it is no longer soluble in organic solvents and must first be cleaved into smaller units before it can easily be solubilized by organic solvents. The molecular weight of the HMW isolate is a continuum as shown by its behavior on GPC. This fraction begins to elute at the solvent front of our column, which has a nominal lower molecular weight limit of 7000 a.m.u., and continues to elute until just prior to the elution of the pyropheophorbide-*a* steryl esters (PSEs) which have an average molecular weight of 950 a.m.u.. With GPC elution volume, the total absorbance at 410 nm of this fraction increases until just prior to the elution of the PSEs when the absorbance at 410 and 665 nm decreases, indicating that the amount of phorbin in the HMW fraction increases with decreasing molecular weight. The major differences between the HMW and AEX isolates are solubility properties, the degree of unsaturation, and the quantity of incorporated

phorbin, while both isolates are highly aliphatic, relatively non-polar, and contain only low amounts of phorbin.

Structural characterization of the phorbins in HMW and AEX isolates

The phorbins seen in the visible spectra of the HMW and AEX fractions can be released from the macromolecular structures by further reaction with 25% H_2SO_4/MeOH. Degradation of HMW with acid to form the acidified HMW fraction (AC-HMW) did not produce a decrease in the measurable amount of phorbin in the visible spectrum and the relative contribution of phorbin to the Soret maximum remained constant at 0.53. The HPLC chromatogram of AC-HMW contains three well resolved peaks eluting between 22 and 28 minutes, all of which are phorbins (Fig. 4-12a; Table 4-3). Upon reaction with 25% H_2SO_4/MeOH, the AEX extract (AC-AEX) showed no loss of chlorophyll degradation products as measured at the red band, though the relative contribution of phorbin to the Soret maximum decreased from 0.57 to 0.48. Upon analysis of the extract by HPLC, we found that the chromatogram of AC-AEX is identical with that of the 50% acid extract (Fig. 4-11c). The broad peak at 35 minutes is greatly reduced in the chromatogram of AC-AEX and five well resolved peaks appeared between 23 and 28 minutes (Fig. 4-12b; Table 4-3). Two of the five compounds released by hydrolysis from the AEX have S/R ratios characteristic of porphyrins. Integration of the chromatogram showed that loss of absorption from the broad peak can be accounted for by the absorption of the five peaks. The second peak of AC-HMW to elute by HPLC has the same retention time (R_t) as the first peak in AC-AEX but has a different visible spectrum. The third peak of HMW coelutes with the fifth peak in AEX and also has the same visible spectrum. This data suggests that the HMW and AEX isolates are not only chromatographically similar, but may contain similar phorbins.

The phorbins and porphyrins released by acid hydrolysis can be isolated from the AC-AEX and AC-HMW samples by TLC. Using TLC, AC-HMW and AC-AEX can be divided into two fractions. Prior to rehydrolysis of the AEX and HMW fractions, these isolates can not be separated by TLC. The more rapidly eluting green band on the TLC plate (AC-HMW-G and AC-AEX-G) consists of several adjacent, fine bands (R_f = 0.76 - 0.81). There are two fine green bands for the HMW fractions and three for the AEX fractions. When collected as one band, the visible spectrum is phorbin-like with very little base-line absorption (phorbin content at Soret maximum = 0.65 for AC-HMW-G and 0.63 for AC-AEX-G). When analyzed by HPLC, the green bands from both AC-HMW and AC-AEX contain almost exclusively the distinct peaks seen in the HPLC chromatogram of the unfractionated sample. Very little base-line rise is seen in these chromatograms. The

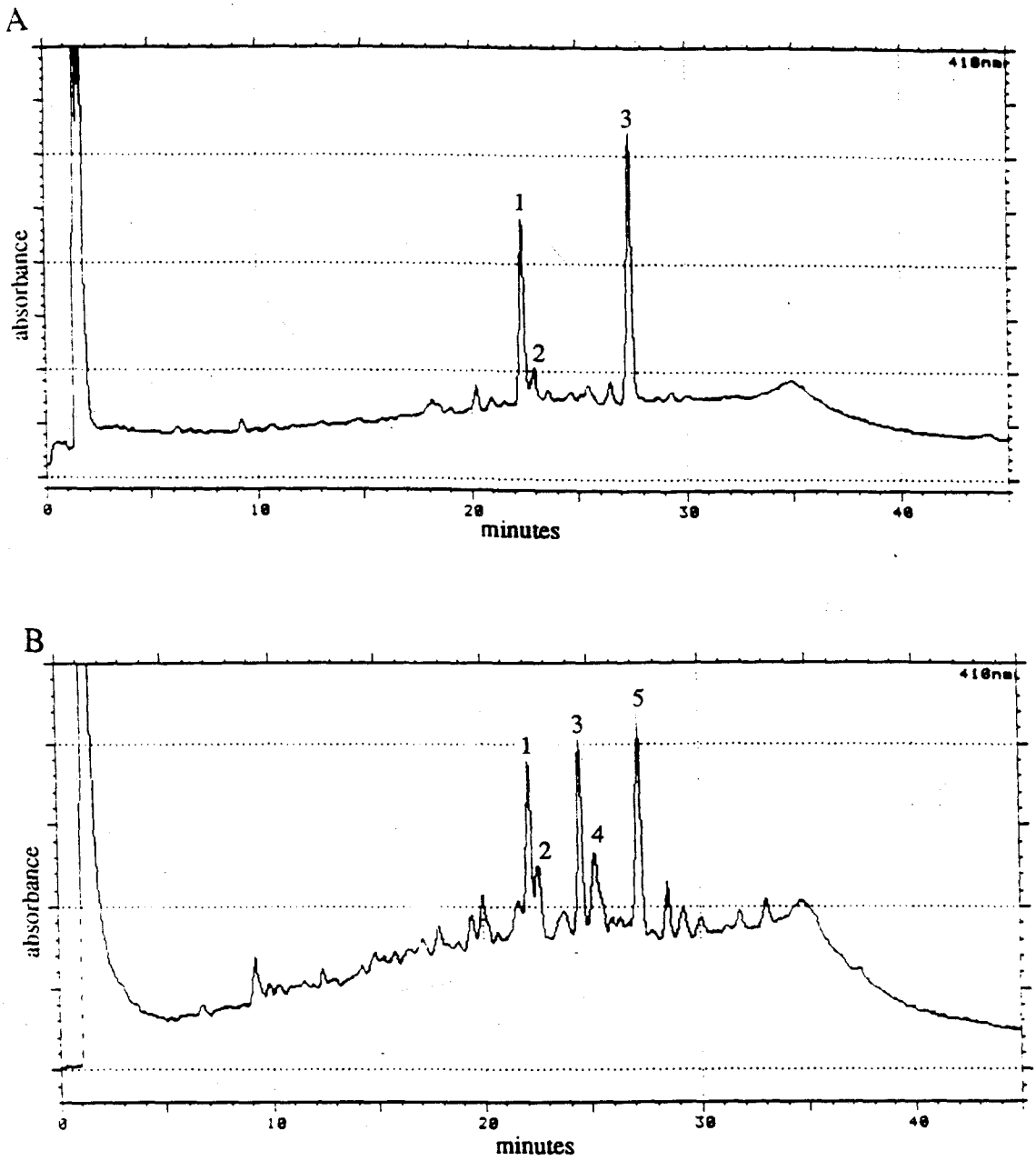

Fig. 4-12 Comparison of reversed-phase HPLC chromatograms with detection at 410 nm of (a) AC-HMW and (b) AC-AEX isolates.

Table 4-3

Visible Spectra and HPLC Retention Times for HMW and AEX Chlorophyll Degradation Products

Compound	R_t (minutes)	HPLC diode array Soret(nm)	red (nm)	S/R	off-line (100% acetone) Soret(nm)	red (nm)	S/R
AC-HMW-G-1	22.4	410	665	2.5	408	664	2.7
AC-HMW-G-2	23.0	410	665	2.7	407	661	3.2
AC-HMW-G-3	27.6	410	665	2.6	410	666	2.4
AC-AEX-G-1	23.0	395	670	3.7	400	667	4.3
AC-AEX-G-2	23.4	400	660	3.7	405	661	5.1
AC-AEX-G-3	25.0	400			404	662	14.
AC-AEX-G-4	25.6	405			406	662	14.
AC-AEX-G-5	27.6	410	670	2.6	409	666	3.1

HPLC chromatogram of AC-AEX-G contains much more of the base-line rise seen in the HPLC analysis of the total sample than does the HPLC chromatogram of AC-HMW-G. The increased base-line rise seen in AC-AEX-G is due to the relatively lower amount of the green isolate in the AEX fraction (28%) than in the HMW fraction (36%), and to the lower resolution of the green and brown bands (AC-HMW-B, and AC-AEX-B) in the AEX than in the HMW fraction. The brown band ($R_f = 0.66$) is wide and is not completely resolved from the green band in the AEX fraction. The visible spectrum of AC-HMW-B and AC-AEX-B is similar to that of the total sample but has much less phorbin-like character (phorbin content at Soret maximum = 0.46 for AC-HMW-B and 0.39 for AC-AEX-B). This is consistent with the HPLC trace of the brown band which consists almost exclusively of the base-line rise with no broad peak at 35 minutes The base-line rise of AC-HMW-B and AC-AEX-B possess a phorbin visible spectrum similar to that of off-line visible spectra of the total fraction. Once the green and brown isolates are separated, the individual phorbins and porphyrins were isolated from the HMW and AEX material by HPLC.

Three phorbins were isolated from the AC-HMW-G, and three phorbins and two porphyrins were isolated from the AC-AEX-G (Table 4-3). Each of these was examined by visible spectrophotometry, both on-line with an HPLC diode array detector and off-line

in 100% acetone, and by CI-MS. Differences exist between the on-line and off-line visible spectra of the isolated compounds since the on-line spectra are background corrected, and the off-line spectra contain any compounds which coelute in the base-line by HPLC. Comparisons of the on-line and off-line visible spectra of authentic chlorophyll-*a* derivatives shows that shifts in the wavelength of maximum absorbance for the Soret and red bands due to solvent effects are negligible. In order to obtain clean mass spectra, it was necessary to further purify each fraction using SiO_2 TLC. The purified compounds were then analyzed by CI-MS.

Based on their mass spectrometric and visible spectrophotometric data, structural characteristics for the isolated compounds can be suggested. Based on their visible spectra, the compounds isolated from AC-HMW-G, AC-HMW-G-1, -2, and -3 (Table 4-3), are all chlorophyll-*a* derived phorbins. From their mass spectra, AC-HMW-G-1 and AC-HMW-G-3 are pheophorbide-*a* methyl ester and pyropheophorbide-*a* methyl ester respectively. The quality of the mass spectrum of AC-HMW-G-2 is poor, but, based on retention time as well as spectral characteristics, we suggest that this compound is the epimer of pheophorbide-*a* methyl ester. The retention times of AC-HMW-G-1, AC-HMW-G-2, and AC-HMW-G-3 correspond to those of standard pheophorbide-*a* methyl ester and its epimer and of pyropheophorbide-*a* methyl ester, providing more evidence for the identification of AC-HMW-G-1, AC-HMW-G-2 and AC-HMW-G-3 as pheophorbide-*a* methyl ester, pheophorbide-*a'* methyl ester, and pyropheophorbide-*a* methyl ester.

The identities of the compounds isolated from AC-AEX-G are not as clear as those isolated from AC-HMW-G. The spectral and chromatographic characteristics of AC-AEX-G-5 are identical to those of AC-HMW-G-3, and therefore AC-AEX-G-5 is pyropheophorbide-*a* methyl ester. From their visible spectra, AC-AEX-G-1, -2, -3, and -4 do not appear to be directly related to chlorophyll-*a*. The Soret maxima in the visible spectra of these compounds is shifted 5 - 15 nm to shorter wavelengths. The S/R ratios of these four compounds indicate that AC-AEX-G-3 and -4 are porphyrins and AC-AEX-G-1 and -2 are phorbins. The Soret band of AC-AEX-G-2, a phorbin, is 5 nm shorter than that of AC-AEX-G-4, a porphyrin, and the Soret band of AC-AEX-G-1, a phorbin, is 5 nm shorter than that of AC-AEX-G-3, a porphyrin. The additional unsaturation in rig IV in porphyrins as compared to phorbins could explain the wavelength shifts between these phorbins and porphyrins.

The mass spectra of these four AC-AEX-G isolates appear to contain ions from more than one compound, but suggest structural relationships among the compounds. The contamination in the mass spectra is likely from lipid material which was not sufficiently removed from the isolates. The base peaks of AC-AEX-G-1 and AC-AEX-G-3 (625 and

623 a.m.u. respectively) differ from each other by 2 a.m.u. The combination of visible spectrophotometric and mass spectra data suggests that AC-AEX-G-3 is the porphyrin formed from dehydrogenation of AC-AEX-G-1. The mass spectra of AC-AEX-G-2 and AC-AEX-G-4 are not as clean as those of AC-AEX-G-1 and AC-AEX-G-3. The appearance of major ions in the mass spectra of AC-AEX-G-2 and AC-AEX-G-4 (625 and 623 a.m.u. respectively), which correspond to those of AC-AEX-G-1 and AC-AEX-G-3, suggest that AC-AEX-G-4 is the porphyrin formed from AC-AEX-G-2. When combined with HPLC retention time data, this data further suggests that AC-AEX-G-2 and AC-AEX-G-4 are epimers of AC-AEX-G-1 and AC-AEX-G-3.

The behavior of the HMW and AEX fractions upon treatment with acid is similar. After treatment with acid, both macromolecular fractions produce well resolved peaks. In each fraction, the least polar compound is pyropheophorbide-*a* methyl ester. The more polar peaks in the AEX and HMW fractions do not coelute with each other (Table 4-3). After separation of the individual peaks from the base-line by TLC, the retention characteristics of the phorbins could be more easily analyzed. The compounds in the AEX fraction are slightly more polar than those in the HMW fraction (with the exception of pyropheophorbide-*a* methyl ester which is present in both fractions). Additional structural similarities are suggested by the need to use 25% H_2SO_4/MeOH to release the phorbins from both macromolecular structures.

A major difference between the two fractions is the inclusion of porphyrins into the AEX fraction. Porphyrins are not usually present in non-thermally altered organic matter (Baker and Louda, 1983) and may represent dehydrogenation products of the incorporated phorbins. Whether the porphyrins were formed before or after the original phorbin-type compounds were included in the AEX fraction is not known, but the lack of porphyrins in the HMW fraction which was treated in the same manner as the AEX fraction suggests that the porphyrins are not artifacts of the analytical procedures.

The structural data from the different sources suggests that the organic material in the HMW and AEX fractions are structurally similar. Based on solubility differences, the molecular weight of the AEX material may be greater than that in the HMW fraction, or the AEX may be bound to the mineral matrix in such a way that strong acid is needed to free the structure, possibly through chelation of a metal in the mineral matrix by the free base nitrogens of the phorbin and porphyrin macrocycles, or the polarity of the AEX structure may be such that AEX is not soluble in organic solvents. The molecular weight of the HMW material encompasses a wide range of values as shown by its gel permeation chromatography elution characteristics. It is possible that the molecular weight of the AEX

material also covers a range of weights. Both fractions are highly aliphatic with the HMW fraction being more so, and the AEX may contain a higher degree of aromaticity than the HMW as supported by the NMR data and the inclusion of porphyrins in the AEX isolate. Both fractions contain large amounts of other lipid material to which the phorbins and porphyrins are bound. In both fractions, a portion of the bonds linking the phorbins and porphyrins to the rest of the structure are susceptible to acid hydrolysis. The spectroscopic characteristics of the phorbins and porphyrins released from both the HMW and AEX fractions suggests that these compounds originated as algal chlorophylls, but not necessarily chlorophyll-*a*.

C. ORIGIN OF HIGH MOLECULAR WEIGHT AND ACID EXTRACTABLE CHLOROPHYLL DEGRADATION PRODUCTS

Two possible sources for both the HMW and AEX material readily present themselves: cross-linking of phorbins and porphyrins with other lipid material occuring either in the water column or surface sediments, and direct biological production of this material in the water column with subsequent deposition in the sediments. During early diagenesis, lipid material quickly becomes bound into macromolecular material and may move from the solvent extractable bitumen into the non-solvent extractable bitumen (Taylor *et al.* 1984). The HMW and AEX structures have similarities as demonstrated by HPLC, IR, and degradation studies, but there is no evidence to support the accumulation of AEX through the further condensation of HMW. Down core studies of HMW and AEX (Ch. 7) show constant concentrations of AEX with increasing concentrations of HMW and total phorbin. For AEX to be forming from HMW, the loss of AEX, either through degradation or through the formation of a phorbin reservoir that we have yet to analyze, must occur at the same rate as the formation of AEX.

The direct biosynthesis of biopolymers which are precursors to both the AEX and HMW chlorophyll degradation products is unlikely for two reasons. First, HPLC chromatograms of extracts of phytoplankton and suspended particulate matter do not possess the large base-line hump (Gieskes and Kraay, 1985; Klein *et al.*, 1986; Burkhill *et al.*, 1987; Downs, 1989; Ondrusek *et al.*, 1991) characteristic of the elution of HMW in total sediment extracts. Analysis of suspended particulate material from the surface Black Sea (10, 20, 30, 40 m) does not indicate the presence of HMW chlorophyll degradation products though HMW chlorophyll degradation products do appear to be present in sediment trap samples (Ch. 5). Second, for HMW and AEX to be directly synthesized as biopolymers, the chlorophyll which contributes the phorbin-like appearance to the visible

spectra of the HMW and AEX isolates would have to be bound to the thylakoid membrane. Since chlorophyll is loosely associated, being non-covalently bound, with the thylakoid membrane and its proteins in the chloroplasts of algae (Miller, 1979; Anderson and Barrett, 1986; Kuhlbrandt and Wang, 1991), it is unlikely that the HMW and AEX degradation products are entering the sediments as part of biopolymers. Sun (1992) isolated a fraction of chlorophyll in sediments which could only be released from the sediment matrix by freezing of the sample, and proposed that this fraction represented chlorophyll still associated with the thylakoid membrane. The samples used in this study were frozen prior to analyses, therefore neither HMW nor AEX chlorophyll degradation products represent the "bound" chlorophyll identified by Sun (1992).

A more plausible origin for high molecular weight chlorophyll degradation products is the incorporation of phorbins into larger structures by chemical or microbial reaction. If this process is occuring, it must start very early in the diagenetic process since we have evidence for both HMW and AEX chlorophyll products in sediment trap samples (Ch. 6). Cross-linking of sedimentary lipids with each other and with geopolymers is thought to be a major process in kerogen formation (Tissot and Welte, 1984). In sulfur rich environments, cross-linking of organic matter with sulfur has been proposed to account for the wide variety of identifiable lipids released from bitumen (Kohnen *et al.*, 1991). To determine if sulfur-linkages are involved in the incorporation of phorbins into HMW and AEX, Raney-nickel desulfurization was performed on these samples. Raney-nickel desulfurization failed to release phorbins from HMW and AEX material in any quantity which could be detected spectrophotometrically, suggesting sulfur is not involved in this condensation of phorbins and porphyrins with other lipid material. Comparisons of degradation products of kerogen, insoluble algal residues, and whole algae led Philp and Calvin (1976) and Philp *et al.* (1978) to suggest that lipid material deposited in sediments not associated with macromolecular structures may become associated with the insoluble residues of algae and bacteria. The results of these studies further suggest that sulfur is not necessary for the condensation of organic molecules into geomacromolecules. The presence of sulfur does not appear to be necessary for the inclusion of chlorophyll degradation products into HMW and AEX material.

The work of Oehler further supports the incorporation of phorbins into macromolecular structures. Oehler *et al.* (1974) found that chlorophyll could become incorporated into algal detritus in such a way that it is difficult to extract. He subjected algae to thermal alterations under oxic and anoxic conditions and analyzed the samples for chlorophyll content. Under anoxic conditions, Oehler *et al.* (1974) found that intracellular chlorophyll was altered to pheopigments and, when incubated for 30 minutes at 250°C,

chlorophyll and pheopigments became non-extractable with organic solvents. Pheopigments in the treated algae were not base extractable, but could be extracted with acid, though Oehler *et al.* (1974) did not specify the type or strength of acid which was used. The present study has shown that most of the AEX sedimentary chlorophyll degradation products are not extractable with HCl, but only with strong H_2SO_4. Black Sea surface sediment examined in this study have not been subjected to thermal degradation, but the increased temperatures used by Oehler *et al.* (1974) were used to simulate burial and the passage of time. If the mechanism of inclusion of chlorophyll degradation products into more complex structures under anoxic conditions shown by Oehler *et al.* (1974) is at work in surface sediments, then the HMW fraction may represent the input of intact chlorophyll containing algal cells or biopolymers of algal origin onto which chlorophyll has become grafted. Visible spectra of thermally altered algae under anoxic conditions (Oehler, *et al.*, 1974) resemble the spectra found for both the HMW and AEX material considered in this paper.

Once the initial association of chlorophyll degradation products with other lipid material occurs, whether this material is cell membrane or lipids from other sources, further reaction with other lipid material may occur until the high molecular weight material is no longer solvent extractable. The increasing insolubility of once soluble macromolecules in organic solvents due to continued cross-linking has been proposed by Tegelaar *et al.* (1989) and Kohnen *et al.* (1991). The time frame necessary for condensation of phorbins with other lipid material such in such a manner that the structure is not solvent extractable is unknown, though AEX chlorophyll degradation products have been found in sediment trap samples (Ch. 6). Unequivocal evidence for the early association of chlorophyll in HMW and AEX material rests upon determining the impact of lateral transport of resuspended material on sediment trap samples. The incorporation of phorbins into non-solvent extractable material, as shown in this study, suggests an origin for porphyrins found in kerogens and oils.

IV. CONCLUSIONS

A significant fraction of solvent extractable chlorophyll degradation products (30%) exists in Black Sea sediments in high molecular weight form. Another 30% exists in an acid extractable forms. The molecular weight of the phorbin containing macromolecules is greater than 1000 a.m.u.. Individual phorbins can be freed from the macromolecular matrix by hydrolysis using H_2SO_4/MeOH. One-third of total chlorophyll degradation

products exists in Black Sea sediments in a fraction than can only be released from the sediment matrix using strong acid. This fraction may be further treated with methanolic acid to release discrete phorbins and porphyrins. Spectroscopic and chromatographic data suggest the HMW and AEX fractions are structurally similar and the phorbins and porphyrins are bound in the macromolecular structures with other lipids. Macromolecular and acid extractable chlorophyll containing structures may represent either condensation of chlorophyll degradation products with other sedimentary lipids or deposition of chlorophyll degradation products bound with lipids possibly as intact algal structures.

It remains unclear as to how phorbins are associated with the other constituents of the HMW and AEX material. These studies suggest the phorbins and porphyrins are bound into HMW and AEX through bonding with is at least partly susceptible to cleavage with H_2SO_4. Further work needs to be done to further establish the means through which chlorophyll is incorporated such as oxidation with CuO and RuO_4 to selectively cleave ether linkages and aromatic structures. The stability of phorbins and porphyrins under the conditions used in Raney-nickel desulfurization also needs to be established. Further work is required in order establish the role of H_2SO_4 as an agent for the release of phorbins and porphyrins from sediment samples. It is unknown whether H_2SO_4 acts as an agent for solubilization or bond cleavage in the extraction of AEX. If these compounds represent condensation products, then their identification has wider implications in the preservation of not only chlorophyll, but also for other natural products in sediments, and for the origin of porphyrins found in ancient sediments.

V. REFERENCES

Anderson J. M. and Barrett J. (1986) Light-harvesting pigment-protein complexes of algae. In: Photosynthesis III: Photosynthetic Membranes and Light Harvesting Systems (Eds: L. A. Staehelin and C. J. Arntzen) Springer-Verlag.

Baker E. W. and Louda J. W. (1983) Thermal aspects in chlorophyll geochemistry. *Adv. Org. Geochem 1981*, 401-421.

Barwise A. J. G. and Roberts I. (1984) Diagenetic and catagenetic pathways for porphyrins in sediments. *Org. Geochem.* **6**, 167-176.

Barwise A. J. G. and Whitehead E. V. (1980) Separation and structure of petroporphyrins. *Adv. Org. Geochem. 1979*, 181-192.

Blumer M. and Rudrum M. (1970) High molecular weight fossil porphyrins: Evidence for monomeric and dimeric tetrapyrroles of about 1100 molecular weight. *J. Inst. Pretrol.* **56**, 99-106.

Blumer M. and Snyder W. D. (1967) Porphyrins of high molecular weight in a Triassic oil shale: Evidence by gel permeation chromatography. *Chem. Geo.* **2**, 35-45.

Bonnet R., Brewer P., Noro K., and Noro T. (1972) On the origin of petroporphyrin homologues: the transalkylation of vanadyl octa-alkylporphyrins. *J.C.S. Chem. Comm.* **1972**, 562-563.

Bonnet R., Brewer P., Noro K., and Noro T. (1978) Chemistry of vanadyl porphyrins. *Tetrahedron* **35**, 379-385.

Burkill P. H., Mantoura R. F. C., Llewellyn C. A., and Owens N. J. P. (1987) Microzooplankton grazing and selectivity of phytoplankton in coastal waters. *Mar. Bio.* **93**, 581-590.

Casagrande D. J., and Hodgson G. W. (1971) Geochemical simulation evidence for the generation of homologous decarboxylated porphyrins. *Nature Phys. Sci.* **233**, 123-124.

Cronin J. R. and Morris R. J. (1982) The occurrence of high molecular weight humic material in recent organic-rich sediment from the Nambian Shelf. *Estuarine, Coastal and Shelf Sciences* **15**, 17-27.

Downs J. N. (1989) Implications of the phaeopigments, carbon and nitrogen content of sinking particles for the origin of export production. Ph.D. dissertation, Univ. of Washington.

Ertel J. R. and Hedges J. I. (1983) Bulk chemical and spectroscopic properties of marine and terrestrial humic acids, melanoidins and catechol-Based synthetic polymers. In: Aquatic and Terrestrial Humic Materials (Ed. R. F. Christman and E. T. Gjessing). pp 143-163, Ann Arbor Science.

Fales H. M., Jaouni T. M., and Babashak J. F. (1973) A simple device for preparing etheral diazomethane without resorting to codistillation. *Anal. Chem.* **45**, 2302-2303.

Furlong E. T. and Carpenter R. (1988) Pigment preservation and remineralization in oxic coastal marine sediments. *Geochim. Cosmochim Acta* **52**, 87-99.

Gieskes W. W. and Kraay G. W. (1983) Unknown chlorophyll-a derivatives in the North Sea and the tropical Atlantic Ocean revealed by HPLC analysis. *Limnol. Oceanogr.* **28**, 757- 766.

Gillan F. T. and Johns R. B. (1980) Input and early diagenesis of chlorophylls in a temperate intertidal sediment. *Mar. Chem.* **9**, 243-253.

Holden P. N. and Gaffey M. J. (1990) Practical considerations for using reflectance spectroscopy as a screen tool for geoporphyrins. *Energy Fuels* **4**, 705-709.

Holden P. N., Sundararaman P., and Gaffey M. J. (1991) Estimation of porphyrin concentration in the kerogen fraction of shales using high-resolution reflectance spectroscopy. *Geochim Cosmochim Acta* **55**, 3893-3900.

Keely B. J., Brereton R. G., and Maxwell J. R. (1988) Occurrence and significance of pyrochlorins in lake sediment, Advances in Organic Geochemistry 1987, *Org. Geo.*, **13**, 801-805.

Keely B. J., Prowse W. G., and Maxwell J. R. (1990) The Treibs Hypothesis: An evaluation based on structural studies, *Energy Fuels*, **4**, 628-634.

Klein B., Gieskes W. W. C., and Kraay G. G. (1986) Digestion of chlorophyll and carotenoids by the marine protozoan *Oxyrrhis mariana* studied by h.p.l.c. analysis of algal pigments. *J. Plankt. Res.* **8**, 827-836.

King L. L. and Repeta D. J. (1991) Pyropheophorbide steryl esters in Black Sea sediments. *Geochim. Cosmochim. Acta* **55**, 2067-2074

Kohnen M. E. L., Sinninghe Damste J. S., Kock-van Dalen A. C., and de Leeuw J. W. (1991) Di- or polysulphide-AEX biomarkers in sulphur-rich geomacromolecules as revealed by selective chemolysis. *Geochim. Cosmochim. Acta* **55**, 1375-1394.

Kuhlbrandt W. and Wang D. N. (1991) Three-dimensional structure of plant light-harvesting complex determined by electron crystallography. *Nature* **350**, 130-134.

Louda J. W. and Baker E. W. (1981) Geochemistry of the tetrapyrrole, carotenoid, and perylene pigments in sediments from the San Miguel Gap (Site 467) and Baja California borderland (Site 471), Deep Sea Drilling Project Leg 63. In *Initial Reports of the Deep Sea Drilling Project* (Ed. B. Haq, and R. S. Yeats). Vol. 63, pp. 785-818. U. S. Government Printing Office.

Mackenzie A. S., Quirke J. M. E., and Maxwell J. R. (1980) Molecular parameters of maturation in the Toarcian shales, Paris Basin, France -- II. Evolution of metalloporphyrins. *Adv. Org. Geochem. 1979*, 239-248.

Miller K. R. (1979) The photosynthetic membrane. *Sci. Am.* **241**, 102-113.

Moore J. C. (1964) Gel permeation chromatography. I. A new method for molecular weight distribution of high polymers. *J. Polym. Sci. Pt. A* **2**, 835-843.

Oehler J. H. Aizenshtat Z., and Schopp J. W. (1974) Thermal alteration of blue-Green algae and blue-Green algal chlorophyll. *Amer. Assoc. Petrol. Geo. Bull.* **58**, 124-132.

Ondrused M. E., Bidigare R. R., Sweet S. T., Defreitas D. A., and Brooks J. M. (1991) Distribution of phytoplankton pigments in the North Pacific Ocean in relation to physical and optical variability. *Deep-Sea Res.* **38**, 243-266.

Philp R. P. and Calvin M. (1976) Possible origin for insoluble organic (kerogen) debris in sediments from insoluble cell-wall materials of algae and bacteria. *Nature* **262**, 134-136.

Philp R. P., Calvin M., Brown S. and Yang E. (1978) Organic geochemical studies on kerogen precursors in recently deposited algal mats and oozes. *Chem. Geol.* **22**, 207-231.

Poutanen E.-L. and Morris R. J. (1983) The occurrence of high molecular weight humic compounds in the organic-rich sediments of the Peru continental shelf. *Oceanologica Acta* **6**, 21-28.

Quirke J. M. E., Shaw G. J., Soper P. D., and Maxwell J. R. (1980) Petroporphyrins II. The presence of porphyrins with extended alkyl substituents. *Tetrahedron* **36**, 3261-3267.

Ross D. A., Uchupe E., and Bowin C. O. (1974) Shallow structure of the Black Sea, In: The Black Sea--Geology, Chemistry, and Biology, E. T. Degen and D. A. Ross, Eds. Am. Assoc. Petrol. Geol. pp 1-10.

Sato S. (1980) Diagenetic alteration of organic matter in leg 57 sediments, deep sea drilling project. In *Initial Reports of the Deep Sea Drilling Project* (Ed. Scientific Party), Vol. 61-62, pp 1305-1312. U.S. Government Printing Office.

Sun M. (1992) Early diagenesis of chloropigments in coastal sediments. Ph.D. thesis, State University of New York at Stony Brook.

Taylor J., Young C., Parkes R. J., Eglinton T., and Douglas A. G. (1984) Structural relationships in protokerogens and other geopolymers from oxic and anoxic sediments. *Org. Geochem.* **6**, 279-286.

Tegelaar E. W., de Leeuw J. W., Derenne S., and Largeau C. (1989) A reappraisal of kerogen formation, *Geochim. Cosmochim. Acta* **53**. 3103-3106.

Tissot B. P. and Welte D. H. (1984) Petroleum formation and occurrence, Springer-Verlag. 697 pp.

Van Berkel G. J., Quirke J. M. E., and Filby R. H. (1989) The Henryville Bed of the New Albany Shale -- II. Comparison of the nickel and vanadyl porphyrins in the bitumen with those generated from the kerogen during simulated catagensis. *Org. Geochem.* **14**, 129-144.

CHAPTER 5

PYROPHEOPHORBIDE-*A* STERYL ESTERS IN SEDIMENT TRAP SAMPLES FROM THE BLACK SEA

CHAPTER 5

PYROPHEOPHORBIDE-*A* STERYL ESTERS IN SEDIMENT TRAP SAMPLES FROM THE BLACK SEA

I. INTRODUCTION

Pyropheophorbide-*a* steryl esters, which represent a major sink for chlorophyll in sediments, have been reported previously by King and Repeta (1991; Ch. 3), Prowse and Maxwell (1991), and Eckardt *et al.* (1991). These compounds are formed through the esterification of pyropheophorbide-*a* with sterols, but neither the location nor the mechanism of formation, is known. Based on a comparison of the reported distribution of sterols in Black Sea sediment traps and suspended particulate matter with the distribution of sterols esterified to pyropheophorbide-*a* found in Black Sea sediments, we (King and Repeta, 1991) surmised that the esterified sterol distribution must be influenced by the distribution of planktonic species and primary production. Due to its well documented cycles of primary production and succession of phytoplankton species, the Black Sea is an appropriate location to investigate the relationship of sterols esterified to pyropheophorbide-*a* with the distribution of phytoplankton sterols, and with the cycle of primary production. The results of the present study show pyropheophorbide-*a* steryl esters to be present in sediment trap samples and indicate that the esterified sterols change with season. We therefore compared the concentration of PSEs and the PSE sterol distribution with the annual distribution of producers and the annual production cycle in the Black Sea.

The cycle of primary production in the Black Sea has two major blooms (Sorokin, 1983; Benli, 1987): the spring bloom in March - April, and the fall bloom in August - September. Different phytoplankton species are responsible for the production in each bloom, with diatoms being the major producers during the spring bloom, and coccolithophores being the major producers during the fall bloom (Benli, 1987). The community of producer species should be reflected in the distribution of organic compounds found in the underlying sediments, though the signal will be integrated over time (with sediment depth) and loss of quantitative information will occur during diagenesis.

The quantity of dinosterol found in Black Sea sediments has led to the suggestion that dinoflagellates are a major contributor of phytoplankton biomass in the Black Sea (Boon *et al.*, 1979), but studies of phytoplankton abundances do not support this conclusion (Sorokin, 1983; Benli, 1987). King and Repeta (1991) suggested that the

distribution of non-esterified solvent-extractable sterols found in sediments does not provide an accurate reflection of the sterol distribution produced in the surface waters of the Black Sea, due to selective remineralization in the water column and at the sediment/water interface. We (King and Repeta, 1991) further suggested that the pyropheophorbide-*a* steryl ester sterol distribution may provide a more accurate reflection of the sterol distribution produced in the surface waters than sedimentary sterols due to the protection of the sterols through their esterification to pyropheophorbide-*a*.

As part of our study of the seasonal production of chlorophyll degradation products using sediment traps, and as a follow-up to our earlier studies, we analyzed the distribution of pyropheophorbide-*a* steryl esters in sediment traps to determine if the distribution of compounds changes over the course of a year and how the distribution of esterified sterols relates to producer species. Our data shows a cycle in the flux of total pyropheophorbide-*a* steryl esters which is similar to the cycle of primary production. The distribution of sterols esterified to pyropheophorbide-*a* in sediment traps further suggests that the pyropheophorbide-*a* steryl ester sterol distribution is determined by the community of phytoplankton living in the photic zone at the time of pyropheophorbide-*a* steryl ester production.

II. METHODS

A composite sediment sample from 0 - 4 cm taken from Box Core 5 Station 3 (Fig. 5.1; 43°04.23'N, 33°58.37'E) was sonically extracted 15 minutes with 3 x 25 mL acetone and 1 x 25 mL CH_2Cl_2. The extracts were combined, concentrated by rotary evaporation, and back extracted with 3 x 50 mL 30% hexane/ether. The organic phase was dried over Na_2SO_4, the solvent evaporated, and the residue dissolved in 100 mL acetone. The concentration of total phorbins was determined spectrophotometrically at 665 nm ($\varepsilon = 5 \times 10^4$ L/molxcm). From 2% of the extract, non-esterified solvent-extractable sedimentary sterols were isolated according to the method of Farrington *et al.* (1988), and acylated using 50 µL each of acetic anhydride and pyridine (Volkman *et al.*, 1984).

Pyropheophorbide-*a* steryl esters (PSEs) were isolated from the remaining total organic extract by HPLC on an Alltech absorbosphere 15 cm, 5 mm ID, 3µm column, using 20/80 (v/v) *n*-PrOH/MeOH at a flow rate of 1.5 mL/minutes, with fluorometric detection (excitation at 415 nm and emission at 675 nm). The PSE isolate was then concentrated and PSEs further purified by repeating the same HPLC procedure. Prior to each isolation step, the HPLC column was washed with 500 mL 50% CH_2Cl_2/MeOH.

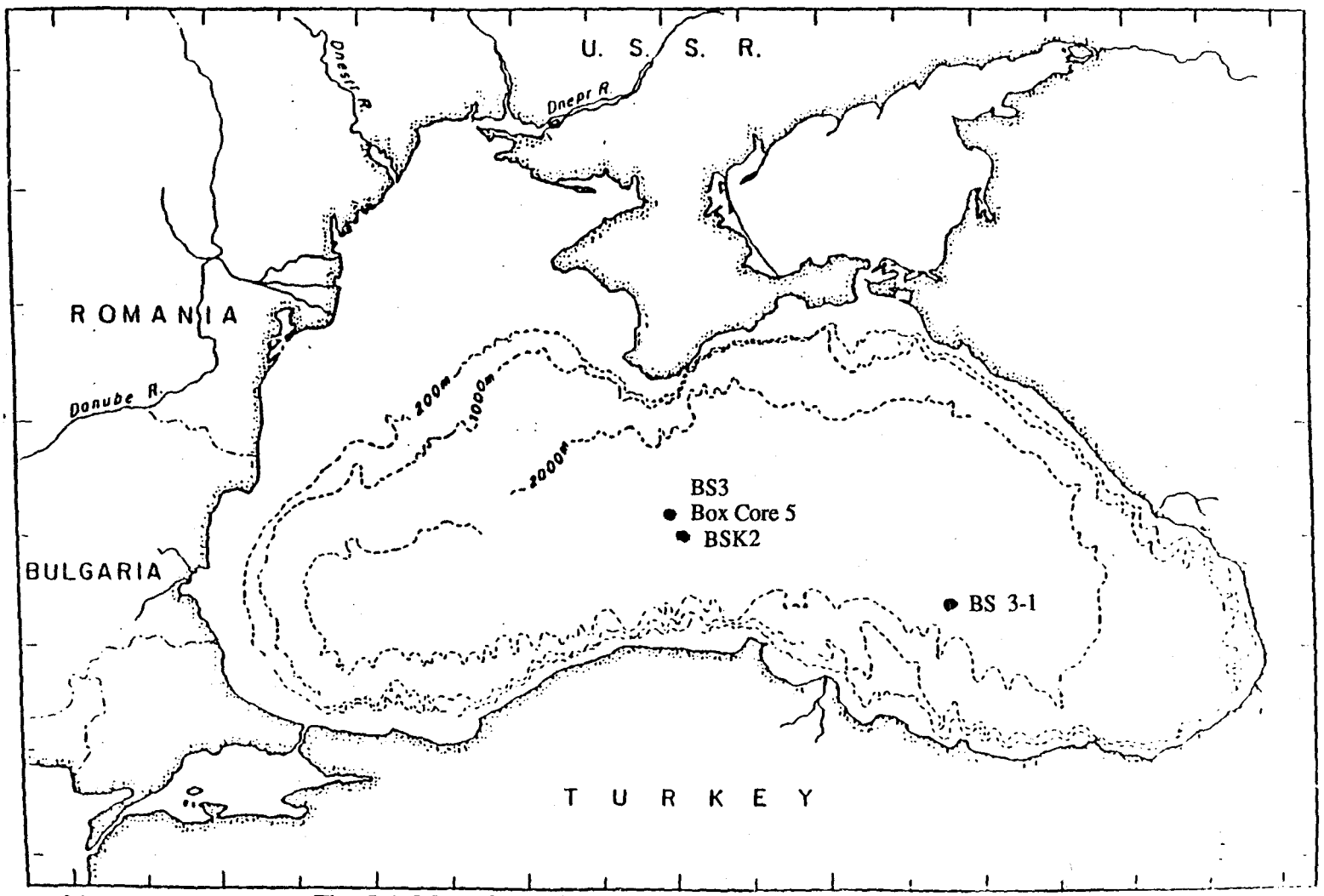

Fig. 5-1 Map of the Black Sea. Sampling locations are indicated.
(Ross *et al.*, 1974)

The PSEs eluted between 30 and 60 minutes. Prior to isolation of the PSEs, the potential for contamination of the PSE isolate with non-esterified solvent-extractable sterols was determined. In order to determine whether non-esterified solvent-extractable sterols would separate from PSEs using the above HPLC method, the retention time of non-esterified solvent-extractable sterols (mixture of authentic sterols) was determined by refractive index detection to be 3 - 10 minutes. After analyzing pure sterols, the HPLC column was washed with 500 mL 50% CH_2Cl_2/MeOH, and then 200 mL of 20% *n*-PrOH/MeOH was pumped through the HPLC column and collected, evaporated, diluted to 1 mL, and analyzed by GC. No sterols were found to be retained by the HPLC column. Following the second HPLC purification step, a fraction of the PSE isolate was reanalyzed by HPLC and determined to contain 90% PSEs.

After isolation and purification, the PSEs were quantified by visible spectrophotometry and split 1:1, and 50% was diluted to 200 µL and 1 µL analyzed by GC to show that no sterols are present in the sample prior to hydrolysis of the PSE esters. This is necessary since non-esterified solvent-extractable sterols are 1000 times more abundant than are PSE sterols in sediments. Low levels of contamination were found prior to the region were sterols elute using our GC program, but no peaks eluted in the sterol region of the gas chromatogram.

Pyropheophorbide-*a* steryl esters were hydrolyzed by dissolving them in 500 µL 5% H_2SO_4/MeOH and allowing the mixture to react overnight. The acidic solution was diluted with 1 mL permanganate distilled water, extracted with 3 x 1 mL 20% ethyl acetate/hexane, and the solvent evaporated. Hydrolysis of synthetic pyropheophorbide-*a* cholesteryl ester indicated that the recovery of the sterol portion of the hydrolyzed PSEs is 95% and the pyropheophorbide-*a* portion is 75%. The hydrolyzed isolate was then acylated using 50 µL each of acetic anhydride and pyridine (Volkman *et al.*, 1984).

Black Sea sediment trap samples for the period covering 1988-89 were obtained from BSK2 (43°00.13'N, 34°00.73'E) and BSK3-1 (42°20.85'N, 37°34.22'E) (Fig. 5-1). The sediment trap samples analyzed are listed in Table 5-1. Samples were split, placed in glutaraldehyde and refrigerated at 4°C. Prior to analysis, samples were filtered onto GF/F filters and rinsed with $KMnO_4$ distilled water. Filters were then ground in 2 - 6 mL cold acetone, transfered to centrifuge tubes, and the grinding stone and tube were rinsed with acetone and the rinse added to the sample. After centrifugation for 10 minutes, the supernatant was evaporated, diluted to 1 - 10 mL of 100% acetone, and analyzed by visible spectrophotometry to determine total phorbin content (665 nm, $\varepsilon = 5 \times 10^4$ L/molxcm). Pyropheophorbide-*a* steryl esters were analyzed by HPLC using a 30 min linear gradient from 100% A to 100% B with an additional 60 min isocratic B, where A is 20/80 (v/v) 0.5

Table 5-1
TRAP DESIGNATIONS AND DATES OF DEPLOYMENT FOR ANALYZED SEDIMENT TRAP SAMPLES

station designation	trap depth (m)	sample designation	dates of deployment	No. days per cup	size fraction
BSK2	477	2ST6S	6/2 - 6/8/88	5.75	<1 mm
		2ST7S	6/8 - 6/14/88	5.75	
		2ST1	8/1 - 8/31/89	30	
		2ST2	8/31 - 10/1/88	30	
		2ST3	10/1 - 10/31/88	30	
		2ST4	10/31 - 12/1/88	30	
		2ST5	12/1 - 12/31/88	30	
		2ST6	12/31/88 - 1/31/89	30	
		2ST7	1/31 - 3/1/89	30	
		2ST8	3/1 - 4/1/89	30	
		2ST9	4/1 - 5/1/89	30	
		2ST10	5/1 - 6/1/89	30	
		2ST11	6/1 - 7/1/89	30	
		2ST12	7/1 - 8/1/89	30	
	1300	2ST1D	8/1 - 8/31/88	30	<1 mm
		2ST2D	8/31 - 10/1/88	30	
		2ST3D	10/1 - 12/1/89	30	
BSK3-1	1172	3ST1 L1	4/26 - 8/1/89	90	<1 mm
		3ST1 G1	4/26 - 8/1/89	90	>1 mm
		3ST2	8/1 - 8/31/89	30	<1 mm
		3ST3	8/31 - 10/1/88	30	
		3ST4	10/1 - 10/31/88	30	
		3ST5	10/31 - 12/1/88	30	
		3ST6	12/1 - 12/31/88	30	
		3ST7	12/31/88 - 1/31/89	30	
		3ST8	1/31 - 3/1/89	30	
		3ST9	3/1 - 4/1/89	30	
		3ST10	4/1 - 5/1/89	30	
		3ST11	5/1 - 6/1/89	30	
		3ST12	6/1 - 7/1/89	30	
		3ST13	7/1 - 8/1/89	30	

N NH_4OAc(aq)/MeOH and B is 20/80 (v/v) *n*-PrOH/MeOH. Pyropheophorbide-*a* steryl esters elute between 65 - 85 minutes. Concentrations of PSEs were determined by integration of the total HPLC peak area, and using a conversion factor determined using synthetic PSEs.

The distribution of PSE molecular weights was determined in select sediment trap samples from BSK3-1 (May - July 1988, November 1988, December 1988, and January 1989) and in sediments by isolating PSEs from the organic extract by TLC (Merck Kieselgel 60, plate washed with acetone and activated 2 hr at 250°C) developed with 25% acetone/hexane. The uppermost band, which contains PSEs and pheophytin-*a* was recovered and analyzed by methane CI-MS. Chemical ionization-MS were collected by applying CH_2Cl_2 solutions of each PSE sample to the platinum wire of the DCI probe. The probe was inserted with the mass spectrometer source temperature at 100°C, the ionization potential at 130eV, and the methane pressure at 0.5 torr. Upon insertion of the probe, the current through the wire was increased from 0 to 3 amps in 7 sec.

Sterols from sediment traps, sediments, and PSEs were analyzed by GC. Gas chromatographic analyses were performed on a Carlo Erba 4160 gas chromatograph equipped with a 30 m, 0.25 mm i.d. fused silica capillary column coated with phenylmethylsilicone (DB-5; J & W Scientific), using H_2 carrier gas and temperature programmed from 80 - 260°C at 3.5°/min, then 4°/min to a final temperature of 310°C which was maintained for 20 minutes. A Finnigan 4510 quadrupole mass spectrometer was used for GC/MS analysis of the acylated sterols from PSEs, sediment traps, and sediments. The GC/MS GC conditions were the same as those used for GC analysis.

III. RESULTS AND DISCUSSION

A. PYROPHEOPHORBIDE-*A* STERYL ESTERS IN BLACK SEA SEDIMENT TRAPS

In Ch. 3 and in King and Repeta (1991), we describe the occurrence and distribution of pyropheophorbide-*a* steryl esters in a Black Sea sediment sample, and postulate that these compounds are formed in the upper water column, possibly through the process of grazing. We further suggest that the sterol distribution in PSEs may approximate the distribution of sterols as produced by phytoplankton. To further investigate the source of PSEs and the origin of their sterol distribution, we examined the distribution of PSEs in samples from two one-year sediment trap time series (Table 5-2) collected in the central and western basins of the Black Sea.

Table 5-2

FLUX OF PSEs AND TOTAL PHORBIN AT SEDIMENT TRAP STATIONS BSK2 AND BSK3-1

	flux (nmol/m^2/d)					
	BSK2				BSK3-1	
	477 m		1300 m		1172 m	
deployment dates	phorbin	PSEs	phorbin	PSEs	phorbin	PSEs
6/2 - 6/8/88	22.	3.0				
6/8 - 6/14/88	19.	2.3				
4/26 - 8/1/89					41.	18.
8/1 - 8/31/89	12.	1.5	25.	3.4	0.33	0.062
8/31 - 10/1/88	11.	0.64	17.	1.2	0.57	0.090
10/1 - 10/31/88	4.7	0.51	11.	0.82	1.5	0.14
10/31 - 12/1/88	21.	0.72			8.0	0.93
12/1 - 12/31/88	3.1	0.35			29.	3.3
12/31/88 - 1/31/89	46.	3.7			13.	3.1
1/31 - 3/1/89	11.	4.0			0.48	0.13
3/1 - 4/1/89	8.7	0.92			0.57	0.14
4/1 - 5/1/89	2.2	1.2			0.31	0.063
5/1 - 6/1/89	0.20	0.15			0.00	0.0
6/1 - 7/1/89	2.2	1.1			0.00	0.0
7/1 - 8/1/89	0.00				0.41	0.065

Total organic extracts of sediment trap samples were analyzed by HPLC and the concentration of total PSEs determined by integration. The flux of PSEs at BSK3-1 and BSK2 is plotted along with total phorbin flux in Fig. 5-2. The annual cycle of PSE flux follows the same trends as total phorbin flux. At station BSK3-1, the most striking differences in the yearly flux cycle of PSE's and total phorbin is the much lower magnitude of the fall flux maximum for the PSEs as compared with total phorbin. Also, the fall PSE flux maximum is spread over two months whereas the fall total phorbin flux maximum occurs in a single month.

A comparison of PSE and total phorbin flux at BSK2 produces results similar to BSK3-1 (Fig. 5-2), with the PSE flux maximum again spread over two months at BSK2 as at BSK3-1. At BSK2, the magnitude of the total phorbin flux increased during November, decreased in December, then maximized in January. The November increase in PSE flux at BSK2 is relatively smaller than that for total phorbin flux, and the

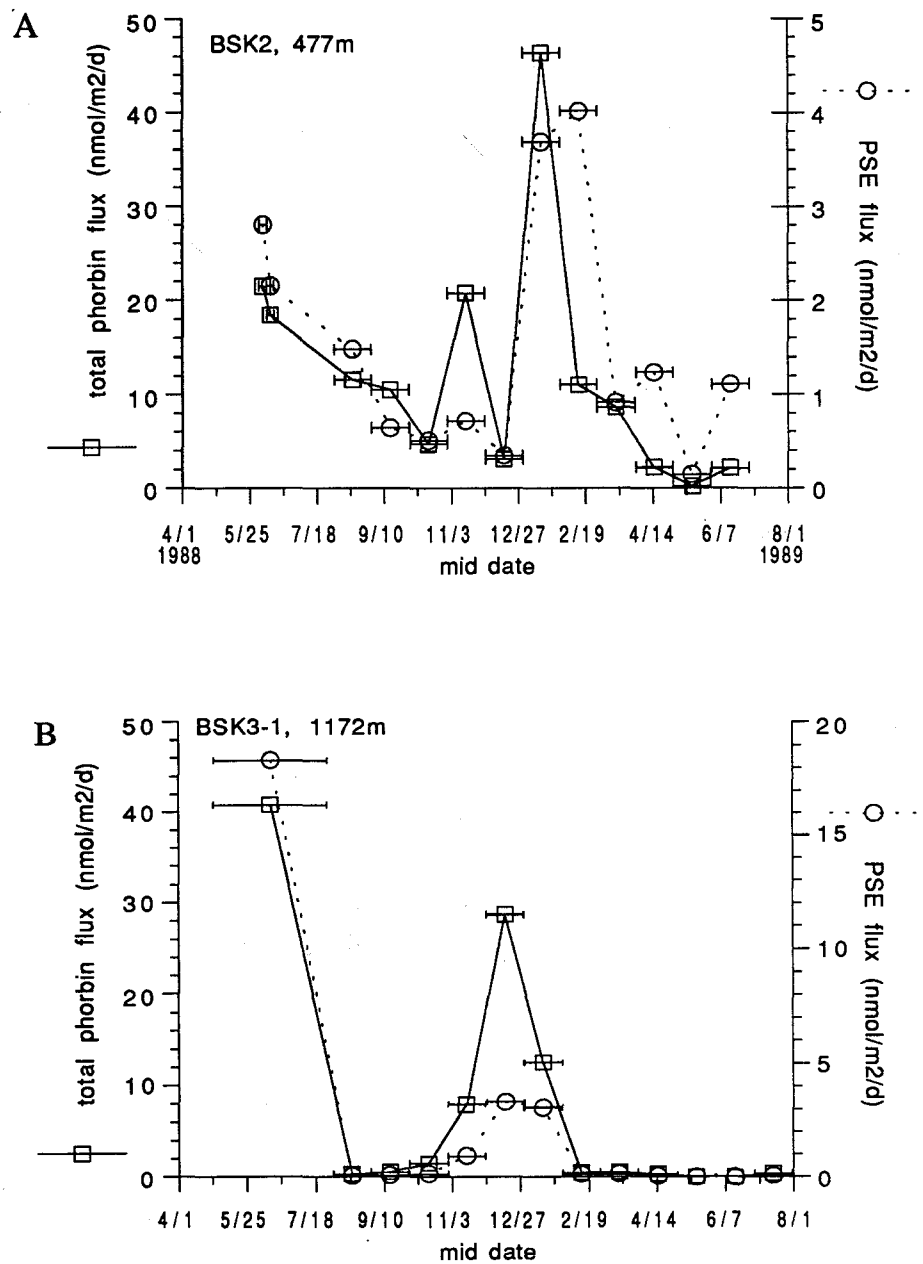

Fig. 5-2 Plots of the total flux of phorbins and PSEs over time in sediment traps at stations BSK2 (A) and BSK3-1 (B).

January/November flux ratio in the PSEs is greater than that for total phorbins, indicating the later increase in PSE flux relative to total phorbin flux, if the December flux data is not considered. This data, along with the timing of the PSE flux maximum, which is spread over two months at both BSK2 and BSK3-1, supports the slightly later occurrence of the PSE flux maximum as compared with the total phorbin flux maximum. Low flux values at 477 m in December are seen in total flux as well as all phorbin type pigments. At BSK2, the only data for the 1988 spring bloom is from two one-week trap samples collected in mid-July, which would place these data in the declining portion of the flux maximum. Therefore, at BSK2, it is again unknown how the total phorbin flux data compare with the PSE data in the spring bloom.

The relationship of PSE flux to that of total phorbin flux is best illustrated by plots of the relative contribution of total PSEs to total phorbin flux (Fig. 5-3). The relative contribution of PSEs to total phorbin flux varies between 2 and 35% at BSK2, and between 9 and 29% at BSK3-1. At BSK3-1, the minimum in relative percent PSEs occurs during October when the total phorbin flux has begun to increase towards the fall flux maximum, and the maximum in percent PSE occurs when the total phorbin flux is approaching its minimum. The cycle of relative percent PSE in the total phorbin flux follows the same trends as the total phorbin flux cycle but with maxima occuring later than the total phorbin flux maxima. At trap site BSK2, the annual cycle of relative percent PSE follows the same pattern as seen at site BKS3-1 (Fig. 5-3). The PSEs account for a progressively larger percentage of total phorbin flux as the phytoplankton bloom progresses and the maximum percentage occurs after the phorbin flux has decreased to its minimum value. This data supports the conclusion that as the phytoplankton bloom (as recorded by phorbin flux) progresses, the importance of PSEs as a degradation product for chlorophyll increases.

Since PSEs have not been reported as occuring in living phytoplankton, there are two potential sources for PSEs occurring in sediment traps. These are production during senescence (Prowse and Maxwell, 1991) and during grazing (Prowse and Maxwell, 1991; King and Repeta, 1991; Ch. 3). Two arguments against the production of PSEs during senescence can be made. First, analysis of suspended particulate matter from Black Sea surface waters (10, 20, 30, 40 m) using the HPLC method used in this study, provides no evidence for PSEs in suspended material. Second, if PSEs were forming in senescent algae, then we would expect to see the highest concentrations of PSEs coincident or just prior to the total phorbin flux maximum when recycling of organic matter in the photic zone is at its lowest (Epply and Peterson, 1978). This is opposite of our observations.

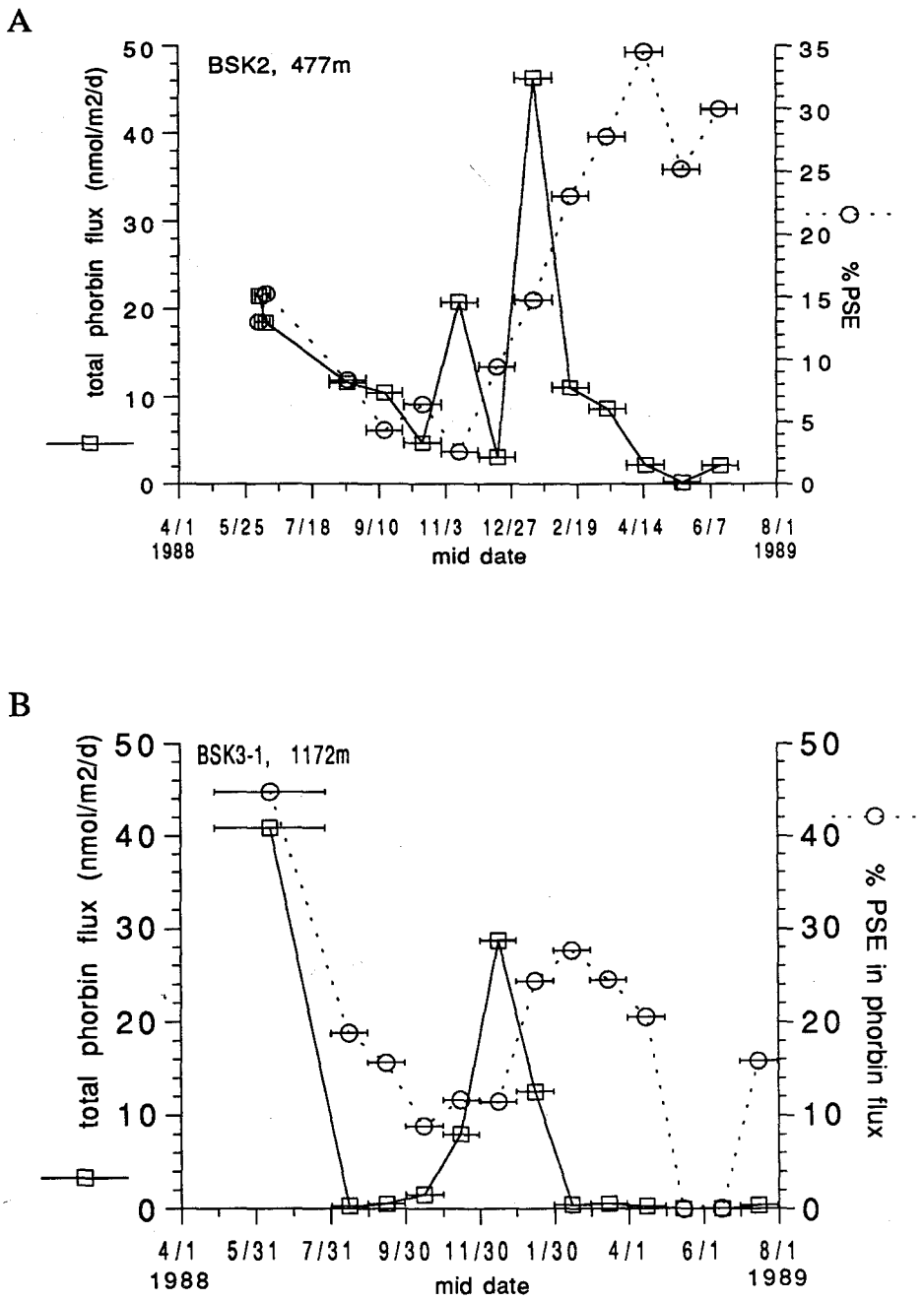

Fig. 5-3 The relative contribution of PSEs to the total phorbin flux over time in sediment traps from stations BSK2 (A) and BSK3-1 (B).

Two different mechanisms for the formation of PSEs during grazing exist. Variations in production of PSEs during grazing caused by changes in zooplankton grazing and food utilization strategies over the course of the phytoplankton bloom may explain the later maxima in PSEs relative to total phorbin. During bloom periods, when phytoplankton numbers are at their maximum, herbivorous zooplankton may graze in such a way that much of the cell contents of the grazed phytoplankton are not ingested (Roy *et al.*, 1989). At high phytoplankton concentrations, the ingestion rate of food by zooplankton is relatively low, and the absorption efficiency of ingested material is maximal (Penry and Frost, 1991; Mayzaud and Razouls, 1992). In culture studies with *Calanus pacificus*, Lopez *et al.* (1988) and Penry and Frost (1991), found that under conditions where *C.pacificus* is conditioned to high food concentrations, 25 - 50% of the ingested chlorophyll-*a* is degraded to colorless products. As food supplies decrease, gut transit times increase and the degradation of chlorophyll-*a* to undetectable material increases (Penry and Frost, 1991). Zooplankton adjust to decreasing food concentrations by decreasing the proportion of chlorophyll-*a* degraded to colorless products (Lopez *et al.*, 1988; Penry and Frost, 1991). This same type of relationship is shown in the relative concentration of PSE produced in the total phorbin flux. After the maximum in primary production is reached, production begins to decrease. At the same time as primary production begins to decrease, the relative production of PSE continues to increase before beginning to decrease.

An alternate explanation for the occurrence of a later flux maximum for PSEs than for total phorbins is succession of grazer species during the course of the bloom. The appearance of different phytoplankton species during the course of a bloom may trigger the increase in numbers of different species of zooplankton, since zooplankton preferentially graze on certain phytoplankton species (Burkhill *et al.*, 1987). Feeding studies have shown that different zooplankton species produce different degradation products of chlorophyll-*a* (Carpenter and Berquist, 1985; Downs, 1989; Roy *et al.*, 1989). The cause of the later PSE flux maximum relative to the total phorbin flux maximum may be that only given species of zooplankton produce PSEs and these species only increase in numbers late in the phytoplankton bloom.

B. TEMPORAL CHANGES IN PYROPHEOPHORBIDE-A STERYL ESTER DISTRIBUTIONS IN SEDIMENT TRAPS

As well as showing variations in the magnitude of flux over the course of a year, the PSEs show qualitative and quantitative variations in the distribution of sterols esterified to pyropheophorbide-*a*. Qualitative changes in the PSE sterol distribution can be seen in

the pattern of HPLC peaks (Fig. 5-4). Studies of the HPLC behavior of PSEs using standards, showed that small variations in sterol structure cause differences in HPLC retention time (Ch. 3). For the months of August 1988 - January 1989, the pattern of HPLC peaks in samples from BSK2 and BSK3-1 are similar, and suggest a similarity in the sterol distributions produced at the two sites. In samples from the months of February, March, April, and May, 1989, the distribution of PSE HPLC peaks at BSK2 is different from that at BSK3-1. The period of February to July, 1989 was characterized by anomalously low level of phytoplankton production during the 1989 spring bloom (Ch. 6). The variations in the PSE distribution at BSK2 and BSK3-1 during this time period, may represent a divergence in sterol production at these two locations in the Black Sea.

At station BSK3-1, analysis of the molecular weight distribution of PSEs in individual sediment trap samples was carried out by CI-MS on the less than 1 mm size fraction of the sample for May - July, and for the less than 1 mm fractions for samples collected in November, December, and January (Fig. 5-5). In each of the three winter samples, the most abundant pseudo-molecular ion is m/z 915 followed by 901, 903, 931, and 929 (molecular weights 914, 900, 902, 930, 928 a.m.u.) (Fig. 5-6). The ratios of the intensity of these four ions to the base peak are greatest in January and lowest in December, indicating that the production of individual PSEs is not constant from month to month. The distribution of PSE pseudo-molecular ions in the samples from November, December, and January (Fig. 5-5, 5-6) is quite different from that of the May - July sample. The difference between the spring and fall bloom samples is best illustrated by the ratio of the intensities of the two ions that are the base-peaks in these two samples. The base peak in the region of m/z 850 - 1000 in May - July is m/z 903, and in January, 915. In May - July, the 903/915 ratio is 3.4 and in January, this ratio is 0.85. All the other ions in the May - July sample have a ratio to m/z 903 (molecular weight of 902) of less than 0.50 (Fig. 5-6).

Based on molecular weights of PSEs, on the known sterols occuring in the Black Sea water column, and on comparisons of the HPLC peak distributions with previous studies (Ch. 3), it is possible to assign the major PSEs in the samples analyzed by CI-MS. Under the assumption that sterols become esterified to pyropheophorbide-*a* in the same relative proportions as they are synthesized, suggestions can be made as to the major groups of phytoplankton contributing organic matter to the sediment trap sample. In the May - July sample, the most abundant PSE, as determined by CI-MS, has a nominal molecular weight of 902 a.m.u. Based on previous studies of PSEs (King and Repeta, 1991); the PSE with a nominal molecular weight of 902 is pyropheophorbide-*a* cholesteryl ester. The May - July sample was collected during the spring bloom when diatoms are the most abundant group of phytoplankton (Benli, 1987), and the most abundant sterol in the

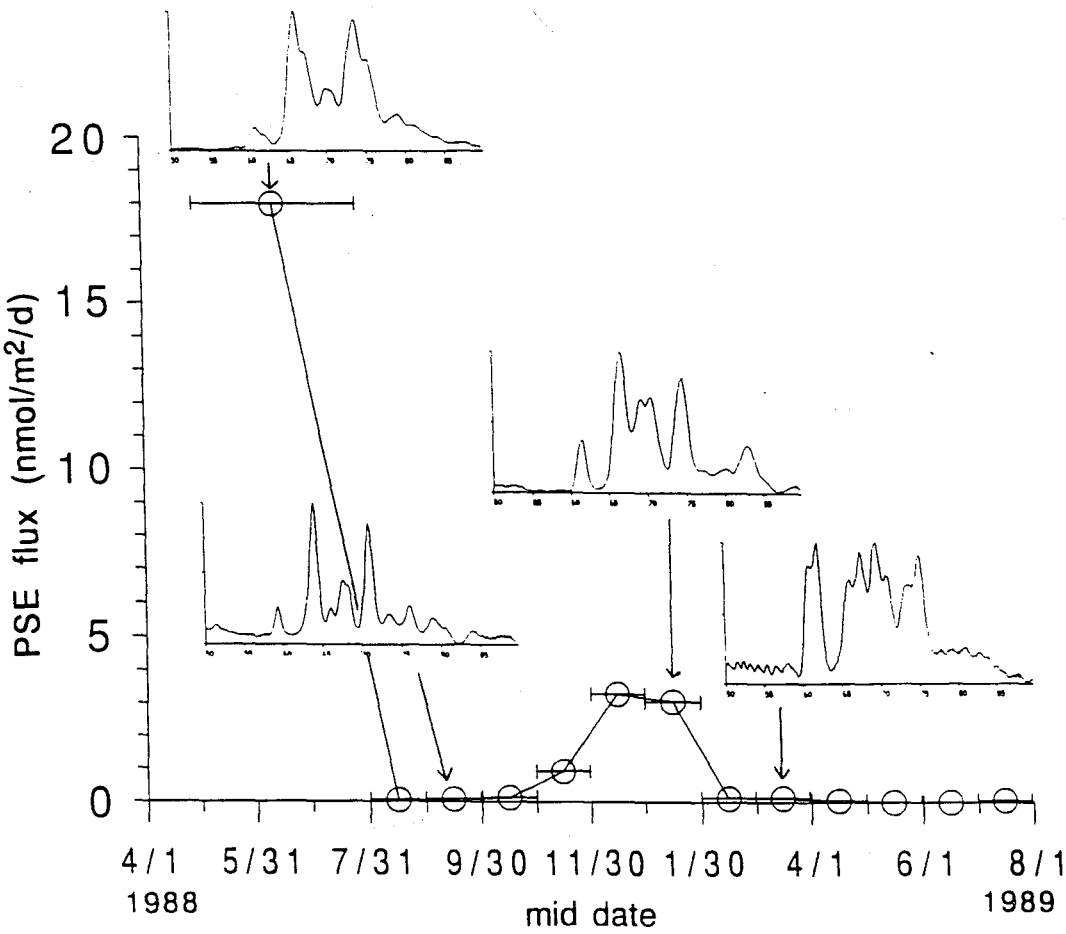

Fig. 5-4 Plot of the variation in PSE flux over the course of a year in sediment traps samples from station BSK3-1. Insets are enlargements of the PSE region of HPLC analysis at the indicated points.

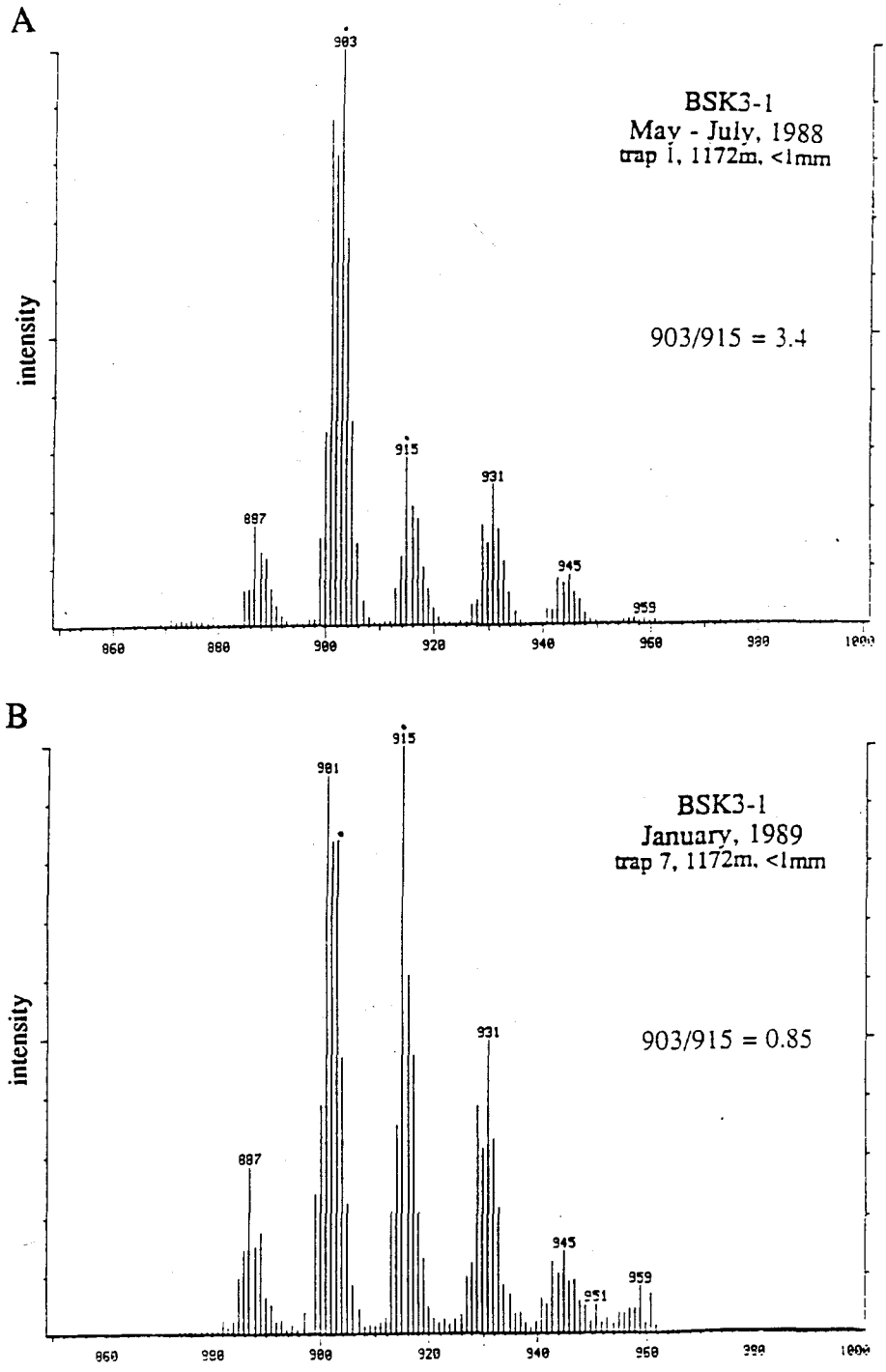

Fig. 5-5 Chemical ionization-MS of total PSE isolates from the May - July, 1988, and January, 1989 sediment trap samples from station BSK3-1.

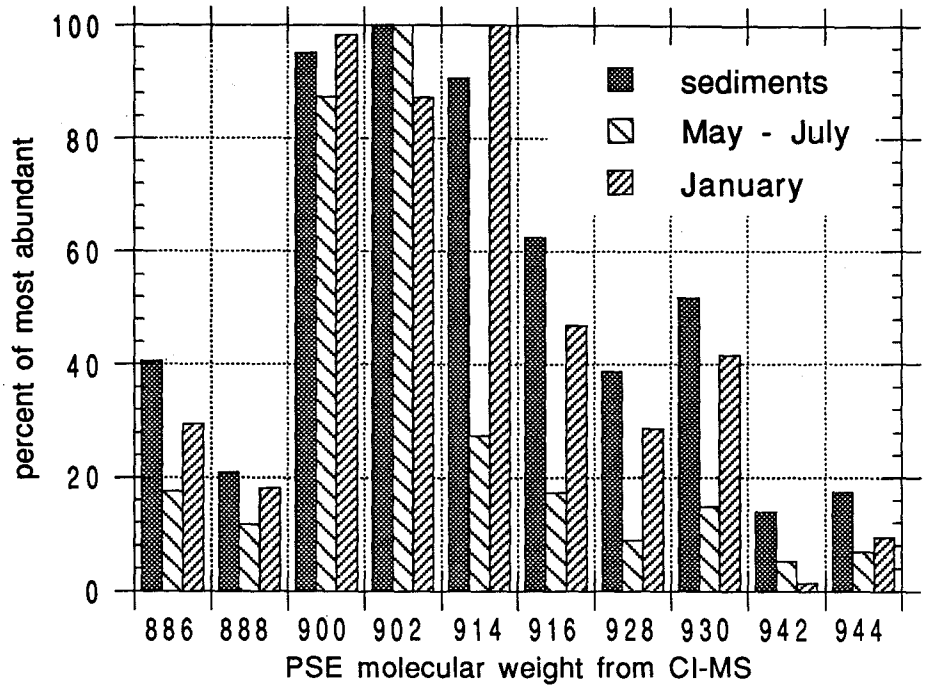

Fig. 5-6 Histogram showing the relative contribution of the individual PSEs to the May - July and January sediment trap samples. Included for comparison is the data for sediments.

dominant diatom species identified in the Black Sea, *Rhizoselenium spp*, is cholesterol (Volkman, 1986; Benli, 1987). The flux of cholesterol increases beginning in June and maximized in early August in sediment trap samples collected in the south western portion of the Black Sea in 1983 (Michaelis *et al.*, 1987). The timing of the cholesterol flux increase corresponds to the time the May - July sample was collected. The second most abundant PSE as determined by CI-MS has a molecular weight of 900 a.m.u. and can be assigned as pyropheophorbide-*a* cholesta-5,22-dien-3β-ol ester. Cholesta-5,22-dien-3β-ol is also a major sterol synthesized by some diatom species, for example *Thalassionema nitzschoides* which live in the Black Sea (Volkman, 1986; Benli, 1987). The assignments of these PSEs are further supported by HPLC studies. The major PSE containing HPLC peaks in the May - July sample correspond to those which were assigned, in Ch. 3 (see Table 3-1) and King and Repeta (1991), as containing Pyropheophorbide-*a* cholesteryl and cholesta-5,22-dien-3β-ol esters.

During the fall bloom, the most abundant phytoplankton are coccolithophores and dinoflagellates (Benli, 1987). In the November, December, and January samples, the major PSE has a molecular weight of 914. This indicates the presence of either, or both, pyropheophorbide-*a* 24-methylcholesta-5,22-dien-3β-ol ester, or pyropheophorbide-*a* 24-methylcholesta-5,24(28)-dien-3β-ol (methylene cholesterol) ester. The sterol 24-methylcholesta-5,22-dien-3β-ol is the major sterol found in coccolithophores (Volkman, 1986), including *E. huxleyi*, the most abundant coccolithophore found in the Black Sea (Benli, 1987). Dinoflagellates, which are also in the fall bloom, synthesize methylene cholesterol, but usually in low quantities (Nichols *et al.*, 1983; Volkman, 1986). The low abundance of the PSE with molecular weight 944 (Fig 5-5 (m/z 945); Fig. 5-6) indicates that pyropheophorbide-*a* dinosteryl ester is in low abundance in this sample. Under the assumption that sterols become esterified to pyropheophorbide-*a* in the same relative distribution as they are produced, the low abundance of pyropheophorbide-*a* dinosteryl ester suggests that dinoflagellates are not a major contributor to this sample. Therefore, pyropheophorbide-*a* methylene cholesterol ester should not be an important PSE in this sample. In November and December, 1983, the flux of methylene cholesterol is below detection limits (Michaelis *et al.*, 1987), and some of the dinoflagellate species identified in the Black Sea, for example *Gonyaulax polygramma* and *Peridinium spp.*, do not possess this sterol (Volkman, 1986; Benli, 1987). The appearance of both the HPLC peaks which contain the two molecular weight 914 PSEs (the two molecular weight 914 PSEs separate by HPLC) suggests that both these sterols are contributing to the PSEs in this sample.

The second most abundant ion in the November, December, and January traps has a molecular weight of 900 indicating that pyropheophorbide-*a* is esterified to either 27-nor-

24-methylcholesta-5,22-dien-3β-ol or cholesta-5,22E-dien-3β-ol. Cholesta-5,22E-dien-3β-ol is found in both diatoms and dinoflagellates (Volkman, 1986), and 27-nor-24-methylcholesta-5,22-dien-3β-ol is found in dinoflagellates (Goad and Withers, 1982). The combination of mass spectral and HPLC data suggests that both coccolithophores and dinoflagellates, as well as diatoms are contributing to the PSE sterols in this sample. These molecular weight and HPLC data suggest that the sterols esterified to pyropheophorbide-*a* in the pyropheophorbide-*a* steryl esters, as determined in sediment traps, may provide a record of sterols produced by phytoplankton species living in the photic zone.

C. COMPARISON OF THE STEROL DISTRIBUTION IN SEDIMENT TRAPS, SEDIMENTS, AND PSEs

In the above discussion, we suggest that the distribution of sterols esterified to pyropheophorbide-*a* as measured in sediment traps reflects the distribution of sterols produced by phytoplankton, and in Ch. 3 and King and Repeta (1991), we suggest that the distribution of PSE sterols in sediments reflects the sterol distribution produced in the water column by phytoplankton. In order to determine whether the sterol distribution in the water column is preserved in pyropheophorbide-*a* steryl esters found in sediments, the sterol distribution in PSEs from Black Sea surface sediment collected in the central basin was compared with the distribution of non-esterified solvent-extractable sterols from the same sediment sample and with non-esterified solvent-extractable sterols in the combined BSK2 sediment trap samples. The sediment and sediment trap samples were collected from the same area of the Black Sea (Fig. 5-1).

Qualitatively, the distribution of sterols in the PSEs in sediments is more similar to the distribution of non-esterified solvent-extractable sterols in sediment traps than to non-esterified solvent-extractable sterols from surface sediments (Fig. 5-7). The non-esterified solvent-extractable sterols found in sediment traps and the sterols in the PSEs are: 24-norcholesta-5,22E-dien-3β-ol; 27-nor-24-methylcholesta-5,22-dien-3β-ol; cholesta-5,22E-dien-3β-ol; cholest-5-en-3β-ol; cholestanol; 24-methylcholesta-5,22-dien-3β-ol; 24-methylcholest-22-en-3β-ol; 24-methylcholesta-5,24(28)-dien-3β-ol; 24-methylcholesta-5-dien-3β-ol; 24-methylcholestanol; 23,24-dimethylcholesta-22-dien-3β-ol; 24-ethylcholesta-5,22E-dien-3β-ol; 23,24-dimethylcholest-5-en-3β-ol; dinosterol; and 23,24-dimethylcholestanol. As well as possessing the above sterols, non-esterified solvent-extractable sterols found in surface sediments also include: 23,24-dimethylcholest-22-en-3β-ol, 24-ethylcholest-22-en-3β-ol, 4α,24-dimethylcholestanol, 4α,22,23-trimethylcholestanol, and 4α,22,24-trimethylcholestanol.

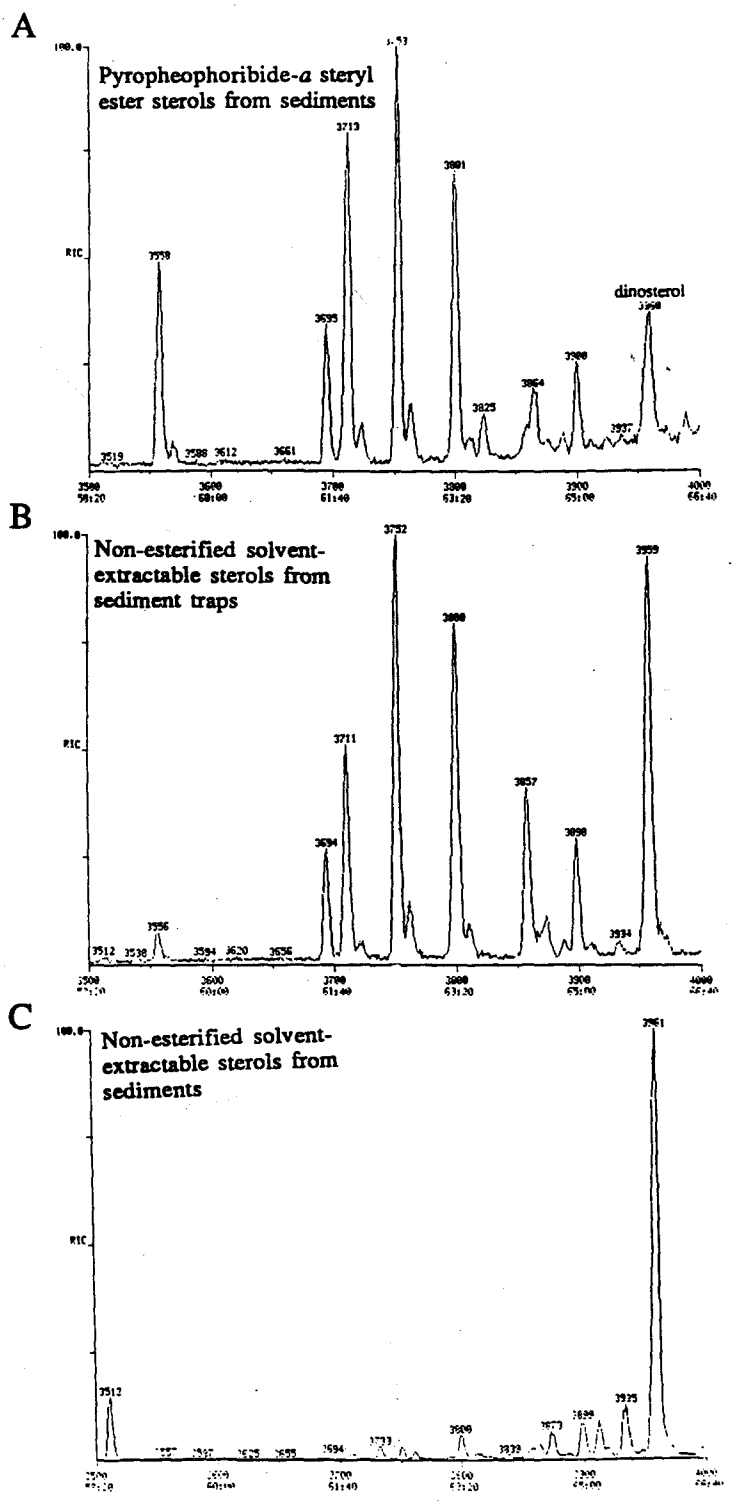

Fig. 5-7 Gas chromatograph-MS total ion current chromatograms of sterol acetates from PSEs, BSK2 sediment traps, and sediments. The PSE sterols and non-esterified solvent-extractable sterols from sediments were obtained from the same sediment sample.

Qualitatively, the greatest difference in the non-esterified solvent-extractable sterol distribution in sediments as compared with the distribution of sterols in PSEs and the distribution of non-esterified solvent-extractable sterols in sediment traps is the presence of large quantities of 4-methylsterols in the non-esterified solvent-extractable sterols in sediments. Only one 4-methylsterol, dinosterol, was identified in the PSE and sediment trap sterol samples. Others may be present but in concentrations which are below detection limits. There are also larger numbers of stanols in the non-esterifed solvent-extractable sterol sample from sediments than in the PSEs sterols and non-esterified solvent-extractable sterols sample from sediment traps. This qualitative difference between sediment trap and sediment non-esterified solvent-extractable sterols can be explained by microbial reduction of stenols to stanols (Eyssen, *et al.*, 1973; Gaskel and Eglinton, 1975, 1976; Nishimura and Koyama, 1977; Nishimura, 1978) and by the greater preservation of 4-methylsterols relative to 4-desmethylsterols (Gagosian *et al.*, 1980; Wolf *et al.*, 1986; Harvey *et al.*, 1989) as described in Ch. 3 and King and Repeta (1991).

Quantitatively, each sterol sample is different (Fig. 5-8). As in the qualitative comparison of sterol samples, the largest quantitative difference exists between the non-esterified solvent-extractable sedimentary sterols, and the sterols of the PSE and sediment trap samples. The small quantitative differences between the sterol distribution of the PSE and sediment trap samples can be explained by the different time span each sample represents. The sediment trap sterols were extracted from a sample representing 1 year of deposition, whereas the pyropheophorbide-*a* steryl esters were extracted from a sediment sample which represents approximately 200 years of deposition (Calvert *et al.*, 1987; Jones and Gagnon, 1992). In sediments, dinosterol accounts for approximately 45% of the total non-esterified solvent-extractable sterols whereas in sediment traps and PSEs, it accounts for less than 1%. The quantitative differences in the sterol samples can also be seen in stanol/stenol ratios. In sediment traps and PSEs, stanol/stenol ratios range between 0.1 - 0.2. For cholestanol/cholestenol this ratio is 0.21 and 0.22 for sediment trap and PSE sterols, respectively, and for 24-methylcholesta-5,22-dien-3β-ol/24-methylcholest-22-en-3β-ol, this ratio is 0.15 and 0.11. In sediments, these same stanol/stenol ratios are 0.66 and 0.75, respectively. In Ch. 3, we present approximations of these data since we were unable to accurately quantify the PSE sterols. The data presented here substantiate the data presented in Ch. 3.

We (Ch. 3; King and Repeta, 1991) explained the differences between the sediment and PSE sterol distributions through microbial reduction of stenols to stanols and preferential removal of 4-desmethyl sterols in sediments. We then conclude that the distribution of sterols as preserved in PSEs more closely resembles the distribution of

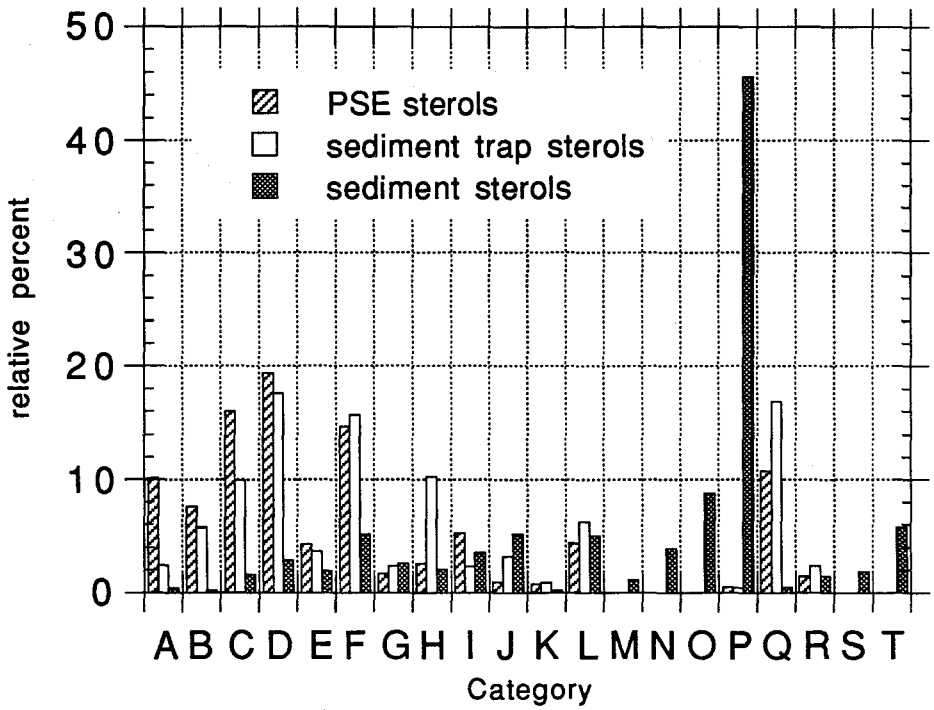

Fig. 5-8 Histogram comparing the relative contribution of individual sterols to total sterols in sedimentary PSEs, BSK2 sediment traps, and sediments. **A**) 24-norcholesta-5,22-dien-3β-ol; **B**) cholesta-5,22E-dien-3β-ol; **C**) cholesta-5,22Z-dien-3β-ol; **D**) cholest-5-en-3β-ol; **E**) cholestanol; **F**) 24-methylcholesta-5,22-dien-3β-ol; **G**) 24-methylcholest-22-en-3β-ol; **H**) 24-methylcholesta-5,24(28)-dien-3β-ol; **I**) 24-methylcholest-5-en-3β-ol; **J**) 24-methylcholestanol; **K**) 23,24-dimethylcholesta-5,22-dien-3β-ol; **L**) 24-ethylcholesta-5,22-dien-3β-ol; **M**) 23,24-dimethylcholest-22-en-3β-ol; **N**) 24-ethylcholest-22-en-3β-ol; **O**) 4a,24-dimethylcholestanol; **P**) dinosterol; **Q**) 23,24-dimethylcholest-5-en-3β-ol; **R**) 23,24-dimethylcholestanol; **S**) 4a,22,23-trimethylcholestanol; **T**) 4a,22,24-trimethylcholestanol.

sterols synthesized by phytoplankton than does the sterol distribution in sediments. By directly comparing sterols in sediment traps, sediments, and PSEs, we present further evidence here to support these conclusion. Through esterification, the 4-desmethyl sterols are protected from selective removal, and through packaging in large particles, stenols are protected from reduction to stanols in the chemocline. Esterification also protects stenols from reduction at the sediment water interface. Each of these arguments is discussed in greater detail in Ch. 3.

Formation of PSEs

A mechanism of formation for pyropheophorbide-*a* steryl esters is suggested by the combination of the presented data: flux data for PSEs and total phorbin, the distribution of HPLC PSE peaks, CI-MS data of sediment trap PSEs, and GC/MS data of non-esterified solvent-extractable sediment trap, non-esterified solvent-extractable sediment, and PSE sterols. The relative amount of PSEs produced during a bloom continues to increase after phorbin flux begins to decrease. The changing distribution of PSE HPLC peaks with season, indicates a changing distribution of esterified sterols with time, and suggests that the source of the sterols going into the PSEs changes with season. The CI-MS data for PSEs from individual sediment traps at BSK3-1 show that pyropheophorbide-*a* is esterified to sterols which have the same molecular weight as the major sterols of phytoplankton species occupying the photic zone at the time the particulate sample was collected by sediment trap. These data suggest that some mechanism is causing the esterification of phytoplankton sterols to a single chlorophyll degradation product. The similarity in the distribution of PSE and sediment trap sterols suggests that the esterification of pyropheophorbide-*a* occurs with sterols in relative proportion to the production of sterols in overlying surface waters. As discussed in King and Repeta (1991; Ch. 3), the low stanol/stenol ratios found in the PSE sterols suggests that these compounds are being transported rapidly through the chemocline, necessitating their being encased in large particles.

To account for these observations, PSEs must have a source in the surface ocean, be transported rapidly out of the photic zone, and have a source which changes over the course of the year. Production of PSEs during zooplankton grazing presents itself as one mechanism which can account for each of these observations. Zooplankton grazing may result in the encasement of pigments into large particles, and if the esterification of sterols to the pigment is non-specific transesterification, then the distribution of esterified sterols should reflect the food source. The increase in the relative contribution of PSEs to the total pigment flux during periods of low primary production may be explained by acclimation of

zooplankton digestive systems to high food concentrations (Penry and Frost, 1991), increased grazing intensity (Roy *et al.*, 1989), or possibly, greater recycling of carbon during periods of low carbon availability (Epply and Peterson, 1979). The sterols in the PSEs are esterified to a common macrocycle, pyropheophorbide-*a*, that is formed through a specific series of degradative reactions from chlorophyll-*a* such as may occur during the enzymatic degradation of phytoplankton carbon during grazing. Pyropheophorbide-*a*, and possibly PSEs (although these compounds have not been definitively identified; Downs, 1989) have been shown to be formed during grazing by some organisms (Downs, 1989). Sediment trap material consists partly of fecal pellets (Urrere and Knauer, 1981) and varying amounts of chlorophyll survives grazing but in the form of pheopigments encased in fecal pellets (Shuman and Lorenzen, 1975; Conover *et al.*, 1986; Lopez *et al.*, 1988; Downs, 1989; Penry and Frost, 1991; Mayzaud and Razouls, 1992). The fluorometric methods used to measure the concentration of pheopigments in grazing experiments would also measured PSEs though they would not be distinguished as such. All these factors suggest that a mechanism exists by which PSE are formed from chlorophyll and phytoplankton sterols during grazing.

IV. CONCLUSIONS

Pyropheophorbide-*a* steryl esters are produced in the surface ocean. The seasonal variation in total PSE flux exhibits the same trends as total phorbin flux, but with flux maxima occuring approximately 15 days later than the total phorbin flux maxima. The relative importance of PSEs as a sink for chlorophyll increases as the phytoplankton bloom progresses. The PSEs are transported out of the photic zone on large rapidly sinking particles and appear to be deposited with little alteration of their sterol distribution. The distribution of PSE sterols in sediment trap samples can be related to the phytoplankton species believed to be contributing to the organic carbon flux in that trap. The esterification of sterols to pyropheophorbide-*a* in a distribution which changes over the course the year, and in a distribution which reflects the phytoplankton community, requires a very specific reaction sequence, such as occurs enzymatically in the guts of organisms. From this data, we suggest that PSEs are produced through the process of grazing by herbivorous zooplankton. We conclude that the sterols in the PSEs reflect the producer community at the time of PSE formation, and the sterol distribution of PSEs in sediments may provide a record of the sterols produced by the phytoplankton community over time.

V. REFERENCES

Benli H. A. (1987) Investigation of plankton distribution in the southern Black Sea and its effects on particle flux. SCOPE/UNEP *Sonderband Heft 62, Mitt. Geol.-Palaeont. Inst. Univ. Hamburg*, 77-87.

Betzer P. R., Showers W. J., Laws E. A., Winn C. D., DiTullio G. R., and Kroopnick P. M. (1982) Primary productivity and particle fluxes on a transect of the equator at 153°W in the Pacific Ocean. *Deep-Sea Res.* **34**, 1-11.

Boon J. J., Rijpstra W. I. C., de Lange F., and de Leeuw J. W. (1979) Black Sea sterol -- a molecular fossil for dinoflagellate blooms. *Nature* **277**, 125-127.

Burkill P. H., Mantoura R. F. C., Llewellyn C. A., and Owens N. J. P. (1987) Microzooplankton grazing and selectivity of phytoplankton in coastal waters. *Mar. Biol.* **93**, 581-590.

Calvert S. E., Vogel J. S., and Southon J. R. (1987) Carbon accumulation rates and the origin of the Holocene sapropel in the Black Sea. *Geology* **15**, 918-921.

Carpenter S. R., and Berquist A. M. (1985) Experimental tests of grazing indicators based on chlorophyll-a degradation products. *Arch. Hydrobiol.* **102**, 303-317.

Conover R. J., Durvasula R., Roy S., and Wang R. (1986) Probable loss of chlorophyll-derived pigments during passage through the gut of zooplankton, and some of the consequences. *Limnol. Oceanogr.* **31**, 878-887.

Cranwell P. A. and Volkman J. K. (1981) Alkyl and steryl esters in a recent lacustrine sediment. *Chemical Geology* **32**, 29-43.

Deuser W. G. and Ross E. H. (1980) Seasonal changes in the flux of organic carbon to the deep Sargasso Sea. *Nature* **283**, 354-365.

Deuser W. G., Ross E. H., and Anderson R. F. (1981) Seasonality in the supply of sediment to the deep Sargasso Sea and implications for the rapid transfer of matter to the deep sea. *Deep-Sea Res.* **28**, 495-505.

Downs J. N. (1989) Implications of the phaeopigments, carbon and nitrogen content of sinking particles for the origin of export production. Ph.D. dissertation, Univ. of Washington.

Eckardt C. B., Keely B. J. and Maxwell J. R. (1991) Identification of chlorophyll transformation products in a lake sediment by combined liquid chromatography-mass spectrometry. *J. Chromatogr.* **557**, 271-288.

Eppley R. W., and Peterson B. J. (1979) Particulate organic matter flux and planktonic new production in the deep ocean. *Nature* **282**, 677,680.

Eyssen H. J., Parmentier G. G., Compernolle G. C., De Pauw G., and Piessens-Denef M. (1973) Biohydrogenation of sterols by *Eubacterium* ATCC 21,408 -- *Nova* Species. *Eur. J. Biochem.* **36**, 411-421.

Farrington J. W., Davis A. C., Sulanowski J., McCaffrey M. S., McCarthy M. A., Clifford C. H., Dickinson P., and Volkman J. K. (1988) Biogeochemistry of lipids in surface sediments of the Peru upwelling area - 15°S. In: *Advances in Organic Geochemistry 1987* (Eds. L. Mattavelli and L. Novelli). *Org Geochem.* **13**, 607-617.

Gagosian R. B., Lee C., and Heinzer F. (1979) Processes controlling the stanol/stenol ratio in Black Sea seawater and sediments. *Nature* **280**, 574-576.

Gagosian R. B., Smith S. O., Lee C. L., Farrington J. W., and Frew N. E. (1980) Steroid transformations in recent marine sediments. In: Advances in Organic Geochemistry 1979 (Ed. A.G. Douglas and J.R. Maxwell) pp. 407-419.

Gaskel S. J. and Eglinton G. (1975) Rapid hydrogenation of sterols in a contemporary lacustrine sediment. *Nature* **254**, 209-211.

Gaskell S. J., and Eglinton G. (1976) Sterols of a contemporary lacustrine sediment. *Geochim. Cosmochim. Acta* **40**, 1221-1228.

Goad L. J., and Withers N. (1982) Identification of 27-nor-(24R)-methylcholesta-5,22-dien-3β-ol and brassicasterol as the major sterols of the marine dinoflagellate *Gymnodinium simples*. *Lipids* **17**, 852-858.

Harvey H. R., O'Hara S. C. M., Eglinton G., and Corner E. D. S. (1989) The comparative fate of dinosterol and cholesterol incopepod feeding: Implications for a conservative molecular biomarker in the marine water column. *Org. Geochem.* **14**, 635-641.

Hassner A. and Alexanian V. (1978) Direct room temperature esterification of carboxylic acids. *Tet. Lett.* **46**, 4475-4478.

Jones G. A. and Gagnon A. R. (1992, submitted) Radiocarbon chronology of Black Sea sediments. *Deep-Sea Res.*

King L. L. and Repeta D. J. (1991) Pyropheophorbide steryl esters in Black Sea sediments. *Geochim. Cosmochim. Acta* **55**, 2067-2074.

de Leeuw J. W., Rijpstra W. I. C., Schenck P. A., and Volkman J. K. (1983) Free, esterified and residual bound sterols in Black Sea Unit I sediments. *Geochim. Cosmochim. Acta* **47**, 455-465.

Lopez M. D. G., Huntley M. E., and Sykes P. F. (1988) Pigment destruction by *Calanus pacificus*: impact on the estimation of water column fluxes. *J. Plank. Res.* **10**, 715-734.

Mayzaud P. and Razouls S. (1992) Degradation of gut pigment during feeding by a subantarctic copepod: Importance of feeding history and digestive acclimation. *Limnol. Oceanogr.* **37**, 393-404.

Michaelis W., Schumman., Ittekkot V., and Konuk T. (1987) Sterol markers for organic matter fluxes in the Black Sea. *SCOPE/UNEP Sonderband Heft 62, Mitt. Geol.-Palaeont. Inst. Univ. Hamburg*, 89-98.

Prowse W. G. and Maxwell J. R. (1991) High molecular weight chlorins in a lacustrine shale. *Org. Geochem.* **17**, 877-886.

Nichols P. D., Volkman J. K., and Johns R. B. (1983) Sterols and fatty acids of the marine unicellular alga, FCRG 51. *Phytochemistry* **22**, 1447-1452.

Nishimura M. (1978) Geochemical characteristics of the high reduction zone of stenols in Suwa sediments and the environmental factors controlling the conversion of stenols into stanols. *Geochim. Cosmochim. Acta* **42**, 349-357.

Nishimura M. and Koyama T. (1977) The occurrence of stanols in various living organisms and the behavior of sterols in contemporary sediments. *Geochim. Cosmochim. Acta* **41**, 379-385.

Penry D. L., and Frost B. W. (1991) Chlorophyll *a* degradation by *Calanus pacificus*: Dependence on ingestion rate and digestive acclimation to food resources. *Limnol. Oceanogr.* **36**, 147-159.

Ross D. A., Uchupe E., and Bowin C. O. (1974) Shallow structure of the Black Sea, In: The Black Sea--Geology, Chemistry, and Biology, E. T. Degen and D. A. Ross, Eds. Am. Assoc. Petrol. Geol. pp 1-10.

Roy S., Harris R. P., and Poulet S. A. (1989) Inefficient feeding by *Calanus Helgolandicus* and *Temora longicornis* on *Coscinodiscus wailesii*: quantitative estimation using chlorophyll-type pigments and effects on dissolved free amino acids. *Mar. Ecol. Prog. Ser.* **52**, 145-153.

Shuman F. R. and Lorenzen C. J. (1975) Quantitative degradation of chlorophyll by a marine herbivore. *Limnol. Oceanogr.* **20**, 580-586.

Sorokin Y. I. (1983) The Black Sea. In: Ecosystems of the world 26 -- Estuaries and Enclosed Seas (Ed. B. H. Ketchum). Elsevier, 253-307.

Urrere M. A., and Knauer G. A. (1981) Zooplankton fecal pellet fluxes and vertical transport of particulate organic material in the pelagic environment. *J. Plank. Res.* **3**, 369-387.

Volkman J. K. (1986) A review of sterol markers for marine and terrigenous organic matter. *Org. Geochem.* **9**, 83-99.

Volkman J. K., Gagosian R. B., and Wakeham S. G. (1984) Free and esterified sterols of the marine dinoflagellate *Gonyaulax polygramma*. *Lipids* **19**, 457-465.

Wakeham S. G. (1989) Reduction of sterols to stanols in particulate matter at oxic-anoxic boundaries in seawater. *Nature* **342**, 787-790.

Wakeham S. G. and Beier J. A. (1991) Organic biomarkers as indicators of particulate matter source and alteration processes in the water column of the Black Sea. *NATO Advanced Research Workshop on Black Sea Oceanography.*

Welschmeyer N. A. and Lorenzen C. J. (1985) Chlorophyll Budgets: Zooplankton grazing and phytoplankton growth in a temperate fjord and the Central Pacific gyres. *Limnol. Oceanogr.* **30**, 1-21.

Wolff G. A., Lamb N. A., and Maxwell J. R. (1986) The origin and fate of 4-methyl steroids -- II. Dehydration of stanols and occurrence of C_{30} 4-methyl steranes. *Org. Geochem.* **10**, 965-974.

Ziegler R., Blaheta A., Guha N., and Schonegge B. (1988) Enzymatic formation of pheophorbide and pyropheophorbide during chlorophyll degradation in a mutant of *Chlorella fusca* SHIHIRA et KRAUS. *J. Plant. Physiol.* **132**, 327-332.

CHAPTER 6

SEASONAL CYCLING OF PHORBIN DEPOSITION AND A MASS BALANCE OF CHLOROPHYLL DEGRADATION PRODUCTS IN THE BLACK SEA

Chapter 6

SEASONAL CYCLING IN PHORBIN DEPOSITION AND A MASS BALANCE OF CHLOROPHYLL DEGRADATION PRODUCTS IN THE BLACK SEA

I. INTRODUCTION

Chlorophyll degradation products can be identified in suspended and sinking particles in the water column, and in sediments. Chlorophyll is produced in the surface ocean by algae. Processes such as photo-oxidation and grazing effect its distribution, but what happens to chlorophyll once it leaves the zone of primary production is poorly understood. In the following, we describe the distribution of chlorophyll and its degradation products in the Black Sea using data from water column suspended particulate matter, sediment traps, and surface sediments, and attempt to create a mass balance of chlorophyll production and sedimentation to identify points in the sedimentation route where major quantities of chlorophyll are lost.

Chlorophyll is produced in surface waters by algae. Algal primary production is fairly uniform throughout the Black Sea, and has a well documented seasonal cycle (Deuser, 1971; Sorokin, 1983; Karl and Knauer, 1991). Two blooms of photosynthetic algae occur annually, a spring bloom in February to April, and a smaller, fall bloom in August to October (Sorokin, 1983). The magnitude of biomass during the spring bloom has been estimated at 1-3 g/m^3. Maximum primary production occurs along the coast, and decreases offshore. In the central basin, primary production is at intermediate levels, and is lowest in the center of the eastern and western basins (Sorokin, 1983). Estimates for basin wide average production range from 75 to 230 $gC/m^2/yr$ (Deuser, 1971; Sorokin, 1983; Karl and Knauer, 1991).

The annual cycle of primary production drives the annual cycle of the organic carbon flux out of the euphotic zone. The organic carbon flux as measured in sediment traps near the Turkish Coast in the western Black Sea at 250 m and 1200 m, shows two distinct maxima (Honjo *et al.*, 1987; Hay, 1987; Hay *et al.*, 1990). The first maximum, with an average organic carbon flux of 25 $mg/m^2/d$, occurs in mid summer, from June to September, and the second, from November to January, when the flux may reach 20 $mg/m^2/d$.

Very few studies have been made of the distribution and flux of chlorophyll and its degradation products in the surface waters of the Black Sea. Repeta and Simpson (1991)

report detailed analyses of pigment distributions with depth in the water column at several stations. They found chlorophyll-*a* to occur to depths of 1000 m on suspended particulate matter, though concentrations dropped sharply between 40 and 50 m. Only very low concentrations of pheophorbide and pheophytin were observed.

Chlorophyll can be lost from the euphotic zone by one of three processes; grazing, photo-oxidation, and cell sinking (Welschmeyer and Lorenzen, 1985). The primary means for removal of chlorophyll from the photic zone is grazing, with the primary products of grazing being pheophytins and pheophorbides (Downs, 1989; Vernet and Lorenzen, 1987). The conversion of chlorophyll to pheopigments, demetallated chlorophyll degradation products, through grazing is not quantitative and a portion of the chlorophyll grazed is metabolized to colorless compounds or CO_2 (Klein *et al.*, 1986; Conover *et al.*, 1986; Kiorboe and Tiselius, 1987; Lopez *et al.*, 1988; Pasternak and Drits, 1988; Downs, 1989; Penry and Frost, 1991; Mayzaud and Razouls, 1992). A portion of the chlorophyll grazed by microzooplankton and incorporated into small fecal pellets remains suspended in the photic zone and is subject to photo-oxidation (Welschmeyer and Lorenzen, 1985; SooHoo and Kiefer, 1982). Chlorophyll and pheopigments suspended in surface waters has a half-life of only 10 days due to photo-oxidative removal (SooHoo and Kiefer, 1982). Chlorophyll which survives photo-oxidation and grazing through removal from the photic zone on large sinking particles, either as chlorophyll or a recognizable degradation product of chlorophyll, is deposited in the surface sediment where it continues to undergo diagenesis.

Prior to this thesis, there were few reports about sedimentary chlorophyll diagenesis in the Black Sea. As part of the 1969 *Atlantis II* Black Sea expedition, products of chlorophyll diagenesis were analyzed in recent sediments. Peak *et al.* (1974) report 1.6 mg/gdw of phorbins in surface sediments and 2.2 mg/gdw at a depth of 68 cm. The suite of pigments they isolated and characterized spectroscopically, contained red visible absorption bands at 670 and 690 nm indicating that pheophytins and pheophorbides, as well as other chlorophyll degradation products, were present. Other studies of chlorophyll degradation in Black Sea sediments were conducted by Lorenzen (1974) who measured concentrations of pheopigments over the upper 5 m of the sediment column. Pheopigments, measured either spectrometrically or fluorometrically, were found to reach concentrations of over 2 mg/gdw in the upper meter of sediment, increasing from approximately 0.5 mg/gdw at the surface (Lorenzen, 1974).

The objectives of the present study are two-fold. First, we present a detailed inventory of chlorophyll degradation products in the water column and surface sediments. The degradation products analyzed are solvent extractable free phorbins, solvent extractable

macromolecular phorbins, and phorbins which can only be extracted from sediment using acid. The second objective is to use the phorbin inventory to construct a quantitative model of chlorophyll degradation in the Black Sea which considers primary production, flux of chlorophyll through the water column, and accumulation of chlorophyll degradation products in surface sediments.

II. METHODS

Black Sea sediment trap samples for the period covering 1988-89 were obtained from 477 m and 1300 m at BSK2 (43°00.13'N, 34°00.73'E; Fig. 6-1) and from 1172 m at BSK3-1 (42°20.85'N, 37°34.22'E; Fig. 6-1) (Hay *et al.*, 1988). Sample collection dates, depths, and size fractions are given in Table 5-1. Samples were extracted with organic solvent and the extract quantified and analyzed as in Ch. 5. The residues from each of the traps in the 1 year time series at BSK3-1 were combined and extracted with acid as described in Ch. 4. The sediment trap residues were suspended in 10 mL MeOH. The solution was purged with N_2 while stirring and 1.3 mL concentrated H_2SO_4 was added until a solution of 25% H_2SO_4/MeOH (w/w) was reached. The mixture was stirred and continuously purged for 1 hour. After filtration, the filtrate was diluted with 100 mL distilled H_2O and extracted with 3 x 20 mL methylene chloride. The methylene chloride solution was dried over Na_2SO_4 and rotary evaporated to dryness. Total phorbins in the acid extractable fraction were determined by visible spectrophotometry at 665 nm as described previously (Ch. 4).

Sediment samples from 0 - 10 cm (BS2-0-10; 187 g dry wt.) and 13 - 18 cm (BS2-13-18; 66.4 g dry wt.) were taken from Box Core 2, Station 2 (42°51'N, 31°57'E, water depth of 2129 m; Fig. 6-1), and a sediment sample from 0 - 4 cm (BS5-0-4; 10.2 g dry wt.) was taken from Box Core 5 Station 3 (43°04.23"N, 33°58.37"E; Fig. 6-1). These samples were collected during Leg 2 of the 1988 *R/V Knorr* Black Sea Expedition. The cores were immediately sectioned and frozen after recovery. Sediment samples were extracted in acetone (9x) and methylene chloride (3x). The extract was concentrated by rotary evaporation and then back extracted into 30% hexane/ether, dried over Na_2SO_4, evaporated to dryness, and then diluted to 100 mL in acetone. The extract was analyzed by visible spectrophotometry in acetone (665 nm, $\varepsilon = 5 \times 10^4$ L/mol·cm) to determine the total phorbin concentration, and analyzed by HPLC to identify and quantify the HPLC separable chlorophyll degradation products. Extracts from BS2-0-10 and BS2-13-18 were fractionated by gel permeation chromatography (Chs. 4 and 7). Each gel column fraction

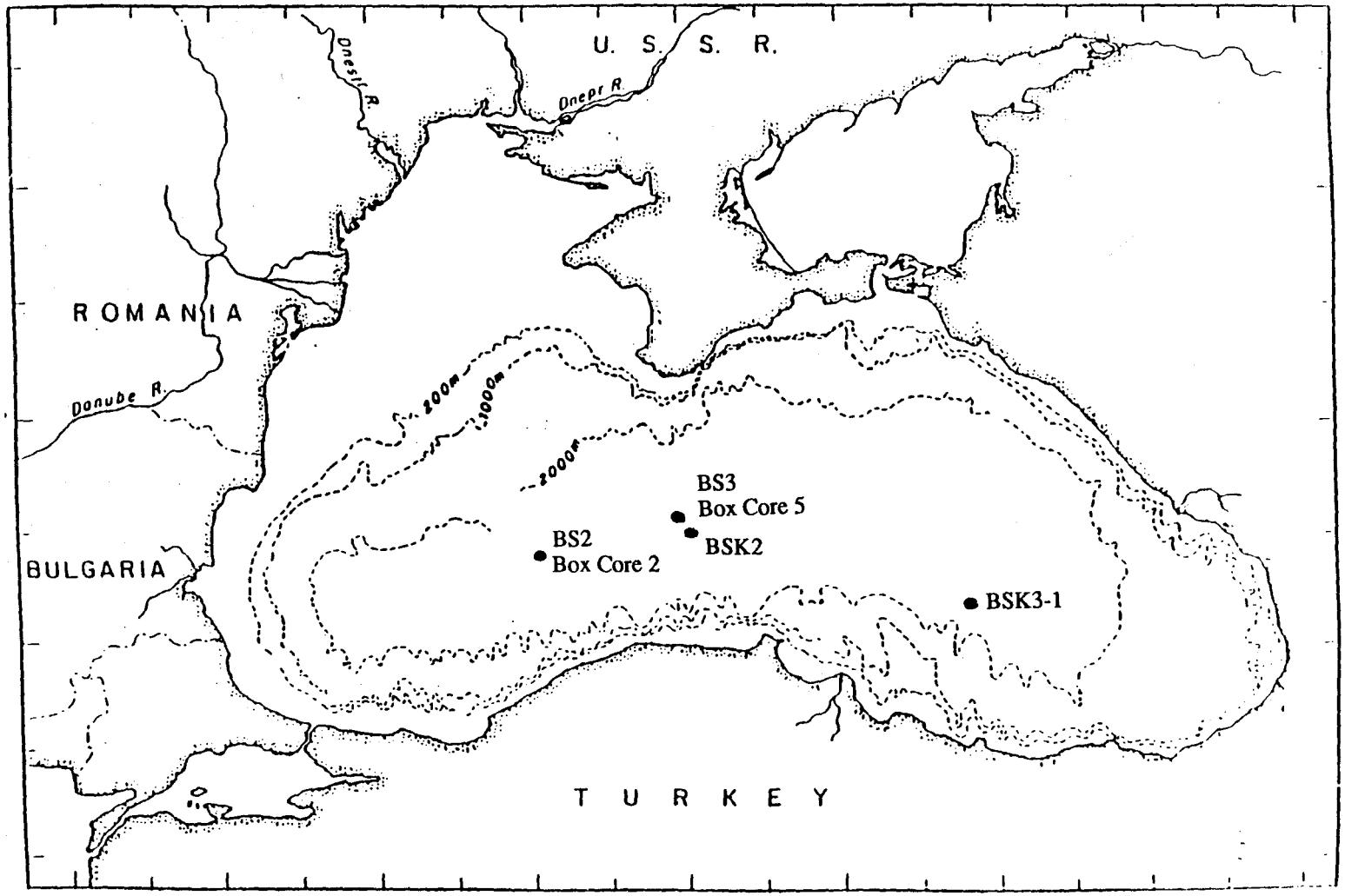

Fig. 6-1 Map of the Black Sea. Sampling locations are indicated.
(Ross *et al.*, 1974)

was analyzed by visible spectrophotometry and HPLC to identify and quantify the chlorophyll degradation products.

Individual peaks in the HPLC chromatograms of the total extracts were identified and quantified. Individual phorbins were identified by HPLC coelution with authentic compounds and chemical ionization mass spectrometry. Quantification was performed using conversion coefficients derived from replicate analysis of authentic compounds. For quantification purposes, the HPLC chromatogram of the total sediment extract was used.

Solvent extracted sediment was then further extracted three times with 25% H_2SO_4/MeOH (Ch. 4). The acid extract was diluted, and the pigments were partitioned into CH_2Cl_2. The CH_2Cl_2 solution was dried over Na_2SO_4, rotary evaporated, and diluted to a known volume with acetone The total acid extractable chlorophyll degradation products were quantified by visible spectrophotometry at 665 nm as for the total solvent extract.

III. RESULTS AND DISCUSSION

A. DISTRIBUTION OF CHLOROPHYLL DEGRADATION PRODUCTS

Distribution of Chlorophyll Degradation Products in Sediment Traps

Individual chlorophyll degradation products as well as the spectroscopically observable phorbin concentration (total phorbin) were analyzed in each sediment trap sample (Tables 6-1a and 6-1b). The major components of the phorbin flux identified throughout the year include pyropheophorbide-*a*, pheophytin-*a*, pyropheophytin-*a*, and pyropheophorbide-*a* steryl esters (PSEs) (Fig. 6-2a). Chlorophyll-*a* was identified in low concentrations throughout the year at BSK2 and only during the spring bloom at BSK3-1. Pheophorbide-*a* occured in low concentrations only after the fall bloom at BSK2 and during the spring bloom at BSK3-1. Also identified as one of the major components in the sediment trap samples was a pyropheophorbide-like pigment with a molecular weight of 532 a.m.u. (referred to as MW532 pyropheophorbide, spectral properties described in Ch. 7), 2 a.m.u. less than that of pyropheophorbide-*a*.

In Ch. 4, we provide evidence for the presence of phorbins incorporated into a solvent extractable high molecular weight form (HMW) and also into a form which can only be extracted with strong acids (AEX). Due to the limited amount of sediment trap sample, it was not possible to separate the solvent extractable HMW phorbins from the free phorbins by gel permeation chromatography, but comparison of HPLC data from sediment trap and sediment extracts suggests that HMW is present in sediment trap samples (Fig. 6-

Table 6-1a

FLUX OF CHLOROPHYLL DEGRADATION PRODUCTS AT BSK3-1

sample designation	deployment dates	flux (nmol/m^2/d) total phorbin	chl-*a*	ptn-*a*	pptn-*a*	pbd-*a*	ppbd-*a*	PSEs	MW532
3ST1 L1	4/26 - 8/1/89	4.1E+01	4.8E+00	2.6E-01	6.3E+00	8.0E-01	7.8E-01	1.8E+01	2.7E+00
3ST2	8/1 - 8/31/89	3.3E-01	0.0E+00	3.8E-03	1.5E-02	0.0E+00	6.2E-03	6.2E-02	0.0E+00
3ST3	8/31 - 10/1/88	5.7E-01	0.0E+00	0.0E+00	2.7E-02	0.0E+00	2.0E-02	8.9E-02	0.0E+00
3ST4	10/1 - 10/31/88	1.5E+0	0.0E+00	9.7E-02	1.1E-01	0.0E+00	7.1E-02	1.4E-01	1.7E-01
3ST5	10/31 - 12/1/88	8.0E+00	0.0E+00	6.4E-01	1.6E-01	0.0E+00	2.6E-01	9.3E-01	4.1E-01
3ST6	12/1 - 12/31/88	2.9E+01	0.0E+00	3.0E+00	6.6E-01	0.0E+00	8.2E-01	3.3E+00	1.7E+00
3ST7	12/31/88 - 1/31/89	1.3E+01	0.0E+00	4.3E-01	7.0E-01	0.0E+00	5.4E-01	3.1E+00	2.1E+00
3ST8	1/31 - 3/1/89	4.8E-01	0.0E+00	1.2E-02	4.4E-02	0.0E+00	1.5E-02	1.3E-01	1.4E-01
3ST9	3/1 - 4/1/89	5.7E-01	0.0E+00	0.0E+00	3.9E-02	5.8E-03	2.5E-02	1.4E-01	7.6E-02
3ST10	4/1 - 5/1/89	3.1E-01	0.0E+00	0.0E+00	1.5E-02	0.0E+00	2.1E-02	6.3E-02	1.2E-01
3ST11	5/1 - 6/1/89	0.0E+00	0.0E+00	0.0E+00	0.0E+00	0.0E+00	0.0E+00	0.0E+00	0.0E+00
3ST12	6/1 - 7/1/89	0.0E+00	0.0E+00	0.0E+00	0.0E+00	0.0E+00	0.0E+00	0.0E+00	0.0E+00
3ST13	7/1 - 8/1/89	4.1E-01	7.0E-03	0.0E+00	6.6E-03	0.0E+00	3.9E-02	6.5E-02	6.1E-02

Table 6-1b

FLUX OF CHLOROPHYLL DEGRADATION PRODUCTS AT BSK2

sample designation	deployment dates	flux (nmol/m^2/d) total phorbin	chl-*a*	ptn-*a*	pptn-*a*	pbd-*a*	ppbd-*a*	PSEs	MW532
2ST6S	6/2 - 6/8/88	2.1E+01	0.0E+00	0.0E+00	3.9E-01	0.0E+00	7.1E-01	3.0E+00	1.9E+00
2ST7S	6/8 - 6/14/88	1.8E+01	0.0E+00	0.0E+00	2.5E-01	0.0E+00	5.8E-01	2.3E+00	1.3E+00
2ST1	8/1 - 8/31/89	1.2E+01	7.6E-01	8.3E-01	5.3E-01	0.0E+00	8.2E-01	1.5E+00	1.3E+00
2ST2	8/31 - 10/1/88	1.0E+01	3.9E-01	2.4E+00	4.0E-01	0.0E+00	6.1E-01	6.4E-01	9.4E-01
2ST3	10/1 - 10/31/88	4.7E+00	4.3E-01	7.1E-01	1.5E-01	0.0E+00	2.9E-01	5.1E-01	4.5E-01
2ST4	10/31 - 12/1/88	2.1E+01	3.6E+00	1.6E+00	2.5E-01	0.0E+00	8.0E-01	7.2E-01	9.6E-01
2ST5	12/1 - 12/31/88	3.1E+00	2.1E-01	1.8E-01	8.5E-02	0.0E+00	2.0E-01	3.5E-01	4.2E-01
2ST6	12/31/88 - 1/31/89	4.6E+01	1.8E+00	0.0E+00	1.6E+00	1.6E-01	7.9E-01	3.7E+00	3.7E+00
2ST7	1/31 - 3/1/89	1.1E+01	5.5E-01	1.1E-01	2.1E+00	3.4E-01	4.7E-01	4.0E+00	2.0E+00
2ST8	3/1 - 4/1/89	8.7E+00	2.2E-02	3.3E-02	2.4E-01	6.8E-03	7.8E-02	9.2E-01	2.4E-01
2ST9	4/1 - 5/1/89	2.2E+00	4.9E-02	2.5E-02	3.5E-01	1.9E-02	1.5E-01	1.2E+00	3.7E-01
2ST10	5/1 - 6/1/89	2.0E-01	2.5E-03	2.9E-03	4.7E-02	0.0E+00	2.7E-02	1.5E-01	4.9E-02
2ST11	6/1 - 7/1/89	2.2E+00	3.1E-02	3.3E-02	2.8E-01	8.8E-03	1.2E-01	1.1E+00	2.4E-01
2ST12	7/1 - 8/1/89	0.0E+00	0.0E+00	0.0E+00	0.0E+00	0.0E+00	0.0E+00	0.0E+00	0.0E+00
2ST1D	8/1 - 8/31/88	2.4E+01	4.1E-01	2.4E+00	1.1E+00	0.0E+00	1.5E+00	3.4E+00	3.0E+00
2ST2D	8/31 - 10/1/88	1.7E+01	5.3E-01	2.0E+00	5.9E-01	0.0E+00	1.0E+0	1.2E+00	1.6E+00
2ST3D	10/1 - 12/1/89	1.1E+01	0.0E+00	9.6E-01	2.6E-01	0.0E+00	5.2E-01	8.2E-01	1.3E+00

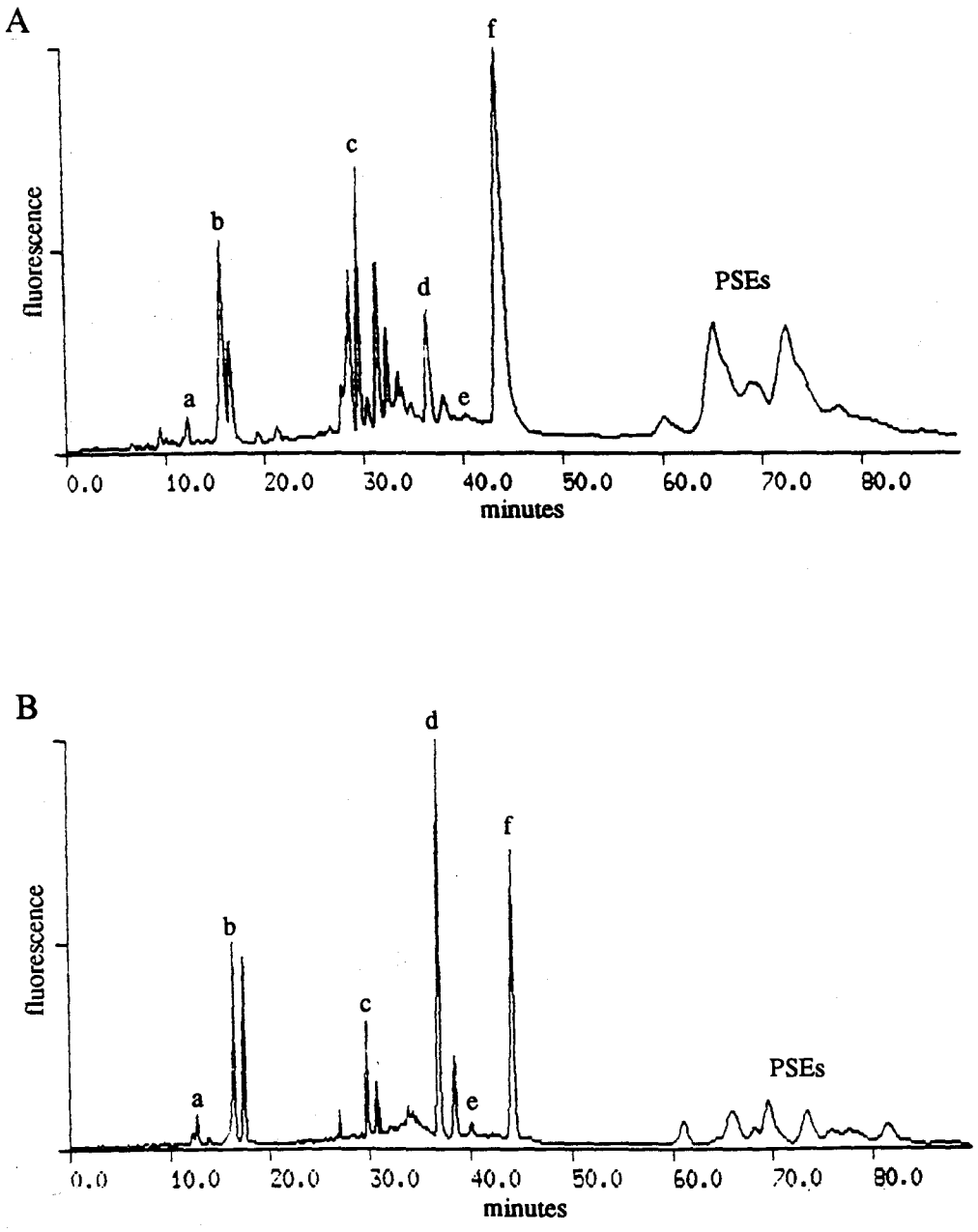

Fig. 6-2 High pressure liquid chromatogram with fluorescent detection of (a) sediment trap sample BSK3-1 L1, and (b) sediment sample BS2-0-10. Peak identifications same as those in Fig. 3-2.

2). The HMW material in sediments appears as a rising base-line between 30 and 38 minutes in HPLC chromatograms of sediment samples. A rise in the base-line, similar to the one seen for sediment samples, is also apparent in the HPLC chromatogram of sediment trap samples. The only estimates which can be made as to the concentration of this phorbin reservoir in individual sediment trap samples from the data available are by subtracting the sum of the individual phorbin concentrations from the spectroscopic yield. For the combined sediment trap samples at BSK3-1 from May, 1988 to April, 1989, the HMW contributes approximately 40 nmol out of a total 97 nmol, or 41% of the solvent-extractable chlorophyll degradation products for the entire year. To determine if AEX chlorophyll degradation products are present in sediment trap samples, the residues from the sediment trap extractions from BSK3-1 were combined and acid extracted according to the procedure described in Ch. 4. Using this method, 8.1 nmol of phorbin were extracted. The studies of phorbin recovery by acid extraction presented in Ch. 4, suggest that one acid extraction will remove approximately 65% of the acid extractable phorbin. We therefore suggest that the 8.1 nmol recovered with acid from the combined sediment trap samples is a lower limit to the concentration of acid extractable chlorophyll degradation products in these samples.

There are two distinct annual blooms of photosynthetic algae in the Black Sea, the first, and largest occurs from February to April and the second, which is about one-half the magnitude of the first, from August to October (Sorokin, 1983). The total flux in our study exhibits maxima from May - July 1988 and December 1988 (Honjo and Manganini, pers. comm.) (Fig. 6-3a), offset from the average recorded timing of the phytoplankton blooms. Results of 5 years of sediment trap studies show that the timing of the flux maximum is variable (Honjo *et al.*, 1987; Hay *et al.*, 1990). The variability in the timing of total flux maxima suggests that the timing of phytoplankton blooms, which drive the flux maxima, is also variable.

The annual cycle of chlorophyll degradation product flux in the Black Sea follows the cycle of primary productivity. The flux of total phorbin, the sum of all chlorophyll degradation products, at BSK3-1 exhibits maxima in May - July 1988, and again from November 1988 to January 1989 (Fig. 6-3c). The May - July measurement is from a 3 month trap, so the exact month and magnitude of the spring maximum phorbin flux could not be determined. Total phorbin flux at BSK2 also exhibits two maxima coinciding with the maxima in primary production (Fig 6-3d). The maximum value and timing of the spring phorbin maximum at BSK2 also can not be determined since only two one week samples during the month of July were available for study (no samples prior to July, 1988 were analyzed at BSK2). The fall maximum in total phorbin content at BSK2 shows a

maximum one month later than that at BSK3-1; in January at BSK2 as compared with December at BSK3-1.

The same annual cycle seen in the total phorbin flux at BSK3-1 and BSK2 is seen in the flux of pheophytin-*a*, pyropheophytin-*a*, pheophorbide-*a*, pyropheophorbide-*a*, MW532 pyropheophorbide-*a*, and the pyropheophorbide-*a* steryl esters (Figs. 6-5 to 6-7). Each of these components of the total phorbin flux exhibit maxima within one month of the maximum total phorbin flux, but with variations in magnitude (Table 6-1a, b). At BSK3-1, the flux maximum of pheophytin-*a* and pyropheophytin-*a* are separated by one month. During the spring maximum in phorbin flux, the pheophytin-a/pyropheophytin-a ratio is 0.04, whereas during the winter flux maximum, the ratio is 4.3. The annual cycles of pheophorbide-*a* and pyropheophorbide-*a* flux at sediment trap station BSK3-1 (Table 6-1; Fig. 6-4b) show trends similar to those of pheophytin-*a* and pyropheophytin-*a* (Fig. 6-4a). During the spring maxima, the pheophorbide-*a*/pyropheophorbide-*a* ratio is 1.0, while at the winter flux maxima, pyropheophorbide-a is below detection limits. The flux of MW532 pyropheophorbide also showed maxima during the May to July bloom and again during the winter bloom (Fig. 6-4d). The maximum value for MW532 pyropheophorbide flux recorded during both blooms was substantially greater than those for pheophorbide-*a* and pyropheophorbide-*a* . The trends in flux of pyropheophorbide-*a* steryl esters are more similar to that of pheophorbide-*a* than to that of their parent compound, pyropheophorbide-*a* (Fig 6-7; Ch. 5), but the PSEs display a flux maxima spread over two months unlike any other pigments analyzed in these samples.

At station BSK2, the measured flux cycles of pheophytin-*a* and pyropheophytin-*a*, and of pheophorbide-*a* and pyropheophorbide-*a*, are different from each other as described for station BSK3-1 (Figs. 6-8, and 6-9). One noticeable difference between BSK2 and BSK3-1, is that during the winter flux maxima at BSK2, the pheophytin-*a*/pyropheophytin-*a* ratio is much less than 1, whereas this ratio is greater than 1 at BSK3-1. The ratio of pheophorbide-*a*/pyropheophorbide-*a* at BSK2 is 0.7, whereas at BSK3-1 pheophorbide-*a* could not be detected. This suggests that different mechanisms are controlling the formation of pheopigments at each station.

At BSK2, the maximum in pheophorbide-*a* flux occurs one month later than the maximum pyropheophorbide-*a* flux, similar to BSK3-1, and the MW532 pyropheophorbide (Fig. 6-5d) has a much larger flux than that of pheophytin-*a*, pyropheophytin-*a*, pheophorbide-*a*, and pyropheophorbide-*a*, as it does at BSK3-1. The flux maximum for each pigment measured at BSK2 occurs one month later during the fall-winter bloom than it does at BSK3-1. The pyropheophorbide-*a* steryl esters also show a broad flux maxima, as they did at BSK3-1 (Fig. 6-5c). No data is available at BSK2 for

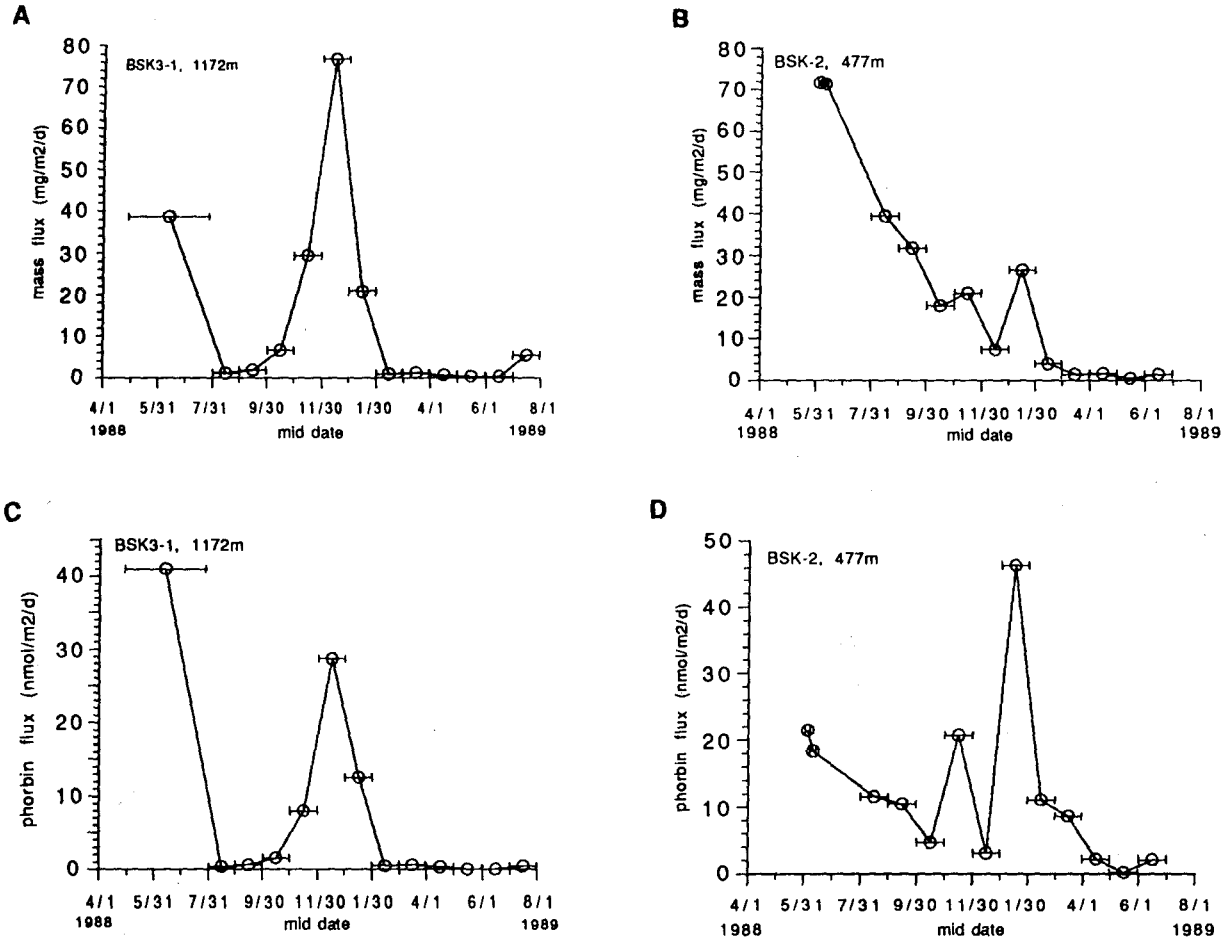

Fig. 6-3 Total mass flux and total phorbin flux at BSK3-1 and BSK2 for May, 1988 - July, 1989: a) total mass flux at BSK3-1 (Manganini, pers. comm.), b)total mass flux at BSK2 (Manganini, pers. comm.), c) total phorbin flux at BSK3-1, and d) total phorbin flux at BSK2.

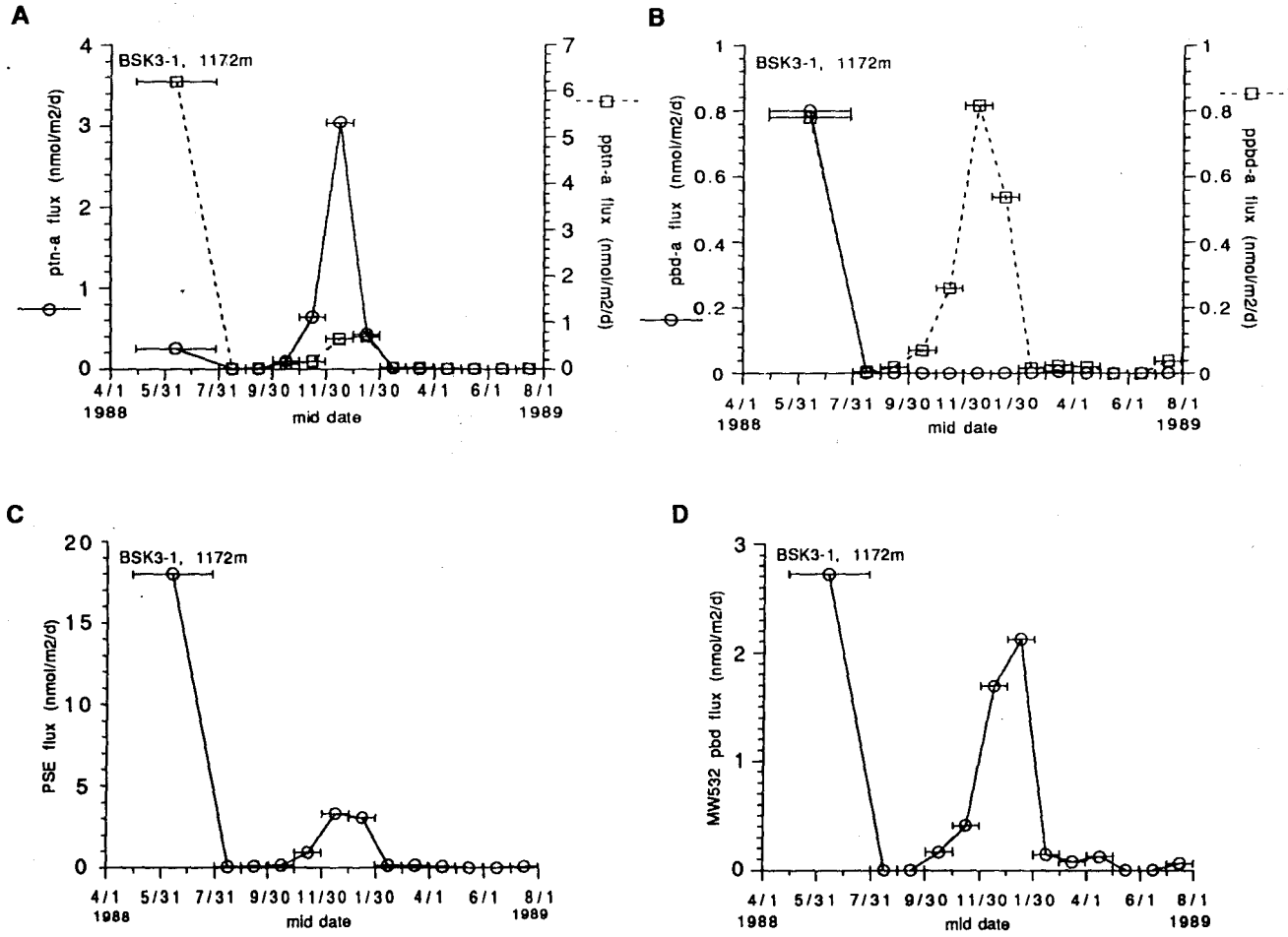

Fig. 6-4 Flux of the major components of the total phorbin flux from May, 1988 - July, 1989 at BSK3-1: a) pheophytin-*a* and pyropheophytin-*a*, b) pheophorbide-*a* and pyropheophorbide-*a*, c) phorbin steryl esters, and d) MW532 pheophorbide.

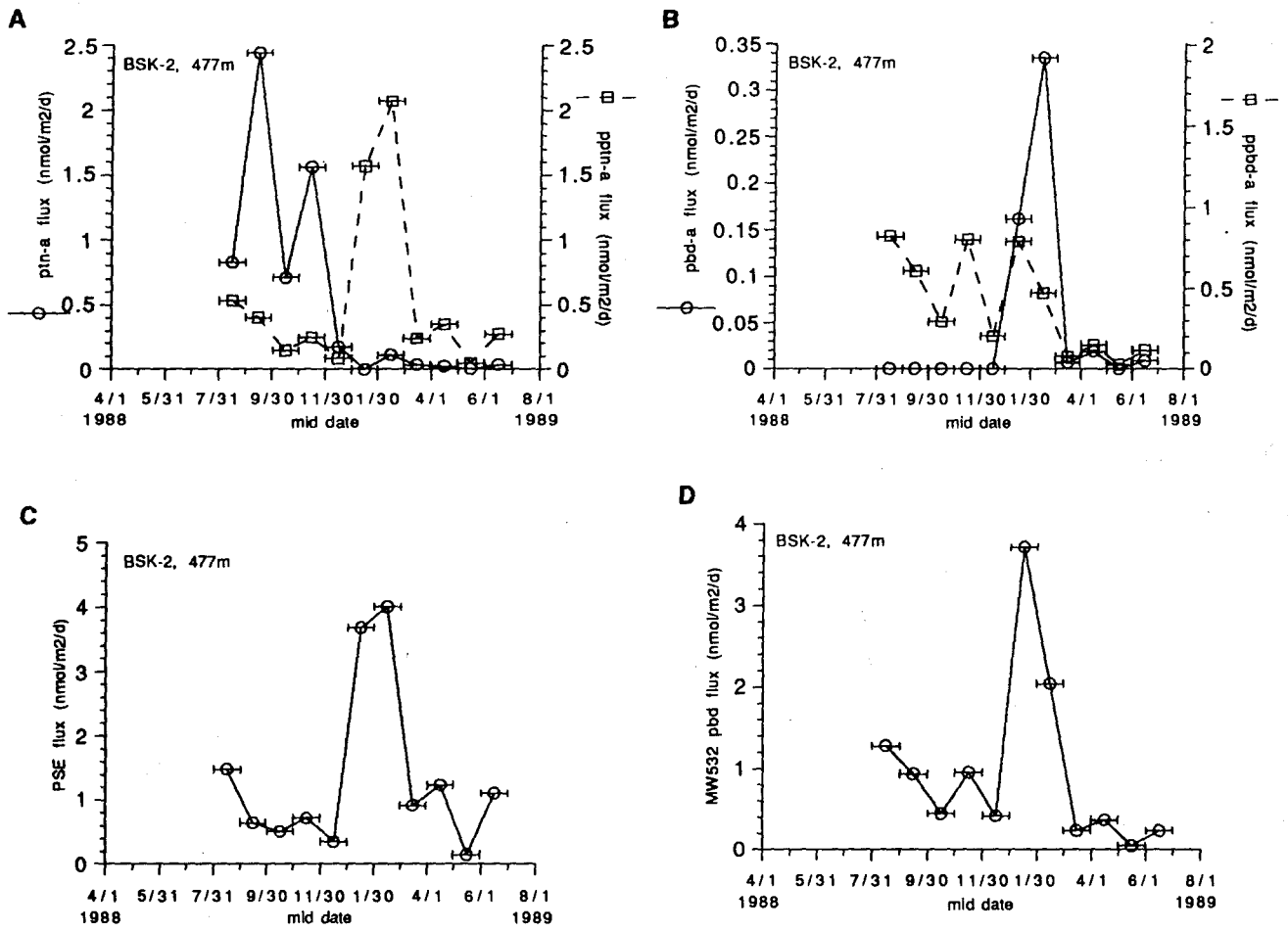

Fig. 6-5 Flux of the major components of the total phorbin flux from May, 1988 - July, 1989 at BSK2: a) pheophytin-*a* and pyropheophytin-*a*, b) pheophorbide-*a* and pyropheophorbide-*a*, c) phorbin steryl esters, and d) MW532 pheophorbide.

the spring bloom, so these comparisons with BSK3-1 can not be made for the spring bloom.

A comparison of the total phorbin flux data at 1300 m at BSK2 (samples 2ST1D, 2ST2D, and 2ST3D; Table 6-1b) with the corresponding samples at 477 m shows that the phorbin flux magnitude is similar, but with a 1 month offset. Hay (1988) calculated an average settling velocity of 65 m/d for particulate matter in the Black Sea. At this settling velocity, it would only take 13 days for material to settle from a depth of 477 m to 1300 m. If the flux maxima is arriving at the upper trap toward the latter part of the month, then with a 13 day settling time between traps, the flux maxima could arrive at the deeper trap in the first part of the following month. Allowing for a 1 month offset in the data between the 477 m trap and 1300 m trap, there does not appear to be any loss of phorbins as particles settle through the anoxic water column of the Black Sea.

The differences in the timing of the flux maxima for pheophorbide, pyropheophytin, and pyropheophorbide-*a* steryl esters, versus pheophytin, pyropheophorbide, and MW532 pyropheophorbide, suggests that different mechanisms are controlling the production of these compounds in the water column, and therefore their flux out of the photic zone. A one month delay in the flux maxima of pyropheophytin-*a* as compared with pheophytin-*a* and total phorbin flux as seen at BSK3-1 and BSK2, has previously been noted at a depth of 55 m in Dabob Bay, Washington, U.S.A. (Downs, 1989). In Dabob Bay, the flux maxima for pyropheophytin-*a* was also weaker than that for pheophytin-*a* (Vernet and Lorenzen, 1987) as observed in the Black Sea. The maximum in pyropheophorbide-*a* flux corresponded to the maximum in pheophytin-*a* flux in Dabob Bay, with only very low concentrations of pheophorbide-*a* (Vernet and Lorenzen, 1987) as it did at BSK3-1 in the Black Sea. These similarities in flux trends suggest that similar mechanisms are controlling the flux of pheopigments in both Dabob Bay and the Black Sea.

Downs (1989) also noted variations in the ratio of pheophorbide-*a*/pyropheophorbide-*a* in Dabob Bay. She noted that the ratio of pheophorbide-*a*/pyropheophorbide-*a* varies with depth with values greater than 1 at the surface, and values less than 1 at depth (Downs, 1989). Both trap sites in the Black Sea are below the photic zone and pyropheophorbide-*a* was the more prominent of the pheophorbide-*a* - pyropheophorbide-*a* pair, as expected from the results of Downs (1989).

One very noticeable point in each of the plots of pigment flux from both trap sites is the lack of any noticeable rise in flux during the months of May - June, 1989. During the period of May to July 1988 at BSK3-1, each pigment exhibited large flux values. Since the

only source of chlorophyll is photosynthetic algae, and since the maxima in the flux of chlorophyll degradation products occurs synchronously with bloom conditions, the lack of any noticeable peak in pigment flux during spring 1989, suggests that either the 1989 spring bloom did not occur or that it was greatly reduced compared to that of 1988. The spring bloom is generally the larger of the two blooms in the Black Sea. The fact that no increase in pigment flux is seen at both trap sites suggests that the greatly reduced spring bloom during 1989 was not a localized phenomenon.

An inventory of chlorophyll degradation products in sediments

The quantitative data for chlorophyll degradation products in sediment samples BS2-0-10 and BS2-13-18 are tabulated in Table 6-2. In both the 0 - 10 cm (BS2-0-10) and 13 - 18 cm (BS2-13-18) sediment samples, the concentration of spectrophotometrically determined total solvent extractable sedimentary chlorophyll degradation products is similar. Upon analysis of the total organic extracts of the two samples by HPLC with fluorometric detection, the similarity between the two samples is evident (Fig. 6-6). We also examined the samples by spectrometric detection at 436 nm. At this wavelength, the greatly reduced amount of carotenoid pigments in the more deeply buried sample, BS2-13-18, as compared to the shallower sample, BS2-0-10, is apparent (Fig. 6-7).

Individual phorbins are identified by HPLC coelution with standards, comparison of visible spectra, CI-MS, and LC-MS (Ch. 7). Thirteen phorbins and a series of pyropheophorbide-*a* steryl esters (PSEs) were identified. These are, in order of increasing retention time: MW532 pyropheophorbide, pheophorbide-*a*, pheophorbide-*a*', pyropheophorbide-*a*, chlorophyll-*a*, chlorophyll-*a*', pheophytin-*b*, pheophytin-*b*', pheophytin-*a*, pheophytin-*a*', pyropheophytin-*b*, pyropheophytin-*a*, and PSEs Each of these compounds appeared in sample BS2-0-10, and six appeared in BS2-13-18 (Table 6-2). Chlorophyll-*a* and pheophytin-*b* did not appear in BS2-13-18.

The relative concentration of the individual phorbins varies between the two samples. In both samples, the total PSEs are the quantitatively most important chlorophyll degradation products as determined by HPLC (Ch. 3; King and Repeta, 1991). The PSEs represent 17% and 21% of the solvent extractable phorbins in BS2-0-10 and BS2-13-18, and 13% and 16% of the total sedimentary phorbins, respectively. When considering only non-PSE phorbins, pheophytin-*a* and pyropheophytin-*a* are each quantitatively more important than pheophorbide-*a*, pyropheophorbide-a, and chlorophyll-*a* together, with pyropheophytin-*a* being the most concentrated in BS2-0-10, and pheophytin-*a* being the most concentrated in BS2-13-18. Pheophorbide-*a* is the quantitatively least important chlorophyll-*a* derived phorbin in both samples.

Table 6-2

CONCENTRATION OF CHLOROPHYLL DEGRADATION PRODUCTS IN BLACK SEA SEDIMENTS

	BS2-0-10		BS2-13-18	
pigment	nmol/gdw	% of total	nmol/gdw	% of total
[1]pheophorbide-*a*	1.08		1.46	
pyropheophorbide-*a*	3.37		3.80	
MW532 pyropheophorbide	3.76		3.08	
chlorophyll-*a*	3.36		0.0	
pheophytin-*a*	12.3		9.50	
pyropheophytin-*a*	9.85		9.70	
pheophytin-*b*	3.85		0.0	
pyropheophytin-*b*	5.57		6.64	
total	43.	**28**	34.	**23**
PSEs	20.	**13**	24.	**16**
HMW	30.	**20**	34.	**23**
total identified by HPLC	93.	**61**	92.	**61**
[2]spectroscopic total	118.	**77**	110.	**73**
[3]spectroscopic yield - HPLC yield		**17**		**13**
total acid extracted	35.	**23**	40.	**27**
total sedimentary phorbins	**153**	**100**	**150**	**100**
gel fraction A		19		23
B		34		34
C		4		7
D		20		10

[1]sum of the concentration of the more common isomer and its epimer

[2]total solvent extractable as determined by visible spectrophotometry at 665 nm

[3]In BS2-0-10 and BS2-13-18, 8% and 6%, respectively may be due to a series of polar compounds, some of which are porphyrins, which elute in gel fraction D, but are not seen using the fluorometric detection system employed here.

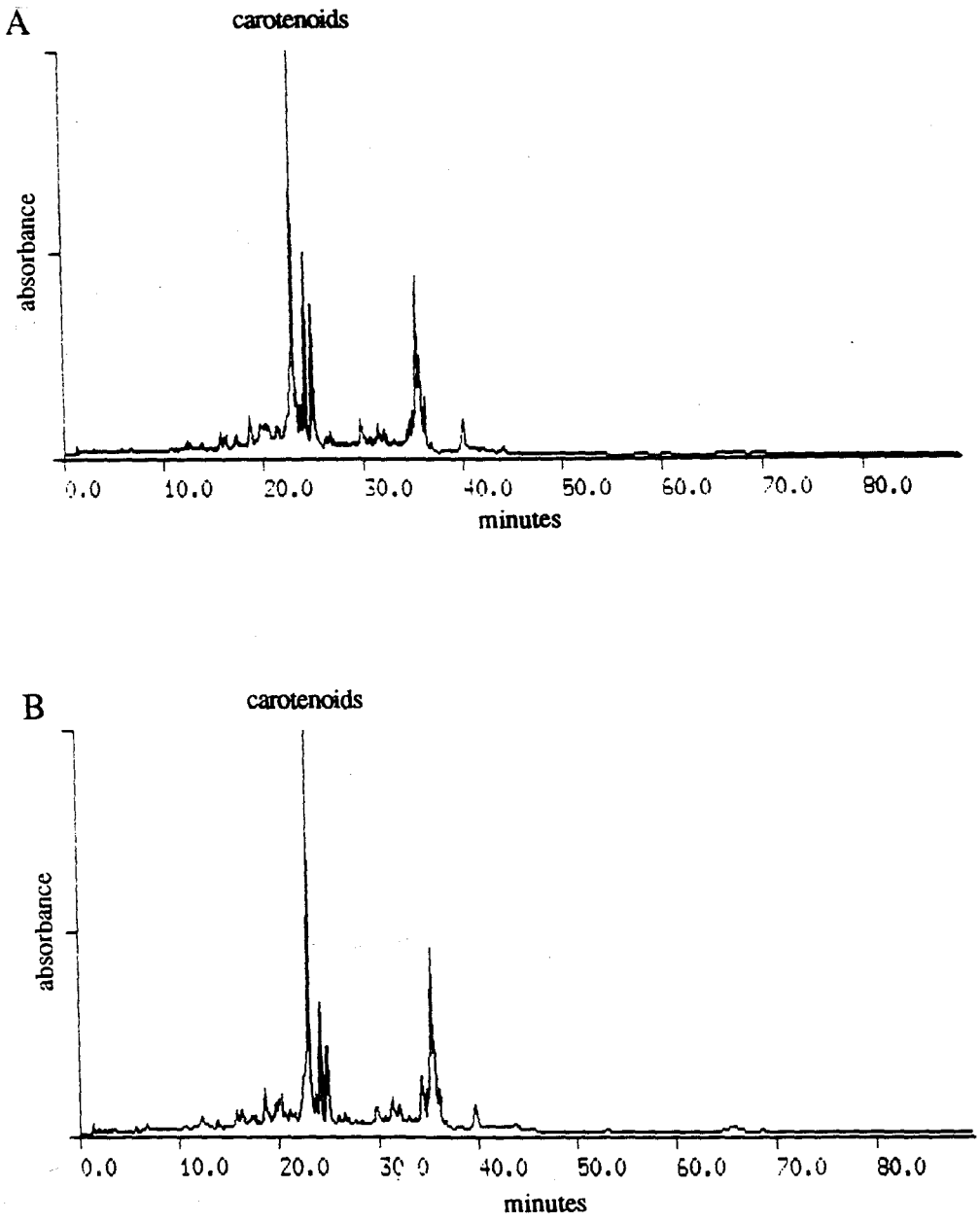

Fig. 6-6 High pressure liquid chromatograph with detection at 436 nm of the total organic extract of sediment samples (a) BS2-0-10 and (b) BS2-13-18.

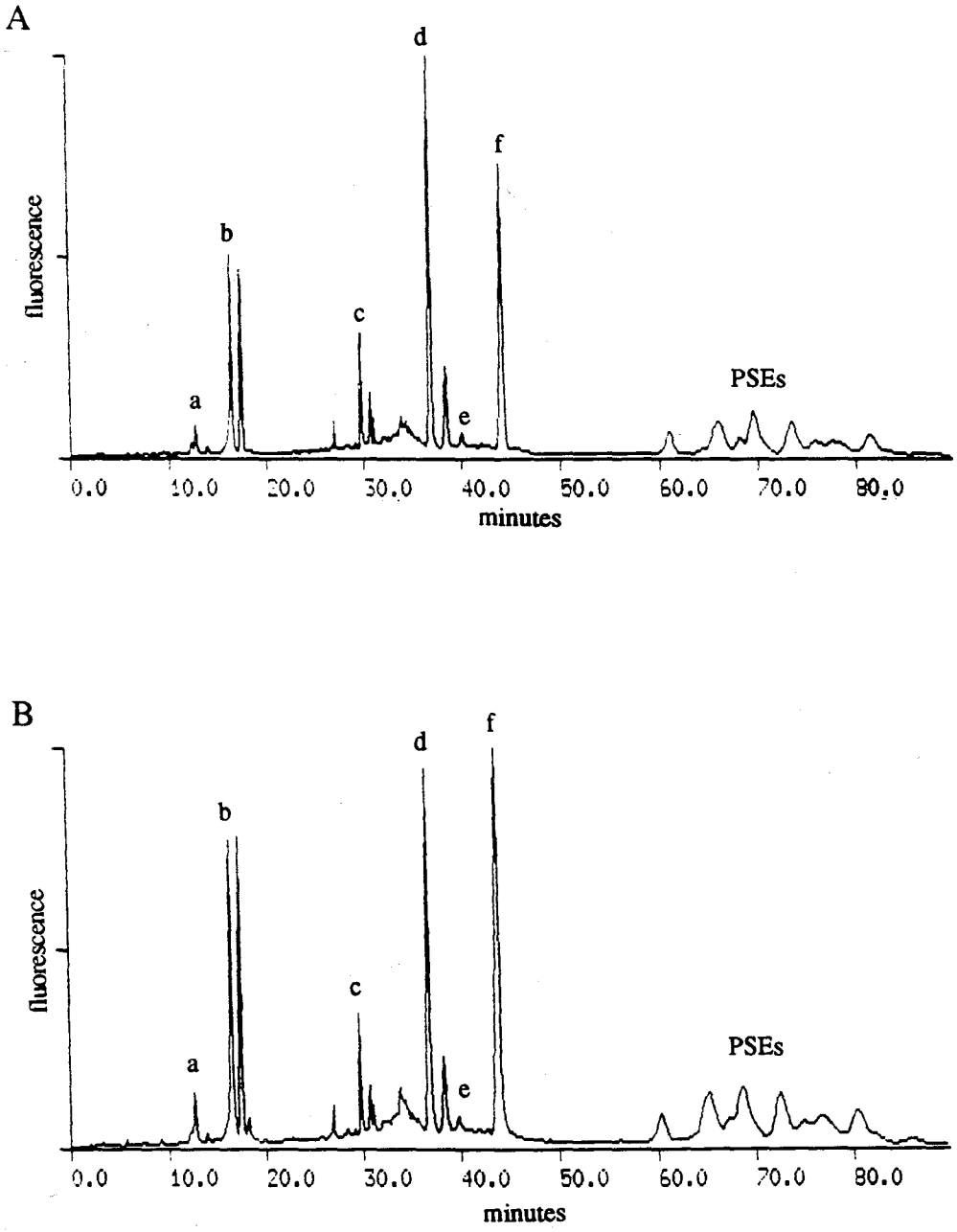

Fig. 6-7 High pressure liquid chromatograph with fluorescence detection of the total organic extract of sediment samples (a) BS2-0-10 and (b) BS2-13-18. Peak identifications are the same as those used in Fig. 3-2.

One notable difference between the two sediment samples is the significantly reduced quantity of chlorophyll-*b* derived pigments in sample BS2-13-18 as compared to BS2-0-10. Only one degradation product of chlorophyll-*b* occurs in BS2-13-18 whereas two occur in BS2-0-10. Since the concentration of the chlorophyll-*a* derived compounds remains relatively constant between the two samples, the reduced concentration of chlorophyll-*b* phorbins in the deeper sample suggests that either the chlorophyll-*b* derived phorbins are considerably less stable than the chlorophyll-*a* derived phorbins, a conclusion not supported by previous studies (Gouterman, 1961; Keely and Brereton, 1986). Alternatively the input of chlorophyll-*b* to the sediments has changed over time. Chlorophyll-*a* is also no longer present in BS2-13-18. The rapid demetallation of chlorophylls in sediments has been reported previously (Keely and Brereton, 1986).

Both sediment samples were fractionated by gel permeation chromatography (GPC). Upon fractionation of the total solvent extracts by gel permeation chromatography (Fig. 6-8), a high molecular weight phorbin containing fraction (fraction **A**) is isolated (Ch. 4 and 7). The quantity of total phorbin in each gel column fraction was determined by visible spectrophotometry and corrected for recovery. The high molecular weight fraction represents 24% and 31% of the total solvent extractable chlorophyll degradation products, and 19% and 23% of total sedimentary phorbins, in BS2-0-10 and BS2-13-18, respectively (Table 6-2). Fraction **B**, which contains the pyropheophorbide-*a* steryl esters, pheophytin-*a*, pyropheophytin-*a*, pheophytin-*b*, and pyropheophytin-*b*, contains the highest concentrations of phorbin, and fraction **D**, which contains the pheophorbide-*a*, pyropheophorbide-*a*, chlorophyll-*a*, and a suite of unknown polar compounds believed to be porphyrins (Ch. 7), contains the least. Fraction **C** contains almost exclusively carotenoids along with a small amount of phorbin due to incomplete separation of the factions.

The total spectroscopically determined phorbin concentration in each gel fraction was compared with the HPLC determined quantity of phorbins which elute in a given gel fraction. The quantity of phorbin determined spectrally in gel fraction **B** was similar to that determined by HPLC for both sample BS2-0-10 and BS2-13-18. For gel fraction **D**, the quantity of phorbin determined spectrally was greater than that determined by HPLC. For sample BS2-0-10, the disparity between the two measurements represented 8% of the total sedimentary phorbin, and in BS2-13-18, the disparity represented 6% of the total sedimentary phorbin. The missing spectrally determined phorbin in fraction **D** might at least partially be accounted for by the suite of compounds believed to be porphyrins (Ch. 7) since these compounds represent up to 5% of the total solvent extractable chlorophyll

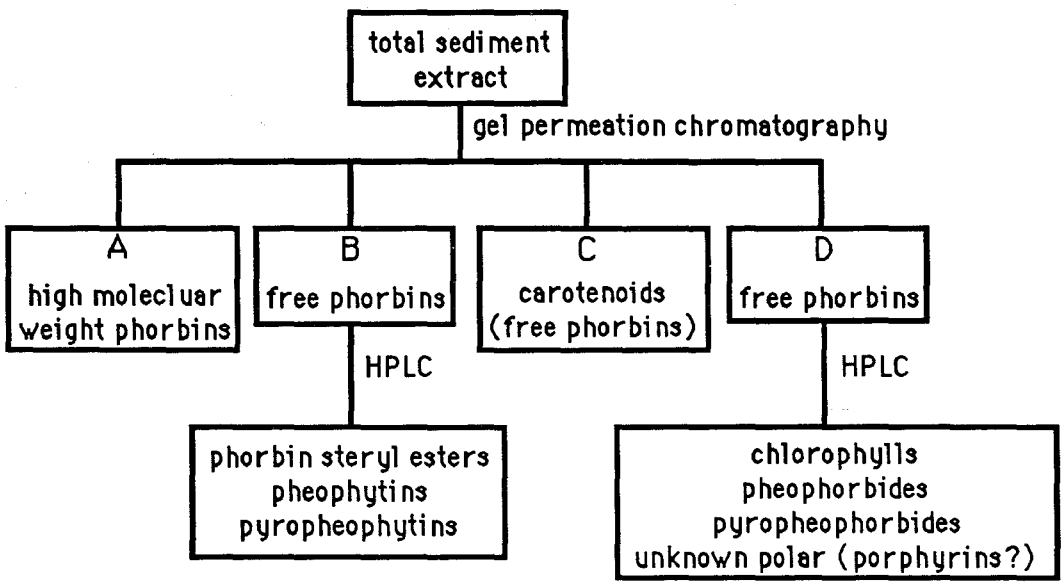

Fig. 6-8 Diagram indicating the groups of pigments eluting in each gel column fraction.

degradation products and they are not detected by the fluorometric detection system used in conjunction with the HPLC in this study.

An inventory of chlorophyll degradation products can also be established by quantifying the individual compounds from HPLC. When considering the compounds isolated and identified by HPLC (including the porphyrins) and the HMW phorbins, 88 and 90% or the total phorbin measured spectrophotometrically in BS2-0-10 and BS2-13-18, respectively, have been identified. The discrepancy between the amount identified and the amount measured by visible spectrophotometry may be attributed to the different ways in which compounds were quantified. The total amount of phorbins in each sample was measured by visible spectrophotometry at 665 nm using an average extinction coefficient. Some error may be incurred using this extinction coefficient, since not all phorbins absorb with the same intensity at 665 nm. The quantity of the individual compounds, not including the high molecular weight fraction which was also quantified by visible spectrophotometry, was determined by HPLC using conversion factors determined for each pigment from standards. In quantification of pigments from the total sediment extract by HPLC, errors in integration are incurred.

The total HPLC separable phorbins normally determined in studies of chlorophyll degradation products (*ie.* pheophytins and pheophorbides, not including PSEs) account for 28 and 23% of sedimentary chlorophyll degradation products respectively for BS2-0-10 and BS2-13-18 with the PSEs accounting for an additional 13 and 16% of the degradation products (Table 6-2). The high molecular weight fraction represents another 20 and 23%. This gives a total of 61 and 62% of the total sedimentary chlorophyll degradation products for BS2-0-10 and BS2-13-18 respectively. Inclusion of the compounds which may be porphyrins brings this total to 69 and 68% of the sedimentary chlorophyll degradation products measured in these two samples.

Additional chlorophyll degradation products were removed from the solvent extracted sediment using methanolic sulfuric acid. Summing the recovered phorbins from three extractions, 32 nmol/gdw was recovered from BS2-0-10 and 37 nmol/gdw from BS2-13-18. This brings the total sedimentary chlorophyll degradation products recovered from BS2-0-10 to 153 nmol/gdw and from BS2-13-18 to 150 nmol/gdw. This is 4 times more sedimentary chlorophyll degradation products than can be accounted for when considering only the HPLC resolvable phorbins (not including the PSEs that have not previously been routinely measured).

A total inventory of sedimentary chlorophyll degradation products can be written as:

$$\underline{\text{total}} = \underline{\text{AEX}} + \underline{\text{HMW}} + \underline{\text{PSEs}} + \underline{\text{phorbins}} \qquad (1)$$

where total is the total sedimentary chlorophyll degradation products with a recognizable macrocycle and absorbance peak at 665 nm; AEX is the concentration of chlorophyll degradation products in the acid extractable fraction; HMW is the concentration of chlorophyll degradation products in the solvent extractable high molecular weight fraction, PSE is the concentration of pyropheophorbide-*a* steryl esters; phorbins, those chlorophyll degradation products with a macrocycle possessing a C-7 - C-8 saturation and an isocyclic ring, is the total concentration of free chlorophylls, pheophytins, pheophorbides, and polar phorbins and porphyrins eluting between 0 and 10 minutes in the reversed-phase HPLC chromatograms. Not included in this inventory of sedimentary chlorophyll degradation products is a term for remineralization, which most likely occurs through ring opening. In the mass balance for water column chlorophyll degradation presented below, we show that within a factor of two, the flux of chlorophyll degradation products which leaves the Black Sea photic zone accumulates in surface sediments. We therefore assume that eq 1 includes all sedimentary reservoirs for chlorophyll degradation products in the Black Sea, and that remineralization in sediments is a minor process.

B. MASS BALANCE OF CHLOROPHYLL DEGRADATION IN THE BLACK SEA

Approach and Assumptions

In order to fully understand the process of chlorophyll degradation, it is important to understand where the major losses of chlorophyll and chlorophyll derived pigments occur in the water column and sediments. We therefore mass balance chlorophyll production with chlorophyll sedimentation, to determine how much chlorophyll degradation product is lost prior to sedimentation and if the loss occurs in the surface ocean or during transport to sediments. In order to create a mass balance of chlorophyll production and sedimentation in the Black Sea it is necessary to consider data for total organic carbon, chlorophyll production, and primary production from the literature with the phorbin flux and sedimentary phorbin concentration data gathered in this investigation. In doing this, assumptions have been made in how the literature data relates to our experimental results. From the literature data, we assume that primary production in the eastern and western basins are similar (Sorokin, 1983; Honjo *et al.*, 1987) and that integrated chlorophyll production and primary production are linearly related (Hayward and Venrick, 1982). We also assume that the relationships of chlorophyll production and chlorophyll flux, and primary production and carbon flux, measured immediately below the chemocline, at a specific time and location in the Black Sea, are representative of the annual averages of these relationships. The model is presented in two parts. In the first part, the

relationship of chlorophyll production and sedimentation at two specific locations for a given month is examined. In the second part the model is extended to an annual average and to cover the entire Black Sea. The mass balance of chlorophyll and its degradation products for the Black Sea is summarized in Fig. 6-9 and Tables 6-3 and 6-4.

In order to create a mass balance of chlorophyll and its degradation products in the Black Sea water column, the water column is divided into two regions; the oxic zone which encompasses the entire photic zone and the suboxic region of the water column, and the anoxic zone which encompasses the water column from oxic/anoxic interface to the sediments. These two zones are separated by a strong chemocline in where a bacterial community lives. In the oxic zone, there is only one source of chlorophyll, production of chlorophyll by phytoplankton (Fig. 6-9). To balance this production, there exists two modes of loss of chlorophyll from the photic zone. These are sinking of particles, either of whole cells or of large fecal pellets produced by macrozooplankton following grazing; and photo-oxidation (Welschmeyer and Lorenzen, 1985). In the anoxic zone, we assume there is again only one source. This is the chlorophyll and its degradation products which fall through the chemocline into the anoxic zone encased in large particles. Loss of pigment through remineralization in the anoxic water column and burial in the surface sediments balances the input of chlorophyll and its degradation products entering the anoxic zone from the oxic zone (Fig. 6-9). In making the assumption of only one source to the sediment traps, we ignore the possibility of resuspension and lateral transport contributing a portion of the material to our trap samples. Hay *et al.* (1990) use lateral transport of resuspended material from the Turkish coast to explain the higher organic flux at 1200 m than at 250 m. Unlike the sediment trap studies of Hay *et al.* (1990), our sediment traps were moored in the center of the basins and away from the influence of riverine input. Due to the rapid photo-oxidation of chlorophyll and its degradation products (SooHoo and Kiefer, 1982), it is unlikely that the input of phorbins from terrigenous runoff will have a significant influence on the flux of phorbin. It is possible that the presence of high molecular weight and/or acid extractable chlorophyll degradation products in the deep traps could represent input through resuspension, though these compounds may be forming in the water column.

The second assumption that we make in our model, is that total phorbin is equal to total chlorophyll-*a* and chlorophyll-*a* derived pigments. Total phorbin fluxes and concentrations were determined spectrophotometrically at the red band (665 nm). The contribution of chlorophyll-*b* derived pigments to this measurement in less than 10%. In our studies we did not identify derivatives of chlorophyll-*c* or of bacteriochlorophylls. Since chlorophyll-*c* and its derivatives are true porphyrins, their absorbance at the red band

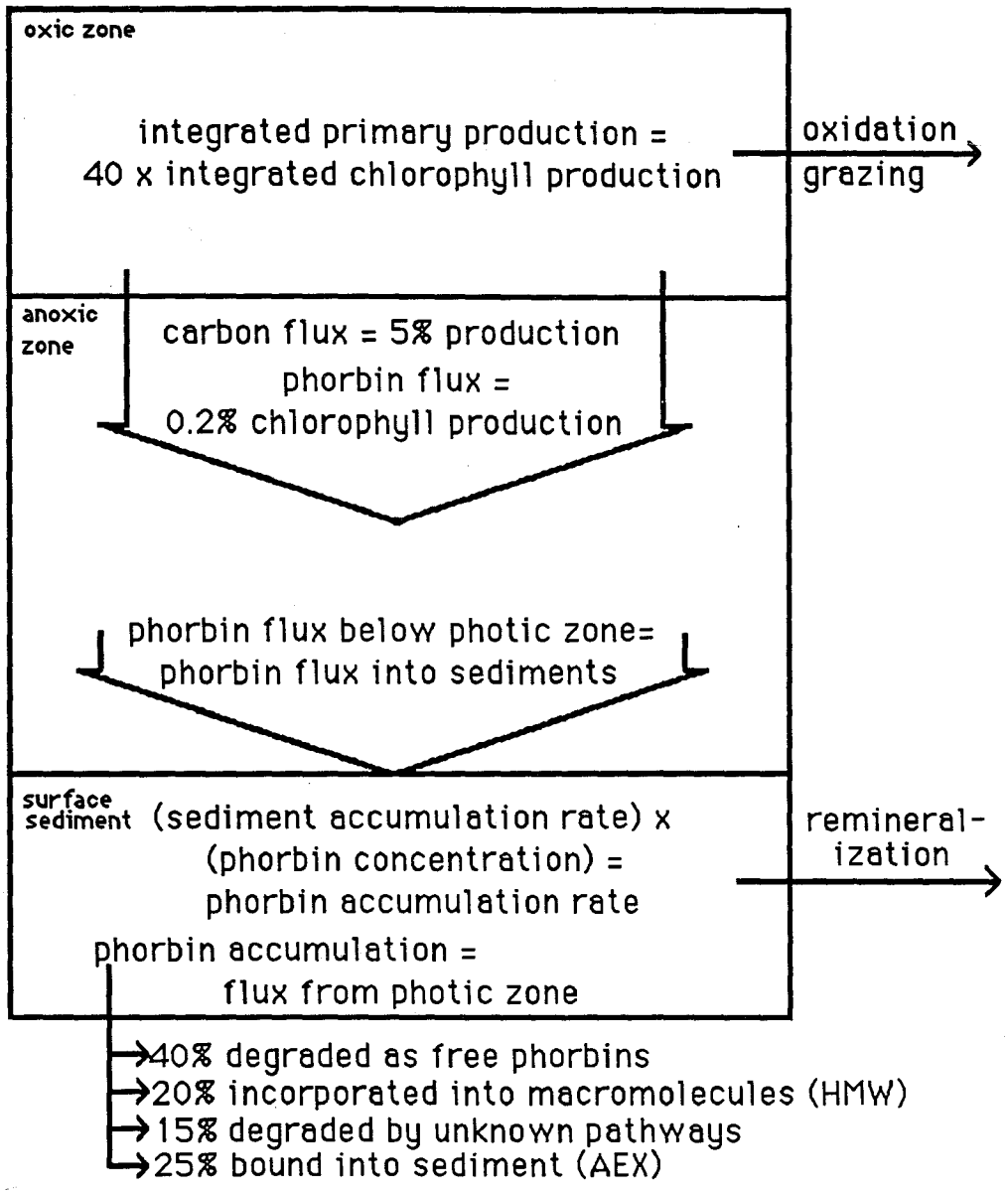

Fig. 6-9 Schematic representation of the mass balance of chlorophyll production and sedimentation for the Black Sea.

is approximately 1/5 that of chlorophyll-*a* derivatives and chlorophyll-*b* derivatives. The contribution of chlorophyll-*c* pigments to the red band absorbance, if they are present, will only be a few percent. At times when the chemocline intersects the photic zone, photosynthetic bacteria are present and produce bacteriochlorophyll-*e*. Unlike other bacteriochlorophylls, bacteriochlorophyll-*e* is a dihydroporphyrin and therefore the red band absorbance occurs at 660 nm. We did not detect bacteriochlorophyll-*e* using our HPLC method, since the Soret maximum is at 460 nm (100% acetone) and we used an excitation wavelength of 417 nm in our HPLC fluorescence detector. The contribution of bacteriochlorophyll-*e* to the red band absorbance of the total extract of sediment trap samples is unknown. Sediment samples were also analyzed using a photodiode array detector as well as the fluorescence detector, and we did not identify bacteriochlorophyll-*e* in the sediment samples.

To determine the relationship of chlorophyll production with chlorophyll sedimentation, we compare primary production, chlorophyll production, and carbon flux data from the literature with our measured phorbin flux and sedimentary phorbin concentrations. In the central Black Sea, we use phorbin flux data from BSK2 and sedimentary phorbin concentration from box core 5 (sample BS5-0-4). We combine our measured phorbin flux at sediment trap station BSK3-1, in the eastern basin, with our measured sedimentary chlorophyll concentration (BS2-0-10), and primary production and carbon flux data from the literature for the western basin. Studies of primary production in the Black Sea suggest that average primary production in the eastern and western basins are similar (Shimkus and Trimonis, 1974; Sorokin, 1983; Honjo *et al*, 1987) or slightly higher in the western basin. We therefore assume that primary production in the eastern and western basin are similar and that sediment trap data from the western basin can be applied to the eastern basin. Sedimentary Ca/Al and C_{org}/Al ratios, suggest that primary production in the western basin of the Black Sea is slightly higher than in the eastern basin (Hay and Honjo, 1989; Hay *et al.*, 1991), but it is unclear whether variations in these ratios are due to primary production or to changes in sediment dilution. No Ca/Al or C_{org}/Al data is given for the upper 5 cm of core from the eastern basin, which was taken as station BSK3-1, but prior to this interval the measurements in the eastern and western basins are similar.

Implicid in our comparison of sediment trap flux measurements to phobin accumulation rates in sediments, is the assumption that phorbin production and accumulation has been constant over the 700 years of deposition represented by our sediment samples. Measurements of organic carbon accumulation rates suggest that organic carbon accumulation has not varied over a factor of two during the deposition of

Unit I (Hay, 1988; Calvert et al., 1991). If the majority of organic carbon is marine derived, as suggested by Calvert and Fontugne (1987), then the constant organic carbon accumulation rates suggest that organic input to the sediments has been constant, within a factor of two, during Unit I.

The portion of our model in the oxic portion of the water column, which determines the input into the anoxic water column, depends entirely on data from the literature. Only one measurement of integrated chlorophyll production exists. We therefore estimate integrated chlorophyll from existing measurements of integrated primary production (Hayward and Venrick, 1982). In our model, we assume that the C:chl ratio calculated from integrated primary production and integrated chlorophyll production at a specific location in the Black Sea (Repeta and Simpson, 1991; Karl and Knauer, 1991) is valid for the entire Black Sea.

A Mass Balance of Chlorophyll Degradation Products in the Western Basin and Central Black Sea

In the Western Basin and the Central Black Sea we compare the measured flux of phorbin to the accumulation rate of phorbin calculated from the total sediment accumulation rate (Calvert *et al.*, 1991) and sedimentary phorbin concentration. For the month of July, 1988, at BSK2, the measured flux at 1300 m is 16 $\mu g/m^2/d$, similar to the value of 14 $\mu g/m^2/d$ at 477 m, suggesting little loss of phorbin as it settles through the anoxic water column. Measurement of organic carbon by sediment traps at two depths in the south western Black Sea water column, suggest that the flux of organic carbon at 250 m and 1200 m is similar, (Honjo *et al.*, 1987; Hay, 1987; Hay *et al.*, 1990). These data suggest that remineralization rates of rapidly sinking particulate organic carbon in the anoxic water column are low. The similarity of the phorbin fluxes at 1300 m and 477 m suggests the remineralization rates of phorbins in the anoxic zone of the water column is low.

Flux of phorbin and total organic carbon through the water column can be compared to the accumulation rates of phorbin and total organic carbon if the total sediment accumulation rate and concentrations of total organic carbon and total phorbin are known. We measured the average total phorbin flux in the central Black Sea (BSK2) at 477 m to be 7.4 $\mu g/m^2/d$ (Table 6-3), and in the eastern basin (BSK3-1) to be 10 $\mu g/m^2/d$. As discussed previously, in this mass balance, we assume the primary production in the eastern and western basin to be similar. Therefore, we compare the total phorbin flux in the eastern basin to the phorbin accumulation rate in the western basin.

The upper unit of Black Sea sediment is finely laminated, alternating between organic carbon rich and calcareous bands. The sediment accumulation rate of the upper

Table 6-3

MASS BALANCE OF CHLOROPHYLL SEDIMENTATION IN THE CENTRAL AND WESTERN BLACK SEA

		western basin			central basin		
		literature value	measured value	[a]calculated value	literature value	measured value	[a]calculated value
water column data for May 1988	integrated primary production ($mgC/m^2/d$)	573[1]			339[1]		
	integrated chlorophyll production ($mg/m^2/d$)	15[2]					8.9
	C:chl			38.2			38.1
	total carbon flux out of photic zone ($mgC/m^2/d$)	28[1,2]					17
	total chlorophyll flux out of photic zone($\mu g/m^2/d$)	32[2]				14	18
	C:chl below photic zone			875			1214
	chlorophyll flux at depth ($\mu g/m^2/d$)		27			16	
yearly averages	average phorbin flux ($\mu g/m^2/d$)		10			7.4	
	sediment accumulation rate ($g/m^2/yr$)	38.7[3]			35.7[3]		
	phorbin concentration in sediments ($\mu g/gdw$)		100			105	
	phorbin accumulation rate ($\mu g/m^2/d$)			10.5			10.3
	carbon accumulation rate ($gC/m^2/yr$)	2.16[3]			1.81[3]		
	% terrigenous organic carbon	29[4,5]			29		
	marine carbon accumulation rate ($gC/m^2/yr$)	1.53			1.43		
	C:chl			399			380

[1] Karl and Knauer, 1991

[2] Repeta and Simpson, 1991

[3] Calvert *et al.*, 1991

[4] Shimkus and Trimonis, 1974

[5] Calvert *et al.*, 1987

[a] calculated from eqs 2 - 7 provided in text

Black Sea sediments has been determined by varve counting (Degens *et al*, 1978; Degens *et al.*, 1980; Hay, 1988; Hay *et al.*, 1991), radiocarbon dating of organic carbon and calcium carbonate (Degens and Ross, 1972; Calvert *et al*, 1987; Calvert *et al.*, 1991), and ^{210}Pb dating (Crusius and Anderson, 1992; Benitez and Buesseler, 1992). The sedimentation rates vary between 38.7 g/m^2/yr (radiocarbon, Calvert *et al.*, 1991) and 150 g/m^2/yr (varve counting, Hay, 1988). In five years of sediment trap collections, one year occured where no coccolithophorid bloom was recorded in the contents of the sediment trap (Honjo *et al.*, 1987; Hay *et al.*, 1990), suggesting that periodically the coccolithophorid blooms which contribute the majority of the carbonate for the white laminae do not occur. This, and the lack of agreement of the results of the radio-isotope dating techniques (both ^{14}C and ^{210}Pb) with the varve counting technique, suggests that varve counting will not produce an accurate sediment accumulation rate for Unit I Black Sea sediments.

We determined the total phorbin content of the surface 10 cm of sediment (sample BS2-0-10) from the western basin to be approximately 100 μg/gdw. Using the sediment accumulation rate of 38.7 g/m^2/yr determined using radiocarbon dating by Calvert *et al.* (1991) for a location near our sediment sample site, we calculate a total phorbin accumulation rate of 10.5 μg/m^2/d. This accumulation rate is similar to the average total phorbin flux of 10 μg/m^2/d measured by sediment trap at 1172 m.

To determine the sedimentary C:chl for sediments in the western basin, we use the organic carbon accumulation rate of 2.16 gC/m^2/yr determined by Calvert *et al.* (1991) from a core in the western basin. This gives a C:chl ratio of 524, a value approximately 1/2 that determined for the C:chl ratio leaving the photic zone. Only 2/3 to 3/4 of sedimentary organic carbon is believed to be marine in origin (Shimkus and Trimonis, 1974; Calvert *et al.*, 1987), therefore to compare the C:chl ratios between the upper anoxic water column and sediments, the carbon accumulation rate must be corrected for the contribution of terrigenous organic carbon. Allowing sedimentary organic carbon to be 70% marine in origin, the marine C:chl is approximately 400, substantially lower than that measured in the upper anoxic water column.

As we did for the western basin, we compare how the flux of phorbin in the central basin with the phorbin accumulation rate in sediments. To do this, we use the phorbin flux determined at 477 m at BSK2 and the sedimentary phorbin concentration determined for sample BS5-0-4. At Black Sea station BSK2, the total phorbin flux averaged over the year at 477 m is 7.4 μg/m^2/d. Calvert determined the organic carbon accumulation rate in the central basin sediments to be 1.8 gC/m^2/yr. Allowing for the contribution of terrigenous organic carbon, the marine carbon accumulation rate in the central basin is 1.4 gC/m^2/yr. If all the phorbin leaving the photic zone reaches the sediment, as suggested by the

comparison of the phorbin flux data at 477 m and at 1300 m, the phorbin accumulation rate at this location is 7.4 $\mu g/m^2/d$ to give a C:chl ratio of 529. Based on a sediment accumulation rate of 35.7 $g/m^2/yr$ (Calvert *et al.*, 1991) and a measured total sedimentary phorbin concentration of 105 μg/gdw (from sample BS5-0-4), the phorbin accumulation rate is 10.3 μg/m2/d; 140% of that calculated from the average phorbin flux. The marine C:chl ratio calculated from the sedimentary phorbin accumulation rate is 380. One point to note about the measured average phorbin flux data at 477 m at BSK2 is the lack of spring bloom data in both 1988 and 1989, and therefore the average phorbin flux measurement at BSK2 is low by some unknown amount. At station BSK3-1, we incorporated the data from the three month trap representing the spring bloom into our average phorbin flux. We have no comparable data for station BSK2, but instead only two one week phorbin flux measurements in July. As discussed previously, the increase in phorbin flux due to the spring bloom is not seen in spring 1989 at either BSK2 or BSK3-1. The lack of spring bloom data, for both 1988 and 1989, in the central basin will force the average phorbin flux measurement to be low at BSK2 as seen in our model calculations.

Using data from the literature, we can compare the flux of total phorbin in the anoxic water column to that in the overlying oxic water column. We also compare the flux of total organic carbon out of the oxic zone as determined by Karl and Knauer (1991) to the total organic carbon accumulation rate determined by Calvert *et al.* (1991). In so doing, we compare the relative preservation of total organic carbon and total phorbin and compare the major sources of loss for total organic carbon and total phorbin.

In the western basin, Karl and Knauer (1991) determined the flux of organic carbon below the chemocline was to be relatively constant with depth with an average value of 28 $mgC/m^2/d$ (Karl and Knauer, 1991). At the same time that Karl and Knauer (1991) did their studies, Repeta and Simpson (1991) determined the chlorophyll-*a* flux below the chemocline (100 m) to be 32 $\mu g/m^2/d$. This gives a C:Chl ratio of 875. At a depth of 1172 m, we measured chlorophyll flux (in the form of total phorbin flux) to be 27 $\mu g/m^2/d$, in the May - July trap at BSK3-1, similar to the value measured by Repeta and Simpson (1991) for the upper anoxic water column.

For the central basin no organic carbon flux, integrated chlorophyll production, or chlorophyll flux data are available, but from the mathematical relationships determined by Karl and Knauer (1991) and Repeta and Simpson (1991) for the western basin, these values can be estimated from the primary production data provided by Karl and Knauer (1991) for the central basin. Karl and Knauer (1991) found that 5% of integrated primary production passes through the chemocline to enter the anoxic portion of the water column

in the western basin. Employing this same ratio for the central basin, we calculate the organic carbon flux in the central basin to be 17 mgC/m^2/d. Employing an average C:chl ratio of 38 to the central basin (Repeta and Simpson, 1991; Karl and Knauer, 1991), we calculate the total integrated chlorophyll production to be 8.9 mg/m^2/d.

Repeta and Simpson (1991) found that 0.2% of the integrated chlorophyll production passes through the chemocline and enters the anoxic water column. This calculation assumes that the sediment traps deployed by Karl and Knauer (1991) in the surface Black do no over or under trap sinking material. Allowing for 0.2% of the calculated integrated chlorophyll production to reach the anoxic water in the central basin, as found by Repeta and Simpson (1991) in the western basin, then we calculate that 18 μg/m^2/d of phorbin should fall into the anoxic zone of the water column. Using the two 1 week traps from July at BSK2, we measured a total phorbin flux of 14 μg/m^2/d. Our measured value is similar to the calculated value.

The results of the organic carbon and total phorbin flux measurements for the upper water column can be expressed mathematically. If the flux of organic carbon below the chemocline equals 5% of integrated primary production and the flux of chlorophyll below the chemocline equals 0.2% of integrated chlorophyll production, then:

$$AP = 0.05\ P \qquad (2)$$

$$AC = 0.002\ C \qquad (3)$$

where P is integrated primary production (mg/m^2/d), AP is primary production reaching anoxic waters (mg/m^2/d), C is integrated chlorophyll production (mg/m^2/d), and AC is total phorbin reaching the anoxic water column (mg/m^2/d). If, below the chemocline, the organic carbon to phorbin ratio increases to 1000, then:

$$(0.05P/0.002C) = 1000 \qquad (4)$$

We have shown that during periods of high productivity, the total phorbin flux out of the chemocline equals the total phorbin flux in the deep anoxic zone. These data suggests that the phorbin flux out of the photic zone reaches the sediments with very little loss. Therefore:

$$AC = SC \qquad (5)$$

where SC is the sedimentary phorbin accumulation rate (μg/m^2/d). Therefore, from equs 1, 2, and 3:

$$SC = 0.002C \quad (6)$$

$$0.05P/1000 = SC \quad (7)$$

In both the eastern and central basins, the C:chl ratio decreases from the anoxic water column to the sediments. Calvert *et al.* (1991) and Lyons (1991) noted elevated organic carbon concentrations in sediments from 0 - 2 cm depth. Beier *et al.* (1991) demonstrated that sediments from 0 - 2 cm also have a different distribution of organic compounds than the sediment immediately below. The carbon accumulation rates used in calculating C:chl ratios were determined using organic carbon contents which did not include the elevated organic carbon levels in surface sediments (Calvert *et al.*, 1991). An increase in organic carbon content in sediment by 1/3 to 1/2 as seen in the very surface sediment (Calvert *et al.*, 1991) would increase the sedimentary C:chl ratios to values which approximate those in the upper anoxic water column. We suggest that total organic carbon is remineralized in the very surface sediments through sulfate reduction and total phorbin is not. The loss or organic carbon through sulfate reduction is discussed in detail below.

A Mass Balance of Chlorophyll Degradation Products for the Entire Basin

Using available data from the literature, the mass balance of chlorophyll degradation products as shown for two locations in May, 1988, can be extended to cover the entire Black Sea (Table 6-4). Estimates for annually averaged primary production for the entire Black Sea basin range from 75 - 250 $gC/m^2/yr$ (Shimkus and Trimonis, 1974; Sorokin, 1983; Lein and Ivanov, 1991). According to the model developed for the western and central basins, the photic zone C:chl ratio is 38. Using this C:chl and the range in primary production from the literature, the range in total photic zone chlorophyll production is 2.0 - 6.6 $g/m^2/yr$. Allowing for 5% of total primary production and 0.2% of total chlorophyll production to pass out of the oxic zone and into the anoxic water column (equs. 1 and 2), then the calculated organic carbon flux in the upper anoxic water column is 3.8 - 13 $gC/m^2/yr$, and the calculated chlorophyll flux is in the range of 4.0 - 13 $mg/m^2/yr$. For a comparison, the only literature data for upper water column organic carbon flux is from sediment trap studies conducted in the southwestern Black Sea (Hay *et al.*, 1990). At this location, the average annual organic carbon flux is 1.46 - 3.43 $gC/m^2/yr$ (Hay *et al.*, 1990). The upper limit of this data agrees with the lower limit of the modelled values. Our model for the central and western basins, which shows a reduction in organic carbon between the upper anoxic water column and sediments, suggests that organic carbon is remineralized at the sediment/water interface, therefore the difference between the literature

Table 6-4

MASS BALANCE OF CHLOROPHYLL SEDIMENTATION FOR THE ENTIRE BLACK SEA

	literature	measured	range	model[a]	extrapolated values[b]
integrated primary production ($gC/m^2/yr$)	75[1] 120-200[2] 200-250[3]		75 250		72 140
integrated chlorophyll production ($g/m^2/yr$)				2.0 6.6	1.8 3.6
C:chl	38[4,5]		38		
total carbon flux out of photic zone ($gC/m^2/yr$)	1.46-3.43[6]		1.5 3.4	3.8 12.5	3.6 7.1
total chlorophyll flux out of photic zone($mg/m^2/yr$)		2.7		4.0 13.2	3.6 7.1
C:chl below photic zone	1000[4]		1000		
chlorophyll flux at depth ($mg/m^2/yr$)		3.7 4.1	3.7 4.1	4.0 13.2	3.6 7.1
sediment accumulation rate ($g/m^2/yr$)	35.7 - 38.7[7] 50 - 55[8] 68±3[9]		35.7 68		
phorbin concentration in sediments (µg/gdw)		107 113	100 105		
phorbin accumulation rate ($mg/m^2/yr$)				3.6 7.1	
carbon accumulation rate ($gC/m^2/yr$)	1.81 - 2.16[7]		1.81 2.16		
% terrigenous organic carbon	25[1] 33[10]		25 33		
marine carbon accumulation rate ($gC/m^2/yr$)				1.2 1.6	3.6[c] 7.1
C:chl				225 330	1000[c]

[1] Shimkus and Trimonis, 1974
[2] Sorokin, 1983
[3] Lein and Ivanov, 1991
[4] Karl and Knauer, 1991
[5] Repeta and Simpson, 1991
[6] Hay *et al.*, 1990
[7] Calvert *et al.*, 1991
[8] Crusius and Anderson, 1992
[9] Benitez and Buesseler, 1992
[10] Calvert *et al.*, 1987

[a] calculated using equs. 1 - 6 provided in text
[b] values extrapolated from sediment phorbin concentrations, and modelled carbon and chlorophyll relationships
[c] values based on extrapolated water column values

and modelled data is not due to remineralization in the water column but either to the sampling sites or to inaccuracies in our mass balance.

For comparison with the model, our measured yearly averaged chlorophyll flux from the upper anoxic water column is available from the present study. This flux is 2.7 $mg/m^2/yr$, and falls below the modelled value of 4.0 - 13 $mg/m^2/yr$ based on the range in primary production from the literature. But as stated previously, the data set from 477 m at BSK2 does not include flux measurements from a spring bloom and our measured average phorbin flux is therefore low.

The model can also be extended into the deep water column. Using measured data from BSK2 and BSK3-1, we calculate the phorbin flux at 1200 m to be within the range of 3.7 - 4.1 $mg/m^2/yr$. This range of values is similar to the measured value at 477 m at BSK2 of 2.7 $mg/m^2/yr$. Based on primary production estimates and the observation in the central basin that the flux of chlorophyll in the shallow and deep anoxic water column is similar, we calculate the deep phorbin flux to be 4.0 - 13 $mg/m^2/yr$. Again, the measured phorbin flux values are similar to the lower limits of the modelled range of chlorophyll flux values.

The basin-wide mass balance of chlorophyll production and flux can be further extended to include sedimentation of chlorophyll and organic carbon. Measurements of Black Sea sediment accumulation rates based on radionuclide measurements range from 35.7 $g/m^2/yr$ (^{14}C; Calvert *et al.* 1991) to 68 $g/m^2/yr$ (^{210}Pb; Benitez and Buesseler, 1992). Sediment accumulation rates determined from varve counting are not considered in this model for reasons previously discussed. The measured range in sedimentary phorbin concentration is 100 - 105 µg/gdw, which when combined with sediment accumulation rates determined from ^{14}C and ^{210}Pb, we calculate a range in phorbin accumulation rate of 3.6 - 7.1 $mg/m^2/yr$. This range in values is similar to both the measured and modelled deep water column phorbin fluxes. As in our May 1988 model, the similarities between the measured phorbin flux and the calculated phorbin accumulation rate suggests that there is little degradation of total phorbin in the anoxic water column or in surface sediments.

In the literature, only one set of estimates of carbon accumulation rates, based on radionuclide studies, appear. Calvert *et al.* (1991) estimate the organic carbon accumulation rate to be between 1.81 - 2.16 $gC/m^2/yr$ from cores collected from each basin of the Black Sea. These values are similar to the upper water column organic carbon flux data of Hay *et al.* (1990), but these organic carbon accumulation rates do not include consideration for the elevated carbon concentrations seen in the surface two centimeters of sediment (Calvert *et al.*, 1991; Lyons, 1992). Studies by Shimkus and Trimonis (1974) and Calvert *et al.* (1987) suggest that sedimentary carbon is between 23 - 33% terrigenous

origin, which gives a marine sedimentary carbon accumulation rate of 1.2 - 1.6 $gC/m^2/yr$. Combined with the phorbin accumulation rate data, these calculated organic carbon accumulation rates give a marine C:chl ratio of 225-330, much lower than the C:chl of 1000 determined by Repeta and Simpson (1991) for the upper anoxic water column, and similar to those calculated previously for the Western basin and central Black Sea. This decrease in C:chl ratio between the upper anoxic water column and surface sediments suggests that total organic carbon is remineralized faster in the Black Sea water column and sediments on average than is total phorbin.

This study represents the first successful attempt to mass balance chlorophyll production with sedimentation. We realize that in a calculation of this type, the errors in using data from many different sources and locations within the Black Sea are large, and that these errors are propagated throughout the calculations. We would like to point out that this mass balance only holds for the Black Sea due to its long anoxic water column and sediments. Under normal marine conditions, chlorophyll degradation products will be remineralized in the water column since it is known that phorbins degrade in the presence of molecular oxygen, and decreases in the concentration of chlorophyll and pheopigments with water depth in oxic environments have been reported (Vernet and Lorenzen, 1987; Furlong and Carpenter, 1988; Downs, 1989).

The effect of sulfate reduction in the water column and surface sediments

Several lines of research in the Black Sea suggest that the major source for TOC loss in through sulfate reduction in surface sediments. Our model suggests that up to 75% of TOC which passes into the anoxic water column will be degraded before it is buried in sediments. Our model also suggests that there is no further loss of total phorbin once phorbin has passed into the anoxic water column. Laboratory studies of ^{14}C labelled chlorophyll-*a* and pheophytin-*a* incubated in sediments under anoxic conditions indicate that chlorophyll-*a* is degraded under anoxic conditions, but at the same time the activity of radiolabelled pheophytin-*a* increased suggesting that chlorophyll-*a* is degraded to pheophytin-*a* (Sun, 1992). In these same experiments, chlorophyll-*a* was also degraded to other unknown colorless components but no loss of ^{14}C was found suggesting that neither chlorophyll-*a* nor pheophytin-*a* were being remineralized under anoxic conditions. Since chlorophyll-*a* represents only 2% of total phorbin measured in our sediment samples, any loss of chlorophyll through degradation to colorless components would be within error of our determinations.

During the 1988 Black Sea expedition, detailed measurements of the concentration of sedimentary organic carbon revealed that there is a surface maximum in TOC which is wide spread over the Black Sea basin (Honjo and Broda, 1988; Calvert *et al.*, 1991; Lyons, 1991). Surface TOC is approximately twice the average Unit I value suggesting that remineralization of total organic carbon is occuring in Black Sea surface sediments. Beier *et al.* (1991) compared the distribution of sterols and fatty acids in sediment traps, sediment floc, and upper 1 cm of sediment (fluff). They found that the relative concentration of reduced compounds is higher in the fluff than in the floc and sediment trap samples. To account for their findings, they suggested that a microbial community lives at the floc/Unit I interface. Microbial mats in surface Black Sea sediments were observed during core collection during the 1988 Black Sea expedition (Honjo and Broda, 1988). Beier *et al.* (1991) did not sample deep enough into the sediment to determine if reduction or organic matter continues below the surface sediment.

Below the chemocline of the Black Sea oxidation of organic carbon occurs by sulfate reduction. The loss of organic carbon in the water column or very surface sediments is demonstrated by the reduction in TOC from 14% in sediment traps to 4% in sediments (Honjo and Broda, 1988). Input of weathered material from resuspension or riverine sources will increase the total sediment accumulation rate and dilute the input of marine organic carbon. Estimates of total organic carbon oxidation by sulfate reduction in the water column and sediments range from 10 - 49 $gC/m^2/yr$ (Deuser, 1971; Lein and Ivanov, 1991). Between 60 and 100 m depth in the water column, Karl and Knauer (1991) found that the organic carbon flux decreased by 110 $mgC/m^2/d$ (but was constant below 110 m). These values were determined for the month of May, but when extended to one year, this decrease in organic carbon flux suggests an average sulfate reduction rate of 40 $gC/m^2/yr$ for the region of the chemocline, similar to the values measured values of sulfate reduction. Our model calculation of organic carbon flux out of the photic zone is greater than the measured values of Hay *et al.* (1990) by up to 11 $gC/m^2/yr$. This difference in values suggests that between 0 - 11 $gC/m^2/yr$ are removed below the oxic zone, which is in agreement with the sulfate reduction rates measured by Lein and Ivanov (1991).

There are two possible explanations for the observed decrease in TOC in the sediment column below the sediment water interface. An increase in input of organic matter to surface sediments would explain this observation. An alternate explanation for the observed decrease in TOC in surface sediments is remineralization of organic carbon in surface sediments through sulfate reduction. Rates of sulfate reduction in Black Sea sediments are 3 - 13 $gC/m^2/yr$ (Vaynshteyn *et al.*, 1985; Lein and Ivanov, 1991). The

difference between the marine carbon accumulation rate calculated in our model from the flux of organic carbon into the upper anoxic water column and the measured marine carbon accumulation rate suggests that 2.4 - 5.5 gC/m2/yr is remineralized in surface sediments. This estimated value of remineralized carbon is low since it does not include the amount of terrigenous carbon which is remineralized. Our modelled organic carbon remineralization rate is similar to the measured sulfate reduction rate in Black Sea sediments (Vaynshteyn *et al.*, 1985; Lein and Ivanov, 1991).

IV. CONCLUSIONS

In the anoxic water column, the total phorbin flux below the chemocline follows the same cycle as does primary production. The individual phorbin identified are pheophorbide-*a*, pyropheophorbide-*a*, chlorophyll-*a*, pheophytin-*a*, and pyropheophytin-*a*. Also identified is a pheophorbide-*a* like compound with nominal molecular weight of 532 a.m.u. Evidence for the existence of high molecular weight and acid extractable chlorophyll degradation products in the water column suggesting that these compounds are formed early in the degradation pathway of chlorophyll. These same phorbins are identified in sediments.

In Black Sea sediments, the chlorophyll degradation products identified spectrophotometrically has been at least partially structurally identified. Solvent extractable sedimentary phorbins consist of free phorbins derived from chlorophylls-*a* and -*b*, phorbin steryl esters, and high molecular weight chlorophyll degradation products. When the phorbin steryl esters, the high molecular weight, and acid extractable fractions are considered, 4 times more sedimentary phorbins can be identified in the Black Sea than by HPLC studies alone. An inventory of chlorophyll degradation products can be established for the Black Sea when all sedimentary sinks for chlorophyll are considered. This inventory can be written as:

$$\text{total} = \text{AEX} + \text{HMW} + \text{PSE} + \text{free phorbins}$$

The recycling of chlorophyll in the photic zone of the Black Sea is highly efficient. Only 0.2% of chlorophyll production can be detected below the chemocline (Repeta and Simpson, 1991). The flux of chlorophyll degradation products leaving the photic zone and surviving the passage through the chemocline varies with primary production. The major compounds found in sediment traps in the anoxic water column are MW532

pyropheophorbide, pyropheophorbide-*a* steryl esters, pheophytin-*a*, and pyropheophytin-*a*. Comparisons of the flux of total phorbin out of the photic zone with the accumulation rate of phorbin suggests that there is very little loss of phorbin during the passage through the anoxic water column. The results of our model study, both for organic carbon and total phorbin flux and accumulation, agree with measured values to within a factor of two.

The results of our work pose many questions. Our results suggest that very little remineralization of phorbins occurs in anoxic waters and further suggests little remineralization of phorbins by bacteria residing at the sediment/water interface occurs, whereas our calculations of organic carbon flux suggests that at the sediment/water interface, significant remineralization of organic carbon does occur. Unfortunately, for this study, only a limited set of samples was available. Before the results of this study can be borne out, multi-year time series studies will have to be done, which include not only detailed phorbin analysis, but also organic carbon analysis, and primary production measurements.

V. REFERENCES

Beier J. A., Wakeham S. G., Pilskaln C. H., and Honjo S. (1991) Enrichment in saturated compounds of Black Sea interfacial sediment. *Nature* **351**, 642-644.

Benitez C. and Buesseler K. (1992) Determination of the sedimentation rate in the Black Sea over the last century using radionuclides. *EOS* **72** (51), 37.

Calvert S. E., Vogel J. S., and Southon J. R. (1987) Carbon accumulation rates and the origin of the Holocene sapropel in the Black Sea. *Geology* **15**, 918-921.

Calvert S. E., Karlin R. E., Toolin L. J., Donahue D. J., Southon J. R., and Vogel J. S. (1991) Low organic carbon accumulation rates in Black Sea Sediments. *Nature* **350**, 692-695.

Conover R. J., Durvasula R., Roy S., and Wang R. (1986) Probable loss of chlorophyll-derived pigments during passage through the gut of zooplankton, and some of the consequences. *Limnol. Oceanogr.* **31**, 878-887.

Crusius J., and Anderson R. F. (1992) Inconsistencies in accumulation rates of Black Sea sediments inferred from Records of Laminae and ^{210}Pb. *Paleoceanography* **7**, 215-227.

Degens E. T., Michaelis W., Garrasi C., Mopper K., Kempe S., and Ittekkot V. A. (1980) Warven-Chronologie und fruhdiagenetische Umsetzungen organischer Substanzen holozaner Sedimente des Schwarzen Meeres. *Neues Jahrb. Geol. Palaeontol. Monatsh.* **5**, 65-86.

Degens E. T. and Ross D. A. (1972) Chronology of the Black Sea over the last 25,000 years. *Chem. Geol.* **10**, 1-16.

Degens E. T., Stoffers P., Colubic S., Dickman M. D. (1978) Varve chronology: Estimated rates of sedimentation in the Black Sea Deep Basin. In: Init. Rep. Deep Sea Drill. Proj.(D. A. Ross *et al.*, eds.). U.S. Gov't Printing Office, 499-508.

Deuser W. G. (1971) Organic-carbon budget of the Black Sea. *Deep-Sea Research* **18**, 995-1004.

Downs J. N. (1989) Implications of the phaeopigment, carbon, and nitrogen content of sinking particles for the origin of export production. Ph.D. thesis, Univ. of Washington, 197 pp.

Furlong E. T. and Carpenter R. (1988) Pigment preservation and remineralization in oxic coastal marine sediments. *Geochim. Cosmochim Acta* **52**, 87-99.

Gouterman M. (1961) Spectra of porphyrins. *J. Mol. Spectrosc.* **6**, 138-163.

Hay B. J. (1987) Particle flux in the western Black Sea in the present and over the last 5,000 years: Temporal variability, sources, transport mechanisms. Ph.D. thesis, WHOI-87-44, 201 pp.

Hay B. J. (1988) Sediment accumulation in the central western Black Sea over the past 5100 years. *Paleoceanogr.* **3**, 491-508.

Hay B. J., Arthur M. A., Dean W. E., Neff E. D., and Honjo S. (1991) Sediment deposition in the late Holocene abyssal Black Sea with climatic an chronological implications. *Deep-Sea Research* **38 suppl. 2**, S1211-S1235.

Hay B. J., Honjo S., Kempe S., Ittekkot V. A., Degens E. T., Konuk T., and Izdar E. (1990) Interannual variability in particle flux in the southwestern Black Sea. *Deep-Sea Research* **37**, 911-928.

Hay B.J., Honjo S., and Konuk T. (1988) Scientific investigations of the water column. Sediment trap work. In: Temporal and Spatial Variability in Sedimentation in the Black Sea: Cruise Report R/V Knorr 134-8, Black Sea Leg 1. WHOI-88-35. 21-30.

Hay B. J. and Honjo S. (1989) Particle deposition in the present and Holocene Black Sea. *Oceanography* **2**, 26-31.

Hayward T. L. and Venrick E. L. (1982) Relation between surface chlorophyll, integrated chlorophyll, and integrated primary production. *Mar. Bio.* **69**, 247-252.

Honjo S. and Broda J. E. (1988) The first recovery of fluff layer from the Black Sea bottom; onboard observation. In: Temporal and Spatial Variability in Sedimentation in the Black Sea: Cruise Report R/V Knorr 134-8, Black Sea Leg 1. WHOI-88-35. 135-140.

Honjo S., Hay B. J., Manganini S. J., Asper V. L., Degens E. T., Kempe S., Ittekkot V., Izdar E., Konuk, Y. T., and Benli H. A. (1987) Seasonal cyclicity of lithogenic particle fluxes at a southern Black Sea sediment trap station. *SCOPE/UNEP Sonderband* **62**, 19-39.

Karl D. M. and Knauer G. A. (1991) Microbial production and particle flux in the upper 350 m of the Black Sea. *Deep-Sea Research* **38 suppl. 2**, S921-S942.

Keely B. J. and Brereton R. G. (1986) Early chlorin diagenesis in a recent aquatic sediment. *Org. Geochem* **10**, 975-980.

Kiorboe T., and Tiselius P. T. (1987) Gut clearance and pigment destruction in a herbivorous copepod, *Acartia tonsa*, and the determination of *in situ* grazing rates. *J. Plankton Res.* **9**, 525-534.

Klein B., Gieskes W. C. C., and Kraay G. G. (1986) Digestion of chlorophylls and carotenoids by the marine protozoan Oxyrrhis marina studied by HPLC analysis of algal pigments, *J Plankton Res*, **8**, 827-836.

King L. L. and Repeta D. J. (1991) Pyropheophorbide steryl esters in Black Sea sediments. *Geochim. Cosmochim. Acta* **55**, 2067-2074.

Lein A. Y. and Ivanov M. V. (1991) On the sulfur and carbon balances in the Black Sea. In: Black Sea Oceanography (E. Izdar and J. W. Murray, ed.) NATO ASI Series, Kluwer Academic Publishers, 307-318.

Lopez M. D. G., Huntley M. E., and Sykes P. F. (1988) Pigment destruction by *Calanus pacificus*: impact on the estimation of water column fluxes. *J. Plank. Res.* **10**, 715-734.

Lorenzen C. J. (1974) Chlorophyll-degradation products in sediments of Black Sea. In: The Black Sea -- Geology, Chemistry, and Biology (E. Degens and D. A. Ross, eds.). *Mem. Am. Assoc. Pet. Geol.* **20**, 426-428.

Lyons T. W. (1991) Upper Holocene sediments of the Black Sea: Summary of leg 4 box cores (1988 Black Sea Oceanographic Expedition). In: Black Sea Oceanography (E. Izdar and J. W. Murray, ed.) NATO ASI Series, Kluwer Academic Publishers, 401-441.

Mayzaud P. and Razouls S. (1992) Degradation of gut pigment during feeding by a subantarctic copepod: Importance of feeding history and digestive acclimation. *Limnol. Oceanogr.* **37**, 393-404.

Pasternak A. F. and Drits A. V. (1988) Possible degradation of chlorophyll-derived pigments during gut passage of herbivorous copepods. *Mar. Ecol. Prog. Ser.* **49**, 187-190.

Peake E., Casagrande J., and Hodgson G. W. (1974) Fatty acids, chlorins, hydrocarbons, sterols, and carotenoids from a Black Sea core. In: The Black Sea -- Geology, Chemistry, and Biology (E. Degens and D. A. Ross, eds.). *Mem. Am. Assoc. Pet. Geol.* **20**, 505-523.

Penry D. L., and Frost B. W. (1991) Chlorophyll *a* degradation by *Calanus pacificus*: Dependence on ingestion rate and digestive acclimation to food resources. *Limnol. Oceanogr.* **36**, 147-159.

Repeta D. J. and Simpson D. J. (1991) The distribution and recycling of chlorophyll, bacteriochlorophyll and carotenoids in the Black Sea. *Deep-Sea Research* **38 suppl. 2**, S969-S984.

Shimkus K. M., and Trimonis E. S. (1974) Modern sedimentation in Black Sea. In: The Black Sea -- Geology, Chemistry, and Biology (E. Degens and D. A. Ross, eds.). *Mem. Am. Assoc. Pet. Geol.* **20**, 249-278.

SooHoo J. B. and Kiefer D. A. (1982) Vertical distribution of phaeopigments -- I. A simple grazing and photooxidative scheme for small particles. *Deep-Sea Research* **29**, 1539-1551.

Sorokin Y. I. (1983) The Black Sea. In: Ecosystems of the world 26 -- Estuaries and Enclosed Seas (B. H. Ketchum, ed.). Elsevier, 253-307.

Sun M.-Y. (1992) Early diagenesis of chloropigments in coastal sediments. Ph.d. dissertaion, State University of New York at Stony Brook.

Vaynshteyn M. B., Tokarev V. B., Shakola V. A., Lein A. Yu, and Ivanov M. V. (1985) The geochemical activity of sulfate-reducing bacteria in sediments in the western part of the Black Sea. *Geokhimiya*, 1032-1044.

Vernet M. and Lorenzen C. J. (1987) The relative abundance of pheophorbide-a and pheophytin-a in temperate marine waters. *Limnol. Oceanogr.* **32**, 352-358.

Welschmeyer N. A. and Lorenzen C. J. (1985) Chlorophyll budgets: Zooplankton grazing and phytoplankton growth in a temperate fjord and the central Pacific gyres. *Limnol. Oceanogr.* **30**, 1-21.

CHAPTER 7

THE DOWN CORE DISTRIBUTION OF CHLOROPHYLL DEGRADATION PRODUCTS IN BLACK SEA SEDIMENTS

CHAPTER 7

THE DOWN CORE DISTRIBUTION OF CHLOROPHYLL DEGRADATION PRODUCTS IN BLACK SEA SEDIMENTS

I. INTRODUCTION

In this thesis, new sinks for chlorophyll degradation products in sediments have been explored. These investigations show that degradation products of chlorophyll may occur in sediments in a number of forms not previously studied, including forms which are solvent extractable high molecular weight, acid extractable, and esterified to sterols. In the previous chapters, we have identified and characterized these sinks in both sediment trap samples and in sediments but have not established the interrelationships between these reservoirs of chlorophyll degradation products. In this paper we present a down core study of the sinks for chlorophyll derived phorbins, explore depth related variations in concentration, and the interrelationships of one degradation product with another. We also relate changes with depth in the total chlorophyll derived phorbin concentration, and in PSE distributions, with changes in the Black Sea environment over time.

Previous studies of sedimentary chlorophyll degradation, both in the Black Sea and elsewhere, have focused on determining the concentrations and identities of those chlorophyll degradation products predicted by Treibs (1936) and more recently by Baker and Louda (1982). Few studies have focused on determining precursor/product relationships in the chlorophyll degradation pathway. In this study, we measure the concentrations and the ratios of concentrations of degradation products of chlorophyll-*a* to examine precursor/product relationships. Except for the conversion of chlorophyll-*a* to pheophytin-*a* (Keely and Brereton, 1986; Sun, 1992), precursor/product relationships based on the increase of product compounds in proportion to the decrease in concentration of the precursor compounds have not been made.

In studies of the early diagenesis of chlorophyll, decreasing concentrations of phorbins are usually found with sediment depth due to the rapid loss of phorbins deposited under oxic conditions (Baker and Louda, 1982; Furlong and Carpenter, 1988). In anoxic depositional environments, the large decrease in phorbin concentration with depth is not found, indicating better preservation of phorbins under anoxic depositional conditions than under oxic conditions (Orr *et al.*, 1958; Swain, 1985; Furlong, 1986; Furlong and Carpenter, 1988; Hurley and Armstrong, 1991; Yacobi *et al.*, 1991). For this reason, we chose the Black Sea, with its anoxic water column and sediments, as the site for this study. The earliest studies of sedimentary chlorophyll degradation in the Black Sea, done as part

of the 1969 R/V *Atlantis II* Black Sea expedition, report the presence of phorbins and porphyrins at all depths. Peak *et al.* (1974) report finding 1.6 mg/gdw of phorbins and porphyrins in surface sediment samples and 2.2 mg/gdw at a depth of 68 cm. The suite of compounds they identified included both pheophytins, pheophorbides, and purpurins. Lorenzen (1974) spectrally measured the phorbin concentrations in Black Sea sediments and found concentrations to increase from approximately 0.5 mg/gdw in Unit I sediments to over 2 mg/gdw in Unit II sediments. In Unit III sediments concentrations dropped to below 50 μg/gdw. The large variations in concentration are suggested by Lorenzen (1974) to reflect variations in productivity, sediment dilution, or nutrient conditions. Changes in each of these variables over time are suggested by the stratigraphy of Black Sea sediments (Ross *et al.*, 1970; Degens and Ross, 1972; Degens and Stoffers, 1980; Calvert *et al*, 1987; Calvert and Fontugne, 1987).

In previous studies of chlorophyll degradation in Black Sea sediments, we report finding steryl esters of pyropheophorbide-*a*, high molecular weight chlorophyll degradation products, and acid extractable chlorophyll degradation products (Chs. 3, 4, and 5), but these studies provide no indication of how the different chlorophyll degradation products relate to one another. By examining the concentration of phorbin in the various chlorophyll degradation product reservoirs down core, we attempt to assess the stability of these compounds under anoxic conditions, and to determine how these compounds correlate with one another. We then use concentration and structural variations in chlorophyll degradation products to examine paleoenvironmental changes in the Black Sea.

Changes in the distribution of PSEs and in C:chl (g organic carbon/g total phorbin) are also explored and related to changes in the Black Sea environment over geological time. Our studies of PSEs (Chs. 3 and 5) suggest that the sterols esterified to pyropheophorbide-a may reflect the distribution of free sterols which passes into the anoxic water column from the photic zone. Changes in the PSE distribution with sediment depth may indicate changes in the composition of the phytoplankton community over time. Fluctuations in the ratio of C:chl with sediment depth may indicate changes in the preservation potential of phorbin relative to total organic carbon. We have shown previously (Ch. 6) that the flux of phorbin in the anoxic water column is approximately equal to the phorbin accumulation rate in sediments, whereas only 25% of the total organic carbon flux is preserved in sediments. Increases in bottom water oxygenation may enhance degradation of phorbin relative to total organic carbon.

In this study, samples from three stratigraphic sedimentary units (Unites I, II, and III) taken from a gravity core collected from the central Black Sea are analyzed. Each sedimentary unit, as defined by Degens and Ross (1972), represents deposition under

different environmental conditions. Unit III, the deepest unit analyzed in the study, was deposited during the last glaciation while the Black Sea was lacustrine. Unit II, a sapropel, was deposited during the transition of the Black Sea from lacustrine to marine conditions, and Unit I, which is currently accumulating, is deposited under full marine conditions. In each sedimentary unit the distribution of chlorophyll degradation products is different and can be related to the environmental conditions under which the sediment accumulated.

II. METHODS

A. SAMPLING

Samples of Black Sea sediment were taken from giant gravity core GGC68 (42°49.21'N, 34°00.30'E; Fig. 7-1) collected during Leg 8 (April 16 - May 7) of the 1988 Black Sea Expedition R/V *Knorr* cruise #134-8 (Arthur *et al.*, 1988). The core was sealed and stored in the core liner at 4°C until it was split in August, 1992, after which it was X-rayed, sectioned, and frozen at -30°C. The absence of iron oxide deposits on the top and outer sediment surfaces of the core suggests that it was sealed in a manner which prevented oxidation of the core. Twelve samples were removed from the core using a #12 cork borer inserted laterally through the core. The samples were placed in centrifuge tubes, weighed, and frozen at -30°C until extracted for analysis. The samples were taken from three the stratigraphic units (Units I, II, and III) found in Black Sea sediments which are represented in core GGC68.

Initial analysis were performed on sample BS2-0-10 taken from Box Core 2 Station 2 (Ch. 3; 42°51'N, 31°57'E; water depth of 2129 m).

B. ANALYSIS

Samples were analyzed according to the scheme outlined in Fig. 7-2. Prior to extraction, samples were allowed to thaw 1 hour in reduced light, and approximately 2 g of sediment was removed for total organic carbon (TOC) analysis. Samples were sonically extracted with 3 x 25 mL acetone and 1 x 25 mL CH_2Cl_2. After sonication, samples were centrifuged, and the solvent decanted. The organic extracts were combined, rotary evaporated, and partitioned between water and 30% hexane/diethyl ether. The aqueous phase was extracted twice more with hexane/diethyl ether, and the organic phases combined and dried over Na_2SO_4. The solvent was then evaporated. The sample was diluted with 100% acetone (100 - 250 mL depending on color) and the visible spectrum

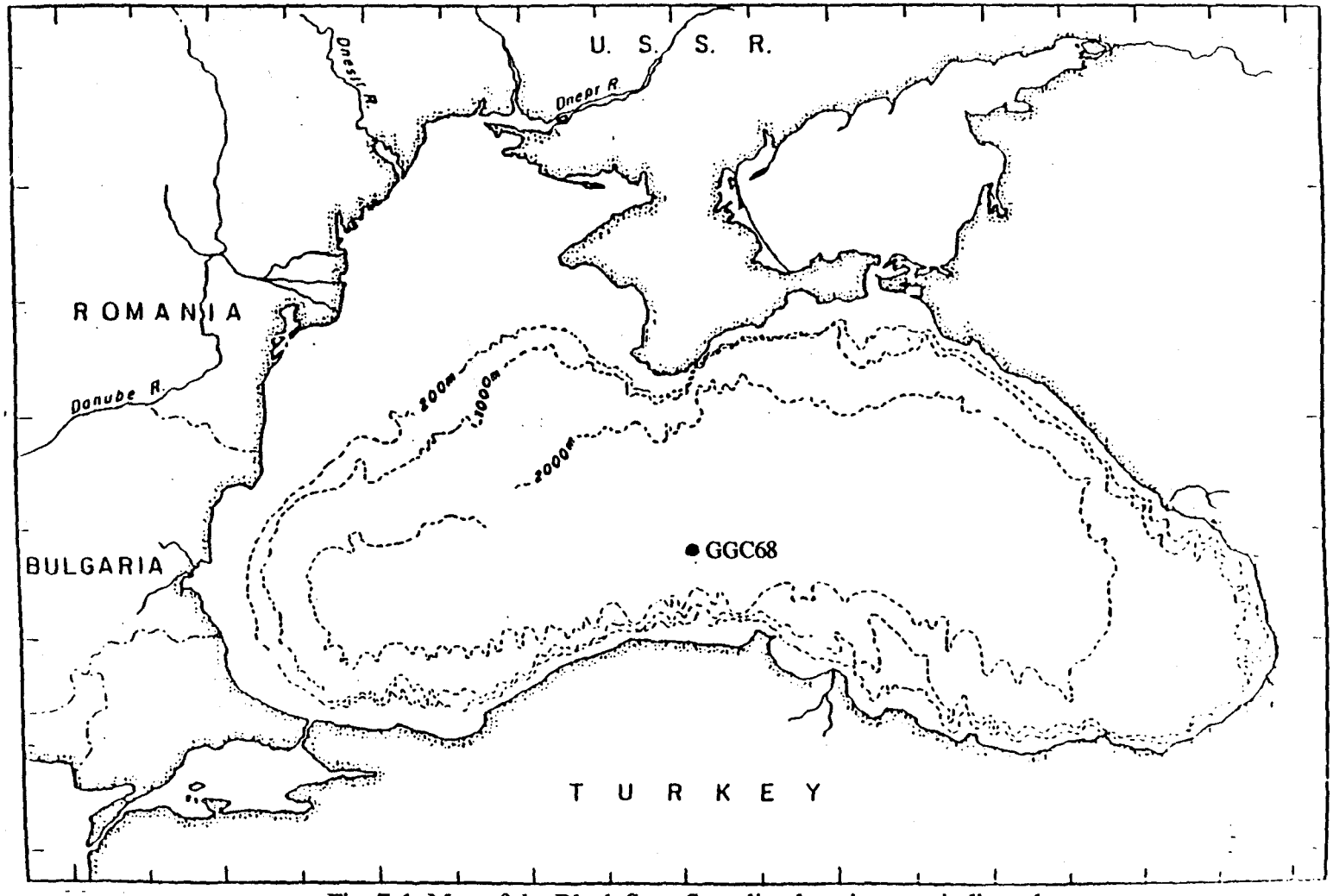

Fig. 7-1 Map of the Black Sea. Sampling locations are indicated.
(Ross *et al.*, 1974)

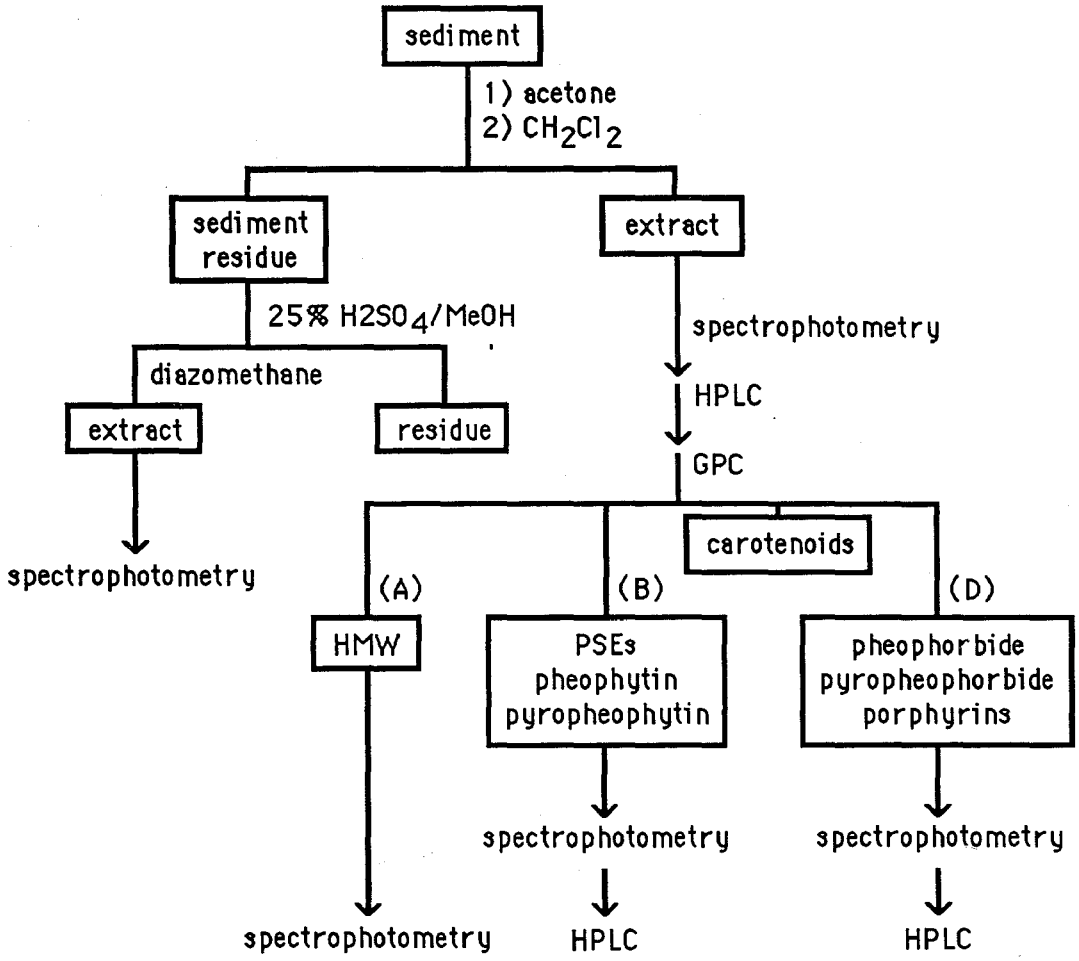

Fig. 7-2 Separation scheme used to analyze sediment samples from core GGC68.

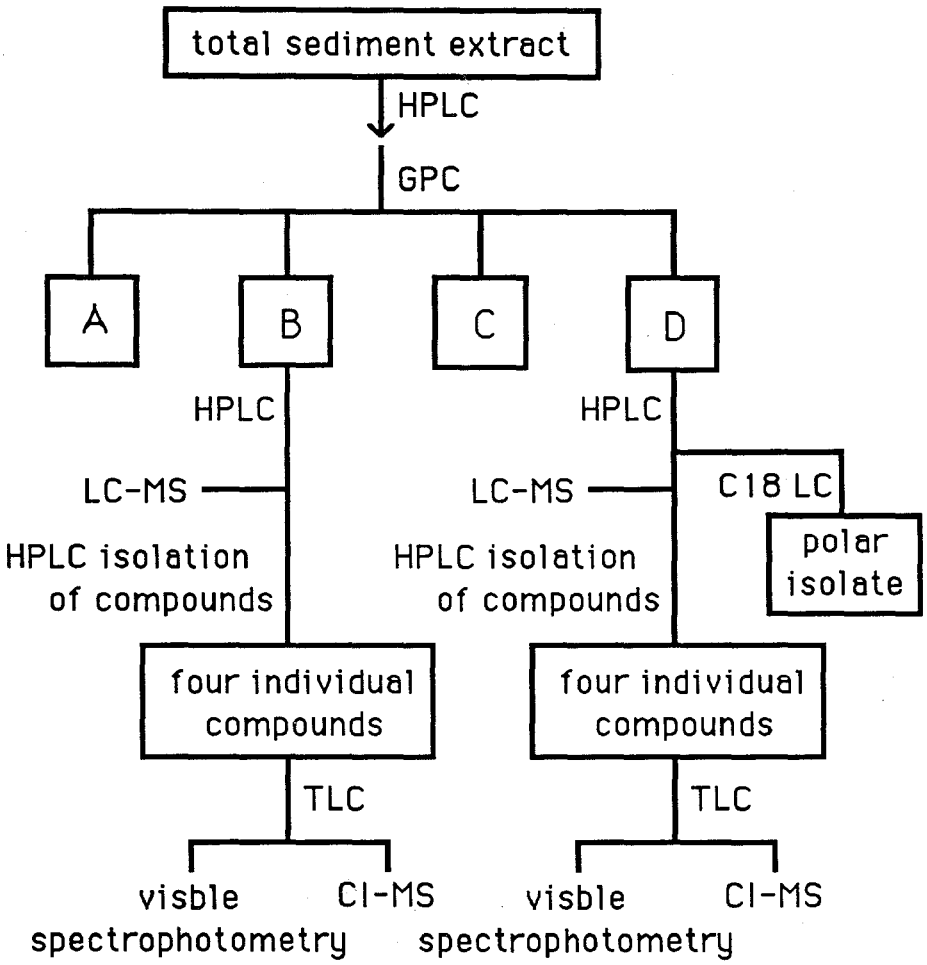

Fig. 7-3 Scheme used in identifying the free phorbins in the total organic extract of sediment sample BS2-0-10.

measured from 350 - 750 nm on a Hewlett-Packard diode array spectrometer referenced to 100% acetone. The concentration of phorbin-like pigments was determined at 665 nm, after background correction, using an extinction coefficient of 5×10^4 L/mol·cm.

Each sample was further analyzed for non-solvent extractable chlorophyll degradation products, as described in Ch. 4, using 2 g solvent extracted sediment, 15 mL MeOH, and 2 mL concd H_2SO_4. The organic residue from the extraction was made up to a known volume with acetone (5 - 10 mL depending on color), and the concentration of phorbin was determined from the visible absorbance at 665 nm after base-line correction.

C. CHROMATOGRAPHY

Total organic extracts were analyzed by reversed-phase high pressure liquid chromatography (HPLC). The HPLC method used was a 30 minute linear gradient from 100% A to 100% B followed by 60 min of isocratic B, where A is 20/80 (v/v) 0.5N $NH_4CH_3CO_2$ (aq)/MeOH and B is 20/80 (v/v) *n*-PrOH/MeOH. A 15 cm 3µ Alltech C_{18} Absorbosphere column was used at a flow rate of 1.5 mL/minute.. Detection was by fluorescence (Hitachi F1000 fluorescence detector) at 685 nm with excitation at 415 nm and by absorbance (Waters 440 visible absorption detector) at 435 nm.

Individual compounds eluting in the HPLC chromatograms of the total extract were identified according to the scheme outlined in Fig. 7-3. Total extracts from sample BS2-0-10 were used to characterize the individual phorbins in surface Black Sea sediments. Seven phorbins were identified by coelution with authentic compounds, off line CI-MS, and LC-MS: chlorophyll-*a*, pheophytin-*a*, pyropheophytin-*a*, pheophorbide-*a*, pyropheophorbide-*a*, pheophytin-*b*, and pyropheophytin-*b*. Chlorophyll-*a*', pheophytin-*a*', pheophorbide-*a*', and pheophytin-*b*' were also identified. The conditions for LC-MS were those used by Eckardt *et al.* (1991). Briefly, a Waters 600 Silk Quaternary HPLC system was used with a Finnigan MAT TSQ 70 Quadrupole mass spectrometer. The interface used was a Finnigan MAT TSP-2 thermospray. Chromatography was performed on 2 Waters Nova-Pak C_{18} cartridge columns using a ternary solvent system involving acetone, MeOH, and H_2O. Quantification of phorbins in total organic extracts of samples from BS2-0-10, and core GGC68 was performed by HPLC using calibration curves constructed from multiple HPLC analyses of authentic compounds (for synthesis and purification see Ch. 2).

Samples BS2-0-10, GGC68-1, GGC68-3, GGC68-5, GGC68-7, GGC68-9, and GGC68-11 were analyzed by gel permeation chromatography according to the method described in Ch. 4. Four fractions were collected: fraction **A** contained the HMW fraction described in Ch. 4; fraction **B**, pheophytins, pyropheophytins, and PSEs; fraction **C**,

carotenoids; and fraction **D**, pheophorbides, pyropheophorbides, chlorophylls, and unknown polar compounds.

In analyzing the total sediment extract of BS2-0-10, HPLC analysis was also performed using a Waters 990 diode-array detector set to measure the spectra of eluting compounds between 300 - 750 nm. Compounds with spectral characteristics similar to those of porphyrins were detected in the first 10 min of the analysis. In order to gather good visible spectra, it was necessary to concentrate this polar fraction. The porphyrin-like compounds were isolated from the total organic extract by low pressure reversed-phase column chromatography. A 1 cm flash column, fitted with a pyrex wool plug and a sand layer, was dry packed with 1.4 g of octadecylsilyl bonded silica (ODS) (C_{18} Sep-Paks, Waters Assoc.) and flushed with 20% H_2O/MeOH (v/v). The sample was dissolved in 0.5 mL 20% H_2O/MeOH by placing the sample vial in a 30°C water bath for approximately 30 sec. The sample was placed on the column and the porphyrin-like compounds were eluted with 36 mL 20% H_2O/MeOH. The remaining pigment was eluted from the column with 100% acetone. The porphyrin isolate was analyzed by HPLC using the conditions previously described.

D. TOTAL ORGANIC CARBON ANALYSIS

Total organic carbon analysis was performed on each sediment sample using a variation of the method of Krom and Berner (1983). Approximately 2 g of each sediment sample were dried at 60°C for three days. The sediment was then ground in a mortar and pestle, and three 100 mg aliquots of each sample were weighed into vials which had been combusted at 450°C overnight. These samples were then combusted overnight at 450°C, and the weight loss determined. Approximately 10 mg of each of the combusted samples and triplicates of the uncombusted samples were then analyzed on a Perken-Elmer 4500 CHN analyzer for total inorganic carbon and total carbon, respectively. The concentrations of inorganic carbon were corrected for weight loss which occured during the combustion process. Total organic carbon content was determined from the difference of the total carbon and total inorganic carbon determinations. Calcium carbonate content was calculated from the total inorganic carbon content assuming 100% of the inorganic carbon was in the form of $CaCO_3$.

II. RESULTS AND DISCUSSION

A. IDENTIFICATION OF PHORBINS IN SAMPLE BS2-0-10

Using the total solvent extract of BS2-0-10, phorbins eluting in gel fractions **B** and **D** were identified. Initial identifications were made by coelution with authentic compounds on HPLC. Using HPLC coelution pheophytin-*a*, pheophytin-*a*', pheophytin-*b*, pheophytin-*b*', pyropheophytin-*a*, and pyropheophytin-*b* were identified in gel fraction **B**, and pheophorbide-*a*, pheophorbide-*a*', pyropheophorbide-*a*, chlorophyll-*a*, and chlorophyll-*a*' were identified in gel fraction **D**. Each of the identified compounds, along with one additional unidentified compound occuring in fraction **D** which did not coelute with any known compound, was isolated from the gel fractions using HPLC. These compounds were further purified by TLC (Ch. 2) and analyzed by CI-MS using the procedure given in Ch. 2. The identities of pheophorbide-*a*, pyropheophorbide-*a*, pheophytin-*a*, and pyropheophytin-*a* were confirmed by comparison of their mass spectra with mass spectra of authentic compounds. The compounds identified as pheophytin-*b*, pyropheophytin-*b*, and chlorophyll-*a* did not give good mass spectra. The identities of pheophytin-*b*, pyropheophytin-*b*, and chlorophyll-*a* were confirmed by mass spectra and visible spectra obtained using LC-MS in conjunction with a diode-array detector. This method was also used to further confirm the identities of the chlorophyll-*a*, pheophytin-*a*, pyropheophytin-*a*, pheophorbide-*a*, and pyropheophorbide-*a*. Phorbins in extracts from core GGC68 were identified by comparing HPLC retention times of pigments with those of the identified peaks in BS2-0-10 and with authentic compounds analyzed periodically throughout the analysis of the core.

The unknown compound isolated from gel fraction **D** eluted at 17 minute by HPLC, just prior to pyropheophorbide-a. From CI-MS and visible spectrophotometry (Fig. 7-4), this compound was determined to be a pyropheophorbide-*a*-like phorbin with nominal molecular weight of 532 a.m.u. (referred to as MW532 pyropheophorbide), 2 a.m.u. less than pyropheophorbide-*a*. The visible spectrum of this compound is identical with that of pheophorbide-*a*, but by HPLC, this compound does not coelute with either pheophorbide-*a* or pyropheophorbide-*a*. MW532 pyropheophorbide is not divinyl pyropheophorbide-*a*, since the Soret band in the visible spectrum of divinyl pyropheophorbide-*a* experience a bathochromic shift of 10 nm relative to pyropheophorbide-*a* (Georicke and Repeta, 1992), and it does not co-elute with divinyl pyropheophorbide-*a*. We suggest this compound may be pyropheophorbide-*a* but with a 7a-7b double bond. The presence of this compound in sediments and sediment traps (Ch. 6) suggests that the methods currently employed to screen water column phytoplankton,

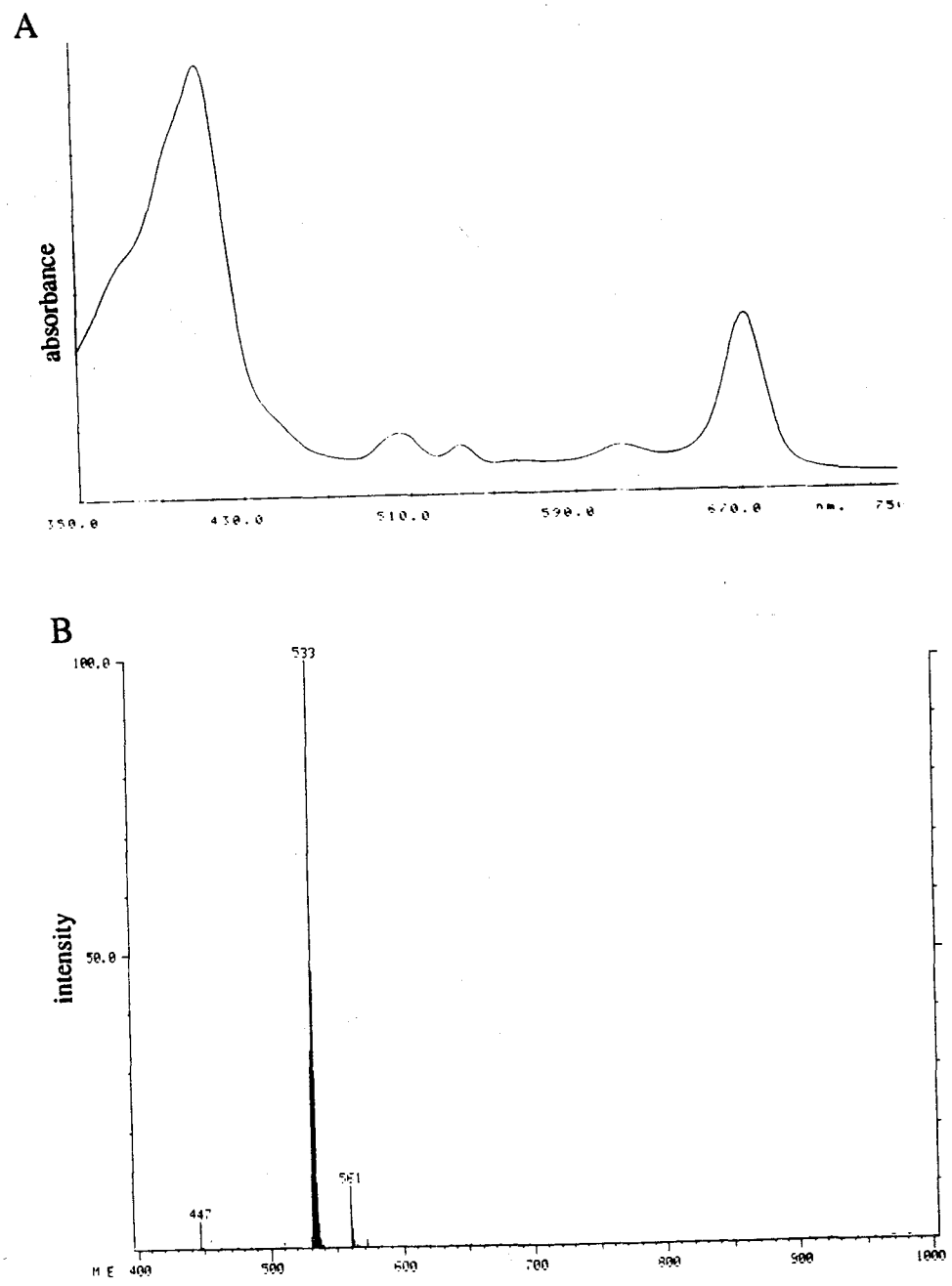

Fig. 7-4 (a) Visible spectra in 100% acetone and (b) chemical ionization-MS of the unknown pheophorbide identified as MW532 pyropheophorbide-*a*.

Table 7-1

VISIBLE SPECTROMETRIC PROPERTIES OF PORPHYRIN ISOLATE ON HPLC

	visible spectrum			solvent composition	
Rt (min.)	Soret (nm)	red (nm)*	S/R	% aqueous+	% acetone+
2.3	395	665	4.0	18.5	1.5
2.5	400	670	8.3	18.3	1.7
2.7	405 (545)	700	5.3	18.2	1.8
3.1	400	660	7.4	17.9	2.1
3.4	400	660	3.5	17.7	2.3
3.5	380	660	5.6	17.6	2.4
3.8	395	700	14.5	17.5	2.5
4.2	400	665	3.5	17.2	2.8
4.7	395	665	5.9	16.9	3.1
5.2	400	660	40	16.5	3.5
5.8	410	700	6.7	16.1	3.9
6.6	400	660	4.3	15.6	4.4
7.6	410			14.9	5.1
9.8	360	670		13.5	6.5
11.3	420			12.5	7.5

*When the concentration of the compound is low, the absorption intensity of the red band may be below detection limits.

+The sum of acetone and 0.5N NH4OAc(aq) in the solution is 20% with the remaining 80% being MeOH.

and sediment samples for pigments may not adequately separate the pigment mixture. The presence of this compound in these samples may suggest that there may be an as yet unidentified chlorophyll synthesized by phytoplankton

In the most polar region of the HPLC chromatogram, before the elution of pbd-*a*, the compounds which comprise the porphyrin isolate elute as a series of peaks which are not well resolved. Based on these elution characteristics, this series of compounds is classified as being polar in nature. As a group, these compounds comprised only 3 - 5% of the pigment determined at 665 nm, and therefore it was necessary to separate them from the rest of the organic extract in order to analyze sufficient quantities by HPLC to gather quality visible spectrophotometric data using the photo-diode array detector. The polar nature of these compounds made it possible, using column chromatography, to elute them as a

concentrated fraction from a large sample of extract, separate from the other pigments except for a slight overlap with pbd-*a*.

Once concentrated, 15 compounds were partially resolved by HPLC. The visible spectra of these compounds suggests that seven are porphyrins (Table 7-1). The Soret bands of the 15 polar compounds identified by HPLC have λ_{max} between 360 and 420 nm. The red band λ_{max} of these 15 compounds vary between 660 and 700 nm, and the ratio of the absorbance intensity of the Soret and red bands (S/R) varies between 3.5 and 15. Based on compilations of S/R ratios of porphyrins, chlorins, and phorbins, compounds with S/R between 1 and 5 have a ring IV with only one unsaturation and are therefore chlorins or phorbins, and S/R ratios greater than 5 are indicative of complete aromatization of the macrocycle (Baker and Louda, 1986). Based on the S/R ratios, 7 of the 15 compounds are porphyrins.

Some structural characteristics of the compounds in the polar isolate may be suggested. Pheophorbide-*a* elutes under the HPLC conditions used in this study at 16.5 minute. For this series of compounds to be more polar than pbd-*a*, it is likely that they have two carboxylic acid groups, or like chl-*c*, which elutes at 7 min, are metallated porphyrins.

In sediment samples BS2-0-10 and BS2-13-18,we expected to see degradation products of chlorophyll-*c* and bacteriochlorophyll-*e*, two compounds which have been identified previously in sediment trap samples (Repeta *et al.*, 1989), but we were unable to detect either of these compounds or their degradation products. Im sediments, Repeta (unpublished) has identified isorenieratene, a carotenoid synthesized by photosynthetic bacteria, suggesting that photosynthetic bacteria are contributing to the organic carbon in Black Sea sediments. Total sediment extracts were analyzed by HPLC using a diode-array detector. Authentic bacteriochlorophyll-e isolated from anoxic Salt Pond sediments and the pheophytins derived from bacteriochlorophyll-*e* were also analyzed by HPLC with diode-array detection. No pigments which coelute with bacteriochlorophyll-*e* were identified in the total sediment extract of Black Sea sediments. The mass balance created in Ch. 6 indicates that the phorbin flux in the anoxic water column equals the phorbin accumulation rate suggesting that very little remineralization of phorbin is occuring in the water column and surface sediments. Bacteriochlorophyll-*e*, also a dihydroporphyrin like chlorophyll-*a*, possesses a methyl group on the δ meso carbon. This may render the bacteriochlorophyll-*e* macrocycle more accessible to cleavage than the chlorophyll-*a* macrocycle.

An alternate explanation for the lack of bacteriochlorophyll-*e* and chlorophyll-*c* in sediment samples may be that these compounds occur in concentrations which are below

the detection limits of the diode-array HPLC detector. In the sediment sample BS2-0-10, the input of bacteriochlorophyll-*e* to the sediment may be low due to movement of the chemocline since bacteriochlorophyll will only be produced when the chemocline intersects the photic zone. When the sediment samples are analyzed using an HPLC fluorescence detector, which has detection limits approximately an order of magnitude lower than the diode-array detector, neither bacteriochlorophyll-*e* nor chlorophyll-*c* would be detected under the conditions used in our analysis. The fluorescence detector used has 10 nm excitation and emission band widths which were centered on 415 nm and 685 nm respectively. Bacteriochlorophyll-*e* and chlorophyll-*c*, have Soret maxima at 463 nm and 442 nm and red bands at 652 nm and 628 nm respectively, rendering our fluorescence detection system insensitive for chlorophyll-*c* and bacteriochlorophylls-*e*. Due to limited sample size, sediment trap samples were only analyzed using the HPLC fluorescence detection system; therefore, we could not identify these compounds in these samples. Bacteriochlorophyll-*e* will only be produced when the chemocline intersects the photic zone.

B. DESCRIPTION OF CORE GGC68

Black Sea sediments are characterized by having distinct stratigraphic units which can be traced throughout the basin. Units I and II were deposited after the termination of the last glaciation, and Unit III was deposited under glacial conditions. Unit I sediments are a laminated calcareous ooze. These sediments contain 2 - 6% total organic carbon (TOC) and up to 40% calcium carbonate (Ross *et al.*, 1970, Ross and Degens, 1974; Calvert *et al.*, 1987) in the form of tests of the coccolithophore *E. huxleyi* (Bukry *et al.*, 1970). Below this sequence is Unit II, a finely laminated sapropel with up to 25% TOC (Ross and Degens, 1974) and 5% calcium carbonate. The calcium carbonate in this sequence occurs in the form of aragonite, and in Unit II, the tests of *E. huxleyi* only appear at the top of the sequence. Both Unit I and Unit II sediments were deposited under marine conditions and the salinity of the Black Sea was greater during deposition of Unit I than Unit II (Calvert *et al.*, 1987; Hay, 1988). Unit III is a typical fresh water sediment, deposited while the Black Sea was isolated from the ocean during the last period of low sea level (Ross and Degens, 1974). This sequence consists of light and dark facies with coarse and fine grained layers, has TOC of approximately 1%, and 10 - 30% calcium carbonate (Ross and Degens, 1974; Calvert, *et al.* 1987).

Core GGC68 is a 346 cm long gravity core (Fig. 7-5; Table 7-2) collected from the central basin of the Black Sea. The upper 7 cm of the core were disturbed. The upper 1.5 cm of the disturbed portion consist of turbidite and the remaining 5.5 cm consist of

Table 7-2

SEDIMENT SAMPLES FROM CORE GGC68

sample	depth (cm)	dry wt (g)	%TOC	sequence	description
GGC68-1	3.0	4.55	4.8	Unit I	laminated immediately below turbidite in disturbed sequence of core top
GGC68-2	27.0	4.42	8.3	transition sapropel - Unit II	wide dark bands in undisturbed finely laminated sequence
GGC68-3	36.5	4.97	8.8	Unit II	fine laminated bands
GGC68-4	46.0	4.85	14	Unit II	wide, dark laminations in undisturbed laminated sequence
GGC68-5	56.2	3.81	14	Unit II	wide, dark laminations in undisturbed laminated sequence
GGC68-6	182.5	8.60	1.4	turbidite	light grey turbidite
GGC68-7	251.8	6.08	2.4	Unit III	dark grey homogeneous
GGC68-8	270.0	7.45	1.2	Unit III	dark grey homogeneous
GGC68-9	276.0	6.22	1.2	Unit III	black, finely laminated
GGC68-10	313.0	6.94	2.0	Unit III	finely laminated sediments
GGC68-11	332.0	7.41	1.2	Unit III	bioturbated
GGC68-12	343.5	7.88	1.3	Unit III	grey homogeneous

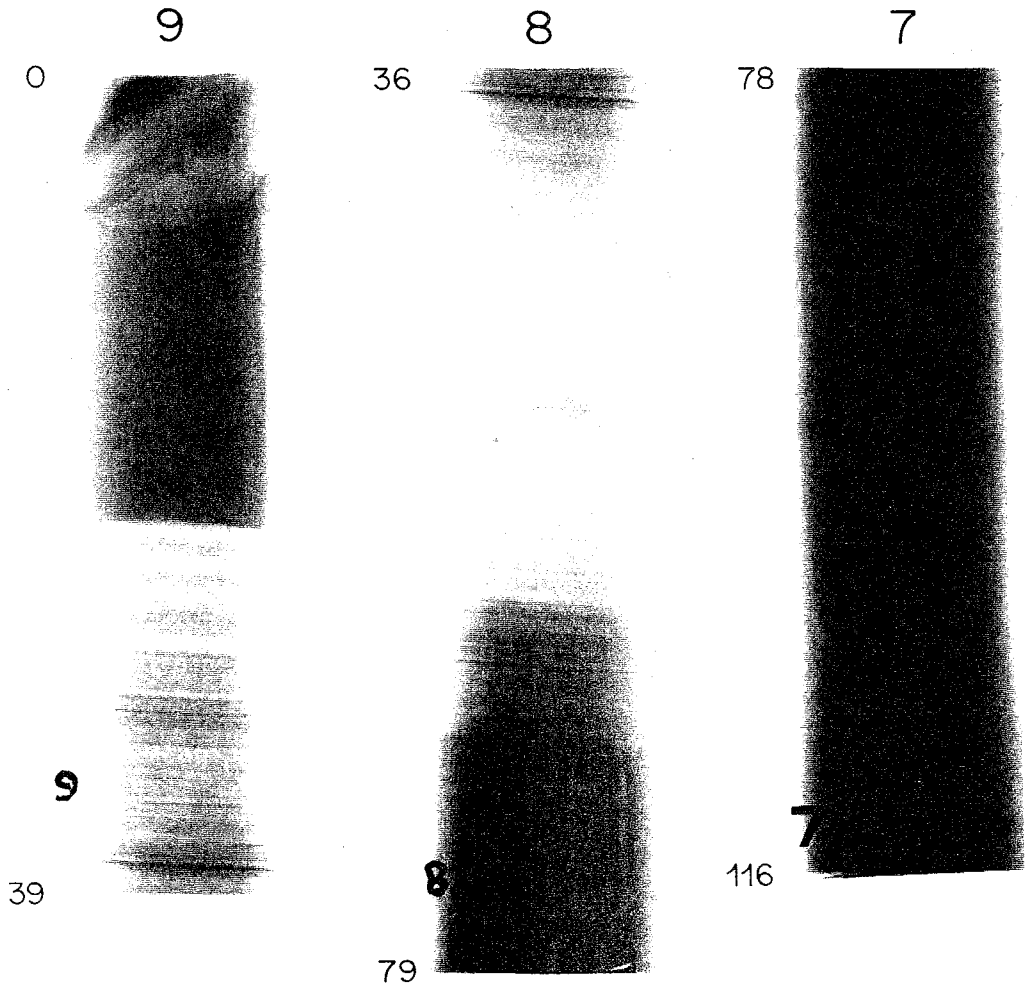

Fig. 7-5 x-radiographs of core GGC68. Section 9 represents the upper most core section of core with section 1 at the bottom. The core is measured from 0 cm at the surface to 342 cm at the base of section 1.

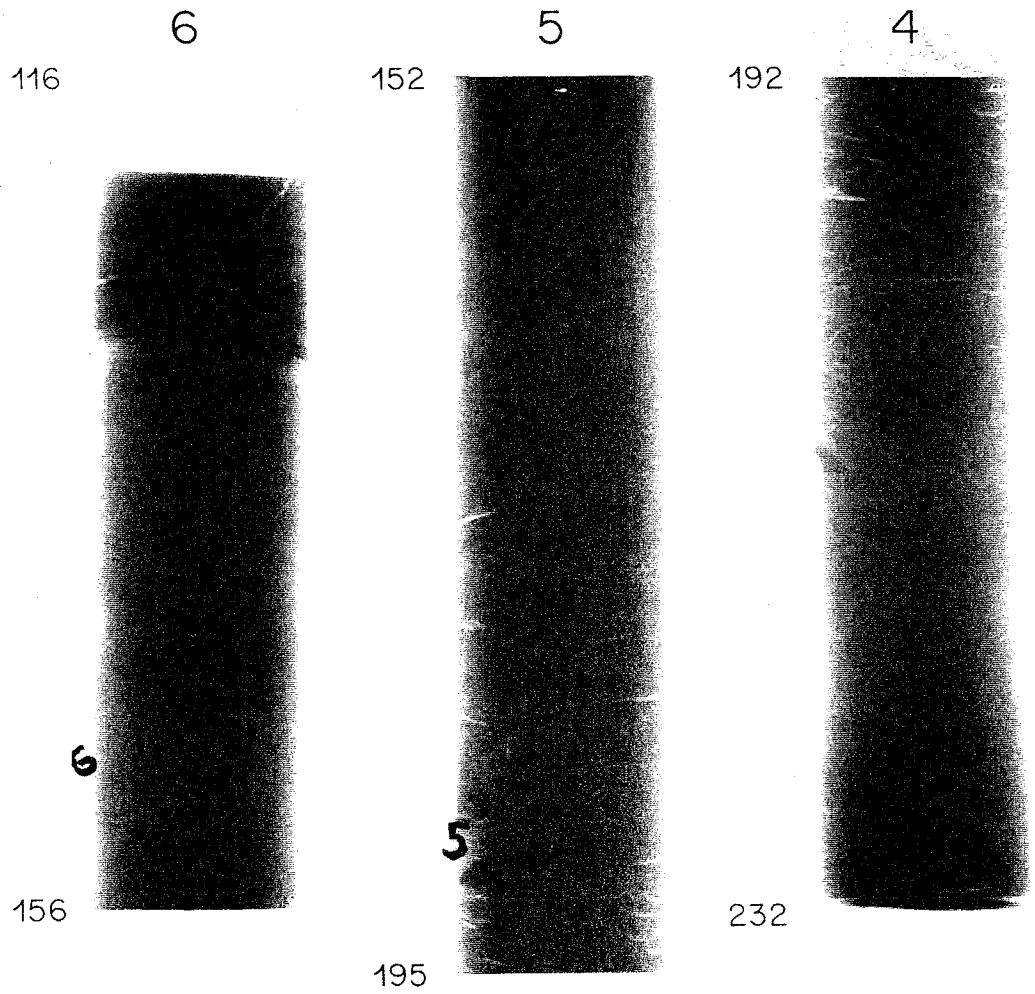

Fig. 7-5 continued.

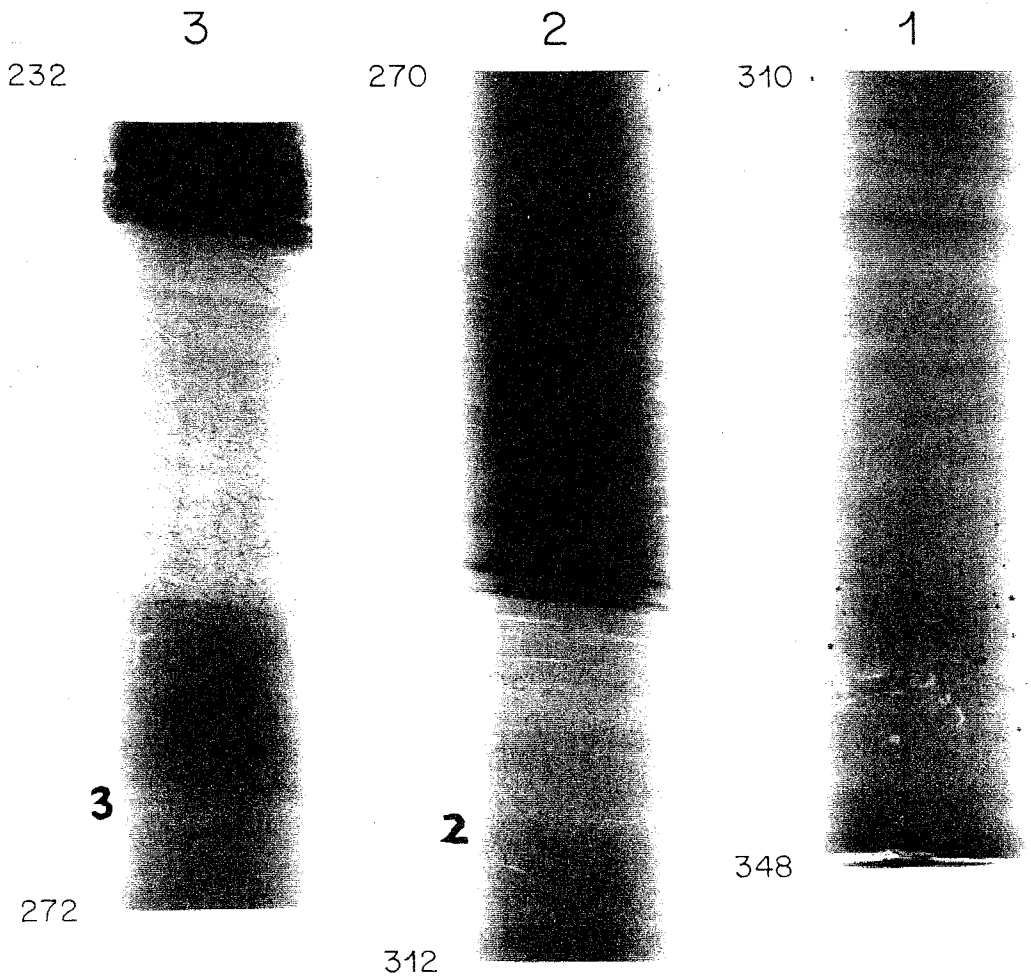

Fig. 7-5 continued.

laminated sediment typical of Unit I. This is the only portion of Unit I recovered in this core. Unit I was also lost in a gravity core collected from nearby, GGC66 (Arthur *et al.*, 1988). The 15 cm below the disturbed layer are turbidite. At 22 cm depth, the finely laminated, high organic carbon sequence typical of Unit II in Black Sea cores begins. The three wide calcium carbonate rich bands at the top of this sequence mark the onset of Unit II, the Holocene Black Sea sapropel. At 68 cm is the beginning of a turbidite which extends down to 240 cm. Below this turbidite is another, lighter colored turbidite, approximately 20 cm in length, which exhibits characteristics of bioturbation. Another, darker turbidite, of approximately 10 cm in length, is embedded in this core beneath the light-colored turbidite. From 240 cm to the bottom of the core is a sediment sequence characteristic of Unit III Black Sea sediments. Interbedded in this sequence are additional turbidites. A turbidite appears at 278 cm and runs to 294 cm. A sequence of interbedded Unit III and turbidite runs from 294 to 320 cm with Unit III running from 320 cm to the bottom of the core at 348 cm.

C. CHLOROPHYLL DEGRADATION PRODUCTS IN CORE GGC68

In sediments deposited under anoxic conditions, preservation of phorbins is generally greater than in sediments deposited under oxic conditions (Orr *et al.*, 1958; Swain, 1985; Furlong, 1986; Furlong and Carpenter, 1988; Hurley and Armstrong, 1991; Yacobi *et al.*, 1991). In sediment with oxic depositional conditions, the concentration of phorbins is seen to decrease rapidly with depth (Orr, 1958; Furlong and Carpenter, 1988). In the present study, we see good preservation of phorbins to sediment depths of 60 cm. Below this depth, the deposition of sediment occurred from an oxic water column, and preservation of total phorbin decreases. The decrease in preservation is suggested by the 100 fold decline in phorbin concentration, and the order of magnitude increase in the C:chl ratio (discussed in detail below). Part of the concentration decrease, and therefore part of the C:chl increase, may be due to a decrease in input.

The concentration of total phorbin was determined in each of the twelve samples from GGC68 by summing the total organic solvent extractable and acid extractable phorbins (Fig. 7-7a). In samples from Unit I and Unit II (GGC68-1 to GGC68-5), total phorbin ranged from 130 nmol/gdw at 3.0 cm to 420 nmol/gdw at 56.2 cm. Phorbin concentrations in the turbidite and Unit III (GGC68-6 to GGC68-12) ranged between 4.2 nmol/gdw at 343.5 cm and 29 nmol/gdw at 251.8 cm. In previous studies of total solvent extractable phorbin in Unit I and Unit II sediments, total phorbin was found to vary between 600 nmol/gdw and 4000 nmol/gdw, and in Unit III total phorbin averaged 400 nmol/gdw (Lorenzen, 1974). Background correction of spectra presented by Lorenzen

(1974) suggests that the actual phorbin concentrations in his samples are up to 40% too high. Lowering Lorenzen's phorbin concentrations by 40% brings his lowest concentrations into range of the upper limits of our data, though our data also include the contribution of acid extractable chlorophyll degradation products whereas Lorenzen's (1974) does not. The lower values found in the present study may be attributed to differences in the locations from which the cores were taken (Lorenzen's core was from the Eastern Basin, ours is from the central basin) since concentration measurements are effected by variations in total sediment accumulation rate, as well as to the inclusion of background correction in our quantitation method.

The chlorophyll-*a* derived phorbins identified in this core were pheophytin-*a*, pyropheophytin-*a*, pheophorbide-*a*, pyropheophorbide-*a*, and chlorophyll-*a*. Also identified was MW532 pyropheophorbide. The concentrations of these compounds vary down core, with the largest variations occuring in the upper 60 cm. Phorbin concentrations in Units I and II are much greater than in the turbidite and in Unit III. In Units I and II, the concentrations of pheophytin-*a* and pyropheophytin-*a* (Fig. 7-6b) increase from 17 nmol/gdw and 26 nmol/gdw, respectively, at 3.0 cm to maxima of 32 nmol/gdw and 61 nmol/gdw, at 27.0 cm, before decreasing to 9.7 and 31 nmol/gdw at 46 cm. The concentrations then increase to 22 nmol/gdw and 64 nmol/gdw, respectively at the bottom of Unit II. The concentrations of pheophorbide-*a* and MW532 pyropheophorbide-*a* (Fig. 7-6c) increase slowly from the sediment surface to 36.5 cm and 27.0 cm, respectively, before sharply increasing to maxima of 6.5 nmol/gdw and 13 nmol/gdw at depths of 46.0 cm and 36.5 cm respectively. The sum of the concentrations of the five chlorophyll-*a* derived free phorbins decreases between 36.5 and 46.0 cm (GGC68-3 and GGC68-4). In this interval, the concentrations of chlorophyll-*a*, pheophytin-*a*, pyropheophytin-*a*, and pyropheophorbide-*a* decrease, but the concentration of pheophorbide-*a* increases.

The lower seven samples from core GGC68 are from sequences of turbidite and Unit III. In sample GGC68-6, from a depth of 182.5 cm, the concentration of total phorbin decreases to 6.2 nmol/gdw (Fig. 7-6a). In this sample, chlorophyll-*a* was not detectable, and chlorophyll-*a* was not found in any sample from deeper within the core. All chlorophyll degradation products, including total phorbin, are more concentrated in sample GGC68-7 than in GGC68-6. The concentration of all phorbins then decrease in sample GGC68-8 and remain constant to the bottom of the core. Pyropheophytin-*a* continues to be the most abundant pheopigment in the lower 7 samples as it is in the five samples from Units I and II, with pheophorbide-*a* being the least abundant phorbin (Fig. 7-6b and 7-11).

Variations in input of individual pheopigments remove trends in concentration caused by the degradation of one pheopigment to another. To remove the effect of input

Table 7-3

CONCENTRATION OF CHLOROPHYLL DEGRADATION PRODUCTS IN CORE GGC68

sample designation	sample depth	concentration (nmol/gdw) total phorbin	HMW	AEX	chl-a	ptn-a	pptn-a	pbd-a	ppbd-a	PSE	MW532
GGC68-1	3.0	1.3E+02	2.4E+01	3.2E+01	5.5E+00	1.7E+01	2.6E+01	6.6E-01	1.7E+01	5.00E+01	7.2E+00
GGC68-2	27.0	2.6E+02	n.d.	4.3E+01	1.3E+01	3.2E+01	6.1E+01	1.1E+00	1.9E+01	1.2E+02	7.7E+00
GGC68-3	36.5	2.4E+02	5.9E+01	3.9E+01	6.6E+00	1.8E+01	5.2E+01	1.6E+00	1.1E+01	8.6E+01	1.3E+01
GGC68-4	46.0	2.4E+02	n.d.	2.7E+01	5.5E+00	9.7E+00	3.1E+01	6.5E+00	1.5E+01	3.7E+01	6.7E+00
GGC68-5	56.2	4.2E+02	1.7E+02	3.2E+01	1.4E+01	2.2E+01	6.4E+01	3.5E+00	1.9E+01	5.4E+01	6.0E+00
GGC68-6	182.5	6.2E+00	n.d.	1.5E+00	0.0E+00	3.4E-01	8.3E-01	1.7E-02	1.2E-01	2.2E+00	7.6E-02
GGC68-7	251.8	2.9E+01	7.1E+00	3.4E+00	0.0E+00	1.6E+00	4.9E+00	4.9E-02	5.2E-01	1.8E+01	2.2E-01
GGC68-8	270.0	6.2E+00	n.d.	1.1E+00	0.0E+00	2.4E-01	6.8E-01	1.2E-02	1.5E-01	2.7E+00	5.4E-02
GGC68-9	276.0	5.7E+00	1.6E+00	3.8E-01	0.0E+00	2.2E-01	7.0E-01	1.3E-02	1.5E-01	2.4E+00	5.7E-02
GGC68-10	313.0	9.3E+00	n.d.	1.1E+00	0.0E+00	5.5E-01	1.0E+00	4.9E-02	9.7E-02	4.0E+00	1.6E-02
GGC68-11	332.0	4.4E+00	9.3E-01	6.1E-01	0.0E+00	1.1E-01	3.2E-01	8.4E-03	9.1E-02	1.4E+00	3.4E-02
GGC68-12	343.5	4.2E+00	n.d.	1.1E+00	0.0E+00	1.2E-01	4.3E-01	1.0E-02	1.2E-01	1.9E+00	4.3E-02

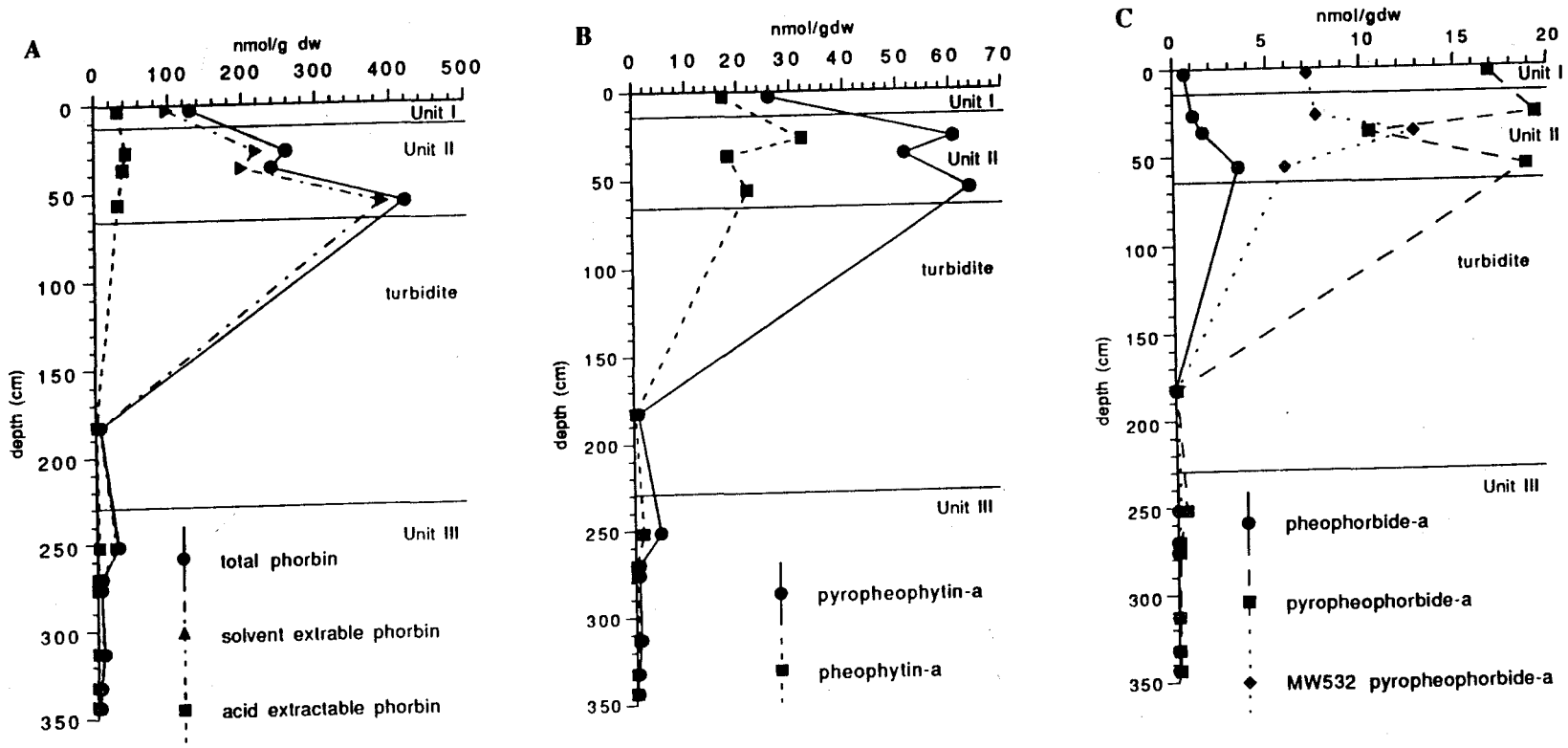

Fig. 7-6 Plots of the concentrations of: a) total phorbin, solvent extractable phorbin, and acid extractable phorbin; b) pheophytins-*a* and pyropheophytin-*a*; and c) pheophorbide-*a*, pyropheophorbide-*a*, and MW532 pheophorbide-*a* down core in GGC68.

variations, ratios of pheopigments are used. The ratio of ptn-*a*/pptn-*a* decreases from 0.7 at the sediment surface to 0.3 at 46.0 cm then levels off, suggesting that pheophytin-*a* is degrading of pptn-*a* but also that pptn-*a* is being deposited in the sediments from the overlying water column. The ratio of ptn-*a*/pbd-*a* decreases with depth in each sedimentary unit analyzed, but the ratio of pbd-*a*/ppbd-*a* increases. This suggests that ptn-*a* is degrading to pheophorbide-*a*, and that the increase in pheophorbide-*a* increases the pbd-*a*/ppbd-*a* ratio. It is generally believed that pheophorbide-*a* is formed from pheophytin-*a*, and pyropheophorbide-*a* from pyropheophytin-*a* during diagenesis (Treibs, 1936; Baker and Louda, 1982; Keely, 1989; Keely *et al.*, 1990). Each of these phorbins is deposited in the surface sediments from the overlying water column in unknown concentrations and the losses and gains in concentration of pheophytin-*a* and pyropheophytin-*a* do not correspond qualitatively nor quantitatively to the gains and losses in concentration of pheophorbide-*a* and pyropheophorbide-*a*, but decreasing ratios of individual pheopigments suggests that pheophorbide-*a* is forming from pheophytin-*a* and that pyropheophytin-*a* is forming from pheophytin-*a*.

The variations in the concentration with depth of solvent extractable macromolecular phorbins (HMW) and acid extractable phorbins (AEX) are quite different from the free phorbins (Table 7-3). In Unit I and Unit II, the concentration of HMW increases from 24 nmol/gdw at the surface to 170 nmol/gdw at 56 cm, following the concentration variations of total phorbin, whereas the concentration of AEX remains constant at approximately 35 nmol/gdw. The AEX therefore becomes a decreasing percentage of the total phorbin concentration with depth. In Unit III, both the HMW and AEX chlorophyll degradation products have fairly constant concentrations. Except for a maximum for HMW at 252 cm, HMW and AEX average 1 nmol/gdw in Unit III. The concentration profiles of HMW and AEX in GGC68 do not suggest the formation of HMW or AEX from free phorbins or from each other.

Phorbin steryl esters in core GGC68

In Ch. 3 and 5 we suggest that the PSEs record, both qualitatively and quantitatively, the sterol distribution as produced by phytoplankton. If this is correct, the distribution of PSEs down core may provide a means of monitoring changes in the phytoplankton community over time. Therefore, the we analyzed the distribution of PSE sterols in our samples.

In Units I and II, PSEs comprise between 13 - 47% of the solvent extractable phorbins, averaging 30%, and in the turbidite and Unit III, PSEs range between 32 - 64% of the total solvent extractable phorbin, and average 43%. The concentration of PSEs in

Unit I and Unit II sediments ranges from 37 nmol/gdw at 46 cm to 120 nmol/gdw at 27 cm. In Unit III, PSE concentrations range from 1.4 nmol/gdw at 332 cm to 18 nmol/gdw at 252 cm (Fig. 7-7, Table 7-2).

As well as showing variations in concentration with depth, the PSEs show variations in the composition of the esterified sterols. This variation with sediment depth can be seen in the distribution of HPLC peaks attributable to PSEs (Fig. 7-7) and in the distribution of molecular ions in the CI-MS of the PSE fractions. These variations in PSE distribution are reflected in the concentration variation of total phorbin with depth. Five different PSE distributions are apparent from the HPLC traces. The first group contains GGC68-1, the second, GGC68-2 and GGC68-3, the third, GGC68-4 and GGC68-5, the fourth GGC68-6 through GGC68-10, and the fifth, GGC68-11 and GGC68-12. Within Unit I and II, the changes in PSE distribution follow the changes in total phorbin concentration. The total phorbin concentration of GGC68-1 represents a surface maximum, which then decreases to a constant concentration in GGC68-2 and GGC68-3, and then increases in concentration in GGC68-5. The concentration of total phorbin varies in samples GGC68-6 to GGC68-10, but is constant in GGC68-11 and GGC68-12.

Based on the distribution of PSE HPLC peaks and CI-MS molecular ions (Fig. 7-8 and 7-9 (PSE molecular weights and sterols given in Table 3-1)) from samples in core GGC68, suggestions can be made as to the identity of the major sterols esterified to pyropheophorbide-*a*. By comparing the PSE HPLC data from this core with analyses of two surface sediment samples, BS2-0-10 (King and Repeta, 1991; Ch. 3) and BS5-0-4 (Ch. 5), of sediment traps (Ch. 5), and of standards (Ch. 3), it is possible to infer the identity of the major esterified sterols in the suites of PSEs in these samples. The HPLC distribution of PSEs in GGC68-1, a sample from the base of Unit I, is similar to that seen in sample BS2-0-10, a sample from the top of Unit I. Under the assumption that the same sterols are producing the PSE distribution in both samples, then the major sterols contributing to GGC68-1 PSE sterols are cholesterol, 24-methylcholesta-5,22-dien-3β-ol, 24-ethylcholest-5-en-3β-ol, and cholesta-5,22-dien-3β-ol. This is supported by CI-MS data which indicates that PSEs with molecular weights of 900 a.m.u. (pyropheophorbide-*a* cholesta-5,22-dien-3β-ol ester), 902 a.m.u. (pyropheophorbide-*a* cholesterol ester), 914 a.m.u. (pyropheophorbide-a 24-methylcholesta-5,22-dien-3β-ol ester), and 930 a.m.u. (pyropheophorbide-a 24-ethylcholest-5-en-3β-ol ester) are the major PSEs. Mass spectral data also indicates that dinosterol occurs in the PSEs at a low concentration. The sterols in these PSEs are made by diatoms, coccolithophores, and dinoflagellates (Volkman, 1986).

In samples GGC68-2 and GGC68-3, HPLC analysis suggests that the major PSEs in these samples are pyropheophorbide-*a* cholesterol ester , and pyropheophorbide-*a* 24-

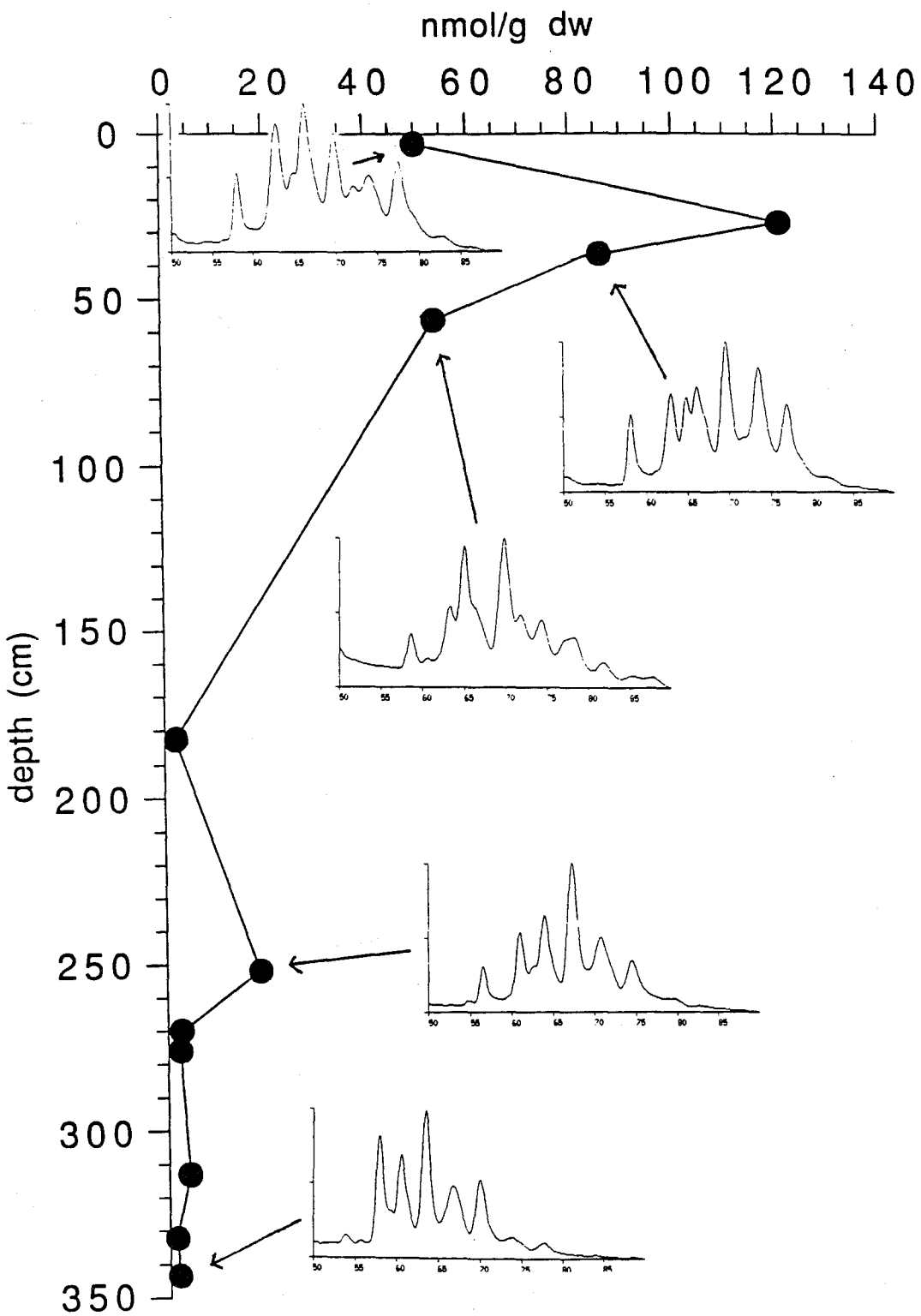

Fig. 7-7 Plot of the concentration of PSEs down core in GGC68 and examples of the PSE region of HPLC chromatograms.

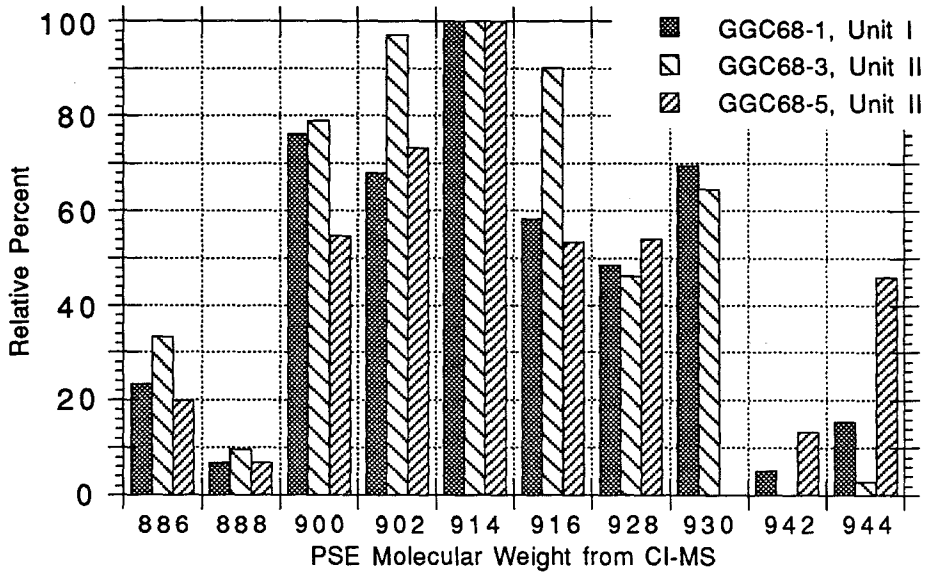

Fig. 7-8 Histogram showing the relative contribution of the PSEs of given molecular weights to the total PSE distributions in Unit I and Unit II sediments as determined by CI-MS in Black Sea sediment core GGC68.

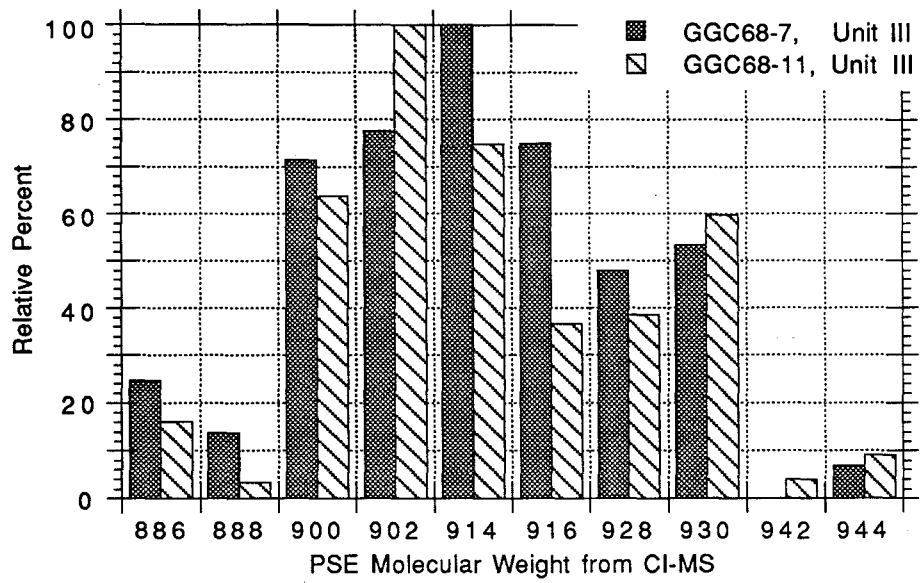

Fig. 7-9 Histogram showing the relative contribution of the PSEs of given molecular weights to the total PSE distributions in Unit III sediments as determined by CI-MS in Black Sea sediment core GGC68.

methylcholest-5-en-3β-ol ester. Mass spectrometry indicates that these sterols represent the second and third most abundant PSEs in GGC68-2. As determined by MS, the molecular weight of the most abundant PSE is 914 a.m.u., but this CI-MS molecular ion represents a mixture of pyropheophorbide-*a* esterified to either (or both) 24-methylcholesta-5,22-dien-3β-ol and 24-methylcholesta-5,24(28)-dien-3β-ol. Since these two PSEs are separated by HPLC, they do not appear by HPLC to be major PSE sterols, and the CI-MS 914 a.m.u. molecular ion represents a mixture of two PSEs. This PSE sterol distribution in GGC68-3 represents an increase in the amount of cholesterol and 24-methylcholest-5-en-3β-ol and a decrease in dinosterol (MW 944 PSE) when compared to GGC68-1, and the low relative amount of dinosterol suggests that 24-methylcholesta-5,24(28)-dien-3β-ol also occurs in relatively low concentrations. This change in the pattern of sterols could represent a decrease in the relative contribution of dinoflagellates to the organic carbon in GGC68-2 and GGC68-3 and a relative increase in diatoms and coccolithophores over that in GGC68-1. The change in PSE sterol distribution in Unit II could also represent the presence of other classes of algae which do not occur in Unit I.

In samples GGC68-4 and GGC68-5, a change in the HPLC distribution of PSEs is again observed. By HPLC analysis, the PSEs in these samples are pyropheophorbide-*a* 24-methylcholesta-5,24(28)-dien-3β-ol ester and pyropheophorbide-*a* cholesteryl ester. The CI-MS data for sample GGC68-5 indicates that cholesterol and either or both 24-methylcholesta-5,22-dien-3β-ol or 24-methylcholesta-5,24(28)-dien-3β-ol is present in the PSE sterols. The large relative contribution of dinosterol to the CI-MS data, three times more than in GGC68-1, and 14 times more than in GGC68-3, indicates that dinoflagellates are once again major contributors to the organic matter in GGC68-5. The large amount of dinosterol also suggests that the contribution of pyropheophorbide-*a* 24-methylcholesta-5,22-dien-3β-ol to the molecular weight 914 molecular ion is reduced over that in GGC68-3, and pyropheophorbide-*a* 24-methylcholesta-5,24(28)-dien-3β-ol is enhanced. Coccolithophores are a relatively less important source for organic matter in GGC68-5 as compared to GGC68-3. The large contribution of dinoflagellates to the organic matter in GGC68-5 is supported by the absence of a measurable concentration of 24-ethylcholest-5-en-3β-ol to the PSE sterols in this sample. This sterol occurs in moderate contributions in most algae but is not found in most dinoflagellates (Volkman, 1986).

In samples GGC68-7 through GGC68-10 from Unit III, HPLC analysis suggests the major PSEs are most likely pyropheophorbide-*a* cholesteryl ester and pyropheophorbide-*a* 24-methylcholesta-5,22-dien-3β-ol ester. This is supported by CI-MS data for sample GGC68-7, and suggests that lacustrine species of diatoms and coccolithophores are contributing to the organic matter in these samples. In the lowest two

samples from this core, the major PSEs as determined by HPLC are pyropheophorbide-*a* 24-norcholesta-5,22-dien-3β-ol ester, pyropheophorbide-*a* cholesta-5,22-dien-3β-ol ester and a previously and as yet unidentified PSE. Diatoms and dinoflagellates synthesize large quantities of cholesta-5,22-dien-3b-ol (Volkman, 1986), and dinoflagellates synthesize 24-norcholesta-5,22-dien-3b-ol (Goad and Withers, 1982). From the CI-MS data no inference can be made as to the identity of these new PSE sterols. The x-radiographs suggest that the bottom 15 cm of this core may be different from those above (Fig. 7-5).

Changes in the phytoplankton distribution in the Black Sea can be inferred by comparing the PSE distribution in samples GGC68-1, GGC68-3, GGC68-5, GGC68-7, and GGC68-11. In GGC68-3, the PSE distribution suggests that this sample contains a much smaller contribution of carbon from dinoflagellates than the strata above and below. The highest contribution of dinoflagellates is to sample GGC68-5. Coccolithophores are found throughout the core. The variations in phytoplankton distribution suggest that changes are occuring in the photic zone of the Black Sea which effect the composition of the phytoplankton community.

D. THE C:CHL RATIO IN BLACK SEA SEDIMENTS

In Ch. 6 we present a mass balance of chlorophyll degradation in the Black Sea which suggests that currently the flux of phorbin which enters the anoxic water column is deposited in surface sediments. This suggests that phorbin does not degrade once it enters anoxic conditions. For TOC, this is not the case. In the anoxic regime of the water column and in surface sediments, our mass balance suggests that 75% of TOC which enters the anoxic water column is remineralized. To examine relative changes in the preservation of TOC and phorbin over time we create a C:chl ratio where C represents TOC and chl represents total phorbin. By ratioing the two concentrations, we remove concentration variations in both TOC and total phorbin due to changes in sediment dilution by inorganic material and variations in input of TOC and phorbin. Since the anoxic regime that currently exists in the Black Sea was in place at the start of Unit II deposition, variations in total phorbin in Units I and II are most likely due to either variations in input from the surface ocean or to dilution from terrigenous input. The sediment analyzed in samples GGC68-1 through GGC68-5 (Units I and II)was laid down under anoxic conditions over approximately the last 8200 years (Jones and Gagnon, 1992).

The percent total organic carbon and calcium carbonate on a total sediment basis are plotted versus depth in Fig. 7-10. To examine changes in TOC and phorbin in Unit I, we must combine data from a surface sample taken from Station 3, Box Core 5 (sample BS5-0-4; Ch. 5) which was collected near our gravity core site, with our data from GGC68.

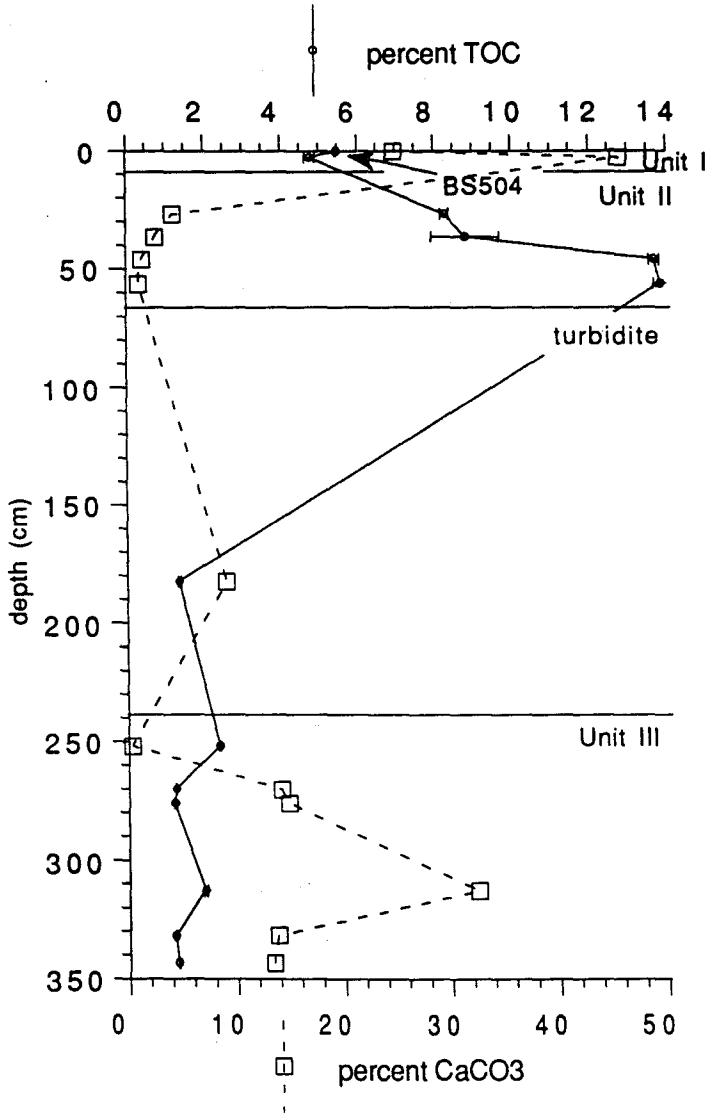

Fig. 7-10 Plot of the percent TOC and $CaCO_3$ in core GGC68.

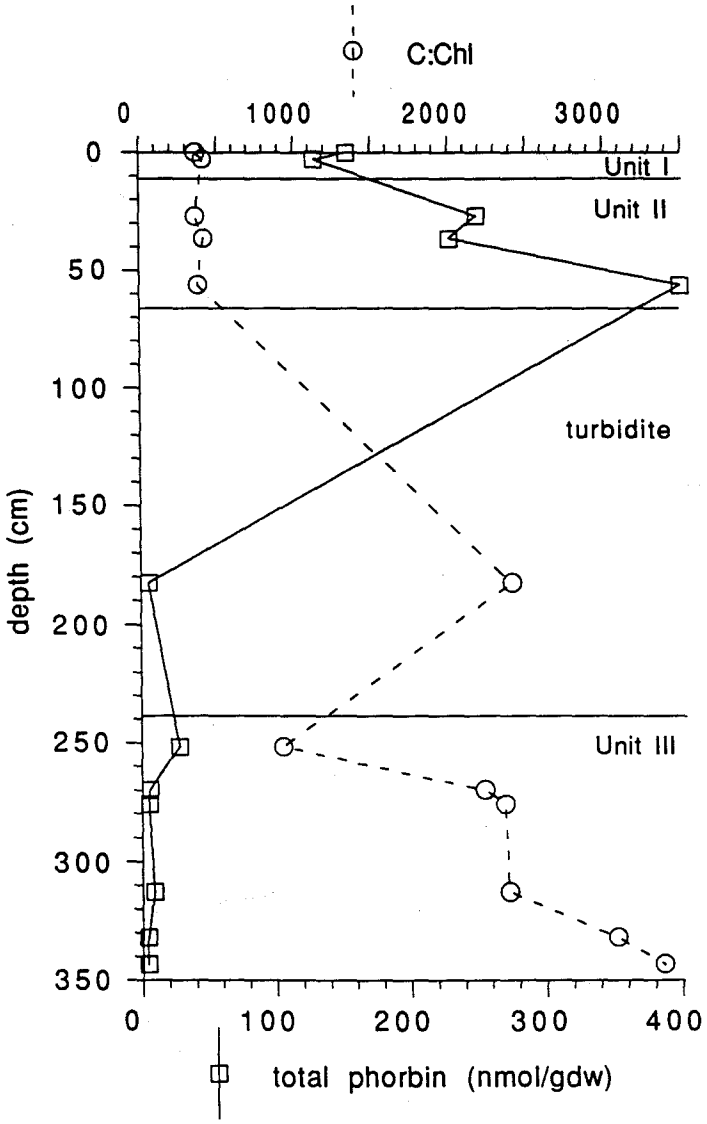

Fig. 7-11 Plot of the C:chl ratio and calculated marine total organic carbon concentration down core in GGC68.

For our single Unit I sample from GGC68, we determined the TOC to be 4.8%, and in the sample from 4.5 cm in BS5-0-4 we determined the TOC to be 5.5%. These values compare well with TOC measurements reported in the literature. Many studies of organic carbon have been carried out in Black Sea sediments (Ross and Degens, 1974; Calvert *et al*, 1987; Calvert and Fontugne, 1987; Hay, 1987, 1988; Lyons, 1991; Wakeham *et al.*, 1991; Calvert *et al.*, 1991), and all have shown that in Unit I sediments, there is very little variation in TOC content from top to bottom of the sequence throughout the Black Sea, and concentrations of TOC from various cores taken in the central basin range from 2 - 6%. In a core collected during the 1988 R/V *Knorr* Black Sea Expedition from a location close to GGC68, Lyons (1991) found TOC to range from 3.5 - 5.5%. From a subcore of the same boxcore, Calvert *et al* (1991) found the average TOC to be 5.1%, and from a core taken from the central basin during the 1975 R/V *Chain* cruise, Hay (1988) found the average TOC to be 4.2%. In these records of TOC, no systematic trends of increasing or decreasing TOC are apparent though fluctuations of 1 -2 % do occur. In Unit II sediments form core GGC68, we found TOC to increase from 8 to 14%. Calvert *et al.* (1987) found TOC in the sapropel to range from 5% to 14%. In extensive studies of TOC in Black Sea cores, Ross and Degens (1974) found TOC to range from 5% to 20% in the sapropel and Hay (1988) found TOC to range from 5% to 15%. Our TOC data agrees well with other published results.

The variation in total phorbin concentration in core GGC68 has been discussed above. To gain another data point in our analysis of the C:chl ratio, we include data from sample BS5-0-4 taken from near our core site. In BS5-0-4, we measured a total phorbin concentration of 160 nmol/gdw. This concentration is similar to that determined for our single Unit I sample (GGC68-1) of 130 nmol/gdw.

In calculating the C:chl ratio in Black Sea sediments, it is necessary to remove the contribution of terrigenous carbon to the sedimentary TOC. In Unit I sediments, Shimkus and Trimonis (1974) estimated the contribution of terrigenous input to TOC to be 33% based on river input and primary production while Calvert and Fontugne (1987) estimated the contribution to be approximately 25% based on stable isotope studies. We therefore correct the TOC content of the samples from Unit I for a contribution of 29% terrigenous carbon. Calvert and Fontugne (1987) used a two endmember mixing model of stable carbon isotopes and found the contribution of terrigenous organic matter to increase slightly from the surface to the base of Unit I. In Unit II, they estimated that TOC becomes almost entirely of marine origin in the center of the sapropel. The low percentage of terrigenous carbon in Unit II is supported by the radiocarbon measurements of organic carbon in Unit II by Jones and Gagnon (1992). They find the radiocarbon ages of the organic carbon in

Unit II to be linear with depth and uniform through out the basin which suggests that there is very little input of organic carbon from advection and lateral transport off the shelf. We also correct the TOC contents in Unit II for a contribution of 29% terrigenous carbon since there is no estimate of the terrigenous contribution in samples that corresponds to our samples. This is likely to be an over correction for contribution of terrigenous TOC in the sapropel and may make our calculated C:chl ratios high by up to 25%. In Unit III, there are no estimates for the contribution of terrigenous carbon so we also correct the TOC for 29% terrigenous carbon.

The C:chl ratios from GGC68 and from our single box core sample are plotted versus sediment depth in Fig. 7-11. In the five samples from Units I and II, the C:chl ratios are constant with depth. In the turbidite and the upper four samples of Unit III, the C:chl ratio increases from the values in Unit I and Unit II by a factor of 6 and in the bottom two samples, the C:chl ratio increases by a factor of 8. Much of these variations are likely due to changes in preservation since Unit III sediments were laid down under oxic conditions.

Variations in TOC and total phorbin may be driven by sediment dilution. Hay (1988) proposed that the invasion of the Black Sea by *E. huxleyi* caused the change in sedimentation from sapropelic sediments to laminated through dilution of the sediment with calcium carbonate. Variations in TOC and total phorbin in the upper five samples of GGC68 are affected by dilution with old carbonate advected off the shelves. The radiocarbon ages of the carbonate in Unit II suggests that it is reworked material which has been advected into the deep basin (Jones and Gagnon, 1992).

The constant C:chl ratio seen in Units I and II suggests that the preservation potential for both TOC and total phorbin has remained constant over the last 8200 years. In Unit III, the C:chl ratio increases by up to a factor of eight over that in Units I and II. This suggests that some change in the conditions either under which carbon is fixed or under which both TOC and phorbin is deposited in sediments occured between Units II and III. The decrease in C:chl towards the top of Unit III, suggests that the change was occuring gradually over time. Baker and Louda (1982) found that in the Gulf of California the C:chl ratio in sediments deposited under oxic conditions to increase rapidly with depth from a value of 370 at the surface to 2500 at 12 cm suggesting that under oxic depositional conditions phorbin is remineralized more rapidly than is TOC. Unit III was deposited under conditions with a longer oxic water column than in Unit II (Degens and Ross, 1974; Calvert *et al.*, 1987; Jones and Gagnon, 1992) and under oxic depositional conditions, phorbin is remineralized more quickly than under anoxic depositional conditions (Sun, 1992). This difference in depositional conditions would explain the differences in C:chl

ratio seen between Unit III and Unit II, since much more phorbin would be lost prior to deposition in Unit III than in Unit II. The gradual decrease in C:chl ratio towards the top of Unit III, suggests that the Black Sea anoxic water column formed during the deposition of Unit III.

The organic carbon budget created by Deuser (1971) suggests that the deep basin of the Black Sea could become anoxic in 1000 years. The Black Sea was reconnected with the Mediterranean Sea approximately 9800 years before present (Stuiver and Pearson, 1986; Bard *et al.*, 1980; Jones and Gagnon, 1992), and the deposition of Unit II began approximately 8200 years before present (Jones and Gagnon, 1992), allowing for 1600 years for the deep basin to become anoxic. The x-radiographs of core GGC68 (Fig. 7-5) indicate that the upper sections of Unit III are laminated. Excluding the turbidites which are interbedded in Unit III, core GGC68 includes 60 cm of sediment from Unit III, 40 cm of which are laminated. Deposition of laminated sediments can only occur when the over lying water is suboxic or anoxic.

Unit III is approximately 65 m in length (Ross and Degens, 1974; Ross et al., 1978) and consists of terrigenous muds. The base of Unit III is believed to have been deposited approximately 25,000 years before present (Ross and Degens, 1974), but no good chronology exists for this unit (Ross and Degens, 1974; Ross et al., 1978). Ross and Degens (1974) estimated the sedimentation rate for Unit III to be on the order of 40 - 90 cm/kyr. Using this sedimentation rate, the the change in C:chl ratio from 3000 to 300 occured over approximately 1000 years, well within the estimates by Deuser (1971) and Jones and Gagnon (1992).

IV. CONCLUSIONS

In core GGC68 from the central Black Sea, total phorbin concentrations range from 4.2 nmol/gdw to 420 nmol/gdw. The major free phorbins identified are pheophorbide-*a*, pyropheophorbide-*a*, MW532 pheophorbide-*a*, pheophytin-*a*, and pyropheophytin-*a*. No precursor/product relationships can be established in the degradation pathway of chlorophyll from the distribution of chlorophyll degradation products. Also identified are the phorbin steryl esters, high molecular weight chlorophyll degradation products, and acid extractable chlorophyll degradation products. In Units I and II, the concentration of AEX remains constant with sediment depth while the concentration of total phorbin and HMW increases with sediment depth. Over the length of GGC68, the relative concentration of PSEs varies from 30 to 60% of the total phorbin concentration.

The distribution of phorbin steryl esters changes with sediment depth in core GGC68. The relative concentration of pyropheophorbide-a dinosteryl ester decreases at the top of Unit II then reaches in maximum concentration near the base of Unit II. In Unit III, the relative concentration of pyropheophorbide-*a* dinosteryl ester again decreases. We suggest that the distribution of sterols esterified to pyropheophorbide-*a* is not altered during degradation and the distribution of esterified sterols can be used to examine the changes in the phytoplankton community over time.

Variations in the C:chl ratio were also examined down core in GGC68. The C:chl ratio is constant in Units I and II but increases by a factor of 8 in Unit III. We suggest the increase in Unit III is due to the oxic water column which existed during the deposition of sediments in Unit III allowing for a greater increase in the remineralization rate over that in Units I and II of phorbins as compared as compared to TOC.

V. REFERENCES

Arthur M. A., Broda J. E., Dean W. E., Derman A. S., Gagnon A. R., Hay B. J., Konuk Y. T., Honjo S., Neff E. D., Pilskaln C. H., and Briskin M. (1988) Black Sea sediments. In: Temporal and Spatial Variability in Sedimentation in the Black Sea: Cruise Report R/V Knorr 134-8, Black Sea Leg 1. WHOI-88-35. 109-129.

Baker E. W., and Louda J. W. (1982), Geochemistry of tetrapyrrole, tetraterpenoid and perylene pigments in sediments from the Gulf of CA: DSDP Leg 64, Sites 474, 477, 479, and 481, and the SIO Guaymas Basin Survey Cruise Leg 3, Sites 10 and 18G, In: *Initial Reports of the Deep Sea Drilling Project* **64**: Washington (U.S. Govt. Printing Office), 789-814.

Baker E.W. and Louda J.W. (1986) Porphyrins in the geological record. In: Biological Markers in the Sedimentary Record. (R. B. Johns, ed.) , 125-225.

Bard E., Hamelin B., Fairbanks R. G., and Zindler A. (1990) Calibration of the ^{14}C timescale over the past 30,000 years using mass spectrometric U-Th ages from Barbados coarals. *Nature* **345**, 405-410.

Bukry D., King S.A., and Horn M.K. (1970) Geological significance of coccoliths in fine-grained carbonate bands of past glacial Black Sea sediments, *Nature* **226**, 156-158.

Calvert S. E. and Fontugne M. R. (1987) Stable carbon isotopic evidence for the marine origin of the organic matter in the Holocene Black Sea Sapropel. *Chem. Geo.* **66**, 315-322.

Calvert S. E., Karlin R. E., Toolin L. J., Donahue D. J., Southon J R., and Vogel J. S. (1991) Low organic carbon accumulation rates in Black Sea Sediments. *Nature* **350**, 692-695.

Calvert S. E., Vogel J. S., and Southon J. R. (1987) Carbon accumulation rates and the origin of the Holocene sapropel in the Black Sea. *Geology* **15**, 918-921.

Degens E. T. and Ross D. A. (1972) Chronology of the Black Sea over the last 25,000 years. *Chem. Geol.* **10**, 1-16.

Degens E.T. and Stoffers P. (1980) Environmental events recorded in Quaternary sediments of the Black Sea. *J. Geol. Soc. London* **137**, 131-138.

Deuser W. G. (1971) Organic-carbon budget of the Black Sea. Deep-Sea Res. 18, 995-1004.

Eckardt C. B., Keely B. J., and Maxwell J. R. (1991) Identification of chlorophyll transformation products in a lake sediment by combined liquid chromatography - mass spectrometry. *J. Chrom.* **557**, 271-288.

Furlong E.(1986) Sediment geochemistry of photosynthetic pigments in oxic and anoxic marine and lacustrine sediments: Dabob Bay, Saanich Inlet, and Lake Washington. Ph.D. dissertation, University of. Washington.

Furlong E. and Carpenter S.R. (1988) Pigment preservation and remineralization in oxic coastal marine sediments, *Geochim. Cosmochim. Acta* **52**, 87-100.

Goad L. J. and Withers N. (1982) Identification of 27-nor-(24R)-methylcholesta-5,22-dien-3β-ol and brassicasterol as the major sterols of the marine dinoflagellate *Gymnodinium simples*. *Lipids* **17**, 852-858.

Goericke R. and Repeta D. J. (1992) The pigments of *Procloracoccus marinus*: The presence of divinyl chlorophyll *a* and *b* in a marine procaryote. *Limnol. Oceanogr.* **37**, 425-433.

Hay B. J. (1987) Particle Flux in the Western Black Sea in the Present and Over the Last 5,000 years: Temporal Variability, Sources, Transport Mechanisms, Ph.D. dissertation, Massachusetts Institute of Technology and the Woods Hole Oceanographic Institution Joint Program in Oceanography, 201p.

Hay B. J. (1988) Sediment accumulation in the central western Black Sea over the past 5100 years. *Paleoceanogr.* **3**, 491-508.

Hurley J. P. and Armstrong D. E. (1991) Pigment preservation in lake sediments: A comparison of sedimentary environments in Trout Lake, Wisconsin. *Can. J. Fish. Aquat. Sci.* **48**, 472-486.

Jones G. A. and Gagnon A. R. (1992, submitted) Radiocarbon chronology of Black Sea sediments. *Deep-Sea Res.*

Keely B. J. (1989) Early diagenesis of chlorophyll and chlorin pigments. Ph. D. dissertation, University of Bristol.

Keely B. J. and Brereton R. G. (1986), Early chlorin diagenesis in a recent aquatic sediment. *Org. Geochem.* **10**, 975-980.

Keely B. J., Prowse W. G., and Maxwell J. R. (1990), The Treibs Hypothesis: An evaluation based on structural studies. *Energy Fuels* **4**, 628-634.

King L. L. and Repeta D. J. (1991) Pyropheophorbide steryl esters in Black Sea sediments. *Geochim. Cosmochim. Acta* **55**, 2067-2074.

Krom M. D. and Berner R. A. (1983) A rapid method for the determination of organic and carbonate carbon in geological samples. *J. Sed. Petrol.* **53**, 660-663.

Lorenzen C. J. (1974) Chlorophyll-degradation products in sediments of Black Sea. In: The Black Sea -- Geology, Chemistry, and Biology (E. Degens and D. A. Ross, eds.). *Mem. Am. Assoc. Pet. Geol.* **20**, 426-428.

Lyons T. W. (1991) Upper Holocene sediments of the Black Sea: Summary of leg 4 box cores (1988 Black Sea Oceanographic Expedition). In: Black Sea Oceanography (E. Izdar and J. W. Murray, ed.) NATO ASI Series, Kluwer Academic Publishers, 401-441.

Orr W. L., Emery, K. O. and Grady J. R. (1958), Preservation of chlorophyll derivatives in sediments off Southern California. *Bull. Amer. Assoc. Petrol. Geo.* **42**, 925-958.

Peake E., Casagrande J., and Hodgson G. W. (1974) Fatty acids, chlorins, hydrocarbons, sterols, and carotenoids from a Black Sea core. In: The Black Sea -- Geology, Chemistry, and Biology (E. Degens and D. A. Ross, eds.). *Mem. Am. Assoc. Pet. Geol.* **20**, 505-523.

Repeta D. J., Simpson D. J., Jorgensen B. B., and Jannasch H. W. (1989) Evidence from anoxygenic photosynthesis form the distribution of bacteriochlorophylls in the Black Sea. *Nature* **342**, 69-72.

Ross D. A. and Degens E. T. (1974) Recent sediments of the Black Sea, In: The Black Sea--Geology, Chemistry, and Biology, E.T. Degen and D.A. Ross, Eds. Am. Assoc. Petrol. Geol.

Ross D. A., Degens E. T., and MacIlvaine J. (1970) Black Sea: Recent sedimentary history. *Science* **170**, 163-165.

Ross D. A., Neprochnov Y., Degens E. T., Erickson A. J., Hsu K., Hunt J. M., Manheim F., Percival S., Senalp M., Stoffers P., Supko P., Traverse A., and Trimonis E. A. (1978) Site 379. In: *Innitial Reports of the Deep Sea Drilling Project* **62**: Washington (U. S. Government Printing Office) 29-54.

Shimkus L. M. and Trimonis E.S. (1974) Modern sedimentation in Black Sea, In: The Black Sea--Geology, Chemistry, and Biology, E.T. Degen and D.A. Ross, Eds. Am. Assoc. Petrol. Geol.

Stuiver M. and Pearson G. W. (1986) High-precision caligration of the radiocarbon time scale, AD 1950-500 BC. *Radiocarbon* **28**, 805-838.

Sun M.-Y. (1992) Early diagenesis of chloropigments in coastal sediments. Ph.D. dissertation, State University of New York at Stony Brook.

Swain E. B. (1985) Measurement and interpretation of sedimentary pigments. *Freshwater Biol.* **15**, 53-75.

Treibs A. (1936) Chlorophyll- und Haeminderivate in organischen mineralstoffen, *Angewandte Chemie* **49**, 682-686.

Volkman J. K. (1986) A review of sterol markers for marine and terrigenous organic matter. *Org. Geochem.* **9**, 83-99.

Wakeham S. G., Beier J. A., and Clifford C. H. (1991) Organic matter sources in the Black Sea as inferred from hydrocarbon distributions. In: Black Sea Oceanography (E. Izdar and J. W. Murray, ed.) NATO ASI Series, Kluwer Academic Publishers, 319-341.

Yacobi Y. Z., Mantoura R. F. C, and Llewellyn C. A. (1991) The distribution of chlorophylls, carotenoids and their breakdown products in Lake Kinneret (Israel) sediments. *Freshwater Biol.* **26**, 1-10.

CHAPTER 8

CONCLUSIONS AND SUGGESTIONS FOR FUTURE RESEARCH

CHAPTER 8

CONCLUSIONS AND SUGGESTIONS FOR FUTURE RESEARCH

I. CONCLUSIONS

This thesis has examined the sedimentary sinks for chlorophyll in the Black Sea, and documents shifts in the relative contribution of chlorophyll to each of these sinks both over a single year and over the past 10,000 years. The approach taken was to extract chlorophyll degradation products from 200 - 1000 g of sediment, to determine spectrally the total concentration of chlorophyll degradation products in the extract, and then to structurally identify all the components contributing to absorption at the red band. We then looked for these same chlorophyll degradation products in sediment traps and down core in sediments. The Black Sea was chosen for the study site due to increased preservation of phorbins under anoxic conditions and to simplify the complexity of the phorbin mixture extracted from sediments, since studies of DSDP samples by Baker and Louda (1982; 1986) have suggested that chlorophyll degradation products deposited in sediments under oxic conditions degraded through a more complex pathway than chlorophyll degradation products deposited in sediments under anoxic conditions.

Four major conclusions can be drawn from the results of the research described in the four preceding chapters of this thesis:

1) There is approximately 3 times more chlorophyll derived phorbin in Black Sea sediments than can be accounted for when considering only individual pheopigments. In anoxic sediments from the Black Sea, the total phorbin concentration can be determined by summing the contributions of organically extractable high molecular weight degradation products, pyropheophorbide steryl esters, pheopigments, and acid extractable macromolecular chlorophyll degradation products.

2) In sediments, the sterol distribution in the pyropheophorbide steryl esters preserves the sterol distribution in surface waters as produced by phytoplankton. Pyropheophorbide steryl esters are preserved in anoxic sediments over the long term.

3) Chlorophyll degradation products which pass through the H_2S chemocline survive quantitatively to accumulate in surface sediments.

4) Based on the distribution of chlorophyll degradation products in Black Sea sediments, no precursor-product relationships can be established.

Previous studies of chlorophyll degradation in sediments have used two different methods to calculate the contribution of chlorophyll degradation products to sedimentary organic matter: by calculating the concentration of phorbins indicated by visible absorption in the red band (Fog and Belcher, 1961; Gorham, 1961; Lorenzen, 1974; Swain, 1985), and by summing the concentration of individual phorbins and porphyrins indicated by HPLC separation of the individual components (Gillan and Johns, 1980; Keely and Brereton, 1986; Furlong and Carpenter, 1988; Yacobi *et al.*, 1991). A comparison of these two methods indicates that the HPLC method accounts for only approximately 1/3 of the total phorbins in organic extracts of sediments. The first study to actually demonstrate this disparity was that of Furlong and Carpenter (1988), but earlier studies by Blumer (Blumer and Snyder, 1967; Blumer and Rudrum, 1970) and Repeta (unpublished) suggested that this discrepancy might exist by demonstrating the presence of solvent extractable high molecular weight phorbin containing compounds. Furlong and Carpenter (1988) oxidized humic and fulvic acids and looked for the oxidation products of phorbins. Their results, for the first time, quantified the amount of phorbin contained within macromolecular compounds and suggested that as much as 1/3 of total sedimentary phorbins may occur in a macromolecular form..

The existence of 3 times more phorbin in the total sediment extract than can be separated and quantified by HPLC is clearly indicated by the work contained within this thesis. By extracting sediments with acid, we showed that there is 50% more phorbin contained within sediment than can be isolated by solvent extraction alone. The concentraton of phorbin in the acid extractable material represents more phorbin than is indicated by studies of humic and fulvic acids.

By comparing the total amount of phorbin analyzed by HPLC with that quantified by solvent and acid extraction, we found that there is approximately 3 times more phorbin in Black Sea sediments than can be accounted for by HPLC analysis alone. This suggests that the degradation of chlorophyll is much more complex than previously suggested by the work of Baker and Louda (1982, 1986) and Keely and others (Keely and Brereton, 1986; Keely *et al*, 1988; Keely, 1989; Keely *et al.*, 1990). We now know that chlorophyll degradation products can be incorporated into macromolecular compounds and into compounds that are not readily accessible to organic solvents, and that this process occurs early in degradation, perhaps before deposition occurs. The presence of acid extractable chlorophyll degradation products in oxic sediments (King and Peeken, unpublished data) indicates that anoxic conditions are not necessary for the formation of these structures.

If these new reservoirs of chlorophyll degradation products are included in the analysis of sedimentary phorbins for use as indicators of paleoproductivity, better results may be obtained. By using only free phorbins or total solvent extractable phorbins as done previously (Fogg and Belcher, 1961; Gorham, 1961; Czeczuga, 1964; Brown *et al.*, 1977; Daley *et al.*, 1977; Guilizzoni *et al.*, 1983; Swain, 1985) a large and potentially important pool of chlorophyll degradation products has not been included in these paleoproduction calculations. Since it is unknown whether phorbins are taken into the macromolecular and acid extractable reservoirs during degradation or released from them, it is unknown how the exclusion of these reservoirs will effect the results of the paleoproduction analysis. In the Black Sea, our data suggests that when each of these reservoirs is summed, the amount of phorbin in Black Sea sediments is equal to that passing through the chemocline. If this relationship holds over time, then total sedimentary phorbin accumulation rates in Black Sea sediments may be useful indicators of paleoproductivity. Our down core analysis of phorbins suggests this relationship might hold in the Black Sea. This will not be true in oxic environments since fecal pellets falling through an oxic water column are subject to further reworking (Bathmann and Liebezeit, 1986) and bottom dwelling organisms continue to rework and remove organic carbon, including phorbins, from sediments (Hawkins *et al.*, 1986; Bianchi *et al.*, 1988).

Another pathway in the degradation of chlorophyll is indicated by the occurrence of pyropheophorbide-*a* steryl esters. The occurence of a mesopyropheophorbide-*a* steryl ester in the Marou oil shale (Prowse and Maxwell, 1991) suggests that pyropheophorbide steryl esters probably continue to degrade in sediments through a pathway similar to that proposed by Treibs (1936) and Baker and Louda (1982). Comparisons of the relative degradation rates of pheophorbides and pheophytins in sediments suggests that pheophytins are more stable than pheophorbides (Hurley and Armstrong, 1990). It is therefore not all together surprising that pyropheophorbide steryl esters persist in sediments when other pheophorbides do not, since pheophorbide steryl esters possess an esterified alcohol like pheophytin. Analysis of the sterol distribution of the PSEs also indicates that the sterol distribution produced in surface waters may be preserved. A comparison of the distribution of sterols esterified to pyropheophorbide at various times of the year shows they are similar to the sterols expected from the distribution of phytoplankton living in the photic zone. A comparison of the sterol distribution of sedimentary PSEs with free sterols in sediment traps and sediments suggests that the sterols in the PSEs preserve the sterol distribution as measured in sediment traps.

Free sedimentary sterols have been used as biomarkers of phytoplankton genera but it is known that the sterol record as found in sediments does not accurately record

phytoplankton populations since stenols are reduced to stanols (Eyssen, *et al.*, 1973; Gaskel and Eglinton, 1975, 1976; Nishimura and Koyama, 1977; Nishimura, 1978) and 4-methyl sterols are preserved relative to 4-desmethyl sterols (Gagosian *et al.*, 1980; Wolf *et al.*, 1986). From free sedimentary sterols, it was suggested that dinoflagellates are important contributors to phytoplankton production in the Black Sea (Boon *et al.*, 1979). Comparisons of sedimentary sterols with sediment trap sterols suggests that dinoflagellates may not be as important as previously thought since dinosterol is a relatively minor sterol in sediment traps (Wakeham and Beier, 1991, and Ch 5). This same conclusion is drawn when the sterol distributions in the sediment trap and sedimentary PSEs are examined, since dinosterol is minor in these sterol reservoirs.

The formation pathway of the phorbin steryl esters is as yet undetermined, but our evidence suggests that they are formed during grazing. Previous studies of zooplankton grazing have looked only at the formation of pheophytin, pyropheophytin, pheophorbide, and pyropheophorbide and the loss of chlorophyll (Shuman and Lorenzen, 1975; Burkill *et al.*, 1987; Downs, 1989; Roy et al., 1989). In studies of chlorphyll loss during grazing, the formation of PSEs does not balance the loss of chlorophyll that occurs during grazing since chlorophyll loss is usually measured by gut fluorescence and this technique would also measure PSEs (Klein et al., 1986; Lopez *et al.*, 1988; Pasternak and Drits, 1988; Penry and Frost, 1991; Mayzaud and Razouls, 1992). In studies identifying the individual chlorophyll degradation products formed during grazing, PSEs would not be determined, however, since very seldom are HPLC runs long enough to insure the elution of these compounds.

Once chlorophyll and its degradation products pass through the Black Sea chemocline, no further loss of phorbin occurs, though alteration or loss of side chains on the macrocycle does occur. The lack of further loss of phorbin during settling to the sediment surface, as found in the Black Sea, is quite unusual for the marine environment. In locations with oxic water columns, the flux of total phorbin decreases with depth in the water column (Yentsh, 1965; Vernet and Lorenzen, 1987). High accumulation rates of chlorophyll in lacustrine environments with anoxic water columns have been reported (Swain, 1985; Hurley and Armstrong, 1991; Yacobi, 1991).

The situation in the sediments is similar to that in the water column. In sediments, our data does not indicate that loss of chlorophyll degradation products is occuring with sediment age over the upper 60 cm of sediment. This situation is comparable to that found in other marine environments where deposition under anoxic conditions occurs (Orr et al., 1958; Swain, 1985; Furlong, 1986; Hurley and Armstrong, 1991), but is quite different from locations with oxic depositional conditions where the concentration of total phorbins

decreases rapidly in the upper few centimeters of sediment until at depth in sediment, a constant concentration is reached (Swain, 1985; Furlong, 1986, Furlong and Carpenter, 1988; Hurley and Armstrong, 1991). In the suite of chlorophyll-*a* degradation products identified in Black Sea sediments, no precursor-product relationships can be suggested. It has previously been suggested that pheophytin persists longer in sediments than does pheophorbide (Hurley and Armstrong, 1990) but our data neither refute nor substantiate this finding. We identified both AEX and HMW chlorophyll degradation products at all depths in our core, but the concentration of AEX remained constant with depth whereas the concentration of HMW varied with the total phorbin concentration.

The suite of free phorbins identified in the water column and sediments of the Black Sea are the same as those previously identified in other locations (Welschmeyer and Lorenzen, 1985; Vernet and Lorenzen, 1987; Downs, 1989). This suggests that the degradation pathways postulated by others (Treibs, 1936; Baker and Louda, 1982; Keely *et al.*, 1990) are functioning in the Black Sea, though the degradation pathway in the Black Sea, and perhaps many other locations as well, is much more complex than previously suggested. Chlorophyll degradation in the Black Sea involves incorporation of phorbins into solvent extractable high molecular weight compounds, into compounds which are only accessible to strong acid, esterification of phorbins to sterols, and degradation of chlorophyll through free phorbins. Each of these degradation pathways begins in the water column, probably in the photic zone, and the intermediates of the early steps in these pathways are deposited in surface sediments.

II. SUGGESTIONS FOR FUTURE RESEARCH

The results of this research project have posed many new questions which have been left unanswered and therefore suggest several lines of research. In this study of the Black Sea, we have found several previously unknown sinks for chlorophyll in sediments, but the Black Sea is a very unique environment, having both an anoxic water column and anoxic sediments. It is unknown whether these new chlorophyll degradation products also occur in other environments as well. The most obvious next step is to choose an oceanic location with oxic water column and bottom waters, and oxic surface sediments, and using methods, such as those used in Chs. 6 and 7 to fractionate the sediment extract, determine if the total phorbin content of the sediments can be accounted for using the relationship derived for Black Sea sediments (Ch. 6):

AEX = bound + HMW + PSE's + free phorbin

Large quantities of sediment will necessarily have to be extracted since the concentration of individual chlorophyll degradation products in oxic sediments is lower than that in anoxic sediment (Furlong and Carpenter, 1988).

The source and complete structure of the high molecular weight and acid extractable chlorophyll degradation products described in Ch. 4 are still unknown. It will likely be impossible to determine an exact structure of these materials. It may be possible to determine how phorbins and porphyrins are bound into these structures using a series of chemical degradative reactions like those used by Richnow *et al* (1991) and Mycke and Michaelis (1986) to selectively cleave sulfur and oxygen containing bonds. Understanding how chlorophyll degradation products are bound with other lipids will help in determining the source of the macromolecular compounds. The results of the current research suggests that these compounds are produced early in the degradation path of chlorophyll, possibly in the water column. To help in source determination, suspended and sinking particulate matter from the surface ocean, including phytoplankton, should be extracted with solvent and acid, and fractionated in a way that will show the presence, or lack thereof, of macromolecular chlorophyll degradation products. Determining the source of macromolecular degradation products and how the phorbins are bound into the structure should provide insight into the transport of organic compounds to the sediments and preservation of organic compounds within sediments.

The discovery of pyropheophorbide steryl esters in both sediment and sediment trap samples has many implications for monitoring the cycle of producer species in a given location, and for biomarker studies. The results of the present studies suggest that the sterol distribution in the steryl esters reflects that produced in the overlying water column, but the source of the steryl esters and their mechanism of formation is still uncertain. To determine the source of these compounds, it will be necessary of collect samples of particulate matter in the photic zone and examine them for pyropheophorbide steryl esters. The samples will have to include phytoplankton, zooplankton, fecal pellets, and detrital material. For samples collected with sediment traps, fecal pellets will have to be removed and the remaining sample fractionated by size to isolate whole phytoplankton. Close examination of fecal pellet extracts will help determine if PSEs are produced as grazing products as suggested in Chs. 3 and 5, and examination of the less than 50 μm fraction will help to determine if these compounds are produced during senescence. Once the source of

the pyropheophorbide steryl esters is determined, the mechanism of formation can be examined.

The last suggestion for research follows directly from the mass balance studies of Ch. 6. The results of the sediment trap studies presented in Ch. 6 suggest that the chlorophyll degradation products which pass through the chemocline of the Black Sea, do not undergo further degradation in the water column, and therefore survive to be deposited in surface sediments. To determine if this mass balance is valid, it will be necessary to take sediment trap samples below the chemocline and at depth over the course of several years, and analyze them for total phorbin content and organic carbon. Measurements of integrated primary production and total chlorophyll production at regular intervals at the trap site will also be necessary to determine if the fraction of chlorophyll and organic carbon which pass through the chemocline is constant. With these measurements, and further measurements of sediment phorbin accumulation rates, it should be possible to test the mass balance, and to make further refinements to it.

This research project was undertaken in an attempt to answer the question of what happens to chlorophyll in anoxic sediments, and how this is related to the production of chlorophyll in the photic zone. In the process of researching this topic, the results have led us to ask many more questions than they have helped us answer. The above suggestions for further research will just begin to answer the questions posed by the results of this thesis.

III. REFERENCES

Baker, E.W., and J.W. Louda (1982) Geochemistry of tetrapyrrole, tetraterpenoid and perylene pigments in sediments from the Gulf of CA: DSDP Leg 64, Sites 474, 477, 479, and 481, and the SIO Guaymas Basin Survey Cruise Leg 3, Sites 10 and 18G, In: *Initial Reports of the Deep Sea Drilling Project* **64**: Washington (U.S. Govt. Printing Office), 789-814.

Baker E.W., and Louda J.W. (1986) Porphyrins in the geological record. In: Biological Markers in the Sedimentary Record. (R. B. Johns, ed.) , 125-225.

Bathmann U. and Liebezeit G. (1986) Chlorophyll in copepod faecal pellets: Changes in pellet numbers and pigment content during a declining Baltic spring bloom. *Mar. Ecol.* **7**, 59-73.

Bianchi T.S., Dawson R., and Sawangwong P. (1988) The effects of macrobenthic deposit-feeding on the degradation of chloropigments in sandy sediments. *J. Exp. Mar. Biol. Ecol.* **122**, 243-355.

Blumer, M., and Rudrum, M. (1970) High molecular weight fossil porphyrins: Evidence for monomeric and dimeric tetrapyrroles of about 1100 molecular weight, *J. Inst. Petr.* **56**, 99-106.

Blumer M. and Snyder W. D. (1967) Porphyrins of high molecular weight in a Triassic oil shale: Evidence by gel permeation chromatography. *Chem. Geo.* **2**, 35-45.

Boon J.J., Rijpstra W.I.C., de Lange F., and de Leeuw J.W. (1979) Black Sea sterol -- a molecular fossil for dinoflagellate blooms. *Nature* **277**, 125-127.

Brown S. R., Daley R. J., and McNeely R. N. (1977) Composition and stratigraphy of the fossil phorbin derivatives of Little Round Lake, Ontario. *Limnol. Oceanogr.* **22**, 336-348.

Burkhill P. H., Mantoura R. R. C., Llewellyn C. A., and Owens N. J. P. (1987) Microzooplankton grazing and selectivity of phytoplankton in coastal waters. *Mar. Bio.* **93**, 581-590.

Cronin J.R. and Morris R.J. (1982) The occurrence of high molecular weight humic material in recent organic-rich sediment from the Nambian Shelf. *Esturine, Coastal and Shelf Sciences* **15**, 17-27.

Czeczuga B. (1964) Quantitative changes in sedimentary chlorophyll in the bed sediment of the Mikolajki Lake during the post-glacial period. *Hydrologie* **27**, 88-98.

Daley R.J., Brown S.R., and McNeely R.N. (1977) Chromatographic and SCDP measurements of fossil phorbins and the postglacial history of Little Round Lake, Ontario. *Limnol. Oceanogr.* **22**, 349-360.

Downs, J.N. (1989), Implications of the phaeopigment, carbon and nitrogen content of sinking particles for the origin of export production. Ph. D. dissertation, University of Washington.

Ertel J.R. and Hedges J.I. (1983) Bulk chemical and spectroscopic properties of marine and terrestrial humic acids, melanoidins and catechol-based synthetic polymers. In *Aquatic and Terrestrial Humic Materials* (Ed. R. F. Christman and E. T. Gjessing). pp 143-163, Ann Arbor Science.

Eyssen H. J., Parmentier G. G., Compernolle G. C., De Pauw G., and Piessens-Denef M. (1973) Biohydrogenation of sterols by *Eubacterium* ATCC 21,408 -- *Nova* Species. *Eur. J. Biochem.* **36**, 411-421.

Fogg G.E. and Belcher J.H. (1961) Pigments from the bottom deposits of an English lake. *New Phycol.* **23**, 129-142.

Furlong E.(1986) Sediment geochemistry of photosynthetic pigments in oxic and anoxic marine and lacustrine sediments: Dabob Bay, Saanich Inlet, and Lake Washington. Ph.D. dissertation, University of. Washington.

Furlong E., and Carpenter S.R. (1988) Pigment preservation and remineralization in oxic coastal marine sediments. *Geochim. Cosmochim. Acta* **52**, 87-100.

Gagosian R.B., Smith S.O., Lee C.L., Farrington J.W., and Frew N.E. (1980) Steroid transformations in recent marine sediments. In: Advances in Organic Geochemistry 1979 (Ed. A.G. Douglas and J.R. Maxwell) pp. 407-419.

Gaskel S. J. and Eglinton G. (1975) Rapid hydrogenation of sterols in a contemporary lacustrine sediment. *Nature* **254**, 209-211.

Gaskel S. J. and Eglinton G. (1976) Sterols of a contemporary lacustrine sediment. *Geochim. Cosmochim. Acta* **40**, 1221-1228.

Gillan F.T. and Johns R.B. (1980) Input and early diagenesis of chlorophyll in a temperate intertidal sediment. *Mar. Chem.* **9**, 243-253.

Gorham E. (1961) Chlorophyll derivatives, sulphur, and carbon in sediment cores from two English lakes. *Can. J. Botany* **39**, 333-338.

Guilizzoni F., Bonomi G., Balanit G., and Ruggiu D. (1983) Relationship between sedimentary pigments and primary production: evidence from core analyses of twelve Italian lakes. *Hydorbiologia* **103**, 103-106.

Hawkins A.J.S., Bayne B.L., Mantoura R.F.C., and Llewllyn C.A. (1986) Chlorophyll degradation and absorption throughout the digestive system of the blue mussel *Mytilus edulis* L. *J. Exp. Biol. Ecol.* **96**, 213-223.

Hurley J. P., and Armstrong D. E. (1990) Fluxes and transformations of aquatic pigments in Lake Mendota, Wisconsin. *Limnol. Oceanogr.* **35**, 384-398.

Hurley J.P. and Armstrong D.E. (1991) Pigment preservation in lake sediments: A comparison of sedimentary environments in Trout Lake, Wisconsin. *Can. J. Fish. Aquat. Sci.* **48**, 472-486.

Keely, B.J. (1989) Early diagenesis of chlorophyll and chlorin pigments. Ph.D. dissertation, University of Bristol.

Keely, B.J., and Brereton R.G. (1986), Early chlorin diagenesis in a recent aquatic sediment, *Org. Geochem.* **10**, 975-980.

Keely, B.J., Brereton, R.G., and Maxwell, J.R. (1988), Occurrence and significance of pyrochlorins in lake sediment, Advances in Organic Geochemistry 1987, *Org. Geochem.*, **13**, 801-805.

Keely, B.J., Prowse, W.G., and Maxwell, J.R. (1990), The Treibs Hypothesis: An evaluation based on structural studies, *Energy Fuels*, **4**, 628-634.

Klein B., W.W.C. Gieskes, and G.G. Kraay (1986) Digestion of chlorophylls and carotenoids by the marine protozoan Oxyrrhis marina studied by HPLC analysis of algal pigments, *J Plankton Res*, **8**, 827-836.

Lopez M.D.G., Huntley M.E., and Sykes P.F. (1988) Pigment destruction by *Calanus pacificus*: impact on the estimation of water column fluxes. *J. Plank. Res.* **10**, 715-734.

Lorenzen C.J. (1974) Chlorophyll-degradation products in sediments of Black Sea. In: The Black Sea -- Geology, Chemistry, and Biology (E. Degens and D. A. Ross, eds.). *Mem. Am. Assoc. Pet. Geol.* **20**, 426-428.

Mayzaud P. and Razouls S. (1992) Degradation of gut pigment during feeding by a subantarctic copepod: Importance of feeding history and digestive acclimation. *Limnol. Oceanogr.* **37**, 393-404.

Mycke B. and Michaelis W. (1986) Molecular fossils from chemical degradation of macromolecular organic matter. *Org. Geochem.* **10**, 847-858.

Nishimura M. (1978) Geochemical characteristics of the high reduction zone of stenols in Suwa sediments and the environmental factors controlling the conversion of stenols into stanols. *Geochim. Cosmochim. Acta* **42**, 349-357.

Nishimura M. and Koyama T. (1977) The occurrence of stanols in various living organisms and the behavior of sterols in contemporary sediments. *Geochim. Cosmochim. Acta* **41**, 379-385.

Orr, W.L., K.O. Emery, and J.R.Grady (1958), Preservation of chlorophyll derivatives in sediments off Southern California, *Bull. Amer. Assoc. Petrol. Geo.*, **42**, 925-958.

Pasternak A.F. and Drits A.V. (1988) Possible degradation of chlorophyll-derived pigments during gut passage of herbivorous copepods. *Mar. Ecol. Prog. Ser.* **49**, 187-190.

Penry D.L., and Frost B.W. (1991) Chlorophyll *a* degradation by *Calanus pacificus*: Dependence on ingestion rate and digestive acclimation to food resources. *Limnol. Oceanogr.* **36**, 147-159.

Prowse W. G. and Maxwell J. R. (1991) High molecular weight chlorins in a lacustrine shale. *Org. Geochem.* **17**, 877-886.

Poutanen E.-L. and Morris R. J. (1983) The occurrence of high molecular weight humic compounds in the organic-rich sediments of the Peru continental shelf. *Oceanol Acta* **6**, 21-28.

Repeta D.J. and Simpson D.J. (1991) The distribution and recycling of chlorophyll, bacteriochlorophyll and carotenoids in the Black Sea. *Deep-Sea Res.* **38 suppl. 2**, S969-S984.

Richnow H.H., Jenisch A., and Michaelis W. (1991) Structural investigations of sulphur rich kerogens and macromolecular oil fractions by sequential chemical degradation. European Association of Organic Geochemists, 15th International Meeting. Programme and Abstracts, p 28.

Roy S., Harris R.P., and Poulet S.A. (1989) Inefficient feeding by *Calanus Helgolandicus* and *Temora longicornis* on *Coscinodiscus wailesii*: quantitative estimation using chlorophyll-type pigments and effects on dissolved free amino acids. *Mar. Ecol. Prog. Ser.* **52**, 145-153.

Sato S. (1980) Diagenetic alteration of organic matter in leg 57 sediments, deep sea drilling project. In *Initial Reports of the Deep Sea Drilling Project* (Ed. Scientific Party), Vol. 61-62, pp 1305-1312. U.S. Government Printing Office.

Shuman F.R., and Lorenzen C.J. (1975) Quantitative degradation of chlorophyll by a marine herbivore. *Limno. Oceano.* 20, 580-586.

SooHoo J.B., and Kiefer D.A. (1982a) Vertical distribution of phaeopigments--I. A simple grazing and photooxidative scheme for small particles, *Deep-Sea Res.* **29**, 1539-1551.

SooHoo J.B., and Kiefer D.A. (1982b) Vertical distribution of phaeopigments--II. Rates of production and kinetics of photooxidation. *Deep-Sea Res.* **29**, 1553-1563.

Swain E.B. (1985) Measurement and interpretation of sedimentary pigments. *Freshwater Biol.* **15**, 53-75.

Treibs, A. (1936) Chlorophyll- und Haeminderivate in organischen mineralstoffen. *Angewandte Chemie* **49**, 682-686.

Vernet, M., and Lorenzen C.J. (1987) The relative abundance of pheophorbide-a and pheophytin-a in temperate marine waters. *Limn. Ocean*, **32**, 352-358.

Wakeham S. G. and Beier J. A. (1991) Fatty acid and sterol biomarkers as indicators of particulate matter source and alteration processes in the Black Sea. *Deep-Sea Res.* **38, Suppl.2**, S943-S968.

Welschmeyer, N.A., and Lorenzen C.J. (1985) Chlorophyll budgets: Zooplankton grazing and phytoplankton growth in a temperate fjord and the Central Pacific Gyres. *Limnol. Oceanogr.* **30**, 1-21.

Wolff G.A., Lamb N.A., and Maxwell J.R. (1986) The origin and fate of 4-methyl steroids -- II. Dehydration of stanols and occurrence of C_{30} 4-methyl steranes. *Org. Geochem.* **10**, 965-974.

Yacobi Y.Z., Mantoura R.F.C, and Llewellyn C.A. (1991) The distribution of chlorophylls, carotenoids and their breakdown products in Lake Kinneret (Israel) sediments. *Freshwater Biol.* **26**, 1-10.

Yentsh C.S. (1965) Distribution of chlorophyll and phaeophytin in the open ocean. *Deep-Sea Res.* **12**, 653-666.

APPENDIX I

THE SPECTRA OF CHLOROPHYLL-*A* AND CHLOROPHYLL-*B* AND THEIR DEGRADATION PRODUCTS

Appendix I

THE SPECTRA OF CHLOROPHYLL-*A* AND CHLOROPHYLL-*B* AND THEIR DEGRADATION PRODUCTS

Here we present the visible, infrared, mass, and nuclear magnetic resonance spectra of each of the authentic chlorophylls and degradation products either isolated or synthesized in Ch. 2. With the exception of the hydrogen chemical ionization mass spectra, the tabulated data is presented in Ch. 2 with an explanation of the spectra. For each of the 10 compounds analyzed, this appendix contains three pages of spectra. The first page presents the molecular structure, molecular formula, molecular weight, visible spectrum, and the infrared spectrum. The second page presents the methane and hydrogen chemical ionization mass spectra, and the third page shows the nuclear magnetic resonance spectrum. For a few of the compounds, mass spectra or infrared spectra are missing, due to difficulties in volatilizing the sample in the case of the missing mass spectra, and to instrumentation problems in the case of the missing infrared spectra.

For the hydrogen chemical ionization mass spectra, each major ion represents either tetra (m/e = 500 - 550), tri (m/e = 300 - 370), di (m/e = 200 - 270), or mono (m/e = 100 - 150) pyrole contained fragments of the parent compound. Ions for tripyroles are not seen in these spectra. For the tri, di, and mono pyrole fragments, four groups of ions appear, one each for the four possible combinations of the presence or lack of meso carbons. The quanlity of these spectra is generally low.

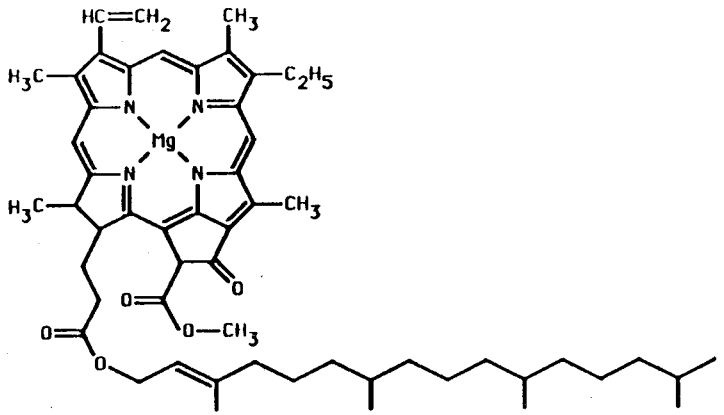

Chlorophyll-a

$C_{55}H_{72}N_4O_5Mg$

893.50

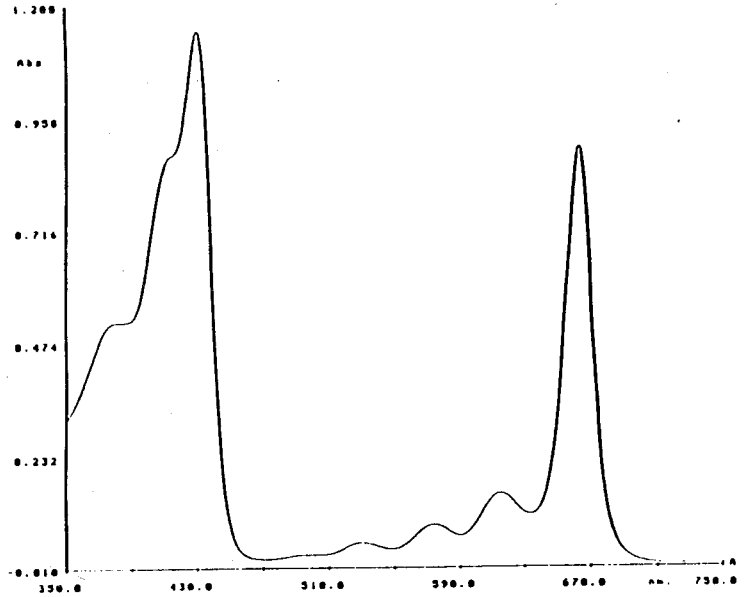

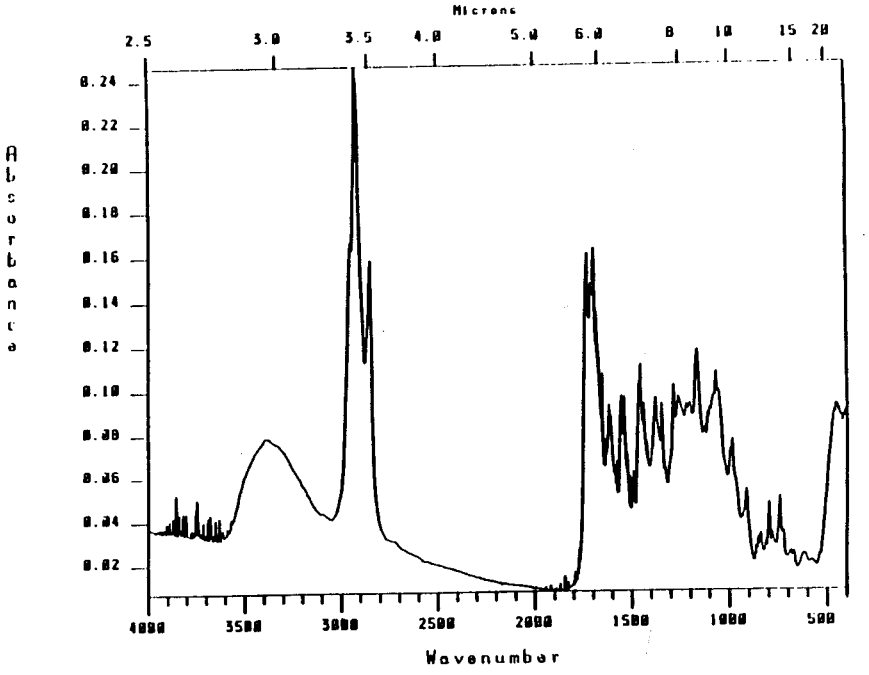

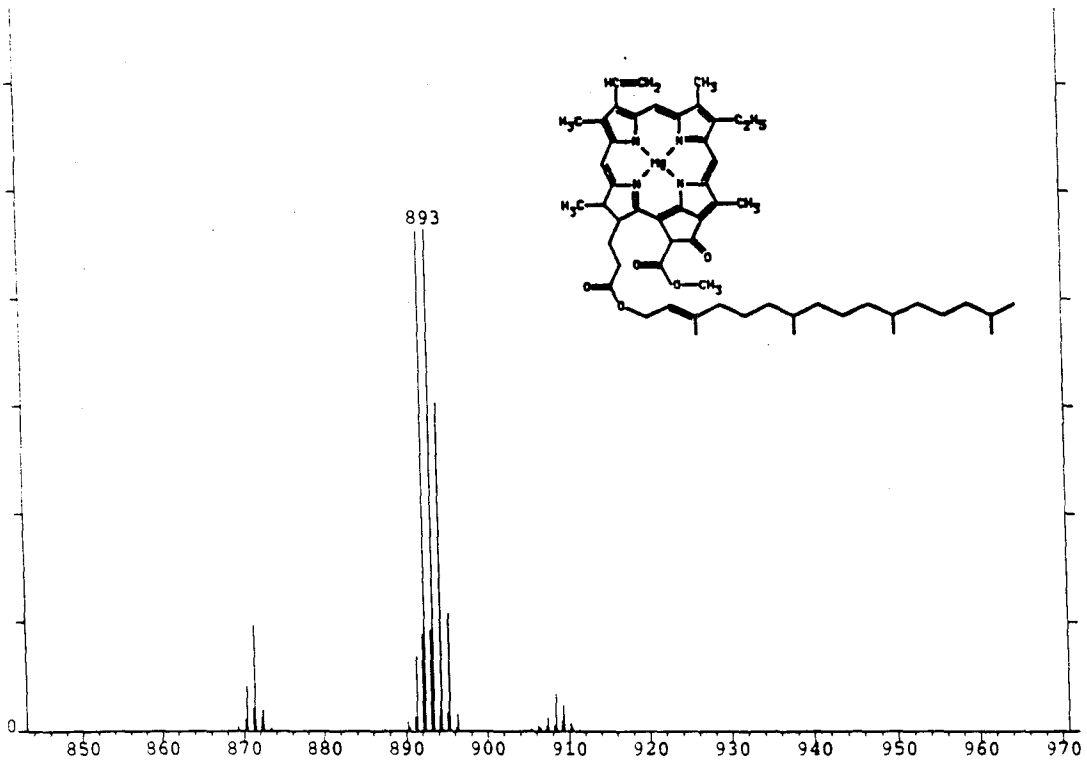

fast-atom bombardment

CHLOROPHYLL-A/C3D6O

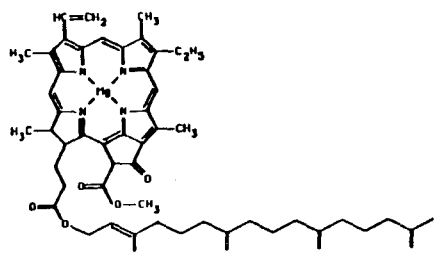

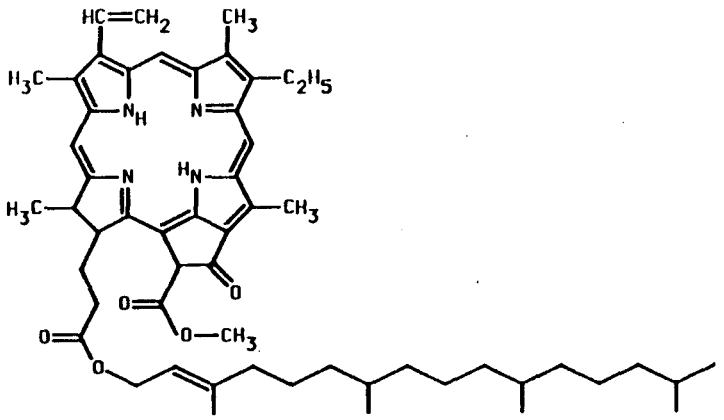

Pheophytin-a

$C_{55}H_{74}N_4O_5$

871.21

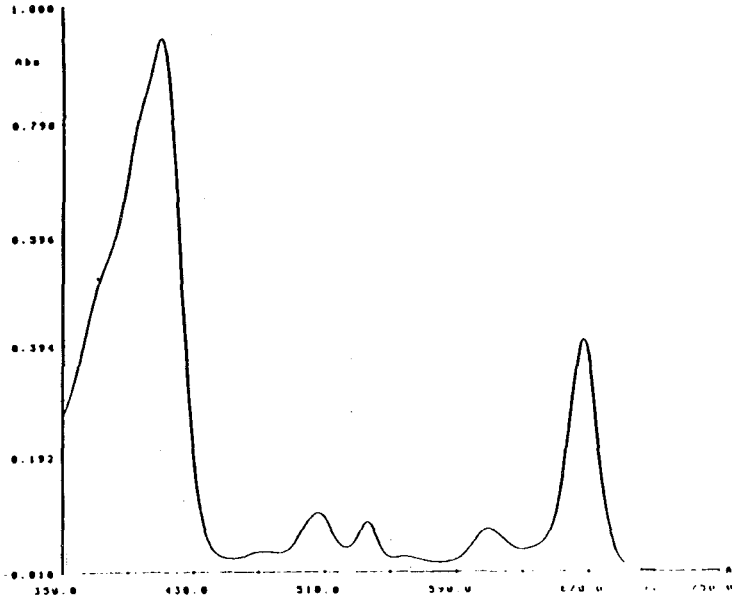

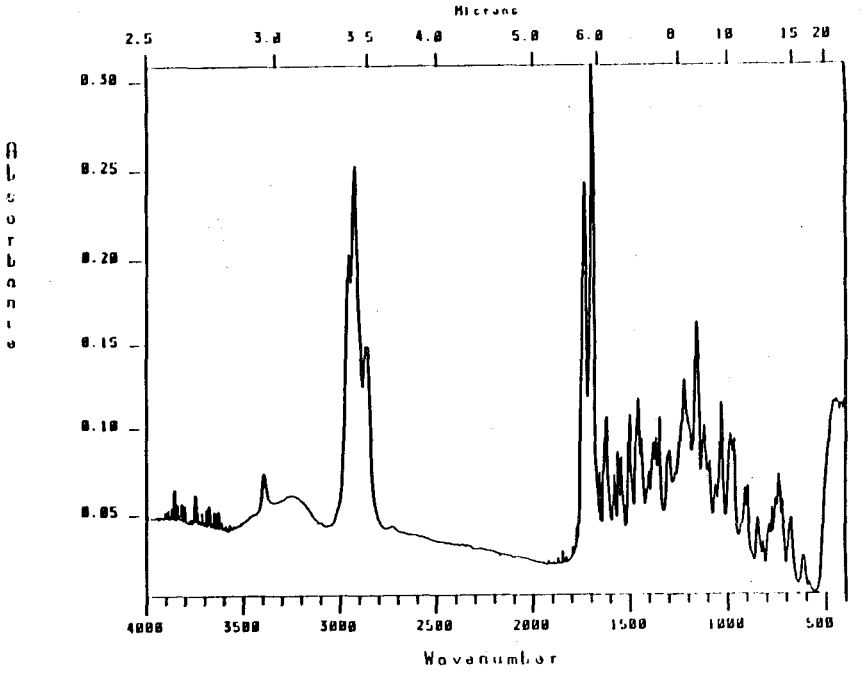

PHEOPHYTIN-A

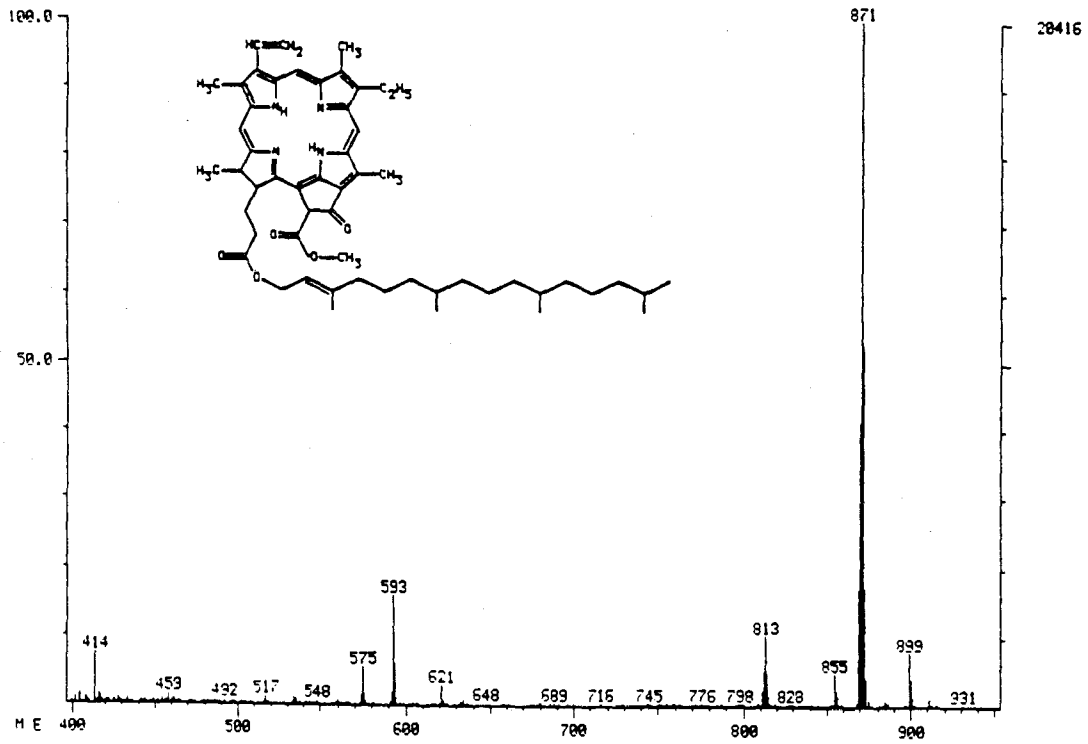

methane chemical ionization

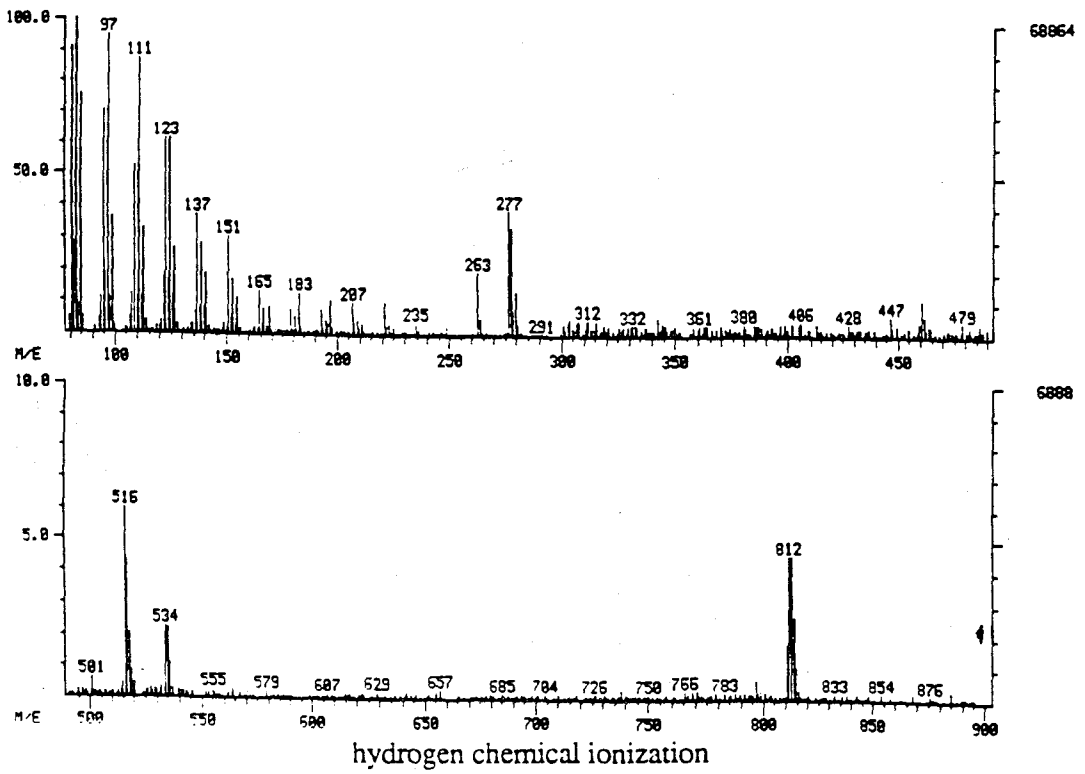

hydrogen chemical ionization

PHEOPHYTIN-A / C_6D_6

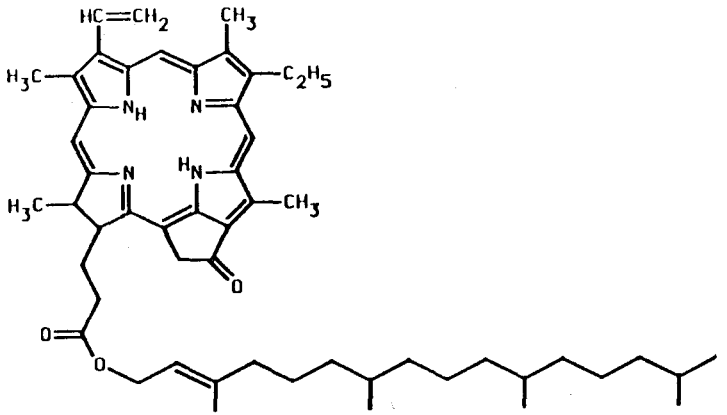

Pyropheophytin-a

$C_{53}H_{72}N_4O_3$

813.18

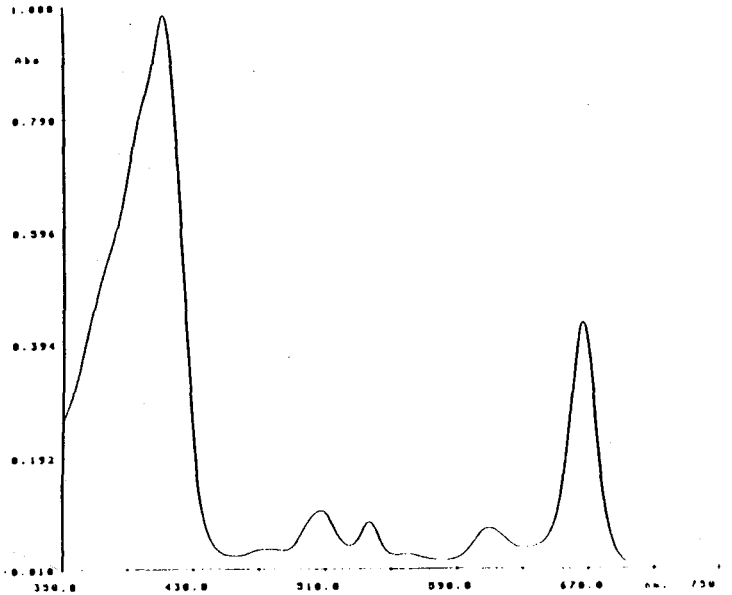

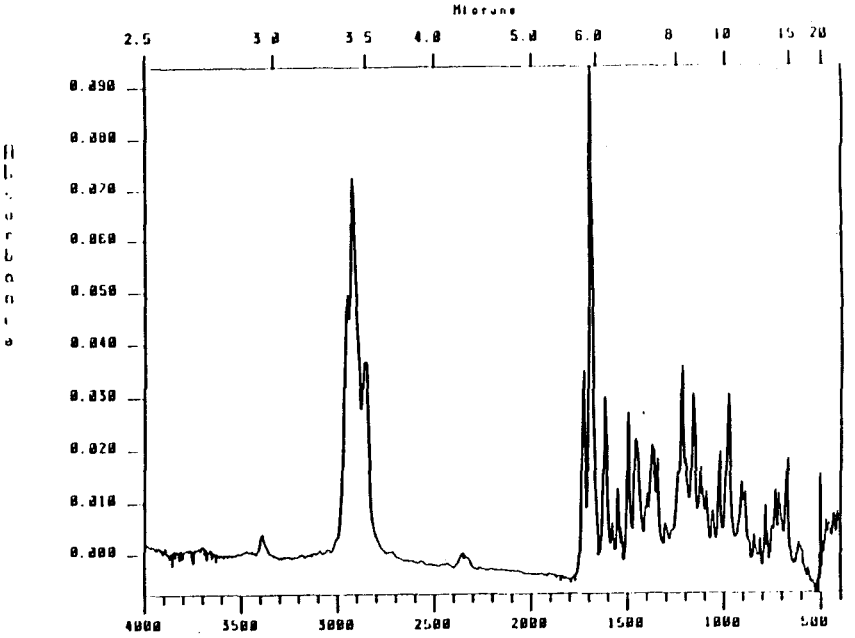

PYROPHEOPHYTIN-A

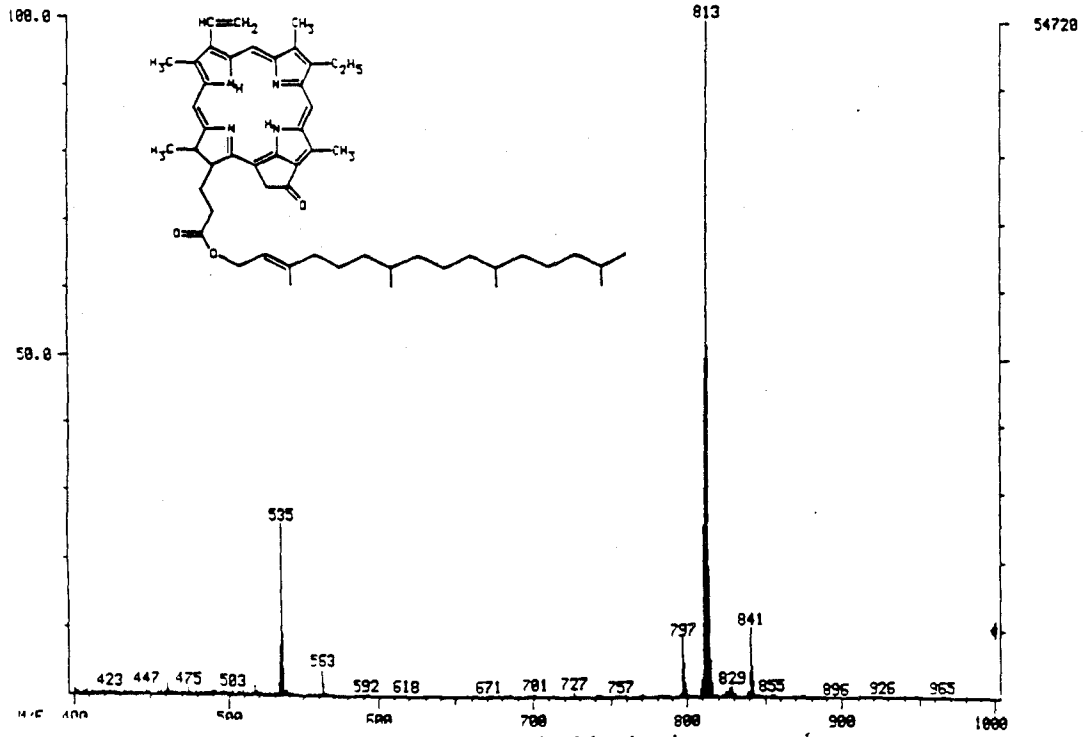

methane chemical ionization

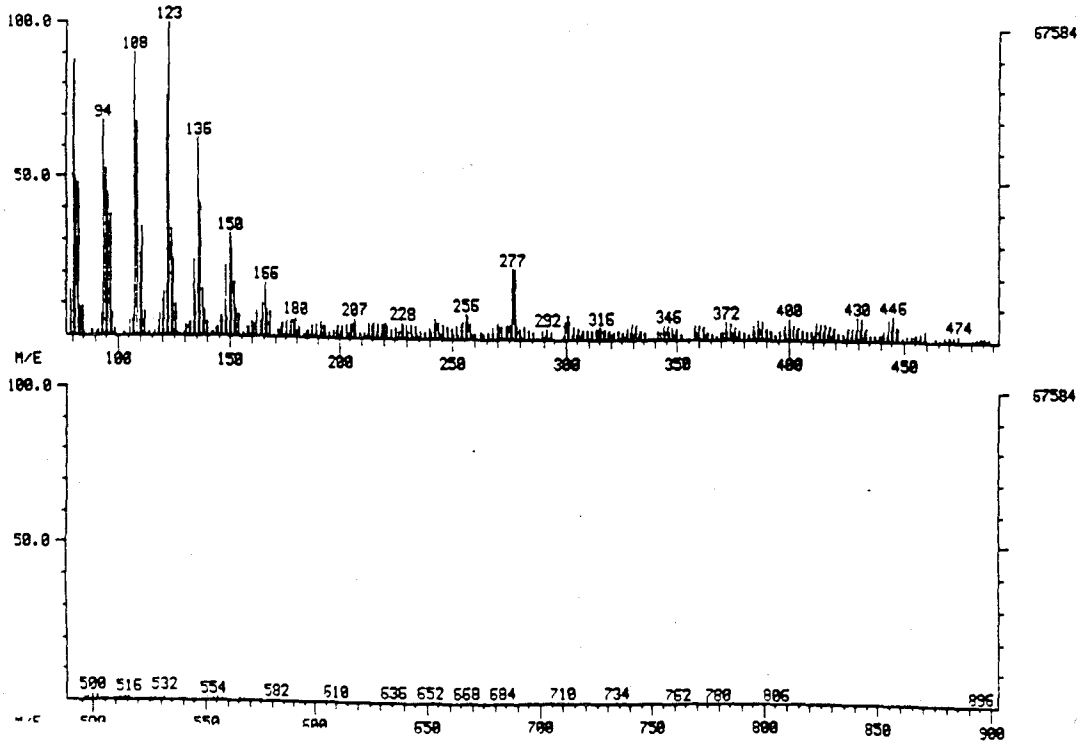

hydrogen chemical ionization

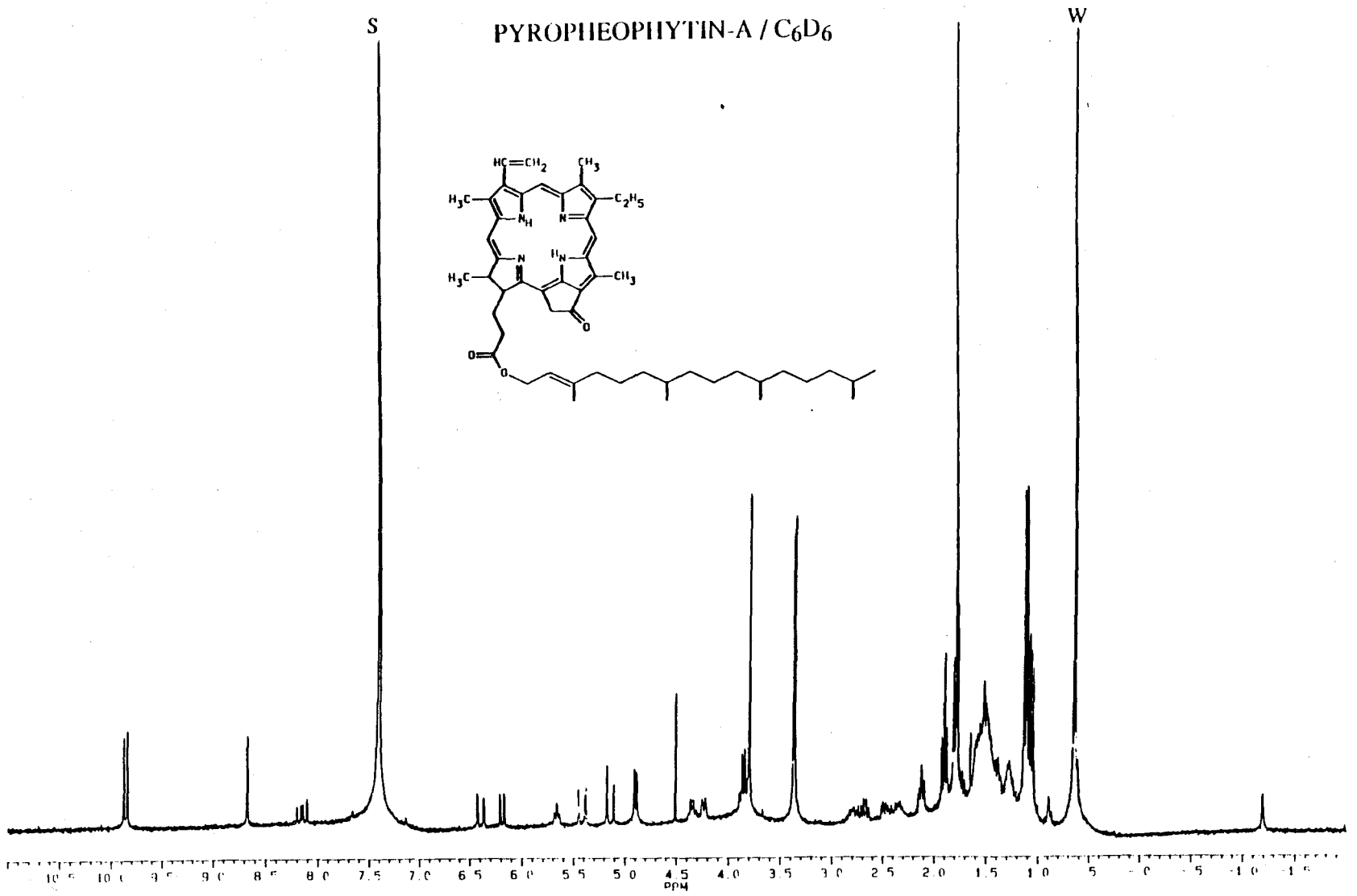
PYROPHEOPHYTIN-A / C_6D_6
S
W
ppm

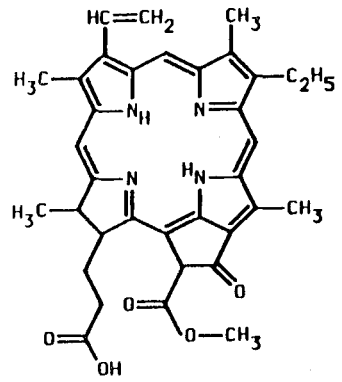

Pheophorbide-a

$C_{35}H_{36}N_4O_5$

592.69

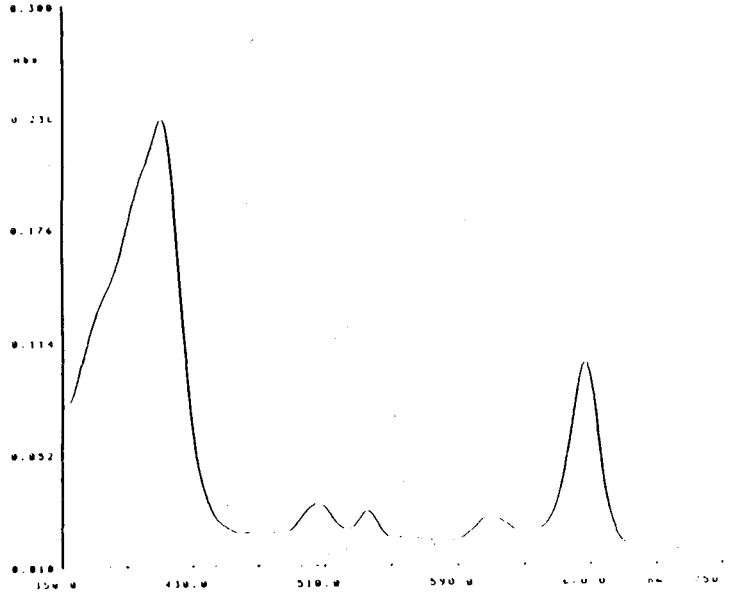

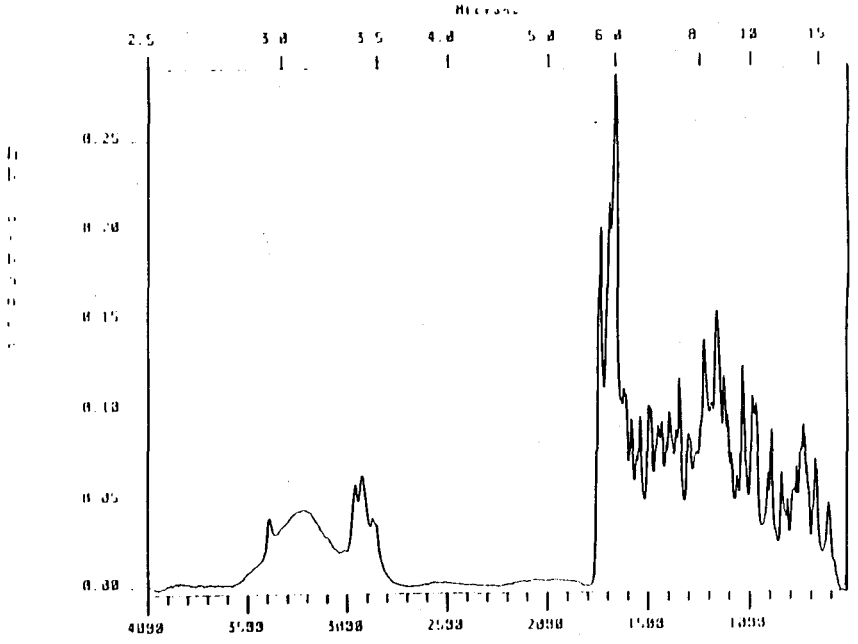

PHEOPHORBIDE-A

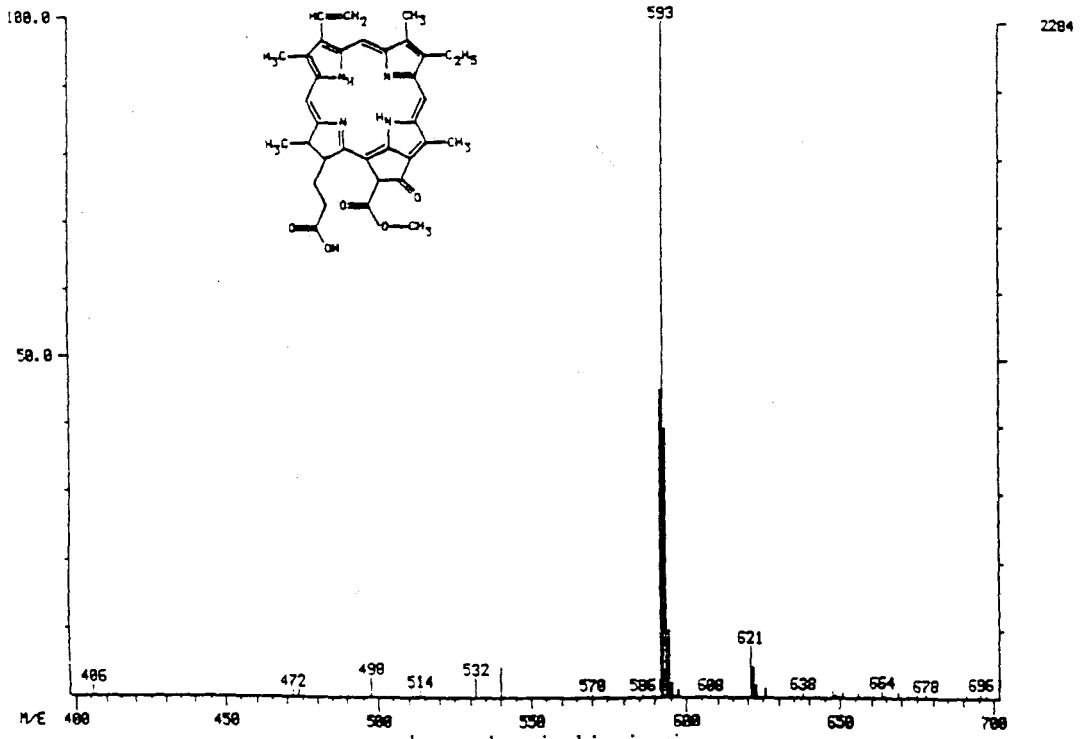

methane chemical ionization

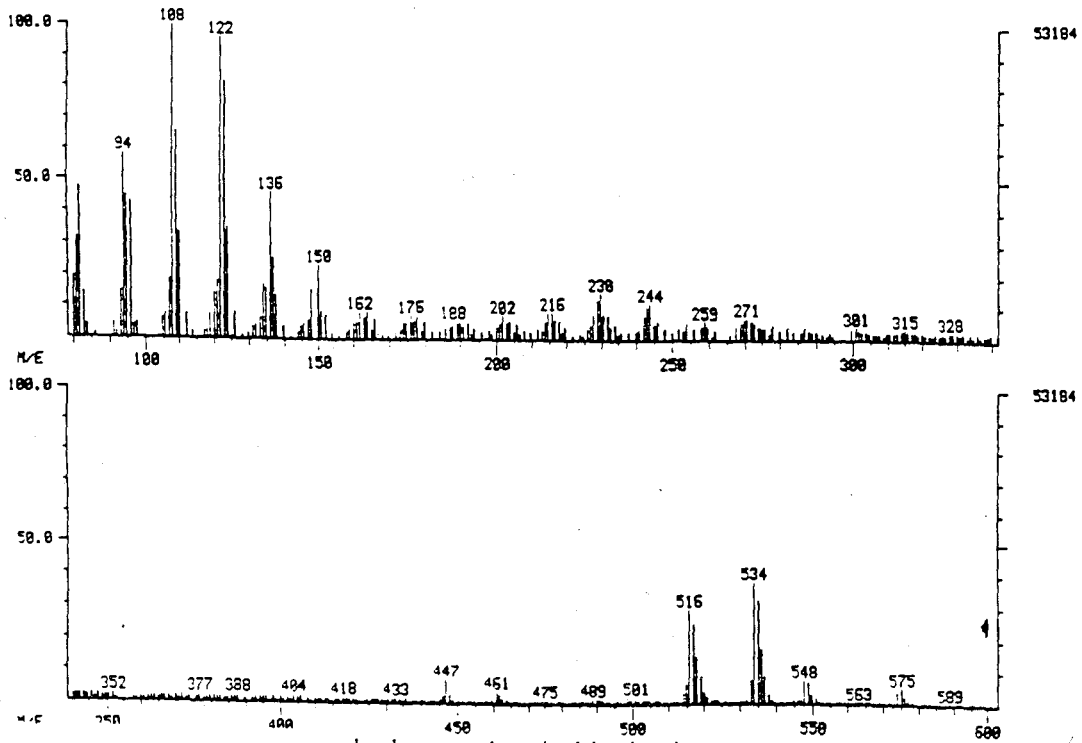

hydrogen chemical ionization

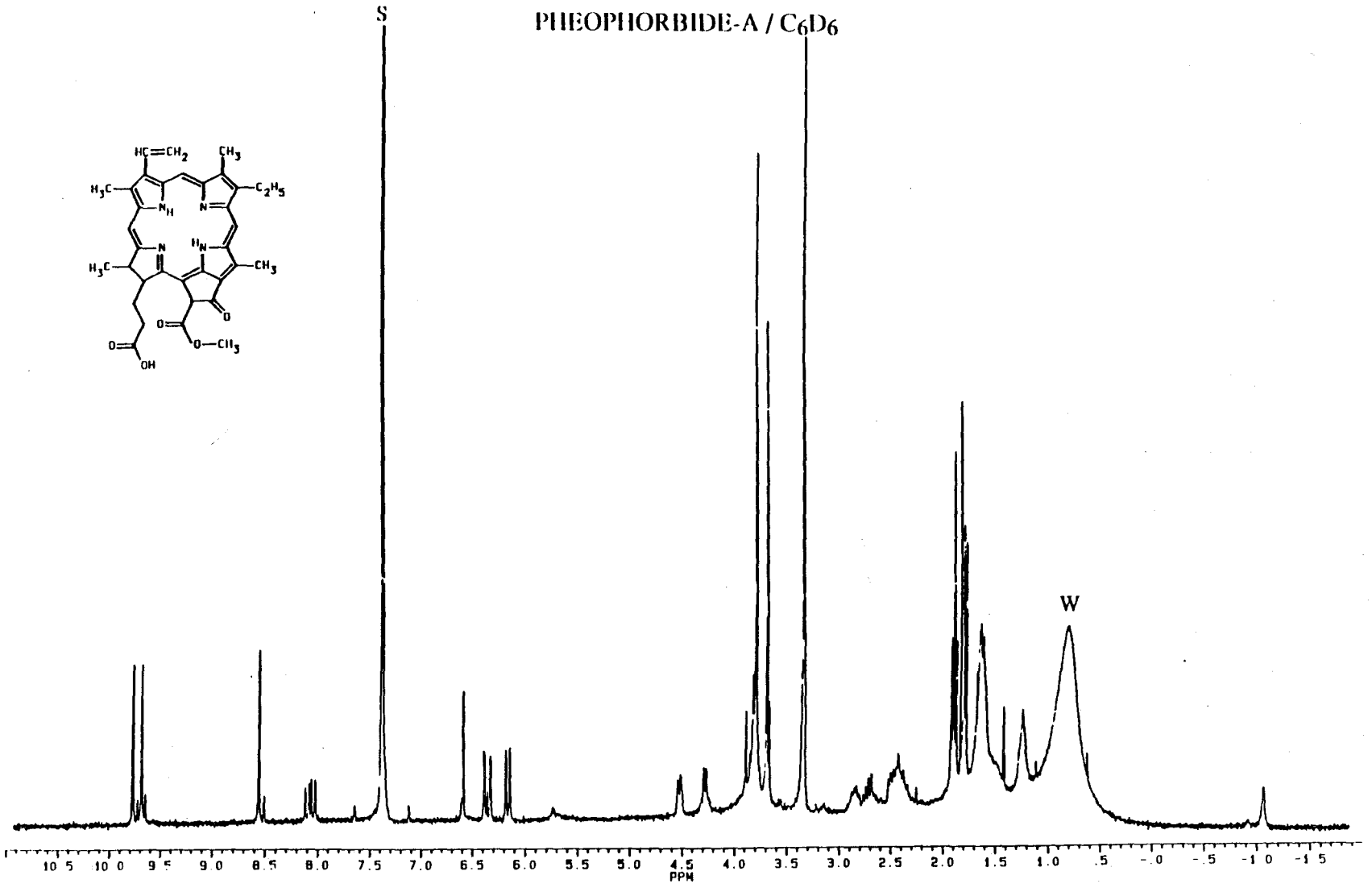
PHEOPHORBIDE-A / C6D6
S
W
HC=CH2
CH3
H3C
C2H5
NH
N
N
HN
H3C
CH3
O
O
O—CH3
O
OH
10.5 10.0 9.5 9.0 8.5 8.0 7.5 7.0 6.5 6.0 5.5 5.0 4.5 4.0 3.5 3.0 2.5 2.0 1.5 1.0 .5 -.0 -.5 -1.0 -1.5
PPM

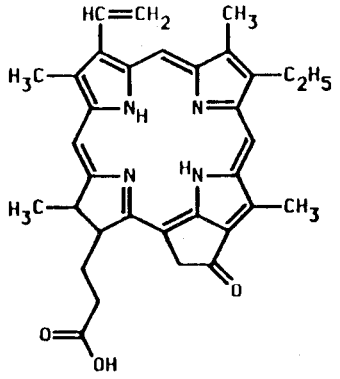

Pyropheophorbide-a

$C_{33}H_{34}N_4O_3$

534.66

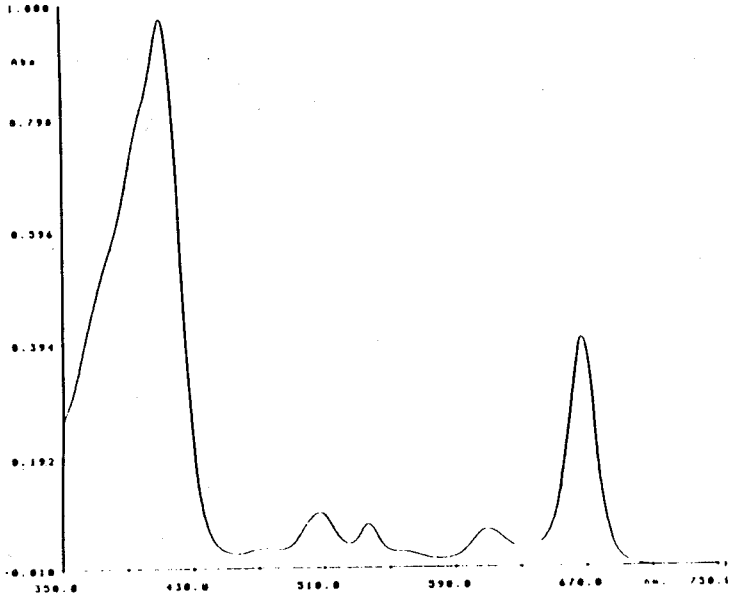

PYROPHEOPHORBIDE-A

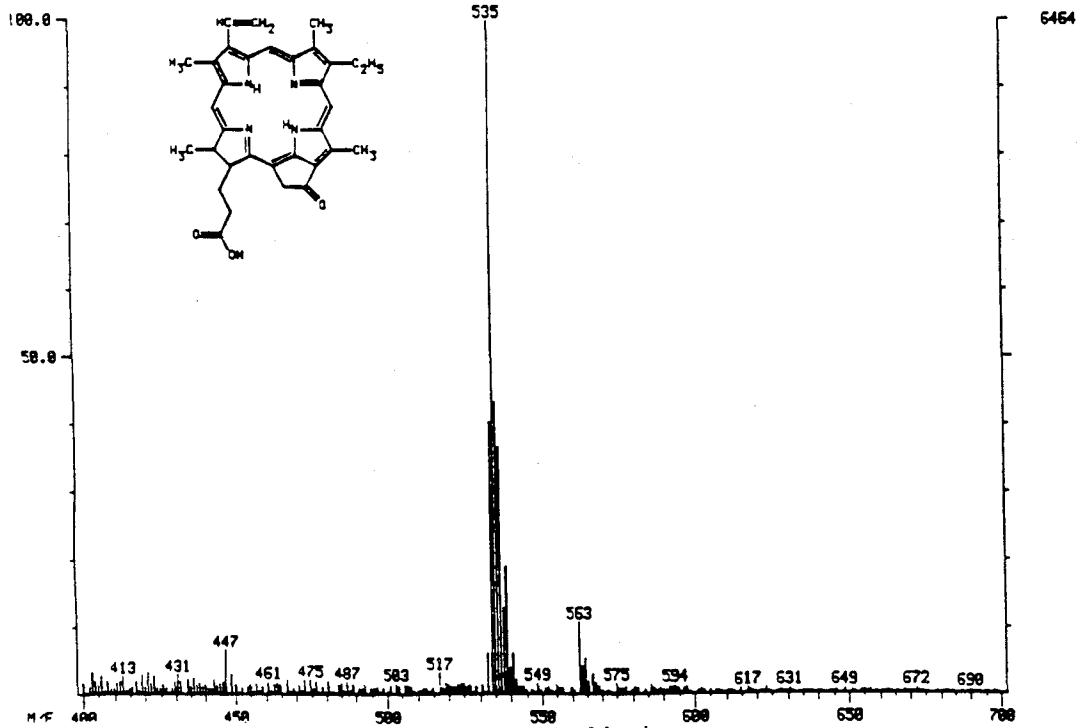

methane chemical ionization

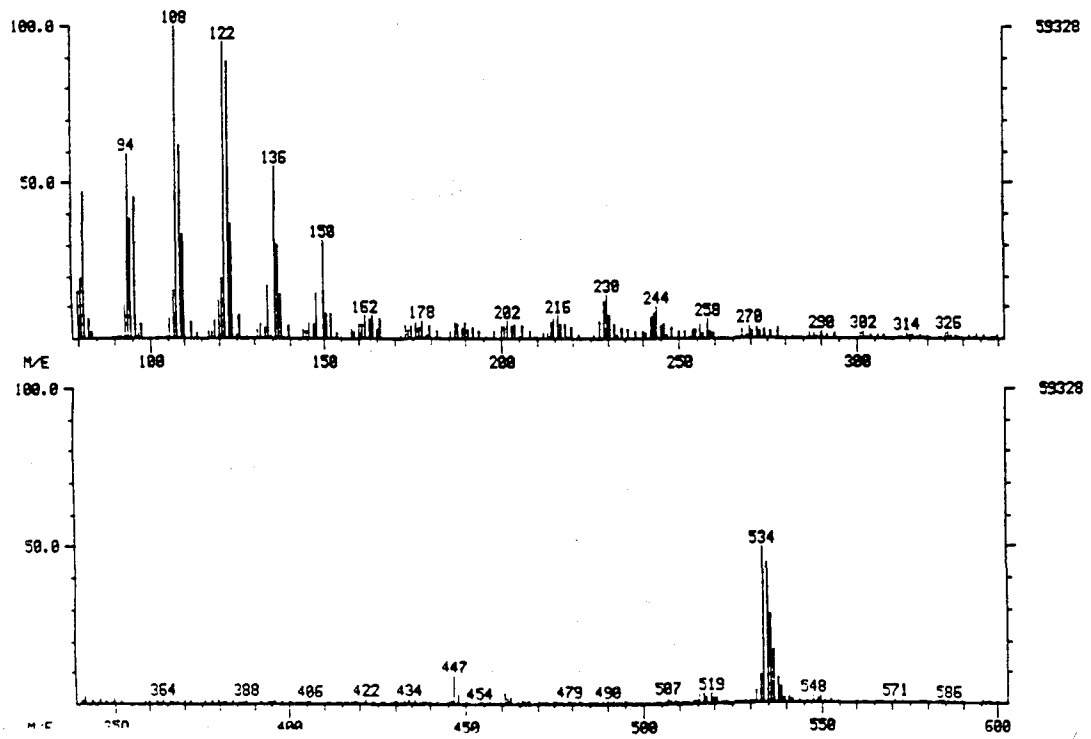

hydrogen chemical ionization

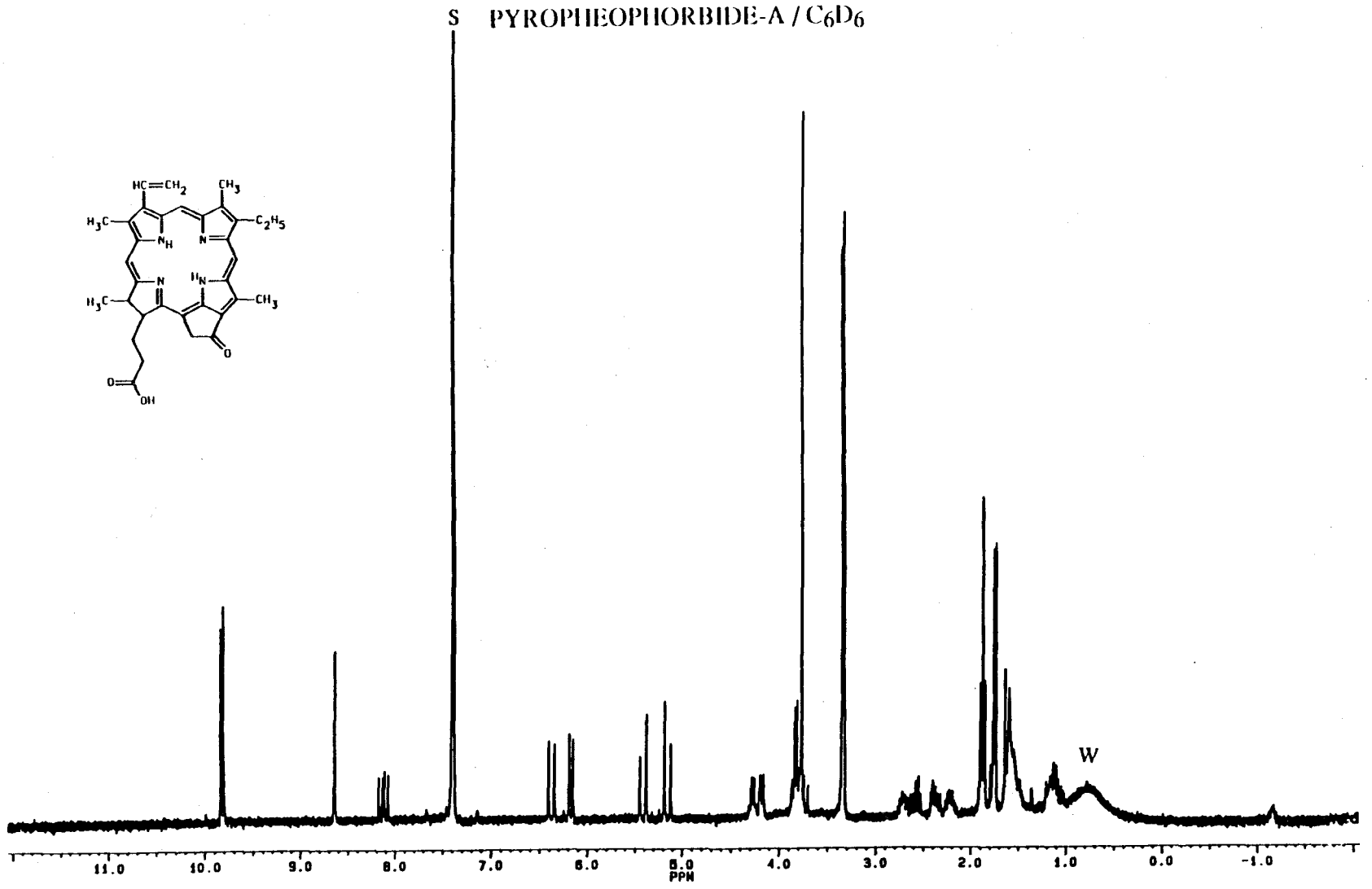
S
PYROPHEOPHORBIDE-A / C_6D_6
W
11.0
10.0
9.0
8.0
7.0
6.0
5.0
PPM
4.0
3.0
2.0
1.0
0.0
-1.0

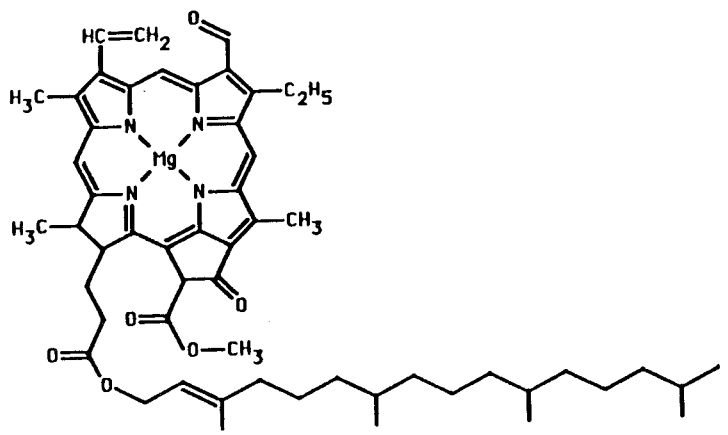

Chlorophyll-b

$C_{55}H_{70}N_4O_6Mg$

MW = 907.49

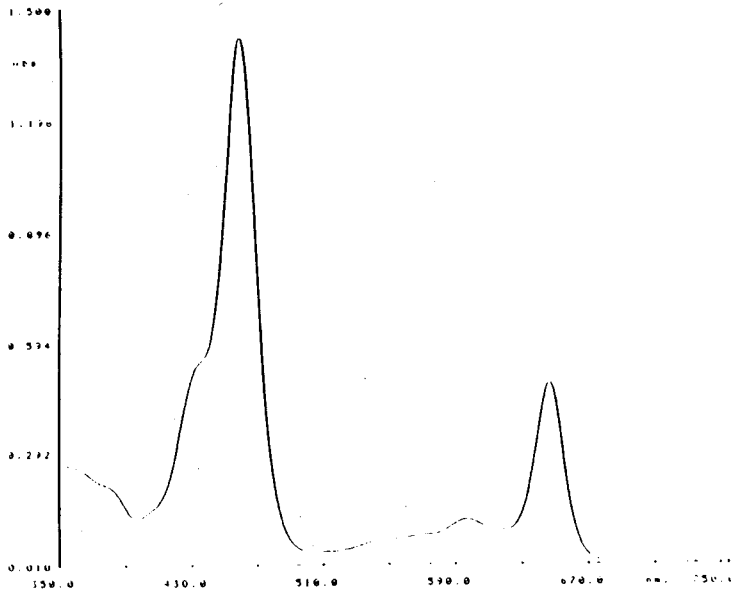

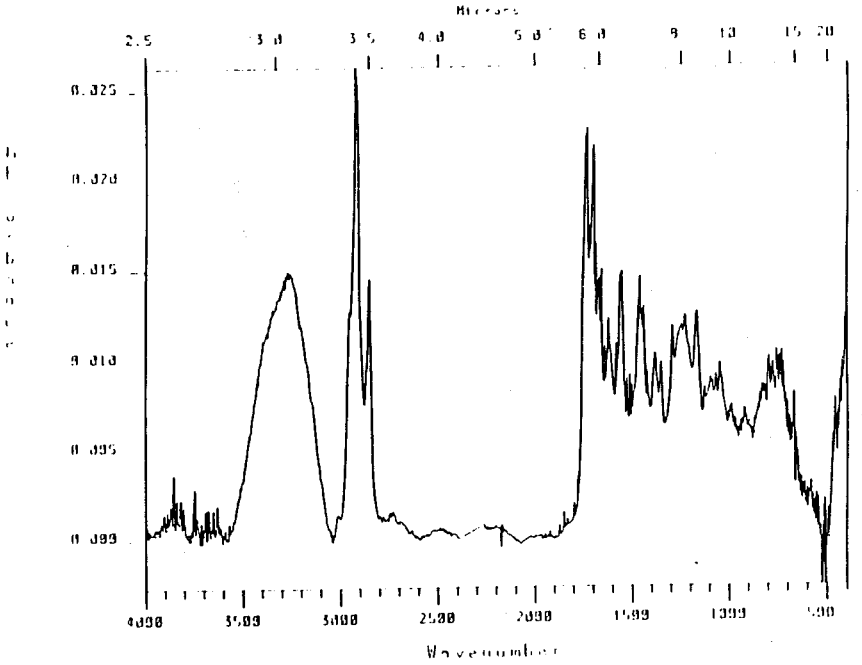

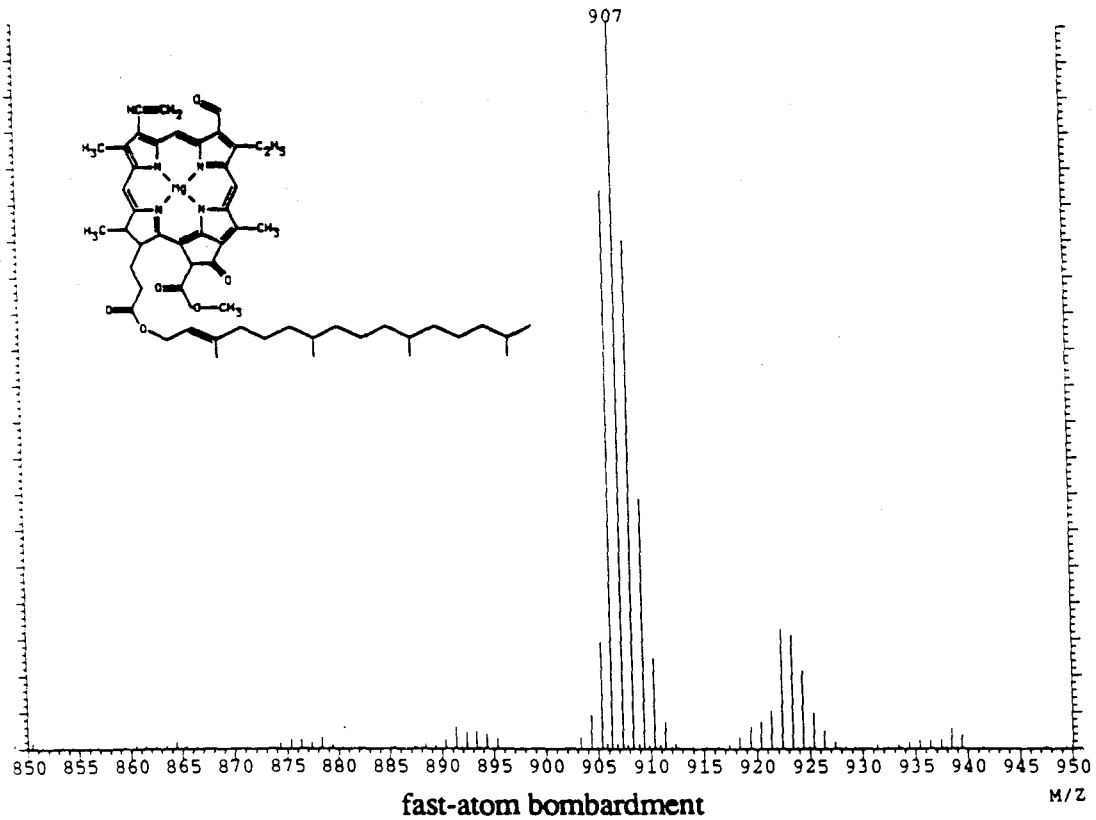

fast-atom bombardment

CHLOROPHYLL-B / Cp26

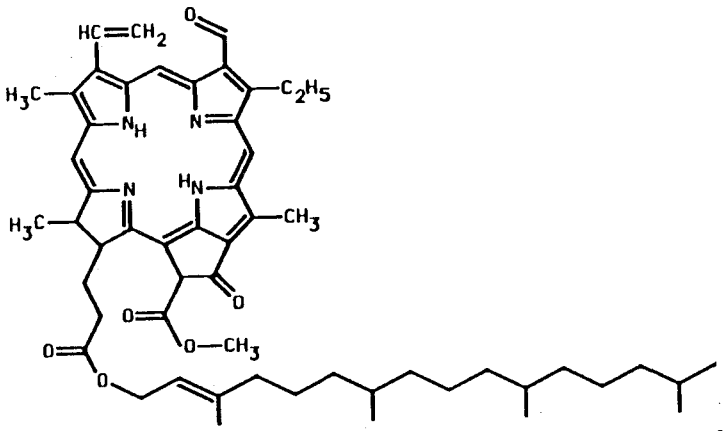

Pheophytin-b

$C_{55}H_{72}N_4O_6$

MW = 885.20

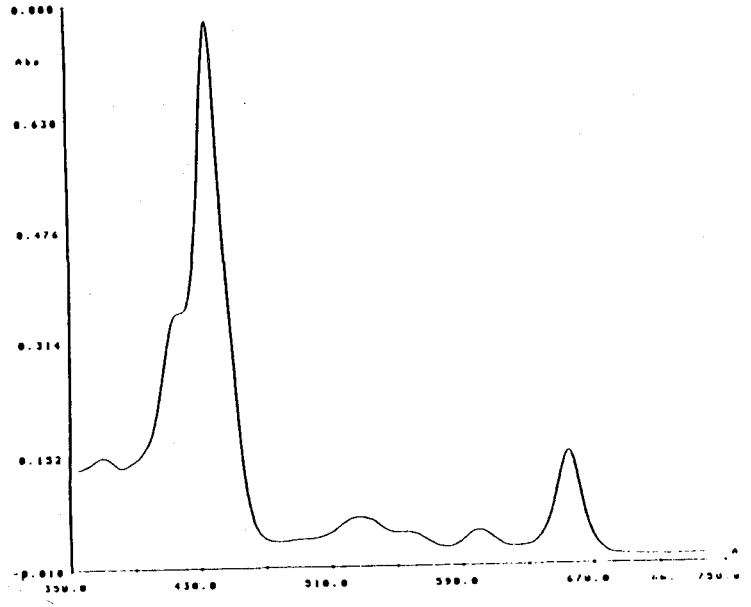

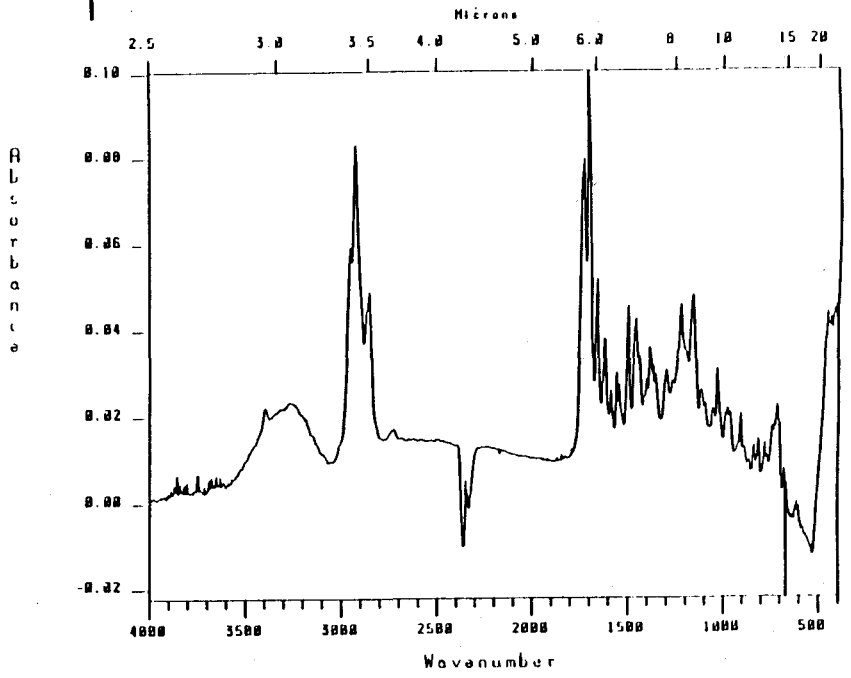

PHEOPHYTIN-B

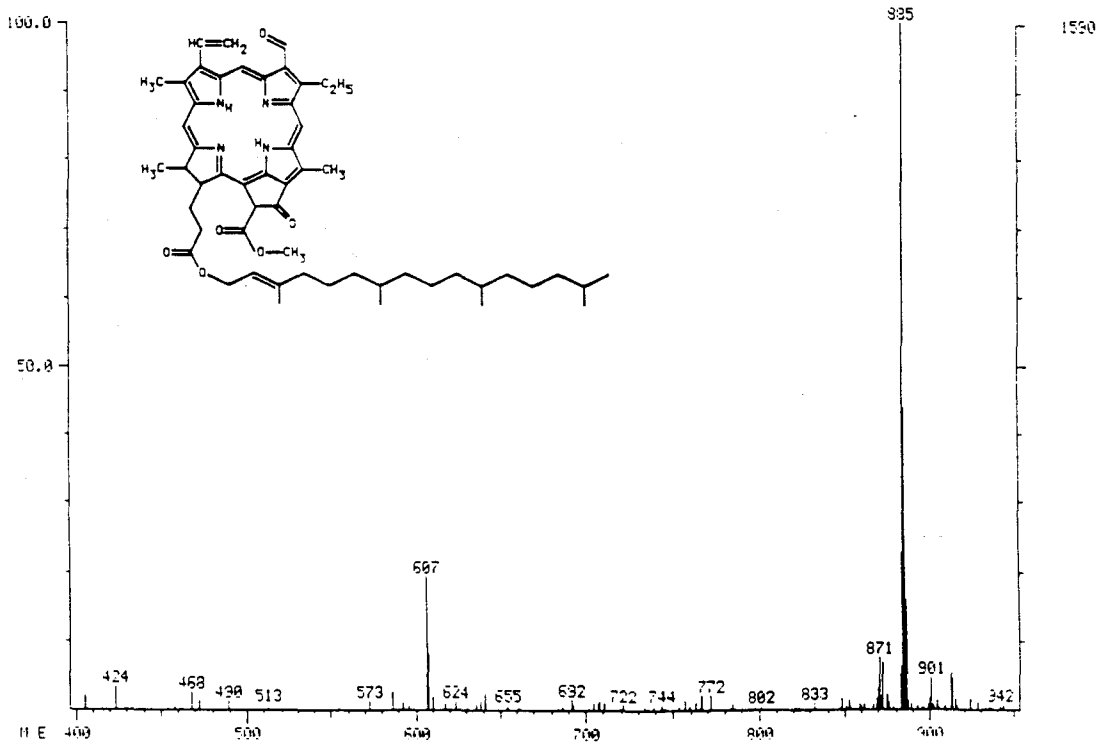

methane chemical ionization

PHEOPHYTIN-B / C_6D_6

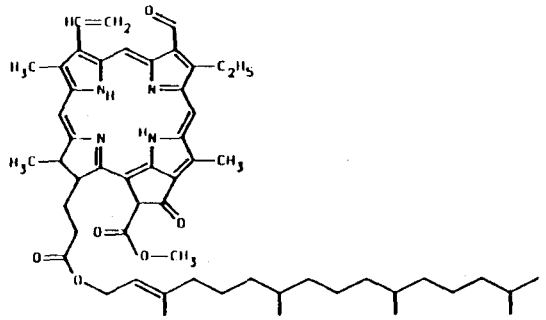

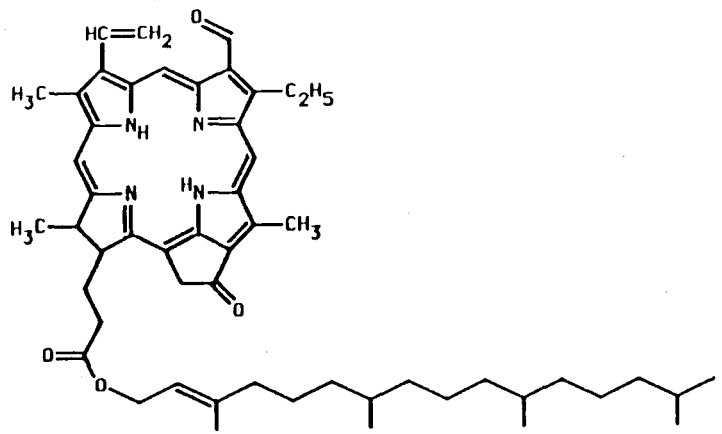

Pyropheophytin-b

$C_{53}H_{70}N_4O_4$

MW = 827.16

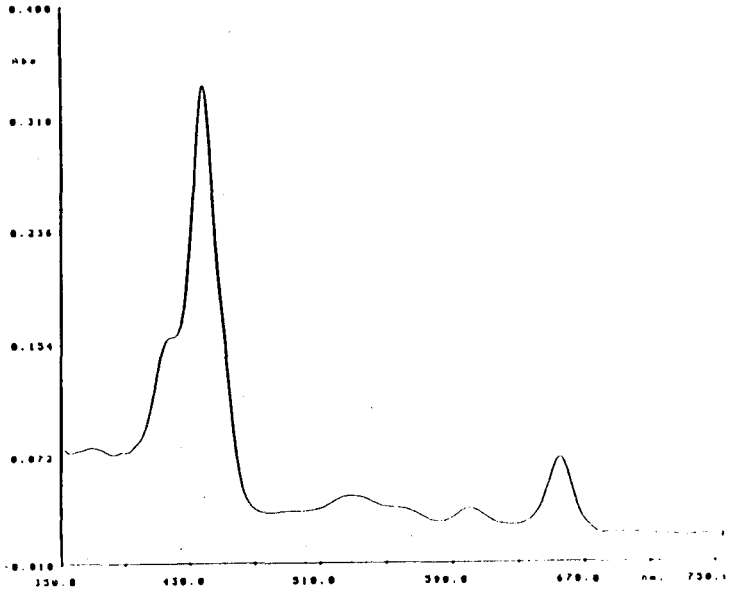

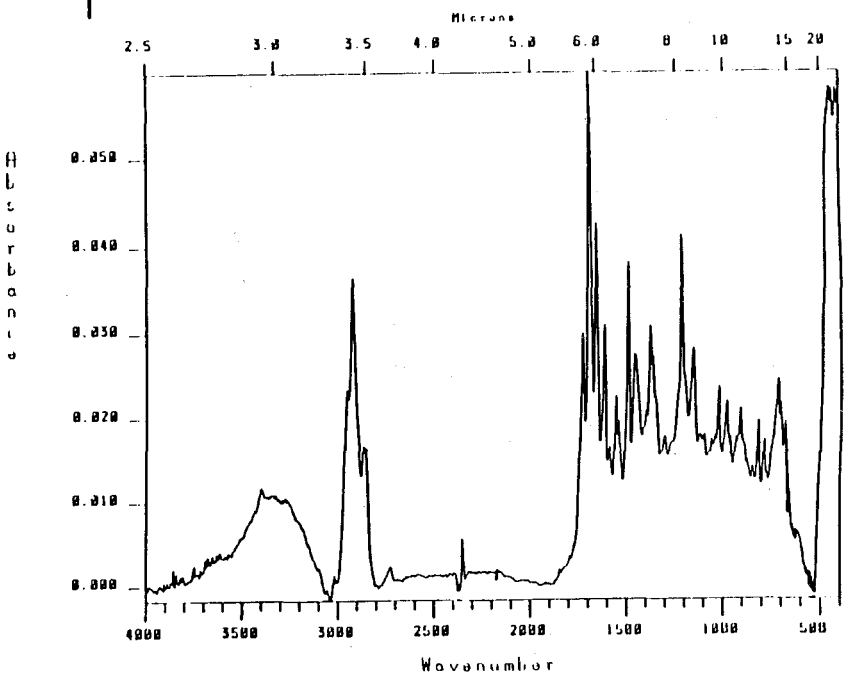

PYROPHEOPHYTIN-B

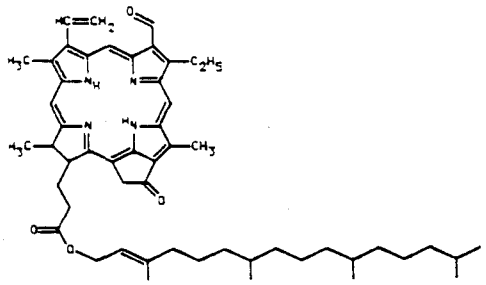

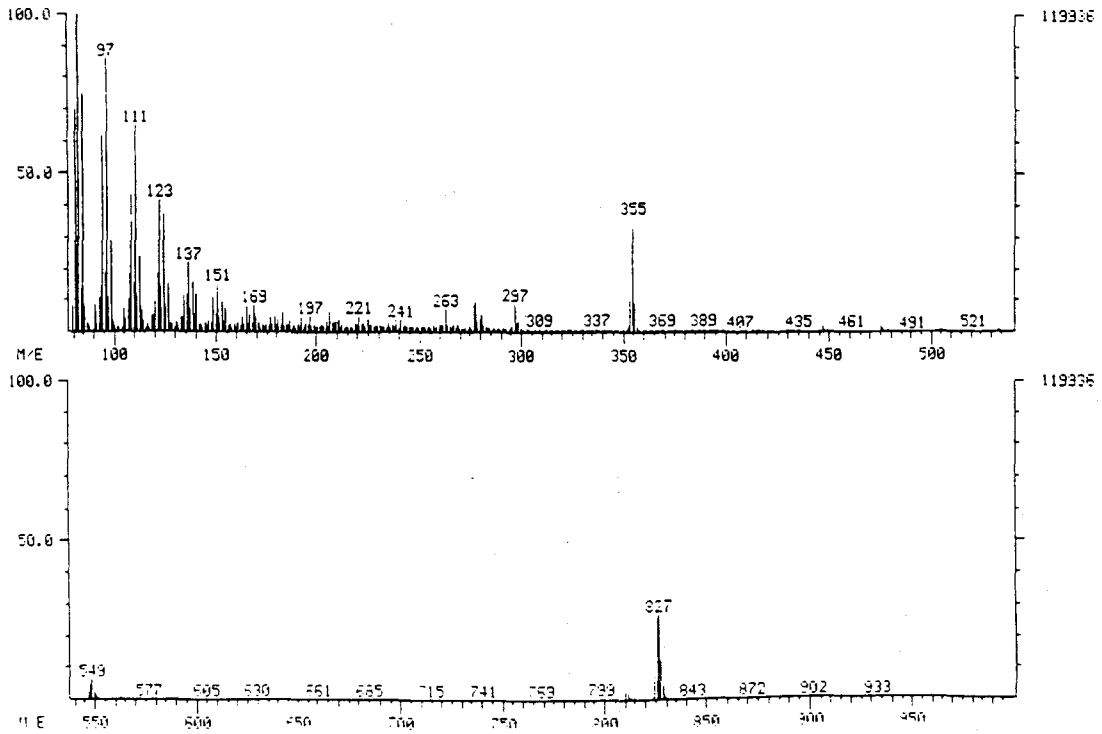

hydrogen chemical ionization

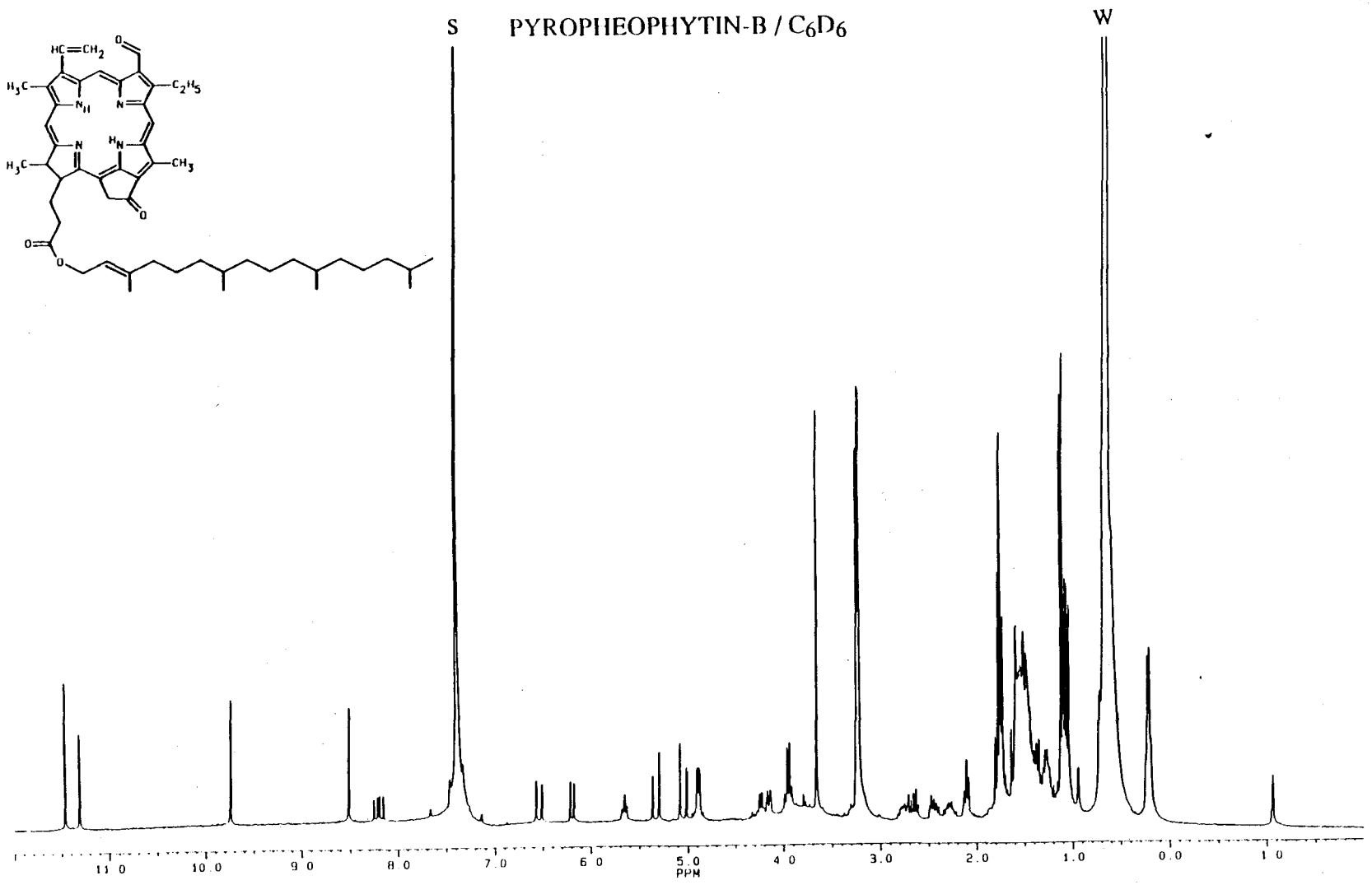
S
PYROPHEOPHYTIN-B / C_6D_6
W
PPM

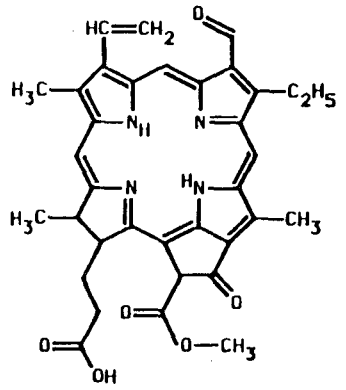

Pheophorbide-b

$C_{35}H_{34}N_4O_6$

MW = 606.68

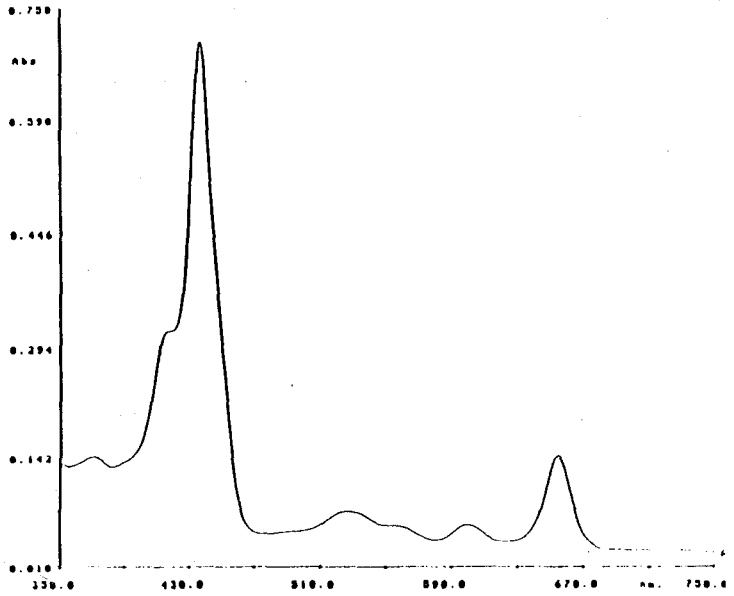

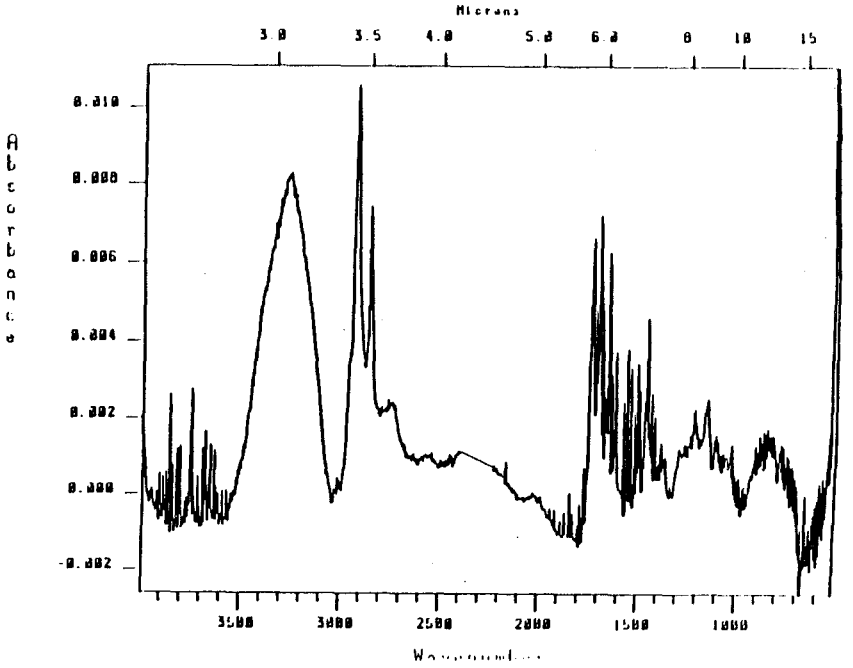

PHEOPHORBIDE-B / C_6D_6

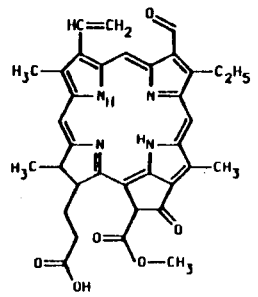

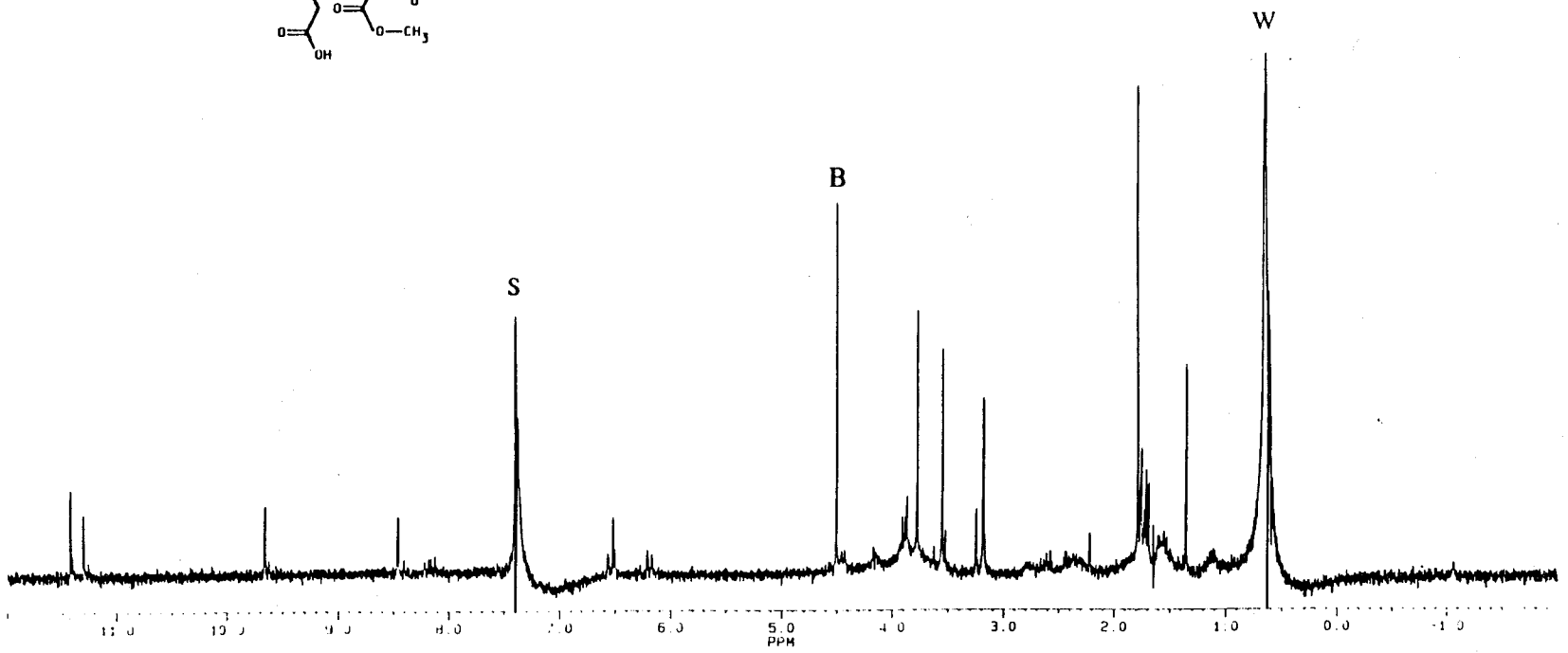

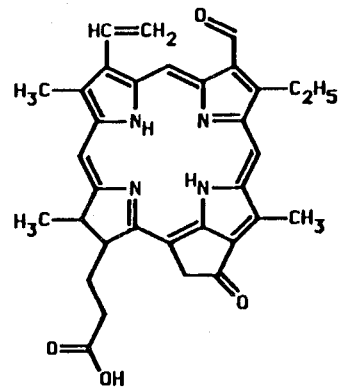

Pyropheophorbide-b

$C_{33}H_{32}N_4O_6$

MW = 580.64

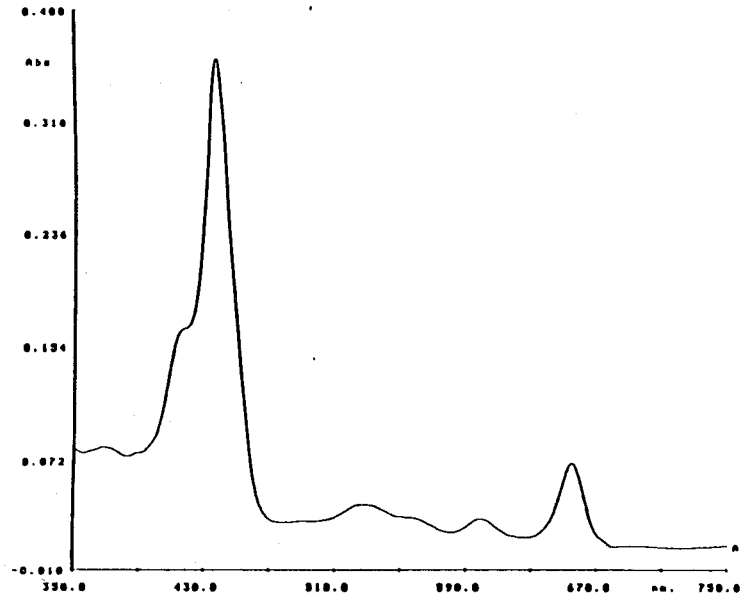

APPENDIX II

THE SPECTRA OF AUTHENTIC PYROPHEOPHORBIDE-*A* STERYL ESTERS

Appendix II

THE SPECTRA OF AUTHENTIC PYROPHEOPHORBIDE-*A* STERYL ESTERS

In Ch. 3 we present the synthesis of four pyropheophorbide-*a* steryl esters: pyropheophorbide-*a* brassicasteryl ester, pyropheophorbide-*a* β-sitosteryl ester, pyropheophorbide-*a* cholesteryl esters, and pyropheophorbide-*a* stigmasteryl ester. In the following, we present the molecular structure, visible spectrum, mass spectrum, and nuclear magnetic spectrum of each authentic pyropheophorbide-*a* steryl ester.

In the mass spectra of pyropheophorbide-a brassicasteryl ester, pyropheophorbide-a b-sitosteryl ester, and pyropheophorbide-a stigmasteryl ester, ions appear at incraments of 14 a.m.u. above the M+1 ion. These ions are probably caused by contaminating sterols in the sterols used in the synthesis.

Pyropheophorbide-*a* brassicasteryl ester

$C_{61}H_{78}N_4O_3$

915.31

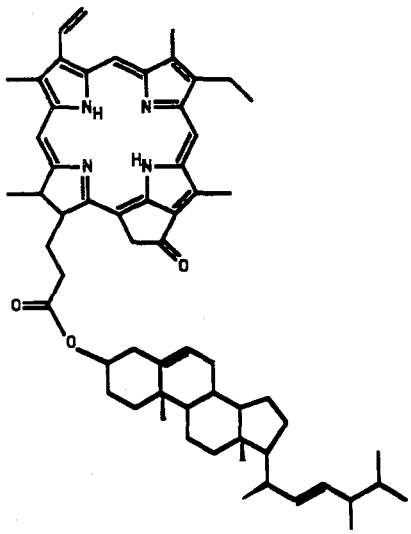

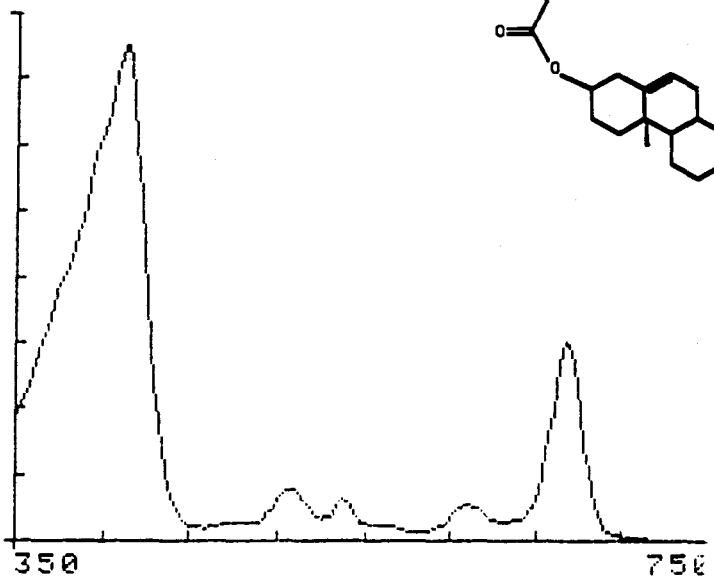

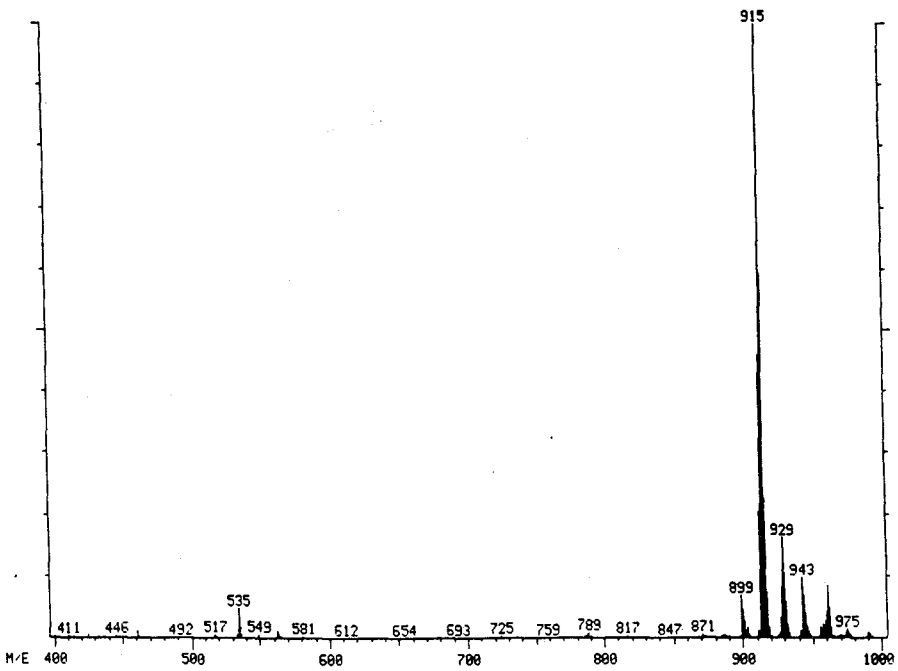

Pyropheophorbide-*a* brassicasteryl ester / d6-benzene

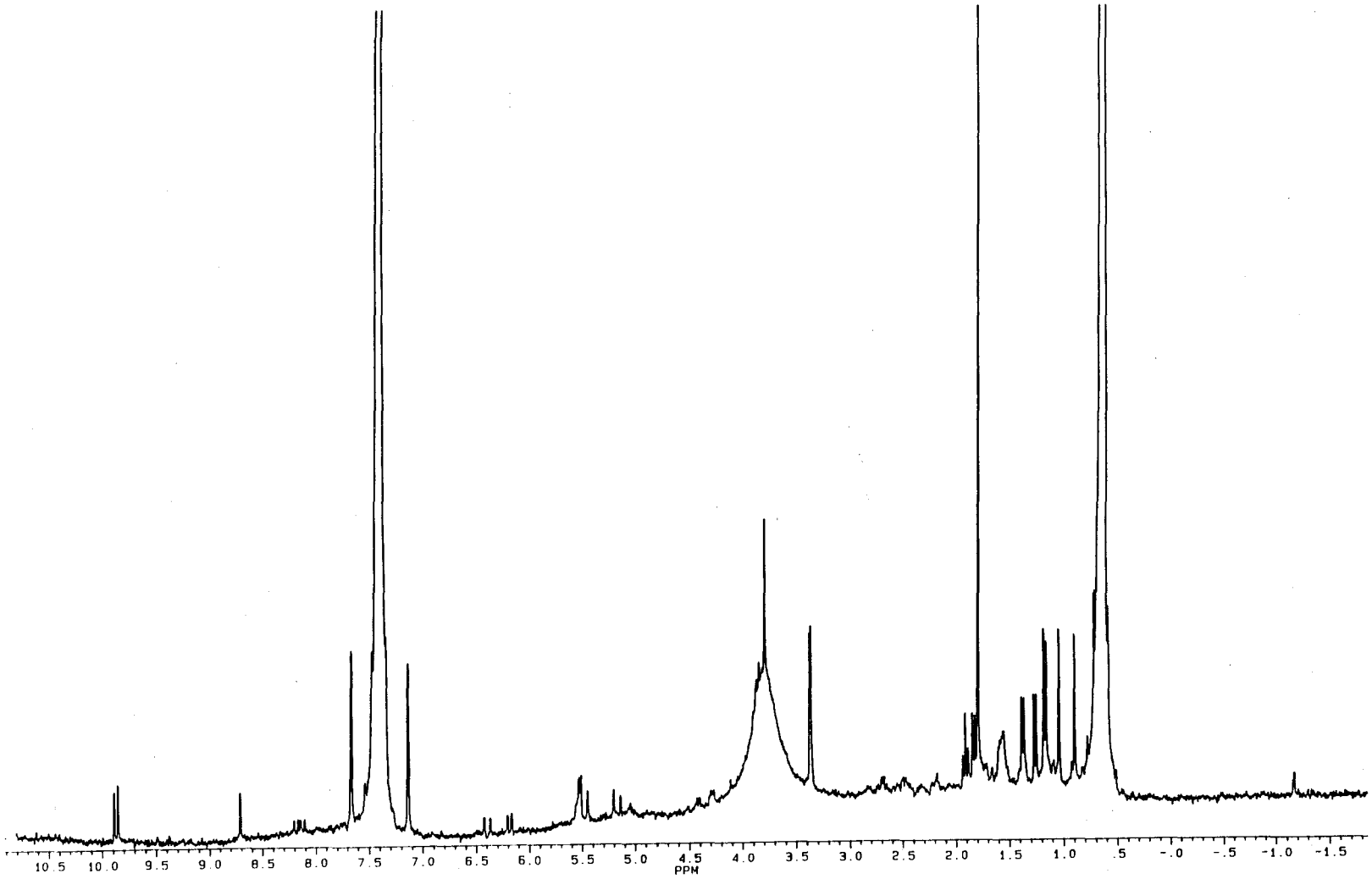

Pyropheophorbide-*a* β-sitosteryl ester

$C_{62}H_{82}N_4O_3$

931.35

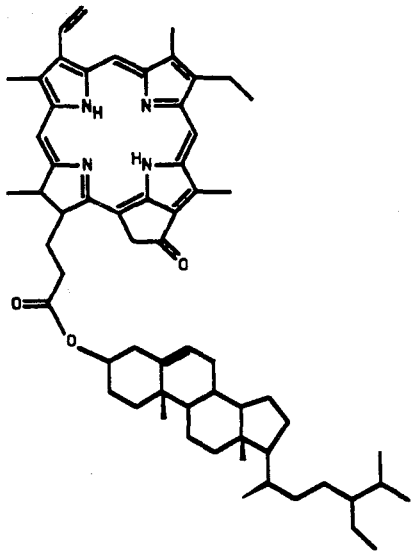

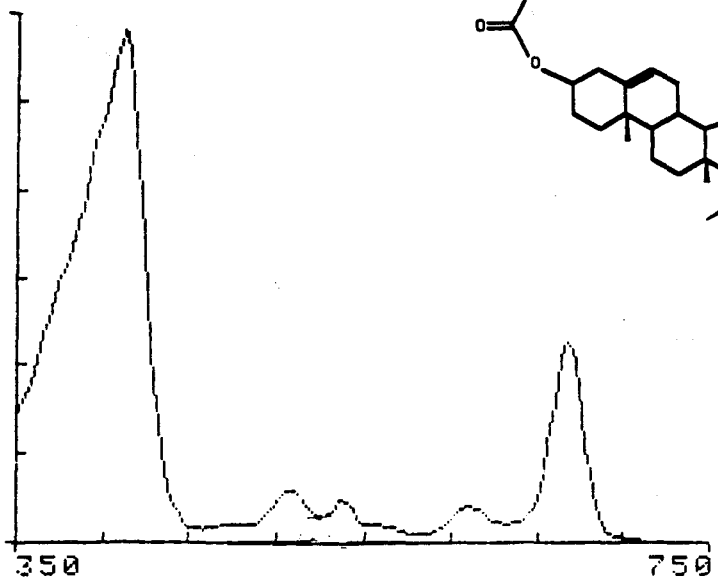

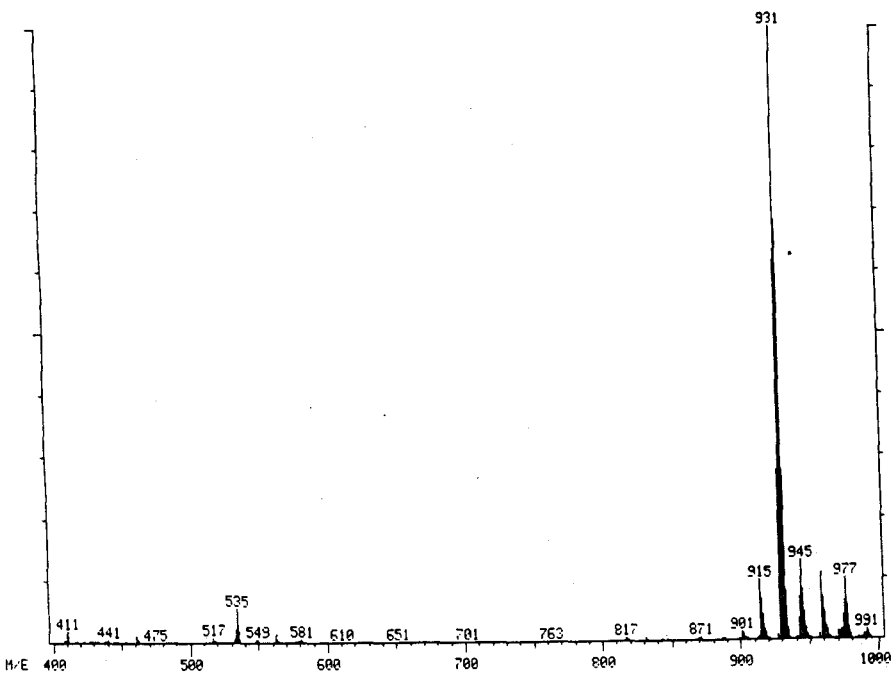

Pyropheophorbide-*a* β-sitosteryl ester / d6-benzene

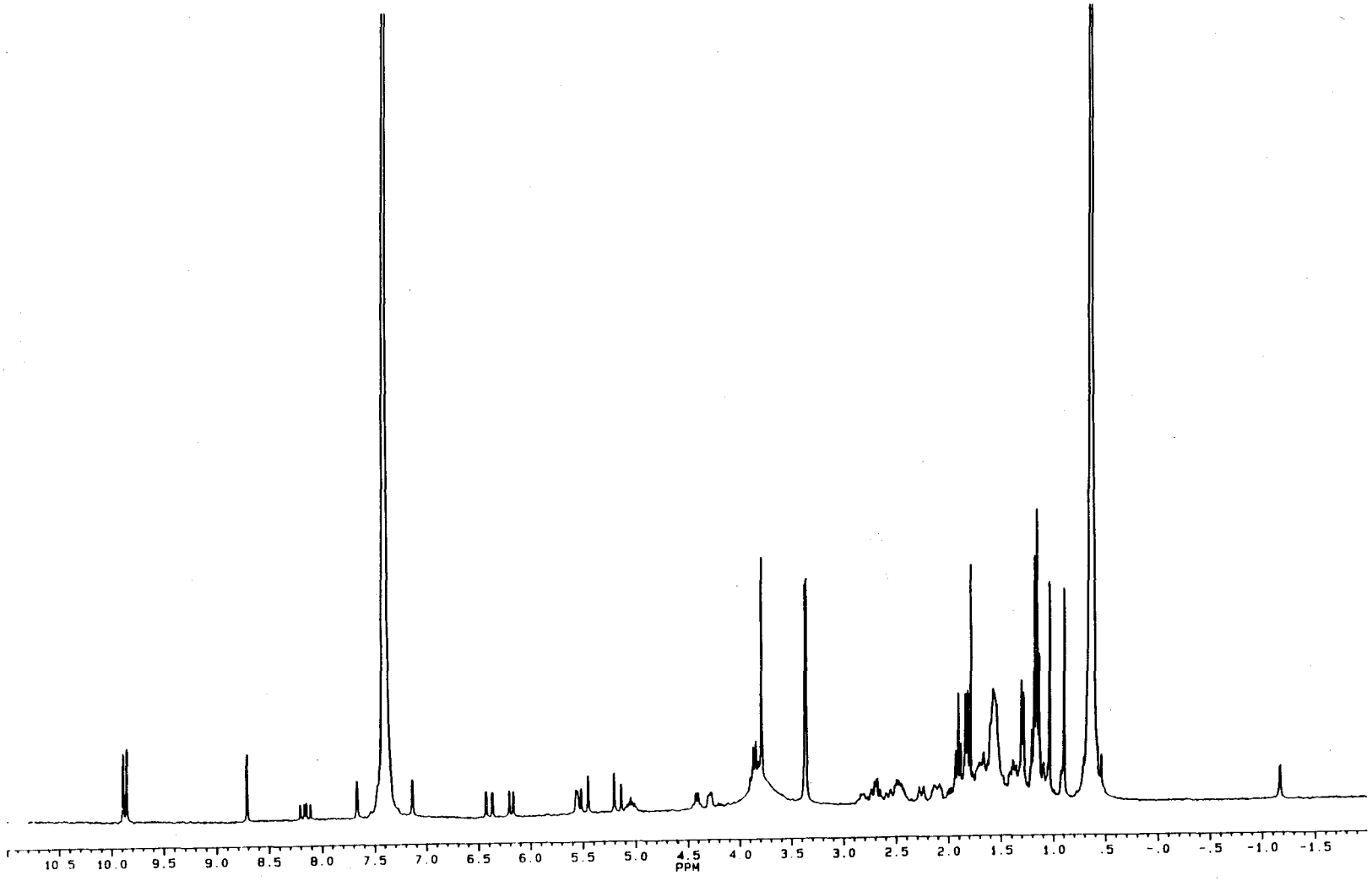

Pyropheophorbide-*a* cholesteryl ester

$C_{60}H_{78}N_4O_3$

903.30

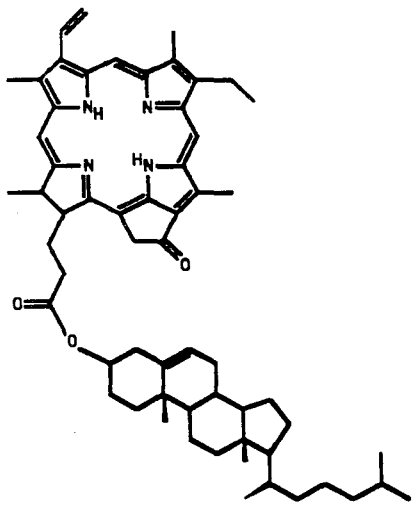

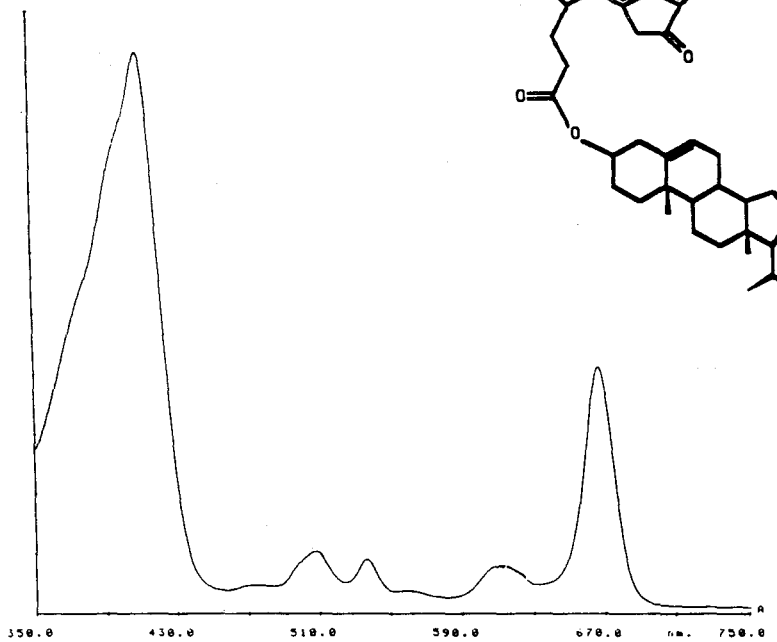

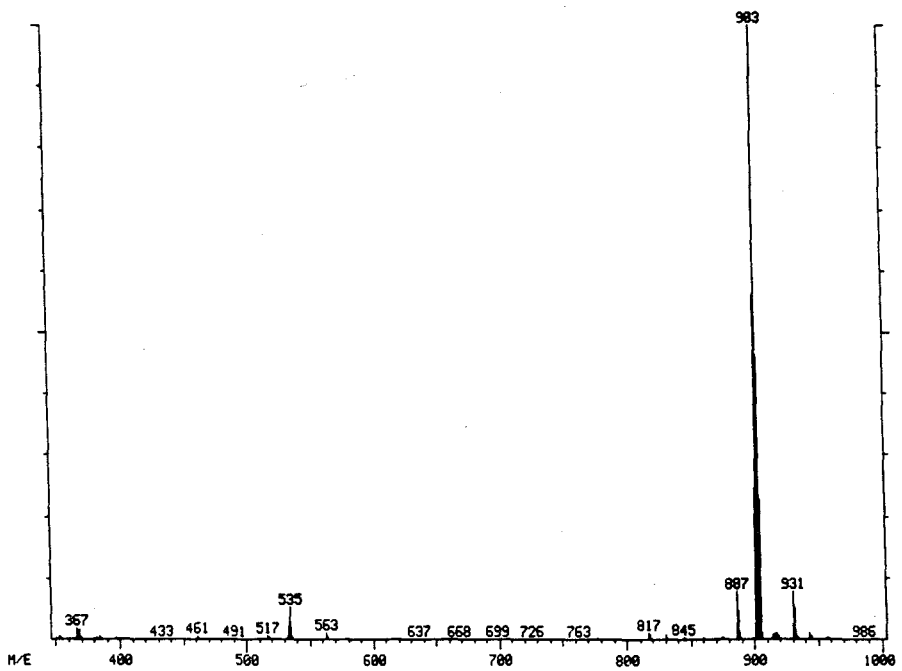

Pyropheophoribide-*a* cholesteryl ester / d6-benzene

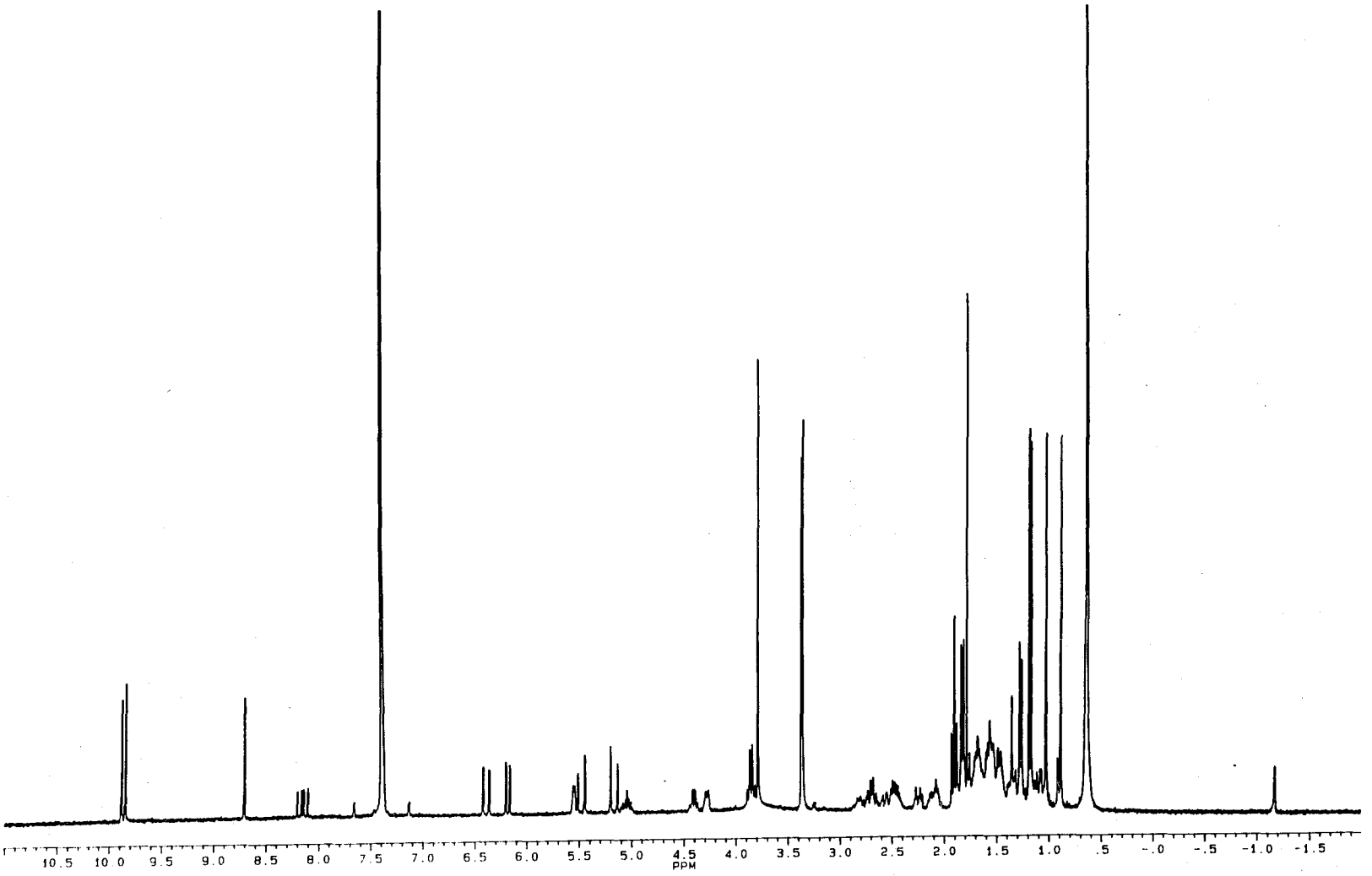

Pyropheophorbide-*a* stigmasteryl ester

$C_{62}H_{80}N_4O_3$

929.34

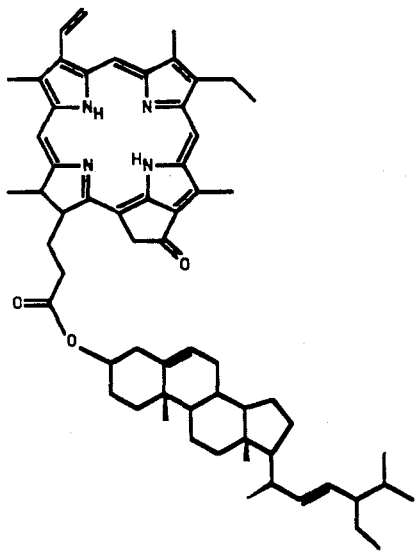

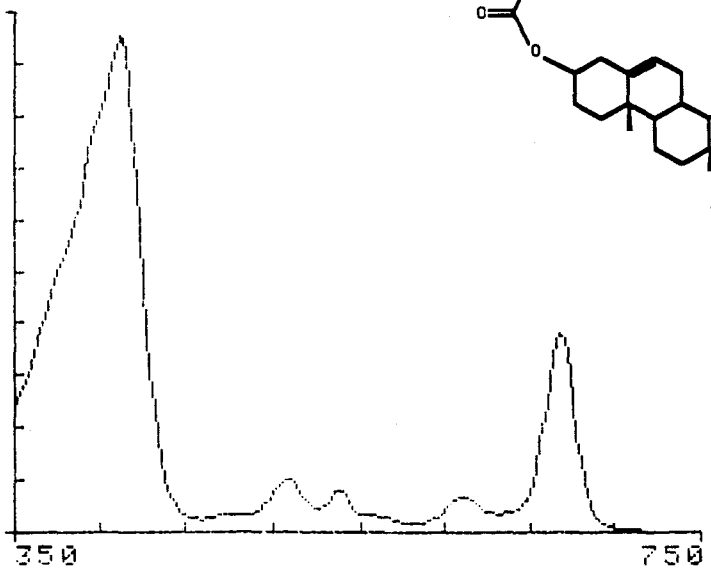

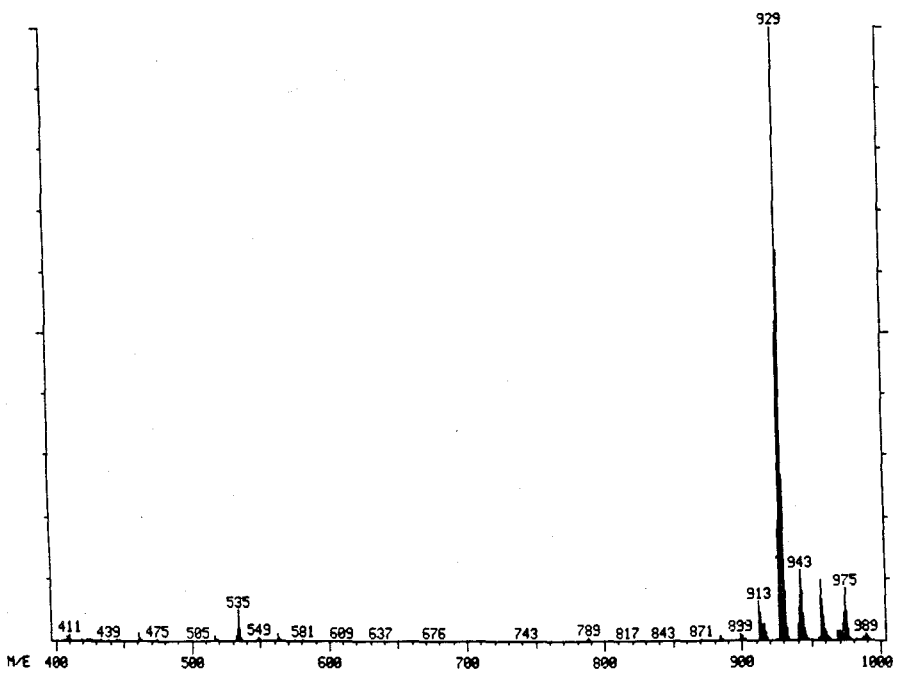

Pyropheophorbide-*a* stigmasteryl ester / d6-benzene

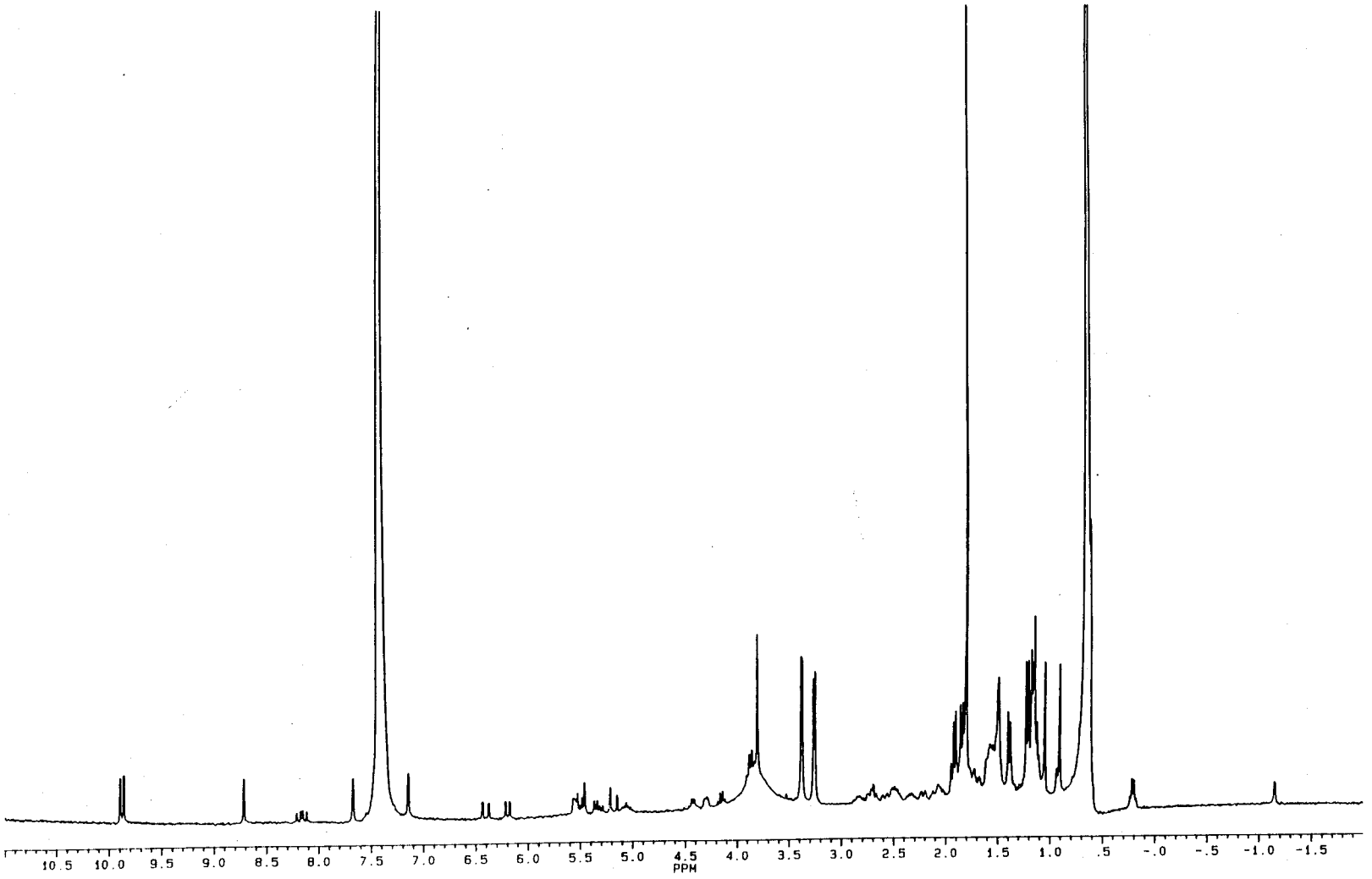

BIOGRAPHICAL NOTE

The author was born in Munich Germany to American parents and was raised in beautiful Virginia, where she spent many starry nights with her father in a boat on the Potomac River. She graduated from Mt. Vernon High School in 1983 and entered Mary Washington College in Fredericksburg, Virginia. She graduated in 1987 with a B.S. in chemistry and departmental and school honors. Her honors thesis was entitled "Chemical Speciation at the Sediment/Water Interface: A Study of Trace Metals in Hazel Run". While working for NASA as a materials engineer during the summer of 1985 and watching the F-16's fly over the Chesapeake Bay, she began thinking about oceanography and received a Summer Student Fellowship at Woods Hole Oceanographic Institution for the summer of 1986. The following summer she returned to W.H.O.I. as a student in the Massachusetts Institute of Technology Woods Hole Oceanographic Insitution Joint Program in Oceanography and Oceanographic Engineering to begin work on her Ph.D.

From her work at NASA and at W.H.O.I., three papers and an abstract have been published:

King, L.L. and Repeta, D.J. (1991) Novel pyropheophorbide-a steryl esters in Black Sea sediments. *Geochim. Cosmochim. Acta* **55**, 2067-2074.

King, L.L. and Repeta, D.J. (1991) New degradation pathways for chlorophyll in Black Sea sediments. In: Organic Geochemistry: Advances and applications in the natural environment (ed. D.A.C. Manning), pp 239-240, Manchester University Press.

Druffel, E.R.M., King, L.L., Belastock, R.A., and Buesseler, K.O. (1990) Growth rate of a deep-sea coral using ^{210}Pb and other isotopes. *Geochim .Cosmochim .Acta* **54**, 1493-1500.

Egli, A.H., King, L.L., and St. Clair, T.L. (1986) Semi-interpenetrating networks of LARC-TPI. *Int. SAMPE Tech Conf: Mater. Space - Gathering Momentum* **18**, 440-453.

The author is continuing to pursue her interest in oceanography and will begin working as a postdoctoral researcher in January, 1992, in the lab of Dr. Stuart Wakeham at the Skidaway Institute of Oceanography, Savannah, Georgia.